

# **From crustal structure to plate kinematics - the role of Large Igneous Provinces in the Pacific Ocean**



Dissertation zur Erlangung des Grades Dr. rer. nat.  
vorgelegt dem Fachbereich Geowissenschaften  
der Universität Bremen  
im November 2015  
von  
**Katharina Hochmuth**



# Erklärung

Hiermit versichere ich,

Katharina Hochmuth  
wohnhaft in der Lilienthalstr. 17, 27568 Bremerhaven

dass ich

1. die Arbeit ohne unerlaubte fremde Hilfe angefertigt habe,
2. keine anderen als die von mir angegebenen Quellen und Hilfsmittel benutzt habe und
3. die den benutzten Werken wörtlich oder inhaltlich entnommenen Stellen als solche kenntlich gemacht habe.

Bremerhaven, den 09.11.2015

---

Katharina Hochmuth

Die vorliegende Dissertation wurde am 14.04.2016 an der Universität Bremen verteidigt. Der Prüfungsausschuss bestand aus Prof. Dr. Wilfried Jokat (erster Gutachter), Prof. Dr. Wolfgang Bach (zweiter Gutachter), Prof. Dr. Cornelia Spiegel, PD Dr. Christian Scheibner, Dr. Karsten Gohl und Rebecca Schlegel.

# Abstract

The bathymetry of the Pacific Ocean is dominated by three Large Igneous Provinces (LIP): the Ontong Java Plateau, the Hikurangi Plateau and the Manihiki Plateau. *Taylor* (2006) proposed their joined emplacement as one "Super"-LIP Ontong Java Nui in the early Cretaceous. Petrological and geochemical data point to this scenario, but geophysical evidence is sparse. To evaluate the hypothesis of Ontong Java Nui, refraction/wide-angle reflection seismic data was collected in 2012, during the RV Sonne cruise So-224 across the two main sub-provinces of the Manihiki Plateau. The modeling and interpretation of P-wave velocity, S-wave velocity and density profiles across the Manihiki Plateau along with available seismic reflection data aims to enhance our understanding of the crustal structure of the Manihiki Plateau and improve the plate kinematic reconstruction of the western Pacific region during the Cretaceous.

If the hypothesis is correct, the Manihiki Plateau exposes break-up margins to all other LIPs of Ontong Java Nui. The Manihiki Plateau itself is fragmented into multiple sub-provinces. The two largest sub-provinces, the High Plateau and the Western Plateaus have been studied intensively in this experiment. The crustal structure of the High Plateau is comparable to other LIPs with a high velocity zone (P-wave velocities  $>7.3$  km/s) in the lower crust and a basaltic to gabbroic crust. The crustal thickness is 20 km. Secondary magmatic phases are strong on the High Plateau expressed in multiple volcanic centers. The Danger Islands Troughs are a series of pull-apart basins, which separate the High Plateau from the Western Plateaus. These plateaus have been subject to massive tectonic deformation such as the gradual decrease in crustal thickness from 17.3 km in the East to 9.1 km in the West. Secondary volcanism is limited to fracture zones and low volume seamount volcanism.

Since the crustal structure of the Western Plateaus points to a joined emplacement, the "Super"-LIP can be reassembled. The data also provides further evidence for a eastern and a northeastern continuation of the Manihiki Plateau by the sudden termination of the high velocity zone in the lower crust towards the East. It has been accounted for subducted LIP-parts, the rotation of LIP fragments such as the Hikurangi Plateau, crustal stretching invoked during the break-up and the crust emplaced during secondary magmatic stages. This calculates to an approximated initial size of Ontong Java Nui of 1.1. % of the Earth's surface. Based on this information I reconstructed the "Super"-LIP Ontong Java Nui and modeled its break-up during the Cretaceous Normal Superchron.

The initial emplacement of Ontong Java Nui can be explained by the interaction of a mantle plume with the Pacific-Phoenix ridge resulting in different crustal thicknesses throughout the plateau. I modeled the motion of different fragments of Ontong Java Nui using mapped fracture zones, traces of former plate boundaries and refined kinematic rotation poles of the western Pacific. Paleogene and Neogene intraplate tectonic activity occurred within the Ellice Basin between the Ontong Java Plateau and the Manihiki Plateau and on the Manihiki Plateau itself.

The eastern and northeastern fragments of the Manihiki Plateau have been captured by the

Phoenix and Farallon Plate, respectively. The eastern fragment subducted analog to the southern Hikurangi Plateau at the eastern Gondwana margin in today's Bellingshausen Sea and Palmer Land region during the Mid-Cretaceous, possibly flattening the slab of the subduction zone. The northeastern fragment collided with the South American craton during the Paleocene. In this amagmatic trench setting, oceanic terranes were accreted to the craton building up today's northern Andes. The Piñón formation of Colombia and Ecuador is a possible candidate to be a remnant of the lower crust of the Manihiki Plateau.

# Zusammenfassung

Die Bathymetrie des pazifischen Ozeans ist durch drei große vulkanischer Provinzen geprägt. Große vulkanische Provinzen werden auch als Large Igneous Provinces oder kurz LIP bezeichnet. Taylor (2006) stellte die Hypothese auf, dass diese drei LIPs - das Ontong Java Plateau, das Hikurangi Plateau und das Manihiki Plateau - zusammen während der frühen Kreide, als eine sogenannte "Super"-LIP namens Ontong Java Nui entstanden sind. Diese Annahme stützt sich besonders auf petrologische und geochemische Daten. Geophysikalische Untersuchungen der Region sind jedoch noch lückenhaft. Um die Entstehung des Manihiki Plateaus und seine Rolle innerhalb des vermuteten "Super"-LIPs besser zu verstehen, wurden 2012 refraktions- / weitwinkelreflektionsseismische Daten, die die zwei größten Unterprovinzen des Manihiki Plateaus, das High Plateau und das Western Plateau, abdecken, erhoben. Ich modellierte und interpretierte P- und S-Wellenmodelle, sowie Dichtemodelle der aufgenommenen Profile. Diese betrachtete ich im Anschluss, zusammen mit den verfügbaren reflexionsseismischen Daten im plattentektonischen Kontext des westlichen Pazifiks. Des weiteren ist die Struktur der Erdkruste der verschiedenen Unterprovinzen des Manihiki Plateaus von Interesse.

Das High Plateau des Manihiki Plateaus zeigt den typischen krustalen Aufbau einer großen vulkanischen Provinz mit Basalten und Gabbros in der oberen und mittleren Kruste und einem Hochgeschwindigkeitskörper (P-Wellengeschwindigkeit  $> 7.3$  km/s) in der unteren Kruste. Die Mächtigkeit der Kruste beträgt 20 km. Spätere vulkanische Phasen haben das Plateau mit mehreren vulkanischen Zentren stark überprägt. Die Danger Islands Troughs sind eine Reihe von Pull-apart Becken, die das High Plateau von den Western Plateaus trennen. Die Western Plateaus zeigen eine starke tektonische Deformation innerhalb der gesamten Kruste, deren Mächtigkeit von Osten nach Westen von 17.3 km auf nur 9.1 km abnimmt. Spätere vulkanische Phasen sind hier schwach ausgeprägt.

Die neugewonnenen Daten zeigen Hinweise auf eine gemeinsame Entstehung der LIPs. Unter Berücksichtigung aller vorhandenen Daten, habe ich die Plateaus wieder zusammengefügt. Hierbei berücksichtigte ich besonders die subduzierten Anteile, die Rotationen der verschiedenen Fragmente, sowie die Dehnung der Kruste und die durch spätere vulkanische Phasen entstandene Kruste. Ontong Java Nui entstand durch die Wechselwirkung eines pulsierenden Manteldiapirs mit dem mittelozeanischen Rücken zwischen der Pazifischen Platte und der Phoenix Platte. Bei seiner Entstehung bedeckte Ontong Java Nui wahrscheinlich 1.1% der Erdoberfläche. Durch das Kartieren von Störungszonen, die die Bewegung der Platten nachzeichnen und ehemaliger Grenzflächen tektonischer Platten, kann die tektonische Bewegung der einzelnen Plateaus nachempfunden werden und die plattenkinematischen Rotationspole des westlichen Pazifiks für die Zeit der Kreide verbessert werden. Während des Paläogen und des Neogens treten platteninterne tektonische Aktivitäten im Bereich des Ellice Basins und des Manihiki Plateaus auf.

Das östliche und das nordöstliche Fragment des Manihiki Plateaus wird im Zuge der platten-tektonischen Reorganisation und des Auseinanderbrechens der "Super"-LIP in die Phoenix,

beziehungsweise die Farallon Platte integriert. Das östliche Fragment trifft innerhalb der mittleren Kreide auf die Subduktionszone am östlichen Gondwanarand auf und wird dort analog zum südlichen Hikurangi Plateau subduziert. Dadurch flachte der Winkel der Subduktionszone im Bereich der heutigen Bellingshausensee und Palmer Land in der Westantarktis ab. Das nordöstliche Fragment kollidiert während des Paläogen mit dem südamerikanischen Kraton. An diesem amagmatischen Graben werden ozeanische Terrane an den Kraton angeschweißt, die die heutigen nördlichen Anden bilden. Die Piñón Formation des heutigen Kolumbiens und Ecuadors ist ein möglicher Kandidat, ein Terran des Manihiki Plateaus zu sein.



# Contents

<b>Abstract</b>	<b>IV</b>
<b>Zusammenfassung</b>	<b>VI</b>
<b>Nomenclature</b>	<b>VIII</b>
<b>List of figures</b>	<b>XIV</b>
<b>List of tables</b>	<b>XV</b>
<b>1 Introduction and motivation</b>	<b>1</b>
1.1 Historic and current volcanic activity and their impact on the global environment	1
1.2 Large Igneous Provinces - massive volcanic eruptions shaping the face of Earth	3
1.3 The Manihiki Plateau and the LIPs of Ontong Java Nui . . . . .	5
<b>2 Research questions</b>	<b>7</b>
<b>3 Datasets, methods and processing</b>	<b>9</b>
3.1 Geophysical Datasets . . . . .	9
3.1.1 New geophysical data acquired during the cruise So-224 . . . . .	9
3.1.2 Pre-existing datasets . . . . .	10
3.2 Refraction/wide-angle reflection seismic data . . . . .	11
3.2.1 Geophysical principle of refraction/wide-angle seismic data . . . . .	11
3.2.2 Data acquisition during So-224 . . . . .	12
3.2.3 Modeling of P- and S-wave arrivals . . . . .	13
3.2.4 Calculation of the Poisson's ratio ( $\sigma$ ) . . . . .	15
3.3 Modeling of gravity anomaly data . . . . .	15
3.4 Plate kinematic model with " <i>GPlates</i> " . . . . .	16
3.4.1 Global plate kinematic models with " <i>GPlates</i> " . . . . .	16
3.4.2 Calculation of new rotation poles for the western Pacific . . . . .	19
<b>4 Contributions to scientific journals</b>	<b>21</b>

<b>5</b>	<b>Multiphase magmatic and tectonic evolution of a Large Igneous Province - evidence from the crustal structure of the Manihiki Plateau, western Pacific</b>	<b>23</b>
5.1	Introduction . . . . .	24
5.2	Geological background . . . . .	25
5.3	Data acquisition, processing, and modeling parameterization . . . . .	28
5.3.1	Data acquisition . . . . .	28
5.3.2	Processing and modeling of seismic refraction/wide-angle reflection data	28
5.3.3	Modeling of gravity data . . . . .	29
5.4	Results of data analysis and modeling . . . . .	30
5.4.1	Bathymetric and sedimentary features . . . . .	30
5.4.2	Upper crustal layers . . . . .	33
5.4.3	Middle crustal layers . . . . .	34
5.4.4	Lower crustal layers . . . . .	35
5.4.5	Crust-mantle boundary and mantle . . . . .	36
5.4.6	Two different magmatic and tectonic regimes on the Manihiki Plateau .	37
5.5	Discussion: Western Plateaus vs. High Plateau – two different crustal environments of the Manihiki Plateau . . . . .	42
5.5.1	Comparison with other oceanic LIPs . . . . .	42
5.5.2	The role of the HVZ in the lower crust of the Manihiki Plateau . . . . .	44
5.5.3	Emplacement scenario of the Manihiki Plateau and its two major sub-provinces . . . . .	45
5.6	Conclusions . . . . .	49
<b>6</b>	<b>Playing jigsaw with Large Igneous Provinces - a plate tectonic reconstruction of Ontong Java Nui</b>	<b>50</b>
6.1	Introduction . . . . .	51
6.2	Geological Setting . . . . .	53
6.2.1	The Large Igneous Provinces of the western Pacific . . . . .	53
6.2.2	The plate tectonic framework of the Pacific during the Cretaceous . . . .	55
6.3	Overview on published and additional data . . . . .	56
6.4	Possible break-up mechanisms on the Manihiki Plateau . . . . .	59
6.5	Plate tectonic reconstruction of the Cretaceous western Pacific . . . . .	60
6.5.1	The emplacement of Ontong Java Nui – plume-ridge interaction and single “Super”-plume head . . . . .	60
6.5.2	The initial break-up of Ontong Java Nui – evaluation of the break-up mechanisms on oceanic LIPs (120-116 Ma) . . . . .	66
6.5.3	Dispersal of Ontong Java Nui over the Pacific Ocean . . . . .	68
6.6	Conclusions . . . . .	72

<b>7</b>	<b>From the western Pacific to the Andes and Antarctica: The Manihiki Plateau on the move</b>	<b>74</b>
7.1	Introduction: Large Igneous Provinces in the plate circuit . . . . .	75
7.2	Geological setting: Ontong Java Nui and its remnants . . . . .	76
7.3	Results of plate kinematic modeling of the Pacific Ocean (Cretaceous – Paleogene)	77
7.3.1	Northeastern Manihiki Plateau fragment . . . . .	77
7.3.2	Eastern Manihiki Plateau fragment . . . . .	78
7.4	The Manihiki Plateau on the move . . . . .	79
7.4.1	Oceanic terranes of the northern Andes: Resting place of Manihiki Plateau fragment . . . . .	79
7.4.2	Palmer Land events: initiated by LIP subduction? . . . . .	81
7.5	Conclusions: The impact of Ontong Java Nui on the Pacific evolution . . . . .	83
<b>8</b>	<b>Conclusions</b>	<b>84</b>
<b>9</b>	<b>Outlook and further research</b>	<b>88</b>
9.1	Crustal structure of the Manihiki Plateau and its margins . . . . .	88
9.2	Enhancement of plate tectonic reconstructions . . . . .	90
9.3	Presence of fragments of the Manihiki Plateau in western Antarctica . . . . .	91
	<b>Bibliography</b>	<b>93</b>
	<b>Danksagung</b>	<b>109</b>
	<b>Appendices</b>	<b>110</b>
<b>A</b>	<b>OBS/OBH data of So-224</b>	<b>111</b>
A.1	Map of deployment locations . . . . .	111
A.2	Performance of OBS/OBH-stations . . . . .	112
A.2.1	AWI-20120100 . . . . .	112
A.2.2	AWI-20120200 . . . . .	113
A.3	OBS/OBH stations of AWI-20120100 . . . . .	114
A.4	OBS/OBH stations of AWI-20120200 . . . . .	145
A.5	Reflection seismic data of So-224 along refraction seismic profile . . . . .	174
A.5.1	AWI-20120101 . . . . .	174
A.5.2	AWI-20120201 . . . . .	175
<b>B</b>	<b>Plate kinematic reconstruction with <i>GPlates</i></b>	<b>176</b>
B.1	Used Plate IDs . . . . .	176

# Nomenclature

approx. ....	approximately
AWI ....	Alfred-Wegener-Institut Helmholtzzentrum für Polar- und Meeresforschung, Bremerhaven
CLIP ....	Caribbean Large Igneous Province
CNS ....	Cretaceous Normal Superchron
DSDP ....	Deep Sea Drilling Program
e.g. ....	for example
FZ ....	Fracture Zone
GEBCO ....	General Bathymetric Map of the Oceans
H.P. ....	High Plateau of the Manihiki Plateau
HVZ ....	High Velocity Zone
incl. ....	inclusive
IODP ....	International Ocean Drilling Project
LIP ....	Large Igneous Province
N.P. ....	North Plateau of the Manihiki Plateau
NZ ....	New Zealand
OAE ....	Oceanic Anoxic Event
OBH ....	Oceanbottomhydrophone
OBS ....	Oceanbottomseismometer
ODP ....	Ocean Drilling Project
Plc ....	refracted P-wave phase from the lower crust
PlcP ....	reflected P-wave phase from the lower boundary of the lower crust
Plmc ....	refracted P-wave phase from the lower-middle crust
PlmcP ....	reflected P-wave phase from the lower boundary of the lower-middle crust
Pmc ....	refracted P-wave phase from the middle crust
PmcP ....	reflected P-wave phase from the lower boundary of the middle crust
PmP ....	reflected P-wave phase from the Moho
Pn ....	refracted P-wave phase from the upper mantle
Puc ....	refracted P-wave phase from the upper crust
PucP ....	reflected P-wave phase from the lower boundary of the upper crust
Pumc ....	refracted P-wave phase from the upper-middle crust

PumcP .....	reflected P-wave phase from the lower boundary of the upper-middle crust
Slc .....	refracted S-wave phase from the lower crust
Slmc .....	refracted S-wave phase from the lower-middle crust
Smc .....	refracted S-wave phase from the middle crust
Sn .....	refracted S-wave phase from the upper mantle
Suc .....	refracted S-wave phase from the upper crust
Sumc .....	refracted S-wave phase from the upper-middle crust
VEI .....	volcanic explosivity index
W.P. ....	Western Plateaus of the Manihiki Plateau



# List of Figures

<b>Introduction and Motivation</b>	<b>1</b>
1.1 Overview on the global distribution of Large Igneous Provinces . . . . .	2
1.2 Different stages of a mantle plume . . . . .	3
1.3 Impact of LIP emplacement . . . . .	4
1.4 Bathymetric map of the research area . . . . .	5
 <b>Datasets, Methods and Processing</b>	 <b>9</b>
3.1 Cruise Logo So-224/225 . . . . .	9
3.2 Overview of existing and newly acquired data . . . . .	10
3.3 Refraction seismic work at sea . . . . .	11
3.4 Sketch of OBS . . . . .	12
3.5 Sketch of OBH . . . . .	13
3.6 Example of refraction seismic data . . . . .	14
3.7 "GPlates"-philosophy . . . . .	16
3.8 Example for rotation hierarchy . . . . .	18
3.9 Workflow of plate kinematic reconstruction . . . . .	19
 <b>Crustal structure of the Manihiki Plateau</b>	 <b>23</b>
5.1 Bathymetric map Manihiki Plateau . . . . .	26
5.2 Data example P-wave arrivals AWI-20120100 . . . . .	31
5.3 Data example S-wave arrivals AWI-20120100 . . . . .	31
5.4 Data example P-wave arrivals AWI-20120200 . . . . .	32
5.5 Data example S-wave arrivals AWI-20120200 . . . . .	32
5.6 Seismic reflection data AWI-20120100 . . . . .	33
5.7 P-wave velocity model AWI-20120100 . . . . .	34
5.8 S-wave velocity model AWI-20120100 . . . . .	35
5.9 P-wave velocity model of AWI-20120200 . . . . .	36
5.10 S-wave velocity model of AWI-20120200 . . . . .	37
5.11 Poisson's Ratio of AWI-20120200 . . . . .	38

5.12 Gravity model of AWI-20120100 . . . . .	39
5.13 Gravity model of AWI-20120200 . . . . .	39
5.14 Geological interpretation AWI-20120100 . . . . .	40
5.15 Geological interpretation AWI-20120200 . . . . .	41
5.16 Comparison of crustal structure of LIPs . . . . .	43
5.17 Evolution of the Manihiki Plateau . . . . .	47
<b>Plate tectonic reconstruction of Ontong Java Nui</b>	<b>50</b>
6.1 Plate tectonic set-up of the Pacific Ocean . . . . .	52
6.2 Tectonic alteration of the Manihiki Plateau . . . . .	53
6.3 P-wave velocity models . . . . .	58
6.4 Classification of margins of Ontong Java Nui . . . . .	61
6.5 Nova Canton Trough . . . . .	63
6.6 Sketch Plume-Ridge Interaction . . . . .	65
6.7 Paleolatitude of Ontong Java Nui . . . . .	67
6.8 Tectonic evolution of the western Pacific during the CNS (125 Ma and 117 Ma) . .	70
6.9 Tectonic evolution of the western Pacific during the CNS (110 Ma, 100 Ma and 83 Ma) . . . . .	71
<b>The Manihiki Plateau on the move</b>	<b>74</b>
7.1 Overview on the LIPs of the Pacific Ocean and their subducted remnants . . . .	76
7.2 Northeastern fragment of the Manihiki Plateau . . . . .	78
7.3 Eastern fragment of the Manihiki Plateau . . . . .	81
<b>Conclusions</b>	<b>84</b>
8.1 Bathymetric map of the research area . . . . .	84
<b>Outlook and further research</b>	<b>88</b>
9.1 Proposed further research: Manihiki Plateau . . . . .	89
9.2 Proposed further research: Western Pacific . . . . .	90
9.3 Proposed further research: Western Antarctica . . . . .	92
<b>Appendices</b>	<b>110</b>
A.1 Deployment positions of OBS/OBH stations . . . . .	111
A.2 Batymetric map of profile AWI-20120200 . . . . .	114
A.3 P- and S-waves station 100st01 . . . . .	115
A.4 P- and S-waves station 100st02 . . . . .	116
A.5 P- and S-waves station 100st03 . . . . .	117
A.6 P- and S-waves station 100st04 . . . . .	118

A.7	P- and S-waves station 100st05	119
A.8	P- and S-waves station 100st06	120
A.9	P- and S-waves station 100st07	121
A.10	P- and S-waves station 100st08	122
A.11	P- and S-waves station 100st09	123
A.12	P- and S-waves station 100st10	124
A.13	P- and S-waves station 100st11	125
A.14	P- and S-waves station 100st12	126
A.15	P- and S-waves station 100st14	127
A.16	P- and S-waves station 100st15	128
A.17	P- and S-waves station 100st16	129
A.18	P- and S-waves station 100st18	130
A.19	P- and S-waves station 100st21	131
A.20	P- and S-waves station 100st22	132
A.21	P- and S-waves station 100st23	133
A.22	P- and S-waves station 100st24	134
A.23	P- and S-waves station 100st25	135
A.24	P- and S-waves station 100st26	136
A.25	P- and S-waves station 100st27	137
A.26	P- and S-waves station 100st28	138
A.27	P- and S-waves station 100st29	139
A.28	P- and S-waves station 100st30	140
A.29	P- and S-waves station 100st31	141
A.30	P- and S-waves station 100st32	142
A.31	P- and S-waves station 100st33	143
A.32	P- and S-waves station 100st34	144
A.33	Batymetric map of profile AWI-20120200	145
A.34	P- and S-waves station 200st01	146
A.35	P- and S-waves station 200st02	147
A.36	P- and S-waves station 200st03	148
A.37	P- and S-waves station 200st04	149
A.38	P- and S-waves station 200st06	150
A.39	P- and S-waves station 200st07	151
A.40	P- and S-waves station 200st08	152
A.41	P- and S-waves station 200st09	153
A.42	P- and S-waves station 200st10	154
A.43	P- and S-waves station 200st11	155
A.44	P- and S-waves station 200st14	156
A.45	P- and S-waves station 200st15	157
A.46	P- and S-waves station 200st18	158

A.47 P- and S-waves station 200st19 . . . . .	159
A.48 P- and S-waves station 200st20 . . . . .	160
A.49 P-waves station 200st21 . . . . .	161
A.50 P- and S-waves station 200st22 . . . . .	162
A.51 P- and S-waves station 200st23 . . . . .	163
A.52 P- waves station 200st25 . . . . .	164
A.53 P- and S-waves station 200st26 . . . . .	165
A.54 P- and S-waves station 200st27 . . . . .	166
A.55 P- and S-waves station 200st28 . . . . .	167
A.56 P- and S-waves station 200st29 . . . . .	168
A.57 P- and S-waves station 200st30 . . . . .	169
A.58 P- and S-waves station 200st31 . . . . .	170
A.59 P- and S-waves station 200st32 . . . . .	171
A.60 P- and S-waves station 200st33 . . . . .	172
A.61 P- and S-waves station 200st34 . . . . .	173
A.62 Seismic reflection data AWI-20120101 . . . . .	174
A.63 Seismic reflection data AWI-20120201 . . . . .	175

# List of Tables

<b>Crustal structure of the Manihiki Plateau</b>	<b>23</b>
5.1 Depth uncertainties intracrustal reflectors . . . . .	29
5.2 Rock densities . . . . .	30
 <b>Plate tectonic reconstruction of Ontong Java Nui</b>	 <b>50</b>
6.1 Paleolatitude Data . . . . .	54
6.2 Margins of Ontong Java Nui . . . . .	62
6.3 Overview on tectonic events . . . . .	69
6.4 rotation poles of Ontong Java Nui . . . . .	72
 <b>Appendices</b>	 <b>110</b>
A.1 Performance of OBS/OBH-stations on profile AWI-20120100 . . . . .	112
A.2 Performance of OBS/OBH-stations on profile AWI-20120100 . . . . .	113
B.1 Plate IDs of the western Pacific . . . . .	176





# 1 Introduction and motivation

## 1.1 Historic and current volcanic activity and their impact on the global environment

Approximately 80 % of the Earth's surface consists of magmatically derived rocks (*Schmincke, 2004*). Most of the volcanic activity is concentrated along plate tectonic boundaries. Oceanic crust is formed at mid-oceanic ridges by a constant production of magma leading to oceanic spreading and the separation of tectonic plates. At convergent plate boundaries, volcanic activity is present at the arc creating mountain ranges such as the Andes or island arcs like the Japanese Islands. Volcanic activity altered not only the shape of the Earth as it creates tectonic plates, but also the climate and the environment. Volcanic eruptions are clear age markers in a variety of proxy reconstructions of the past climate from high-resolution archives such as tree-rings, ice cores and corals (e.g. *Church et al., 2005; Pyle, 1998; Sadler and Grattan, 1999*). The environmental impact of volcanic eruptions can be seen in the geologic and historic records or even our own life span.

In 2010, Europe was kept in suspense by the massive eruptions of the Eyjafjallajökul volcano on Iceland (Fig. 1.1), resulting not only in an interruption of air traffic services, but also in massive increase of fine dust and sulfur concentrations within the atmosphere and on the ground throughout Europe (e.g. *Gudmundsson et al., 2012; Langmann et al., 2012*). Local and regional changes in the atmosphere caused by the eruption ceased within the following months (*Achterberg et al., 2013; Gudmundsson et al., 2012; Langmann et al., 2012*).

A far more dramatic episode of massive volcanic eruptions occurred in Indonesia in the year 1815 (*Briffa et al., 1998; Sadler and Grattan, 1999; Self et al., 2004*). The eruption of the Tambora volcano (Fig.1.1) lead to a decrease in annual summer mean temperatures across Europe of up to 3.5 °C in 1816 and widespread snowfall in North America during the months of July and August 1816 (*Briffa et al., 1998*). This year is often referred to as "Eighteen hundred and frozen to death" or the "year without a summer". The eruption of Tambora volcano was the most severe volcanic episode within historic times. The release of sulfate aerosols to the atmosphere obscured the sky for decades after the initial eruption, reflecting a part of the incoming sunlight (*Self et al., 2004*). This was due to its high volcanic explosivity index (VEI) (7), which is the second highest class on the logarithmic VEI scale. The global extent of the Tambora aerosol cloud can be inferred by the presence of volcanic debris in ice cores from both hemispheres

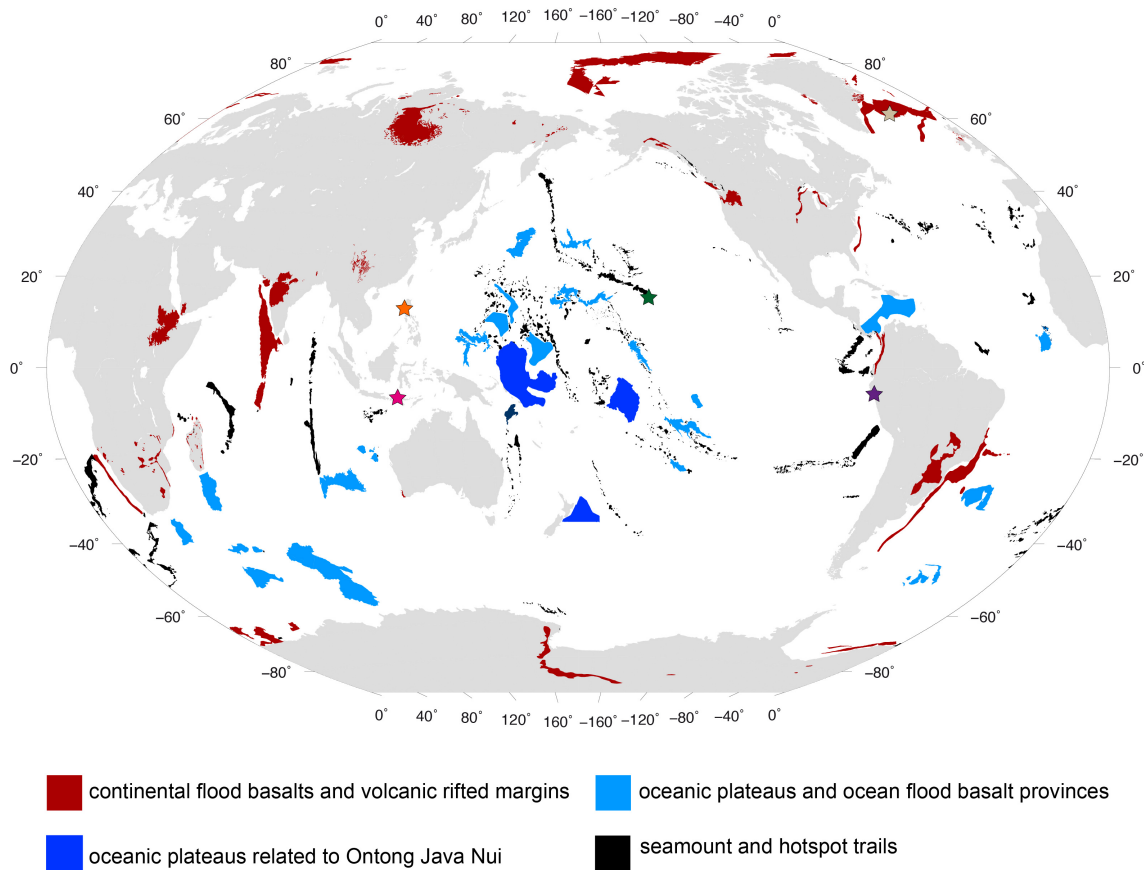


**Figure 1.1:** Overview on the global distribution of Large Igneous Provinces modified after *Bryan and Ferrari (2013)* continental flood basalts and volcanic rifted margins are shown in red, oceanic plateaus and ocean flood basalt provinces are shown in light blue, oceanic plateaus related to Ontong Java Nui are shown in royalblue and seamount and hotspot tracks are shown in black, the position of the locations mentioned in the text are marked with stars: Hawaii hotspot (green), Tambora volcano (pink), Eyjafjallajökul volcano (beige), Huaynaputina volcano (purple) and Pinatubo volcano (orange)

(*Briffa et al., 1998; Self et al., 2004*). The recent eruption of Eyjafjallajökul volcano reached a 4 on the VEI scale, making the eruption of Tambora a thousand times more severe. Over the decade following the Tambora eruption, the global mean temperature was reduced by 0.6 °C (*Briffa et al., 1998; Sadler and Grattan, 1999*). The massive eruption of a single volcano such as Tambora, but also for example of Huaynaputina (Peru) (VEI 6) (*De Silva and Zielinski, 1998*) and most recently the Pinatubo volcano (Phillipines) (VEI 6) (*Church et al., 2005; Self et al., 2004*) lead to a distortion of the global environment. The deposition of volcanic ash endangers flora and fauna over great distances, additionally to the global acid and aerosol fallout. Oceans in the vicinity of the erupting volcano can become anoxic and therefore hazardous to inhabit. The emplacement of volcanic particles into the atmosphere leads to the reduction of solar radiation on the ground, thus cooling the Earth.

Those are eruptions that occur in short time intervals, changing the environment for decades, but their environmental impact, as severe as it seems from the human perspective, is just a

blink of the eye of the eruption of a Large Igneous Province (LIP).

## 1.2 Large Igneous Provinces - massive volcanic eruptions shaping the face of Earth

Large Igneous Province formation is coupled to the third major variety of volcanism on Earth, the intra plate volcanism (Fig. 1.2). The most prominent example for intraplate volcanism is the Hawaiian Islands (Fig. 1.1). The Emperor/Hawaii volcanic chain has been active since the Late Cretaceous or even earlier (Wilson, 1965).

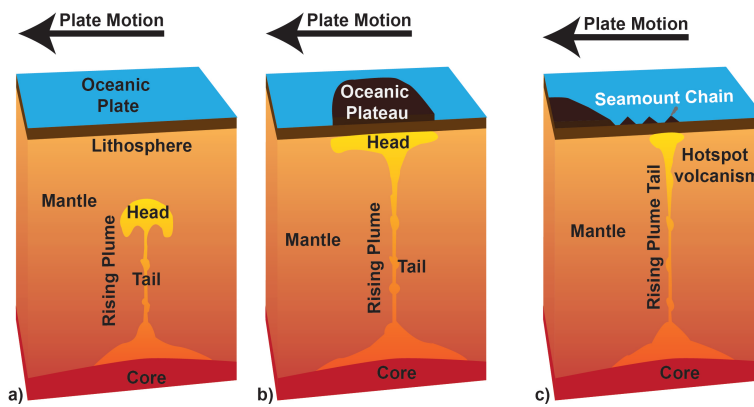


**Figure 1.2:** Different stages of a mantle plume a) mantle plume rising through the mantle b) creation of an oceanic plateau/Large Igneous Province above a surfacing plume head c) hotspot volcanism initiated by a plume tail

The formation of volcanic chains by a hotspot can be related to the presence of a mantle plume (Fig. 1.2). A mantle plume rises from the core-mantle boundary through the mantle to the lithosphere as a mushroom-shaped head followed by its tail (e.g. Griffiths and Campbell, 1990; Richards et al., 1989). The surfacing of the plume head is believed to be the cause of massive volcanic eruptions reshaping and over-

printing large areas in the marine and the continental realm (Coffin and Eldholm, 1993, 1994). Most LIPs are of a mafic to ultramafic composition such as the Deccan Traps in India or the Kerguelen Plateau (Indian Ocean), but also a small number of silicious LIPs exist such as the Sierra Madre Occidental in North America (Fig. 1.1) (Bryan and Ernst, 2008). To differentiate between LIPs and other volcanic formations such as seamounts, the following definition of Large Igneous Provinces was put forward by Bryan and Ernst (2008), which is based on earlier works by Coffin and Eldholm (1994).

*“Large Igneous Provinces are magmatic provinces with areal extents  $> 0.1 \text{ Mkm}^2$ , igneous volumes  $> 0.1 \text{ Mkm}^3$  and maximum lifespans of  $\approx 50 \text{ Myr}$  that have intraplate tectonic settings or geochemical affinities, and are characterized by igneous pulse(s) of short duration ( $\approx 1\text{--}5 \text{ Myr}$ ), during which a large proportion ( $>75\%$ ) of the total igneous volume has been emplaced.”*

This broad definition also includes volcanic rifted margins (e.g. North Atlantic) and Archean Greenstone Belts (e.g. South Africa) (Fig. 1.1) (Bryan and Ernst, 2008). In this dissertation, I will

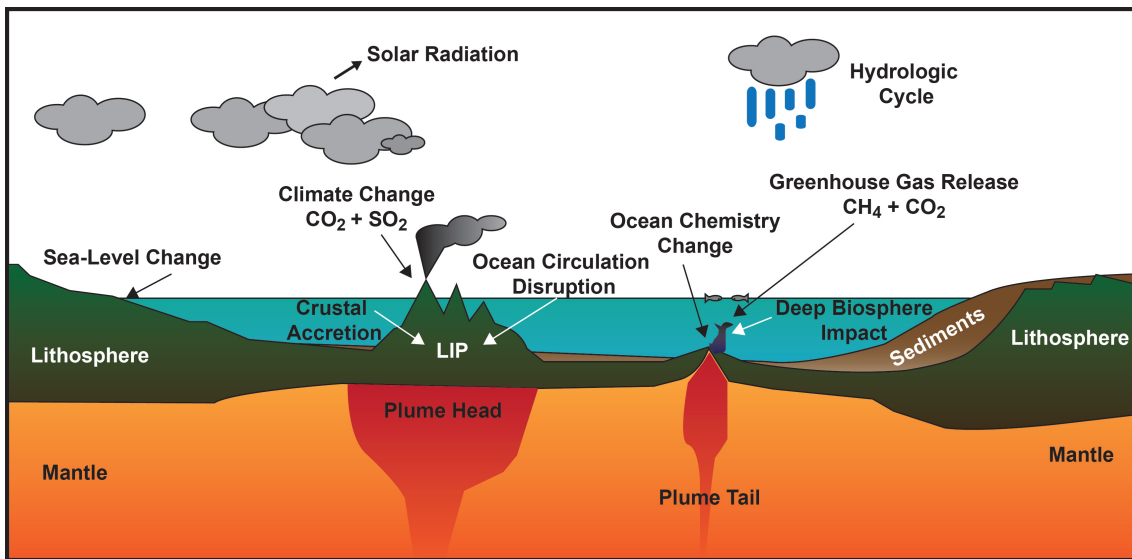


**Figure 1.3:** Impact and consequences of LIP emplacement on the environment modified after *Neal et al. (2008)*

focus on the LIPs of the marine environment, with a special focus on the Pacific Ocean and the LIPs of the Ontong Java Nui event (Fig. 1.1). The oceanic LIPs can be divided into oceanic plateaus such as the Kerguelen Plateau and the LIPs of Ontong Java Nui and ocean basin flood basalts such as the Nauru Basin north of the Ontong Java Plateau (*Bryan and Ernst, 2008*).

Massive volcanic eruptions have of course a tremendous impact on the global environment (Fig. 1.3). The historic volcanic eruptions mentioned above provide a first insight in the complex interplay of volcanic activity and the environment. LIPs form over millions of years and experience an episodic, pulse-like magmatic activity, which peaks in the first 1-5 Ma of the LIP emplacement (*Bryan and Ernst, 2008; Karlstrom and Richards, 2011*). Therefore, LIPs can be linked to radical changes in the global environment such as mass extinction events (e.g. *Sobolev et al., 2011; Wignall, 2005, 2001*). The presence of chalcophile elements (Cu, Au, Ag) within the LIP magmas make them economically attractive for mining, especially if they are obducted onto a continent (*Rosenbaum et al., 2005*)

The release of magmatic volatiles (e.g.  $\text{CO}_2$ ,  $\text{SO}_2$ ) can lead to the depletion of oxygen from the oceans resulting in a biological crisis due to oceanic anoxic events (OAE) (Fig. 1.3). *Tejada et al. (2009)* link samples from the lower Aptian Selli-Level in central Italy, identified as OAE1a, to the initial eruption of the Ontong Java Plateau by using marine Os-isotope ratios ( $^{187}\text{Os}/^{188}\text{Os}$ ). The global occurrence of this event highlights the dramatic changes invoked by a LIP. The content of greenhouse gases within the atmosphere increases, leading to a perturbation of the atmosphere and ocean chemistry (Fig. 1.3). The build-up of the oceanic LIP causes the disruption of the previously established ocean currents and initiates sudden sea level rises (Fig. 1.3).

Additionally, LIPs influence the tectonic behavior of oceanic plates (*Cloos, 1993*). While a 8 km



thick normal oceanic crust subducts easily at a trench, extremely overthickened crust ( $>30\text{km}$ ) can cause the choking of the subduction zone as observed at the Ontong Java Plateau (Mann and Taira, 2004; Taira *et al.*, 2004). Other oceanic plateaus subducted below the continental crust, but cause the build-up of orogens. This is mainly triggered by the phase conversion between basalt and eclogite as it can be observed for the counterpart of the Shatzky Rise and the evolution of the Laramide orogeny (Liu *et al.*, 2010).

This short overview highlights the impact of LIPs on the global environment. Before we can quantify the environmental relevance of LIPs, it is important to understand the nature of their emplacement and further evolution. In the western Pacific a particular interest lays in the interaction between the different LIPs of the area and their tectonic connection. In this thesis I will contribute to our understanding of the emplacement and evolution of a LIP. The main focus is on the crustal structure and the tectonic behavior of the different parts of an oceanic plateau, which can be used as the base of further studies towards understanding the impact of LIPs on the global environment.

### 1.3 The Manihiki Plateau and the LIPs of Ontong Java Nui

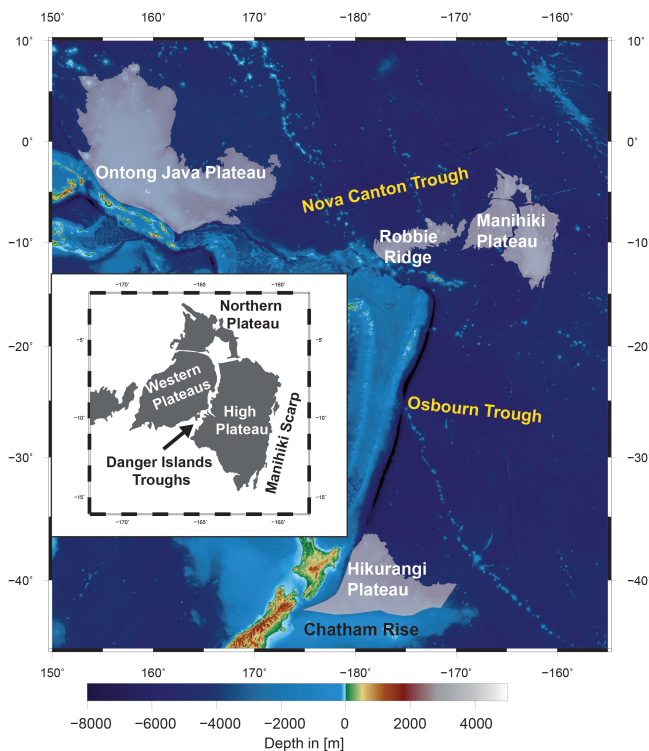


**Figure 1.4:** Bathymetric map of the western Pacific, LIPs of Ontong Java Nui are shaded in white, former spreading centers are marked in yellow, the inlet figure shows a close-up of the Manihiki Plateau

The three largest LIPs of the western Pacific are the Ontong Java Plateau, the Hikurangi Plateau and the Manihiki Plateau (Fig. 1.4), which are believed to have emplaced together as the Super Large Igneous Province Ontong Java Nui during the early Cretaceous (Taylor, 2006) and separated shortly afterwards (Chandler *et al.*, 2012, 2013; Davy *et al.*, 2008; Larson *et al.*, 2002; Taylor, 2006; Viso *et al.*, 2005).

This proposed Super-LIP covered approximately 1% of the Earth's surface during the early Cretaceous. The Manihiki Plateau is the centerpiece of this Super-LIP (Chandler *et al.*, 2012; Taylor, 2006) and therefore should show the evidence of the break-up at all its margins.

Approximately 800 m of sedimentary strata ranging from volcaniclastic material in the deeper layers to calcareous ooze in the upper layers are present on

the plateau (Ai *et al.*, 2008; Winterer *et al.*, 1974). The thickness of the igneous crust is estimated to be about 3.1 times thicker than normal oceanic crust (Hussong *et al.*, 1979), which typically is about 8 km thick. The initial magmatism on the Manihiki Plateau was of tholeiitic nature and occurred approximately between 125 Ma and 110 Ma (Hoernle *et al.*, 2009, 2010; Ingle *et al.*, 2007; Timm *et al.*, 2011). Later alkalic volcanism also referred to as the seamount stage is present between 110 Ma and 43 Ma (Hoernle *et al.*, 2009). An older third stage of magmatic activity forming the nucleus of the plateau can be revealed by seismic reflection data (Pietsch and Uenzelmann-Neben, 2015) and is possibly older than the oldest dated dredge samples.

The Manihiki Plateau is fragmented in multiple sub-provinces: the High Plateau, the Western Plateaus and the Northern Plateau (Fig. 1.4) (Winterer *et al.*, 1974). Gravimetric, reflection, and refraction seismic evidence suggests the former presence of further sub-provinces to the North and the East of the Manihiki Plateau (Pietsch and Uenzelmann-Neben, 2015; Viso *et al.*, 2005). The reason for this fragmentation is currently unknown, but multiple authors (e.g. Davy *et al.*, 2008; Nakanishi *et al.*, 2015; Taylor, 2006) relate the presence of deep troughs such as the Danger Islands Troughs (Fig. 1.4) to the proposed break-up of Ontong Java Nui or the presence of former spreading centers. The break-up of the supposed Super-LIP is not well understood. The separation between the Hikurangi Plateau and the Manihiki Plateau took place at the Osbourn Trough and was finalized with the hard-docking of the Hikurangi Plateau to the continental Chatham Rise at the Gondwana Margin ( $\sim 100$  Ma) (Fig. 1.4) (Billen and Stock, 2000; Davy, 2014; Downey *et al.*, 2007; Worthington *et al.*, 2006). Since there is no clear evidence of a spreading center in the Nova Canton Trough between the Ontong Java Plateau and the Manihiki Plateau (Fig. 1.4), plate tectonic reconstructions have to be achieved by tracing fracture zones (Chandler *et al.*, 2012; Taylor, 2006). The whole separation and integration of Ontong Java Nui took place during the Cretaceous Normal Superchron (CNS) (125 Ma - 83 Ma) (Gee and Kent, 2007). Subsequently, there are no magnetic polarity reversals to guide plate kinematic reconstruction and it is essential to compile all available geological, petrological and geophysical data for plate tectonic reconstructions of the region.

## 2 Research questions

In the following, I provide a condensed overview of the research questions addressed in my dissertation. The prepared manuscripts, which discuss the different topics below, can be found in Chapter 5, Chapter 6 and Chapter 7.

### **Crustal and upper mantle structure of the Manihiki Plateau**

*Winterer et al.* (1974) provided the first insight into the crustal structure of the Manihiki Plateau. Unfortunately, their experiments only revealed data down to the middle crust and no information could be gained on the depth of the Moho or the velocity structure of the lower crust. The Manihiki Plateau is fragmented into sub-provinces, which have been assumed to exhibit a similar crustal structure (*Viso et al.*, 2005). However, gravity anomaly data reveals clear differences between the sub-provinces. Therefore, I investigated the structure of the crust and the upper mantle of the two main sub-provinces of the Manihiki Plateau by refraction/wide-angle reflection seismic experiments.

- *How thick is the crust of the Manihiki Plateau?*
- *Are there differences between the two main sub-provinces, the High Plateau and the Western Plateaus, in crustal thickness and internal structure?*
- *What does the crustal structure imply in regard to the tectonic and magmatic development of the plateau?*

### **The internal fragmentation of the Manihiki Plateau**

The unusual fragmentation of the Manihiki Plateau into multiple sub-provinces lead *Winterer et al.* (1974) and *Taylor* (2006) to interpret the Danger Islands Troughs as an aborted rift system, which separates the High Plateau and the Western Plateaus. *Viso et al.* (2005) postulate a northeastern and an eastern fragment, which were adjacent to the High Plateau of the Manihiki Plateau during its time of emplacement.

- *What tectonic mechanism lead to the formation of the Danger Islands Troughs?*
- *Are there indications for an initial continuation of the Manihiki Plateau towards the East?*

## **The Manihiki Plateau and the proposed "Super" - LIP Ontong Java Nui**

Taylor (2006) proposed the joined emplacement of the three LIPs - Ontong Java, Hikurangi and Manihiki Plateaus - as one single plateau he named Ontong Java Nui. The joined emplacement of the Manihiki Plateau and the Hikurangi Plateau seems to be a well established factor in the literature (Billen and Stock, 2000; Downey et al., 2007; Worthington et al., 2006), but the connection between the Ontong Java Plateau and the Manihiki Plateau is still uncertain, if present at all.

- *Are there indications for a joined emplacement of the Manihiki Plateau and the Ontong Java Plateau?*
- *If the Super-LIP existed, can I provide further constraints on the size, structure and emplacement scenario of Ontong Java Nui?*

## **Plate-tectonic reconstruction of the western Pacific for the Cretaceous Normal Superchron**

The internal fragmentation of the Manihiki Plateau along with the possible presence of sub-provinces to the east and northeast of the High Plateau has so far been ignored by global plate tectonic reconstructions (Seton et al., 2012). Other models, for example by Davy (2014) or Worthington et al. (2006) outline plate tectonic concepts such as the rotation of the Hikurangi Plateau and the existence of a subduction zone at the Wishbone Scarp, but fail to provide plate kinematic reconstructions of the western Pacific within the global context.

- *How did the initial break-up of Ontong Java Nui occur and which role does the Manihiki Plateau play within the break-up scenario?*
- *What constraints can be given for the subsequent dispersal of the LIP across the western Pacific?*
- *What was the ultimate fate of the proposed fragments of the Manihiki Plateau?*

## 3 Datasets, methods and processing

During my dissertation, I modeled refraction/wide-angle reflection seismic data and computed P- wave and S-wave models of two 500 km long profiles, which reveal the crustal structure of the High Plateau and the Western Plateaus of the Manihiki Plateau in the western Pacific. To facilitate the interpretation of the models, I also calculated the Poisson's Ratio and modeled the gravity anomalies of the two main sub-provinces of the Manihiki Plateau. As the final step, I used the newly gained information on the crustal structure to reconstruct the plate motion during the CNS in the western Pacific. In the following, I will outline the different datasets and methods, which I used for the processing and interpretation of the data.

### 3.1 Geophysical Datasets

#### 3.1.1 New geophysical data acquired during the cruise So-224

The project MANIHIKI II (Fig. 3.1) is a cooperation between the Alfred-Wegener-Institut Helmholtz-Zentrum für Polar- und Meeresforschung (AWI) in Bremerhaven (Germany) and the GEOMAR Helmholtz-Zentrum für Ozeanforschung in Kiel (Germany). It was funded by the German Federal Ministry of Education and Research. During MANIHIKI II - Leg 1 (So-224), the AWI collected new geophysical data (Fig. 3.2) aboard the RV Sonne on the Manihiki Plateau (*Uenzelmann-Neben, 2012*). Geological and petrological data was acquired during the subsequent cruise MANIHIKI II - Leg 2 (So-225) by the GEOMAR (*Werner et al., 2013*).



Figure 3.1: Cruise Logo So-224/So-225

During cruise So-224, the AWI recorded two refraction/wide-angle refraction seismic lines (Fig. 3.2), crossing the two main sub-provinces of the Manihiki Plateau along with corresponding reflection seismic profiles to reveal the crustal structure of the Manihiki Plateau and its margins. Those two deep-crustal profiles and the resulting P-wave, S-wave models along with their geological interpretation built the basis of my dissertation. Additionally, 28 reflection seismic lines were

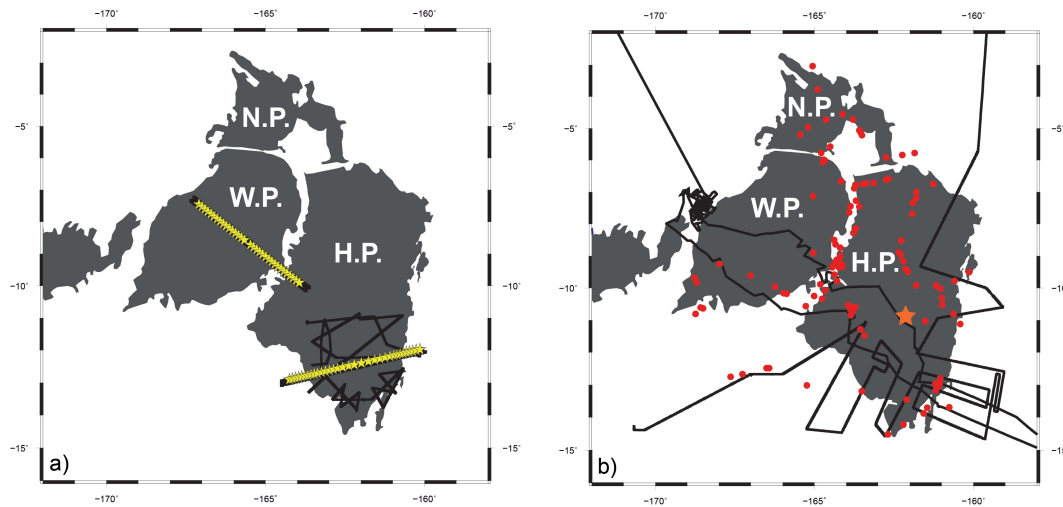


**Figure 3.2:** Overview of the existing and newly acquired data from the Manihiki Plateau; a) data collected during So-224 black thin lines reflection seismic profiles, black thick lines seismic refraction profiles, yellow stars position of OBS/OBH-systems b) pre-existing data black thin lines are single channel seismic reflection profiles, red points indicate rock samples, DSDP leg 33 site 317 is shown by the orange star H.P. stands for the High Plateau, W.P. for the Western Plateaus and N.P. for the North Plateau

recorded on the High Plateau of the Manihiki Plateau (Fig. 3.2), which were processed by R. Pietsch (*Pietsch and Uenzelmann-Neben, 2015*). Bathymetry and sediment echo sounding was recorded throughout the cruise.

### 3.1.2 Pre-existing datasets

In addition to the new datasets from the Manihiki Plateau, I also used multiple pre-existing datasets. Since gravity anomaly data was not recorded during So-224, I reverted to global compilations of gravity data by *Sandwell et al. (2014)* to calculate density models and trace geological lineaments of the oceanic crust. I integrated the bathymetric measurements of So-224 into the global bathymetry grid from GEBCO (2014) (*Weatherall et al., 2015*), to enhance the resolution of the topography within my study area. Magnetic anomaly data was taken from *Maus et al. (2009)*. Additional reflection seismic single channel data was collected by J. Stock and B. Luyendyk during the cruise KIWI Leg 12 on R/V *Revelle* available via <http://www.ig.utexas.edu.sdc> and during the cruise CATO03 presented by *Winterer et al. (1974)* (Fig. 3.2).

Additional to geophysical data from the Manihiki Plateau, rock and sediment samples have been collected from the High Plateau, the margins of the Manihiki Plateau and the internal troughs (Fig. 3.2). Although multiple cruises have been dedicated to the collection of rock samples (e.g. *Clague, 1976; Hoernle et al., 2009, 2010; Ingle et al., 2007; Timm et al., 2011; Werner and Hauff, 2007; Werner et al., 2013*), the coverage with dated rock samples is still sparse (Fig. 3.2) and mainly confined to the deep troughs and the margins of the plateau. The sedimentary column and the uppermost basaltic basement have been drilled by the Deep Sea Drilling



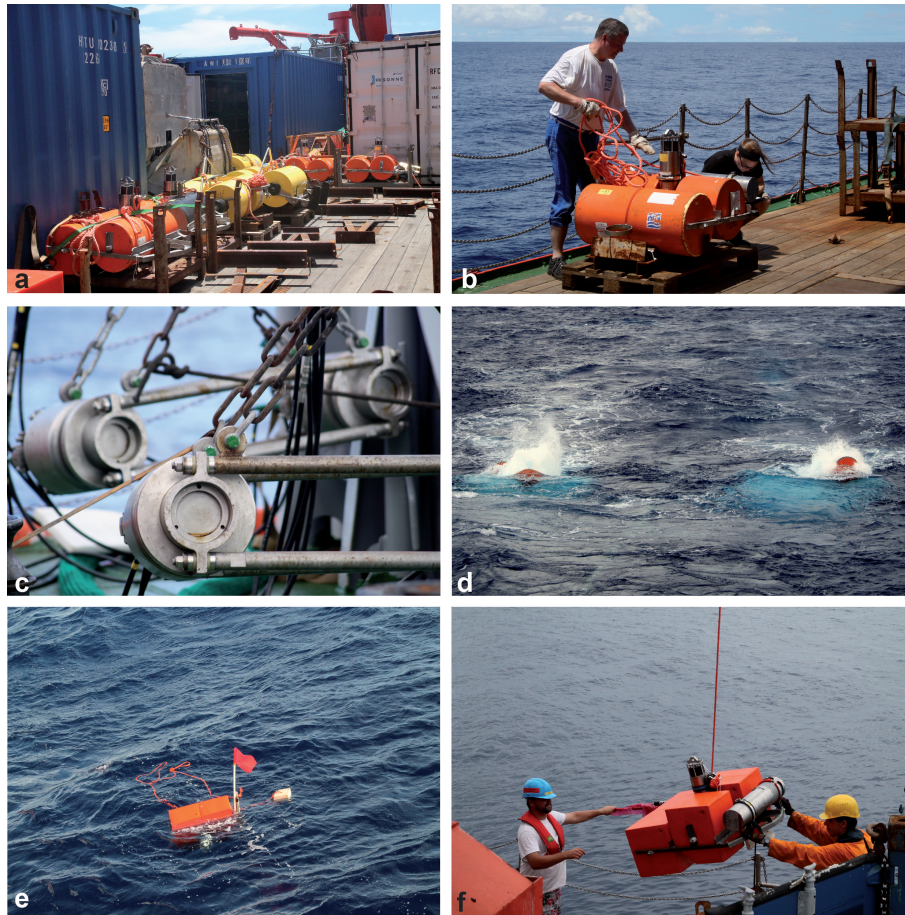


**Figure 3.3:** The steps of refraction seismic profiling at sea; a) OBS assemblage on deck of RV Sonne; b) Preparation for OBS deployment (Photo by J. Grützner); c) G-gun array on deck of RV Sonne (Photo by J. Grützner); d) G-Gun array in use as seismic source (Photo by J. Grützner); e) OBS station floating at sea surface; f) recovery of OBS station

Project (DSDP) Leg 33 Site 317 in 1974 (*Schlanger et al.*, 1976) (Fig. 3.2).

## 3.2 Refraction/wide-angle reflection seismic data

### 3.2.1 Geophysical principle of refraction/wide-angle seismic data

During seismic surveys, the travel-time of seismic waves through the Earth's interior is measured. The seismic wave is emitted at a source and is reflected and refracted at impedance contrasts throughout the subsurface. Receiver units record the arrivals of the different phases of the seismic wave. To image deeper areas of the Earth such as the crust and the upper mantle, the offset between the source and the receiver has to be larger than if the goal is a detailed study of the sedimentary column. For a marine survey, the seismic source is also towed behind the vessel. The receiver units are either a streamer unit, which is as well towed or ocean bottom seismometer stations, which are placed on the seafloor before the data acquisition starts.

After the vessel and therefore the seismic source passed the receiver stations on the seafloor, the stations are contacted and rise to the sea surface to be picked up by the vessel. Detailed information on the experimental set-up of the data used in this dissertation is provided in the following section 3.2.2.

### 3.2.2 Data acquisition during So-224

The data was acquired during the RV Sonne cruise So-224, which started on the 11th of October, 2012 in Suva (Fiji) and ended on the 17th of November 2012 at the same port (*Uenzelmann-Neben, 2012*). The seismic refraction data was recorded on 33 stations on each of the two profiles crossing the two largest sub-plateaus of the Manihiki Plateau. We used 28 Ocean Bottom Seismometer (OBS) stations (Figs. 3.3 and 3.4) and five Ocean Bottom Hydrophone (OBH) stations (Fig. 3.5).

The stations consist of synthetic foam floats mounted on a steel frame (Figs. 3.3, 3.4 and 3.5). An anchoring weight is fixed to the frame via an acoustic/time release unit (type KUMQuat or type IXSEA) to allow the descent of the station to the seafloor. For recording the seismic activity, OBS stations were equipped with a 3-component (4.5s natural period) seismometer and a hydrophone. OBH stations are only equipped with a hydrophone. The recorded data is stored by a seismic data logger (MBS, MLS or MTS-type), which was placed in a pressure cylinder along with a battery pack. The deployment spacing was kept at 14.1 km for profile AWI-20120100 and ranged from 24.1 km to 10.9 km on profile AWI-20120200 to ensure a better data coverage for the margins of the plateau (Fig. A.1).

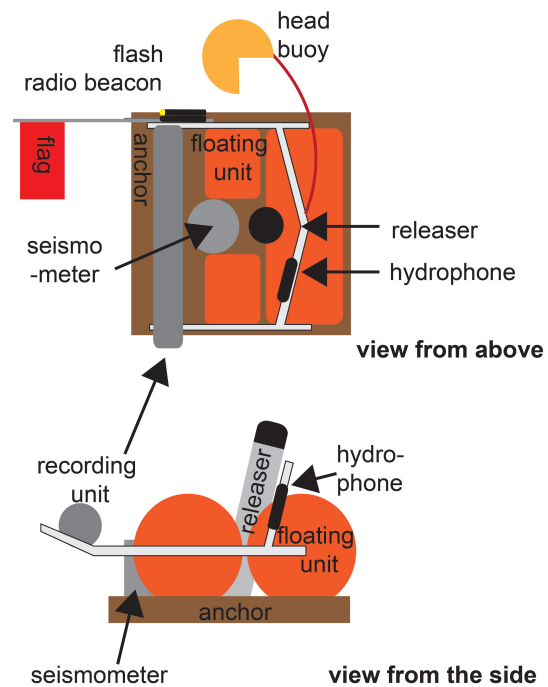


**Figure 3.4:** Sketch of OBS from above and the side

The seismic source used during the seismic refraction experiments were an array of 8 G-Guns (8.5 liters/520 in<sup>3</sup> volume each) with a total volume of 68 liters or 460 in<sup>3</sup> (Fig. 3.3c). The array was towed in 4 x 2 clusters at a water depth of 10 m behind the vessel. The seismic signal was initiated every full minute at 210 bar (Fig. 3.3d). Multichannel seismic reflection data was also collected for the OBS/OBH profiles with the 3000 m long 240-channel hydrophone array streamer (SERCEL SEAL<sup>TM</sup>).



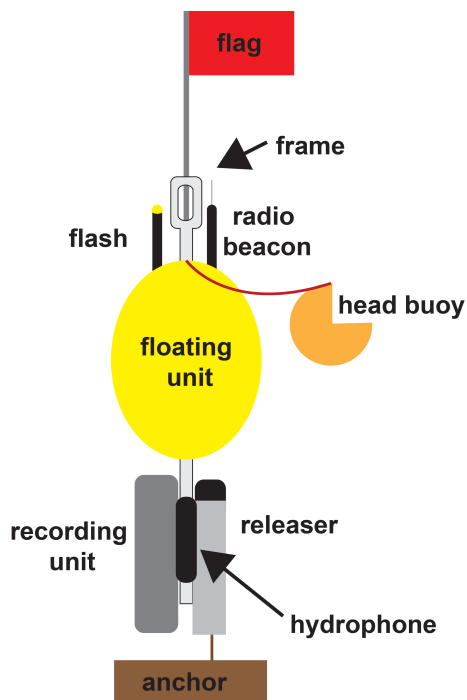


Figure 3.5: Sketch of an OBH station

After the data acquisition the releaser units were triggered acoustically and by unlocking from the anchor weight the station rose to the surface, where it was located and picked up by the vessel (Fig. 3.3e-d). To facilitate the localization, all stations were equipped with a radio and a light signal.

The onboard processing of the refraction seismic data consists of multiple steps, which I will briefly outline below. Navigational data was obtained and reformatted to fit the format requirements given by the program "send2x" (SEND GmbH). The raw data was downloaded from the data storage units. "send2x" demultiplexed the data and corrects the shift of the internal clock of the OBS/OBH-systems. This resulted in four SEGY-files for the OBS-stations and a single file for the OBH-stations. Since the stations may drift during the decent to the seafloor and the ascent to the surface due to

ocean currents, the stations have to be re-located. To correct for this offset, the direct water wave was picked and the difference between the initial deployment coordinate and the first direct water wave arrival was added or subtracted to the data. A first quality control was also carried out during the cruise (Uenzelmann-Neben, 2012).

Data quality was in general very good. Unfortunately, two stations did not record data on profile AWI-20120100 and four stations failed on profile AWI-20120200. Almost all stations show P-wave arrivals of the lower crust and the upper mantle. S-wave arrivals can be observed throughout the profiles for the upper and middle crust. The lower crust and the upper mantle are poorly resolved by S-wave arrivals. For a better overview on the performance of the deployed stations see A.2 in the Appendix. A map of the deployment positions is also provided (Fig. A.1).

### 3.2.3 Modeling of P- and S-wave arrivals

The modeling of P-wave and S-wave velocities was carried out using a standard ray-tracing method implemented in "rayinvr" (Zelt and Smith, 1992). Forward modeling is a widely used technique for refraction/wide-angle reflection data (e.g. Altenbernd et al., 2014; Fromm et al., 2015; Mechie et al., 2009; Mjelde, 2005; Mjelde et al., 2001) and I will only briefly provide the main aspects here. For phase identification and the subsequent picking of the arrivals, I used the software "ZP" (Zelt, 2004). For most stations, the hydrophone channel supplied the most reliable data and was therefore used for the analysis (see A.2). For S-wave identification the horizontal components were also used, but proved to include more noise and internal re-

vibrations than the data collected with the hydrophone. The traveltimes of the different crustal and sedimentary layers are picked and saved with an identifier referring to the specific layer. Within the seismogram, reflected phases appear as hyperbolas, refracted phases are straight to slightly bent (Fig. 3.6). The apparent seismic velocity of the layer is the inverse of the slope.

This picked arrival times were then integrated into a model of the velocity structure of the crust (Fig. 3.6). Since P-wave arrivals are more commonly observed and better constrained, I first obtained the P-wave velocity models for both profiles. I use the software "*rayinvr*" (Zelt and Smith, 1992) for the forward modeling and the graphical interface "*PRay*" (Fromm, 2012), which greatly facilitates the modeling procedure. The initial starting model included the bathymetric measurements acquired during So-224 (Uenzelmann-Neben, 2012), basement reflections from seismic reflection data (Pietsch and Uenzelmann-Neben, 2015) and the crustal structure revealed within the 1-D profiles calculated at the OBS/OBH stations. The position of the OBS/OBH was confirmed by the modeling of the arrival direct water wave. P-wave velocities were assigned manually to each layer from the sedimentary layers to the upper mantle. The P-wave velocities of the sediment layer are in good agreement with the velocities obtained from the reflection seismic data (Pietsch and Uenzelmann-Neben, 2015). The internal structure of the crust is modeled by the interplay of reflections from boundary layers and the nature (direct, reflected, refracted) of the phases. To enhance the model, "*rayinvr*" provides an inversion algorithm. I ran this inversion for selected areas and layers within the model. This algorithm also provides statistical information on the resolution and variability of the model. In order to compare the P-wave and S-wave model I calculated the S-wave model with the same layer distribution (depth nodes) and the same position of the velocity nodes within the model. This also allowed the calculation of the Poisson's ratio ( $\sigma$ ). The calculated P- and S-wave

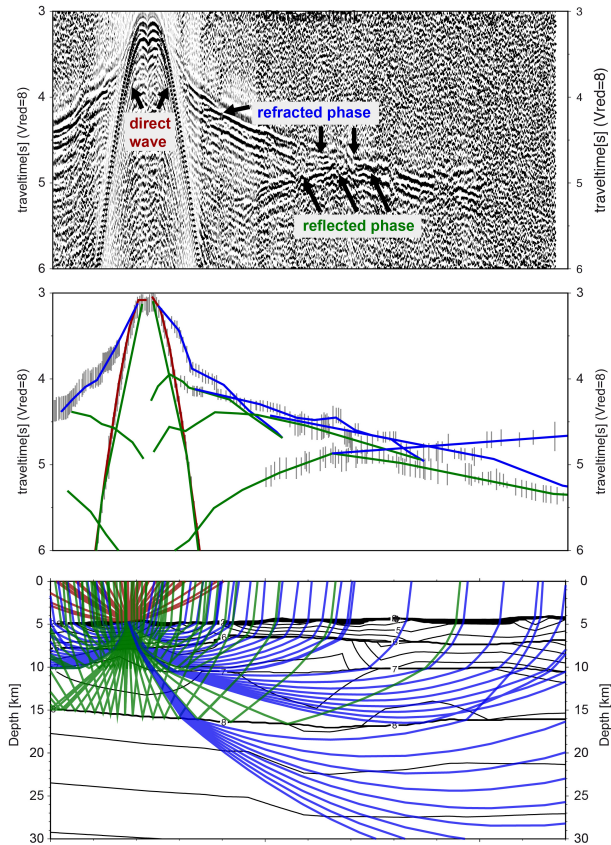


**Figure 3.6:** Example of refraction seismic data top panel seismogram of Station 1 of AWI-20120100 (hydrophone channel), middle panel resulting P-wave model with ray paths (red - direct wave, blue - refracted phase, green - reflected wave), bottom panel picked (thin grey lines) and modeled arrival times

internal structure of the crust is modeled by the interplay of reflections from boundary layers and the nature (direct, reflected, refracted) of the phases. To enhance the model, "*rayinvr*" provides an inversion algorithm. I ran this inversion for selected areas and layers within the model. This algorithm also provides statistical information on the resolution and variability of the model. In order to compare the P-wave and S-wave model I calculated the S-wave model with the same layer distribution (depth nodes) and the same position of the velocity nodes within the model. This also allowed the calculation of the Poisson's ratio ( $\sigma$ ). The calculated P- and S-wave

models are presented in Chapter 5 along with their geological interpretation.

### 3.2.4 Calculation of the Poisson's ratio ( $\sigma$ )

The calculation of the Poisson's ratio ( $\sigma$ ) allows to differentiate rock types. Since the most common rocks within the crust have similar P-wave velocities, the relation to the S-wave velocities can give further indication on the petrological components and the degree of metamorphism, which the rock experienced (*Christensen, 1996*). It allows the differentiation between felsic and mafic rocks as shown by *Grobys et al. (2007)* for the Bounty Trough area offshore New Zealand and the estimation of for example the Mg/Fe ratio within the gabbroic crust (*Mjelde, 2005*). With regards to an LIP the main questions to tackle with the Poisson's ratio ( $\sigma$ ) are to identify possible areas of serpentinization (serpentinite  $\sigma = 0.34 - 0.35$ ; gabbro  $\sigma = 0.29$  (*Christensen, 1996*)) and possibly to recognize changes within the petrology (Fe/Mg-ratio, alkalic and tholeiitic emplacement phases). The Poisson's ratio is calculated by:

$$\sigma = 0.5 \frac{(v_p/v_s)^2 - 2}{(v_p/v_s)^2 - 1}$$

The program package "*rayinvr*" includes a subroutine to convert the P-wave and S-wave velocity models into a model displaying the Poisson's ratio ( $\sigma$ ). Since the S-wave model of AWI-20120100 was restricted to the upper crust, I only present the model calculated for AWI-20120200 (see Chapter 5).

## 3.3 Modeling of gravity anomaly data

To verify and constrain areas of the models with low ray-coverage, I calculated gravity anomaly models of both seismic refraction profiles. I obtained the gravity anomaly data from the global gravity anomaly grid by *Sandwell et al. (2014)*, since there was no gravity data recorded during the cruise So-224. The P-wave velocities obtained by ray-tracing have been converted into blocks of specific densities (*Barton, 1986; Hamilton, 1978*). Modeling of the gravity model was done with "*IGMAS*" (*Götze et al., 2002*). To assure a good comparability between the two methods, I kept the layer boundaries identified within the P-wave velocity model fixed and separated areas of denser or lighter material as additional blocks within the model. The gravity anomaly modeling supports the assumed crustal thickness of the sub-provinces as well as the strong variations within the upper crust of the Western Plateaus. In general, I can report a good fit between the P-wave model and the gravity anomaly data. The misfit ranges between 3.6 mgal and 2.4 mgal. Information on the crustal structure gained by the calculation of the Poisson's ratio ( $\sigma$ ) was also included into the gravity model for example in regard to the possible areas of serpentinization.

### 3.4 Plate kinematic model with "GPlates"

After revealing the crustal structure of the Manihiki Plateau, I prepared plate kinematic models with the software "GPlates", which is an open-source software published and maintained by the Earthbyte Project at the University of Sydney, the Division of Geological and Planetary Sciences at CalTech, the Geodynamics Group at the Geological Survey of Norway and the Centre of Earth Evolution and Dynamics at the University of Oslo. "GPlates" can be downloaded via [www.gplates.org](http://www.gplates.org). "GPlates" allows to perform regional plate kinematic reconstructions and embed them into a global context.

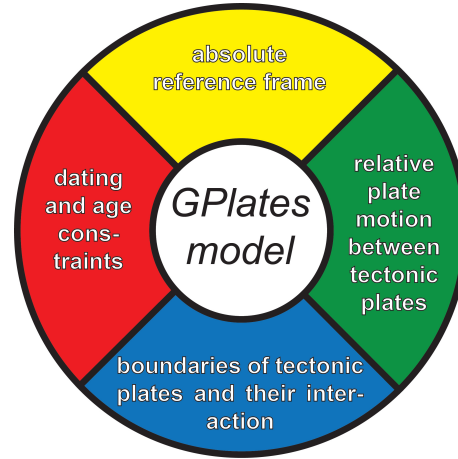


Figure 3.7: "GPlates"-philosophy

It also combines the advantages of a geographical information system with plate kinematic reconstructions, allowing a wide variety of data types. A number of tutorials and datasets can be downloaded along with the software. A deeper insight into the "'GPlates'-philosophy" is provided in various publications such as *Boyden et al. (2011)*.

In the following sections, I will briefly outline the possibilities "GPlates" offers for plate kinematic reconstructions and will focus on the techniques I used for the reconstruction of the western Pacific, which is presented in Chapter 6 and 7.

#### 3.4.1 Global plate kinematic models with "GPlates"

In general, plate kinematic reconstructions performed with "GPlates" are based on four main components: the absolute reference frame, the relative plate motion between the plates, information on the age and timing of the motion and the different plate boundaries (Fig. 3.7). Those corner stones of plate kinematic reconstruction are described in further detail below. For easier identification, Plate IDs are attributed to tectonic plates. These IDs are selected to represent the tectonic realm in their first integer (e.g. Africa - 7 or Pacific - 9). I used the PlateIDs established by the "GPlates" community (*Seton et al., 2012*) and added individual PlateIDs for newly added independent plates (Tab. B.1).

##### Absolute reference frame

The absolute reference frame chosen for the reconstruction is the base of global plate motion and shows the relative motion of the tectonic plates to a fixed reference frame such as a stationary or moving hotspot reference frame or a deep mantle reference frame. Hotspot reference frames include the assumption, that the hotspots of the Atlantic/Indian Oceans and Pa-

cific Ocean are stationary features in the geological environment throughout time, and hotspot trails such as the Hawaiian/Emperor chain are a direct measurement of the plate movement. Because the hotspots experience a motion between each other, recent plate tectonic models use a moving hotspot frame (e.g. *O'Neill et al.*, 2005). For the Pacific realm *Wessel and Kroenke* (2008) proposed an absolute plate motion path for reconstructions starting as far back as 145 Ma, which is the oldest seamount age found on the Pacific Plate. Plate tectonic reconstructions dealing with time frames older than 145 Ma have to refer to a paleomagnetic absolute plate reference system (*Torsvik et al.*, 2008). Such a deep mantle reference frame is based on paleomagnetic data obtained and reconstructed to the rocks initial emplacement region.

The main area of interest in my plate kinematic reconstruction lays in the Pacific Ocean, therefore I used a fixed Pacific Hotspot reference frame (W&KO8-G) (*Chandler et al.*, 2012), which is based on the Pacific hotspot reference frame by *Wessel and Kroenke* (2008). Since the plate kinematic reconstruction by *Chandler et al.* (2012) is the most recent reconstruction of the LIPs of the western Pacific, using the same hotspot reference frame facilitates the comparison between our models.

### Relative motion between tectonic plates

Relative motion between two tectonic plates can be reconstructed by a wide variety of geophysical and geological data. The initial emplacement latitude of magmatic rocks can be calculated along with the declination. Seafloor spreading anomalies within the oceans allow mapping the position of the spreading axis between two tectonic plates at a specific time. Magnetic anomaly data, along with their identification and interpretation can be obtained via the marine magnetic database (*Seton et al.*, 2014). By matching of magnetic anomalies areas of the same age and therefore the same time of emplacement along a mid oceanic ridge are connected. Other seafloor features such as fracture zones (*Matthews et al.*, 2011) can help tracing plate motion. "GPlates" allows the user to chose a point on a plate and trace its motion path throughout the reconstruction. I used this feature to track fracture zones and hotspot tracks.

The motion of plates can be expressed as the rotation of the plate around an axis with a specific angle (Euler's Displacement Theorem). *Seton et al.* (2012) present the most current compilation of global rotation poles integrated into a worldwide plate kinematic reconstruction. The motion of tectonic plates is based on a tree-like hierarchy system within "GPlates". At the top of the hierarchy is the anchored plate, which can be chosen individually regarding the specific research question at hand. All following plates move at a relative rotation to the anchored plate or a plate of higher rank (Fig. 3.8). The anchored plate is most commonly either the hotspot reference frame or the African craton (Fig. 3.8). Since the Pacific Ocean is decoupled from the African continent before the opening of the Bellingshausen Sea (e.g. *Dobrovine and Steinberger*, 2012; *Dobrovine and Tarduno*, 2008; *Seton et al.*, 2012), I choose to use the Pacific Plate as the anchored plate in my models.

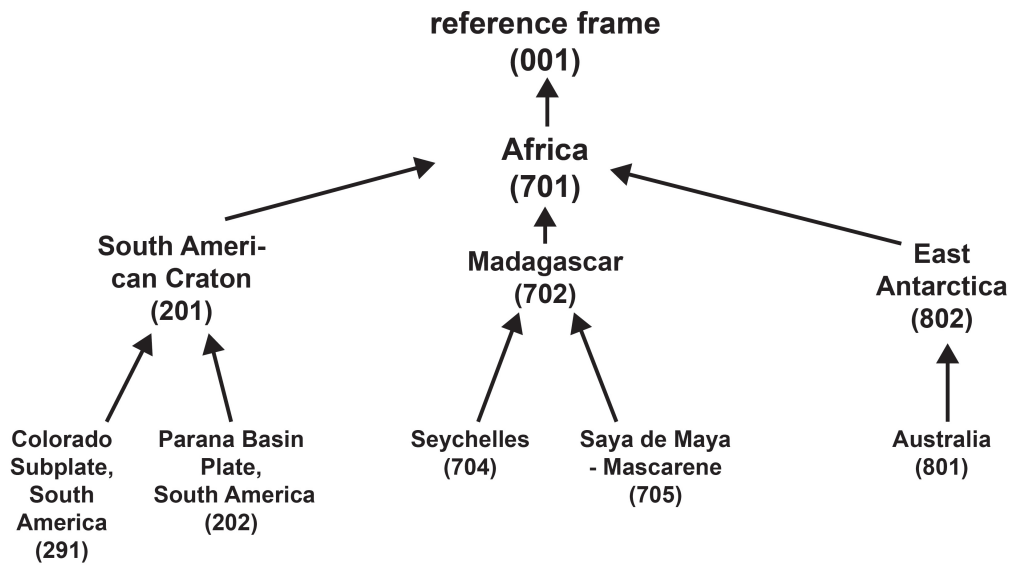


**Figure 3.8:** Example for rotation hierarchy based on the tectonic plates of highest rank from *Seton et al.* (2012) and their Plate IDs. Arrows indicate a relative motion of the lower plate to the upper plate (e.g. Australia (801) moves relative to Antarctica (802), which moves relative to Africa(701))

### Dating and age constraints

After establishing the motion between the different plates it is equally important to constrain the time frame, in which the motion took place. The most recent geological time scale based on magnetic field reversals has been published by *Gee and Kent* (2007). Magnetic anomalies of the seafloor can be related to the described magnetic pole reversals and therefore provide a time frame for the tectonic movement. Since magnetic field reversals are absent within the Cretaceous Normal Superchron (CNS) - the main time frame of the presented study - the seafloor anomalies cannot be used for the reconstruction. During this time *Granot et al.* (2012) identified undulations of the magnetic field offshore northern Africa. Between 110 and 100 Ma, the magnetic field became highly fluctuating. The variability subdued between 90 Ma and 83 Ma. Therefore the CNS can be subdivided in three time periods. This rough estimation may give a better insight into the plate tectonic behavior regarding spreading rates at the mid-oceanic spreading centers, for example. Unfortunately such undulations were not observed within the Pacific Ocean due to the high magmatic activity in the area. Another option to date plate motion is by identifying sudden reorientations (kinks) within fracture zones (*Matthews et al.*, 2012). Dated rock samples from the oceanic crust are rare, but allow the relatively precise identification of emplacement age of the crust. Additional to the dated samples I used major tectonic events such as the collision of the Hikurangi Plateau and the Chatham Rise (*Davy*, 2014), as a time constraint.

### Boundaries of tectonic plates and their interaction

Tectonic plates are changing their appearance and especially their boundaries over geological timescales. Therefore, it is important to let the plates to grow due to spreading or rifting and shrink due to subduction or collision. "*GPlates*" uses continuously closed boundaries (Gurnis *et al.*, 2012), which allows the user to produce a plate kinematic reconstruction without gaps or unwanted overlaps between the plates. I used this feature for oceanic plates throughout the reconstruction, which allows the changeover between different plate boundaries for example from a subducting margin at the Chatham Rise offshore New Zealand to a passive margin (e.g. Davy, 2014). Continental cratons and areas of overthickened oceanic crust such as LIPs can be incorporated into continuously closing plates or even deform for example due to extension as a individual closing plate.

#### 3.4.2 Calculation of new rotation poles for the western Pacific

The plate motion of the western Pacific during the CNS is difficult to constrain, since paleomagnetic reversals are absent. The motion of the plates along with the timing has to be achieved

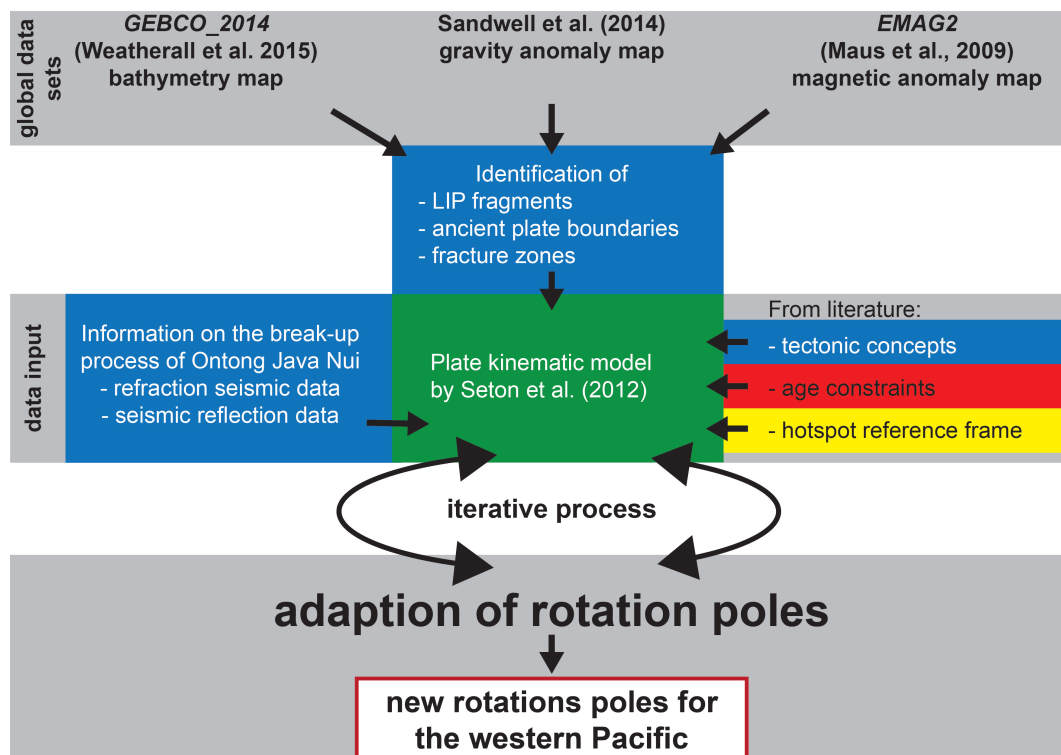


Figure 3.9: Workflow of plate kinematic reconstructions of the western Pacific using "*GPlates*"

by other means than magnetic polarity reversals. Fig. 3.9 illustrates the used data sets and further constraints included into the model. To allow a full comparability and seamless transition from the updated rotation poles between 125 Ma and 80 Ma, the rotation poles published by

*Seton et al.* (2012) were used for the surrounding plates as well as the updated rotation poles for the separation between Zealandia and Marie Byrd Land (*Wobbe et al.*, 2012). After including all available age constraints, I also included tectonic concepts (e.g. *Davy*, 2014; *Worthington et al.*, 2006), which have previously not been modeled from the kinematic point of view. The most important addition to the current model of the western Pacific, is the detailed analysis of the break-up of the "Super"-LIP Ontong Java Nui which revealed multiple microplates and multiple short-lived spreading centers. During the modeling the different rotation parameters were changed interactively in "*GPlates*". The development of a satisfying model includes several iterations to re-evaluate and compare the produced model to the geological evidence. For example, I traced the plate motion and plate velocity along spreading centers throughout the models time frame and compared the outcome of the model to fracture zones. Spreading rates were compared to literature values and the seafloor fabric.



## 4 Contributions to scientific journals

During my dissertation, I prepared three manuscripts as first author, which are presented in Chapters 5 to 7.

### **Multiphase magmatic and tectonic evolution of a Large Igneous Province - evidence from the crustal structure of the Manihiki Plateau, western Pacific**

*K. Hochmuth<sup>1</sup>, K. Gohl<sup>1</sup>, G. Uenzelmann-Neben<sup>1</sup> and R. Werner<sup>2</sup>*

<sup>1</sup>*Alfred-Wegener Institut Helmholtz-Zentrum für Polar- und Meeresforschung*

<sup>2</sup>*GEOMAR Helmholtz-Zentrum für Ozeanforschung*

The manuscript is currently in revision at the *Geophysical Journal International*.

In this paper, the crustal structure of the two main sub-provinces of the Manihiki Plateau is revealed for the first time based on the newly acquired geophysical data. The data shows significant differences between the High Plateau and the Western Plateaus, which lead to the conclusion that secondary volcanism was of lower volume at the Western Plateaus and the crust was severely stretched by the break-up of Ontong Java Nui.

I calculated the P-wave, S-wave and density models, prepared all figures and wrote the manuscript. K. Gohl supervised the work and was the leader of the OBS-Team during So-224. G. Uenzelmann-Neben was Chief Scientist on So-224, leads the AWI-portion of the project MANIHIKI II, supervised the processing of the seismic reflection data and processed parts of the seismic reflection data. R. Werner was Chief Scientist on So-225, as well as the main coordinator of the project MANIHIKI II. He assisted with the petrological interpretation of the data. All authors revised the manuscript and contributed to the discussion.

## Playing jigsaw with Large Igneous Provinces - a plate tectonic reconstruction of Ontong Java Nui

K. Hochmuth<sup>1</sup>, K. Gohl<sup>1</sup> and G. Uenzelmann-Neben<sup>1</sup>

<sup>1</sup>*Alfred-Wegener Institut Helmholtz-Zentrum für Polar- und Meeresforschung*

The manuscript has been published with *Geochemistry, Geophysics, Geosystems* in 2015.

The margins of the Manihiki Plateau provide valuable information on the break-up of the "Super"-LIP Ontong Java Nui. After reevaluating the different margins of the LIPs of Ontong Java Nui and tracing the seafloor fabric emplaced during the CNS, the plate motion was reconstructed. The interaction between the arriving plume and the Pacific-Phoenix ridge explains the different crustal thicknesses of the LIPs. My updated rotation parameters of the western Pacific include the break-up scenario of Ontong Java Nui and previously suggested concepts, which have not been included in the calculation of the plate motion before, such as the rotation of the Hikurangi and Ontong Java Plateaus.

I re-evaluated the available data for the different margin types, mapped the seafloor features used in the reconstruction, executed the plate kinematic reconstruction in "*GPlates*" and prepared the manuscript. K. Gohl supervised the work and was the leader of the OBS team during So-224. G. Uenzelmann-Neben was Chief scientist on So-224 and supervised the processing of the reflection seismic data. All authors revised the manuscript and contributed to the discussion.

## From the western Pacific to the Andes and Antarctica: The Manihiki Plateau on the move

K. Hochmuth<sup>1</sup> and K. Gohl<sup>1</sup>

<sup>1</sup>*Alfred-Wegener Institut Helmholtz-Zentrum für Polar- und Meeresforschung*

The manuscript is currently under review with *Earth and Planetary Science Letters*.

This manuscript traces the plate motion of the northeastern and eastern fragments of the Manihiki Plateau based on the plate kinematic reconstruction of the break-up of Ontong Java Nui. The fragments were incorporated into the Farallon Plate and the Phoenix Plate, respectively. By careful analysis of the projected collision areas of the fragments, the northern Andes and the Bellingshausen Sea, possible remnants of the LIPs are identified and their impact on the plate tectonic framework is assessed.

I executed the plate kinematic reconstruction in "*GPlates*", calculated the rotation poles for the LIP fragments and researched the literature on the structure of the possible areas of subduction. I wrote the manuscript and designed all figures. K. Gohl supervised the work, contributed to the discussion and revised the manuscript.

# 5 Multiphase magmatic and tectonic evolution of a Large Igneous Province - evidence from the crustal structure of the Manihiki Plateau, western Pacific

*K.Hochmuth<sup>1</sup>, K. Gohl<sup>1</sup>, G. Uenzelmann-Neben<sup>1</sup> and R. Werner<sup>2</sup>*

*<sup>1</sup>Alfred-Wegener Institut Helmholtz-Zentrum für Polar- und Meeresforschung, <sup>2</sup>GEOMAR Helmholtz-Zentrum für Ozeanforschung*

## Abstract

The Manihiki Plateau, a Large Igneous Province (LIP) in the western Pacific, has been proposed to be emplaced as part of the “Greater Ontong Java Event” during the early Cretaceous. Shortly after its formation, the Manihiki Plateau fragmented into multiple sub-provinces. Plate tectonic reconstructions ignore this fragmentation, treating the Manihiki Plateau as a single crustal block. By analysing two seismic refraction/wide-angle reflection profiles crossing the two largest sub-provinces of the Manihiki Plateau, we provide new insight into their deep crustal structure and magmatic evolution. Our data indicate that the High Plateau and the Western Plateaus were emplaced as a single unit during an initial phase of massive magmatic activity, but later magmatic stages altered the individual sub-provinces considerably. The High Plateau has a crustal thickness of 20 km and its P-wave velocity distribution is comparable to previously surveyed oceanic LIPs. Strong secondary magmatic phases are visible by eruptive centres and former magmatic pathways in the middle and lower crust. The Western Plateaus, which have a crustal thickness decreasing gradually from 17.3 km (East) to 9.2 km (West), experienced smaller amounts of magmatism mainly along fault zones and on local seamounts. Therefore, we propose a distinct development of the two main sub-provinces of the Manihiki Plateau after their initial joint emplacement. The High Plateau experienced voluminous multi-phase magmatic accretion and extrusion, whereas the thinner Western Plateaus exhibit only relatively minor magmatic growth. Such a large difference in the evolution process has not been reported from any other oceanic LIP so far.

**Keywords**

145 Oceanic hotspots and intraplate volcanism  
146 Oceanic plateaus and microcontinents  
160 Large Igneous Provinces  
169 Crustal structure  
207 Pacific Ocean

**5.1 Introduction**

Large Igneous Provinces (LIP) are large ( $>0.1 \times 10^6 \text{ km}^2$ ) marine and terrestrial areas overprinted by massive volcanic activity (Ai *et al.*, 2008; Bryan and Ernst, 2008; Coffin and Eldholm, 1994; Schlanger *et al.*, 1976; Simoneit *et al.*, 2014). LIPs have a great impact on the environment during and after their emplacement, for instance by the release of greenhouse gases during massive volcanism (Wignall, 2001) or their role in plate motion by thickening of oceanic crust (Bryan and Ernst, 2008; Miura *et al.*, 2004). The emplacement of LIPs can for instance be linked to multiple global mass extinction events (Bryan and Ernst, 2008; Coffin and Eldholm, 1994; Courtillot *et al.*, 1999; Larson and Erba, 1999; Wignall, 2001). LIPs are the result of massive magmatism occurring during a relatively short time period (1-5 M.y.) resulting in an anomalously thick mafic crust (Bryan and Ernst, 2008; Coffin and Eldholm, 1993, 1994; Wignall, 2001). This first magmatic stage of a LIP event is characterized by the emplacement of approximately 75% of its igneous volume (Bryan and Ernst, 2008; Bryan and Ferrari, 2013; Karlstrom and Richards, 2011; Miura *et al.*, 2004). Later magmatic stages can be summarized as secondary magmatism and show longer emplacement periods as well as smaller emplacement rates. The crustal structure of oceanic LIPs commonly consists of a lower crustal layer with high seismic P-wave velocities ( $> 7.3 \text{ km/s}$ ), mafic intrusions in the middle crust, and volcanic flow units in the uppermost crust (Coffin and Eldholm, 1994; Ridley and Richards, 2010). In previous publications, the formation of LIPs on continents and oceans was explained by the impact of a mushroom-shaped plume head at the base of the lithosphere, leading to widespread magmatism (Morgan, 1971; White and McKenzie, 1995). But this scenario has been debated, since this plume head model cannot explain all characteristics of oceanic LIPs (Bryan and Ernst, 2008; Coffin *et al.*, 2002, 2006; Courtillot *et al.*, 1999; Korenaga, 2005; Larson and Erba, 1999; McNutt, 2006). The Manihiki Plateau, located in the western central Pacific, is a LIP with different characteristics within its sub-provinces such as a laterally heterogeneous crustal character. In this paper, we try to unravel the relationship between the two largest sub-provinces of the Manihiki Plateau, the Western Plateaus and the High Plateau, which are separated by the Danger Islands Troughs. Did both sub-provinces experience the same magmatic history? The fragmentation of the Manihiki Plateau poses the question, whether distinct phases of magmatic or tectonic processes led to the fragmentation of the Manihiki Plateau and which role the Danger Islands Troughs played in this scenario. By processing, modeling and interpreting recently acquired seismic

refraction/wide-angle reflection data; the deep crustal structure of both sub-provinces is revealed and interpreted for the first time.

## 5.2 Geological background

The formation of the Manihiki Plateau took place during the early Cretaceous (124-120 Ma) (Clague, 1976; Ingle *et al.*, 2007; Timm *et al.*, 2011) as centerpiece of the “Super-LIP” Ontong Java Nui according to Taylor (2006) and Chandler *et al.* (2012, 2013). This giant LIP covered more than 1% of Earth’s surface (Bryan and Ferrari, 2013; Coffin and Eldholm, 1993; Ingle *et al.*, 2007; Timm *et al.*, 2011; Wignall, 2001) and consisted of the Ontong Java Plateau, the Hikurangi Plateau and the Manihiki Plateau (Fig. 5.1 (inlet)) as well as presumed multiple smaller fragments to the northeast and east of the Manihiki Plateau, which have possibly been subducted (Larson *et al.*, 2002; Viso *et al.*, 2005) or accreted such as the Malaita terranes (Musgrave, 2013).

We refer to today’s Manihiki Plateau and the proposed northeastern and eastern fragment as “Greater Manihiki Plateau” in this manuscript. The plate tectonic reconstructions of Ontong Java Nui are still under debate, especially the fit between the Ontong Java Plateau and the Manihiki Plateau, as the spreading mechanisms of the Ellice Basin between the plateaus remain speculative (Chandler *et al.*, 2012; Taylor, 2006). The coupled emplacement of the Hikurangi Plateau and the Manihiki Plateau appears much more certain, because the Osbourn Trough can be identified as the former spreading center separating the two plateaus (Billen and Stock, 2000; Downey *et al.*, 2007; Worthington *et al.*, 2006). The break-up of Ontong Java Nui took place shortly after its emplacement, since secondary magmatism, which can be related to later magmatic phases with small eruption rates and mainly seamount volcanism, shows different petrological and geochemical characteristics on the three remaining plateaus (Hoernle *et al.*, 2010; Timm *et al.*, 2011). This led to the conclusion, that after the coupled emplacement of the plateaus, the multiple stages of secondary magmatism were supplied by different mantle sources. Seafloor spreading was established possibly around 118 Ma in Ellice Basin (Ontong Java – Manihiki) (Chandler *et al.*, 2012) and at the Osbourn Trough (Hikurangi – Manihiki) (Worthington *et al.*, 2006). The onset and the duration of seafloor-spreading at both locations is difficult to date, since the complete activity of those spreading-centres has occurred within the Cretaceous Normal Superchron. Therefore, no magnetic seafloor-spreading anomalies can be traced, and smaller changes in the magnetic field cannot be observed due to the severe magmatic overprinting (Billen and Stock, 2000).

The Manihiki Plateau itself experienced fragmentation into three sub-provinces, the High Plateau, the Western Plateaus and the North Plateau (Winterer *et al.*, 1974) (Fig. 5.1). Further significant features of the Manihiki Plateau are the Danger Islands Troughs, which are created by rifting and/or transform forces separating the High Plateau from the Western Plateaus (Larson, 1997; Mahoney and Spencer, 1991; Nakanishi *et al.*, 2015; Winterer *et al.*, 1974), the Suvarov Through, and the Manihiki Scarp, a former shear zone at the eastern part of the plateau (Larson *et al.*, 2002). Hussong *et al.* (1979) published first estimates on the crustal structure of the Mani-

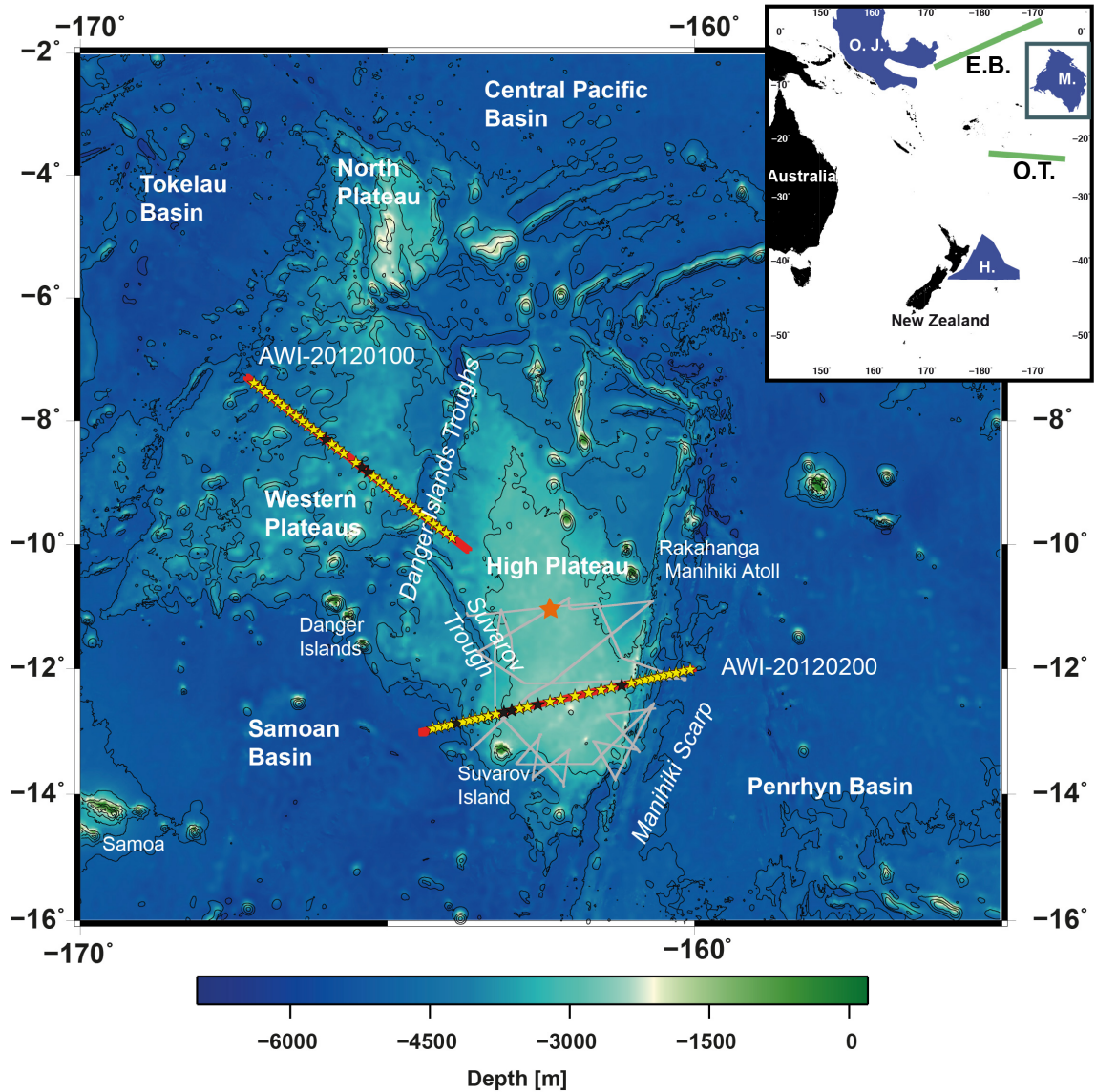


**Figure 5.1:** Bathymetric map (30 arc-second grid GEBCO 2014 (*Weatherall et al., 2015*)) of the central western Pacific, seismic refraction/wide-angle reflection lines of cruise SO-224 are shown in red, seismic reflection lines of SO-224 are shown in grey. Yellow stars depict the positions of the OBS-stations. The black stars are stations, which did not return any data. The borehole DSDP Leg 31 Site 317 is marked by the orange star. In the inlet map the three main components of the Ontong Java Nui related LIPs are shown at their current position (Ontong Java (O. J.), Hikurangi (H.) and Manihiki (M.)). The green lines indicate the former spreading centres of the Osborn Trough (O.T.) and the Ellice Basin (E.B.). The dark green box indicates the study area shown in the larger map.

hiki Plateau. However, their experiment, using seismic sonobuoy data, did not provide data of the lower crustal layers or the upper mantle, but it was inferred that the crust of the Manihiki Plateau was 3.1 times thicker than average oceanic crust and that it showed similar features as described for the crust of the Ontong Java Plateau (Hussong *et al.*, 1979). The upper basement and the sedimentary cover of the Manihiki Plateau has been studied from samples collected by multiple dredges (Beiersdorf *et al.*, 1995a; Clague, 1976; Hoernle *et al.*, 2010; Ingle *et al.*, 2007; Schlanger *et al.*, 1976; Timm *et al.*, 2011; Werner *et al.*, 2013) and short sediment cores. Drilling at Deep Sea Drilling Project (DSDP) Leg 33 Site 317 (Fig. 5.1) reached a basaltic layer in a depth of 910 m below seafloor (Schlanger *et al.*, 1976).  $^{40}\text{Ar}/^{39}\text{Ar}$  dated tholeiitic basement basalts of the Manihiki Plateau reveal a mean age of  $124.6 \pm 1.6$  Ma (Timm *et al.*, 2011). Lava drilled at DSDP Site 317 of the High Plateau exhibit an age of 117 Ma (Hoernle *et al.*, 2010). In the Danger Islands Troughs, tholeiitic basalts ( $^{40}\text{Ar}/^{39}\text{Ar}$  of  $117.9 \pm 3.5$  Ma) with an unusual composition are present, as well as alkalic basalts possibly related to later volcanic stages of a different or altered mantle source ( $^{40}\text{Ar}/^{39}\text{Ar}$  age of  $99.5 \pm 0.7$  Ma) (Ingle *et al.*, 2007). Later stages of episodic volcanism on the Manihiki Plateau are manifested by multiple seamounts and basaltic flow units on the High Plateau (Beiersdorf *et al.*, 1995b; Coulbourn and Hill, 1991) and seamounts on the margins of the Western Plateau (Hoernle *et al.*, 2009; Sandwell *et al.*, 2014; Werner and Hauff, 2007). Seismic reflection data of the High Plateau image several volcanoclastic layers in the lower sedimentary sequences (Ai *et al.*, 2008; Schlanger *et al.*, 1976; Winterer *et al.*, 1974), pointing to a shallow or subaerial environment during the secondary phases of magmatism (Ai *et al.*, 2008; Schlanger *et al.*, 1976; Simoneit *et al.*, 2014). Pietsch and Uenzelmann-Neben (submitted) additionally identify magmatic events occurring within younger strata ( $< 45$  Ma), inferring that the Manihiki Plateau experienced a period of magmatic reactivation, possible due to the overriding over multiple hotspots. In this paper, we use the term initial or first magmatic phase for the initial emplacement of the Manihiki Plateau ( $>120$  Ma). The secondary magmatic stages comprise multiple episodic magmatic activities younger than 120 Ma, which occurred during and after the proposed break-up of Ontong Java Nui. It is important to note, that most of the publications have focused on the High Plateau along with the Danger Islands Troughs and the Manihiki Scarp. Other areas of the Manihiki Plateau, such as the basement of the Western Plateaus, are poorly sampled and therefore the evolution of the different sub-provinces and their magmatic and tectonic relationship to the other parts of the plateau is still poorly understood. Although satellite-derived gravity anomaly maps (Sandwell *et al.*, 2014) indicate different crustal structures of the sub-provinces, plate tectonic reconstructions of the Cretaceous western Pacific (e.g. Chandler *et al.*, 2012, 2013; Davy *et al.*, 2008; Musgrave, 2013; Taylor, 2006) treat the Manihiki Plateau as a single tectonic block and disregard its different sub-provinces and therefore possible indications for the nature of the break-up of the “Super”-LIP.

## 5.3 Data acquisition, processing, and modeling parameterization

### 5.3.1 Data acquisition

During RV Sonne cruise SO-224 in 2012 (*Uenzelmann-Neben, 2012*), the Alfred Wegener Institute (AWI) collected two deep crustal seismic refraction/wide-angle reflection lines (Fig. 5.1), crossing the two main sub-provinces of the Manihiki Plateau: the Western Plateaus (AWI-20120100) and the High Plateau (AWI-20120200). Both seismic lines consisted of 28 ocean-bottom seismometer (OBS) and 5 ocean-bottom hydrophone (OBH) stations spread out over 500 km long profiles each. The OBS stations were equipped with a 3-component (4.5 s natural period) seismometer and a hydrophone. OBH stations were only equipped with a hydrophone. Station spacing varied between a constant 14.1 km on AWI-20120100 and 10.9 km (at the margins) to 24.1 km (on the High Plateau) on AWI-20120200 to ensure better ray-coverage at the plateau margins. An array of 8 G-Guns<sup>TM</sup> (type 520) with a total volume of 68 litres (4160 in<sup>3</sup>) was used as a seismic source. The G-Guns<sup>TM</sup> were towed in four clusters of two guns each at 10 m water-depth and fired at nominally 200 bar operating pressure every full minute. During the acquisition, multichannel seismic reflection data was also recorded with a 3000 m long digital solid streamer (Sercel Sentinel<sup>TM</sup>) of 240 channels. In addition to the seismic experiments, multibeam bathymetry data were collected throughout the cruise with a Kongsberg Simrad EM120, which is permanently installed on RV Sonne.

### 5.3.2 Processing and modeling of seismic refraction/wide-angle reflection data

The OBS/OBH field data were merged with navigation data and converted to SEGY-format. After relocalization of the OBS positions using the direct-wave arrivals, the application of a bandpass filter (6-15 Hz), all refracted and reflected arrival phases were picked with the software "ZP" (*Zelt, 2004*). We assigned picking individual uncertainties to the individual picks taking the signal-to-noise-ratio into account (*Zelt, 2004*). The picking uncertainties range between 0.075 and 0.25s with a median picking uncertainty of 0.1s. P-wave and S-wave velocity-depth modeling was carried out using the forward modeling software "Rayinvr" (*Zelt and Smith, 1992*) and its graphical interface "PRay" (*Fromm, 2012*). We used bathymetric and seismic reflection records obtained during the cruise (*Uenzelmann-Neben, 2012*), in order to constrain modeling parameters for the seafloor and the thickness of the sedimentary cover. The conversion from two-way travel times of the seismic reflection records to the actual depths below seafloor was carried out with the velocity field established by velocity analysis (*Pietsch and Uenzelmann-Neben, 2015*). The layer boundaries and model coordinates of the velocity nodes established by the P-wave model were used for S-wave modeling to ensure comparable models and allow the calculation of the Poisson's ratio. The set-up of the initial model included the following constraints: the topography of the seafloor, the thickness of the sedimentary column and the crustal structure previously published by *Hussong et al. (1979)* and that derived from 1D-Profiles at our OBS/OBH-stations.



Phase	AWI-20120100	AWI-20120200
$P_uP$	+0.4/-0.5	+0.5/-0.4
$P_{um}P$	+0.7/-0.4	+0.6/-0.4
$P_{lm}P$	+0.6/-0.7	
$P_mP$	+0.7/-0.7	+0.8/-0.5

**Table 5.1:** Depth uncertainties within the intracrustal reflectors in km

Refracted and reflected phases in the P- and S-wave models are named respectively to their corresponding layer  $P_{layer}$  and  $P_{layer}P/S_{layer}$  and  $S_{layer}S$ . Reflected phases always represent the reflection at the base of the layer. Mantle phases are called  $P_n/S_n$  for the refracted phase and  $P_mP/S_mS$  for the reflection at the crust-mantle boundary (Moho). We observed three distinct groups of crustal phases

( $P_{uc}/S_{uc}$  (upper crust),  $P_{mc}/S_{mc}$  (middle crust),  $P_{lc}/S_{lc}$  (lower crust)) on the Western Plateaus (Fig. 5.2, Fig. 5.3) and four distinct groups of crustal phases ( $P_{uc}/S_{uc}$  (upper crust),  $P_{umc}/S_{umc}$  (upper-middle crust),  $P_{lmc}/S_{lmc}$  (lower-middle crust),  $P_{lc}/S_{lc}$  (lower crust)) on the High Plateau (Fig. 5.4, Fig. 5.5). The resolution of the S-wave velocity models is generally lower than the resolution of the presented P-wave velocity models. Unfortunately, only little to no information on the S-wave velocity distribution was returned from the lower crust and the mantle. We assessed the uncertainty of layer boundaries of the intercrustal reflections (Tab. 5.1). The depth uncertainties of the individual layers range between 0.4 and 0.8 km, with the largest uncertainties for the Moho depths. This is well in the uncertainty range given by the ray-tracing method. The Poisson's ratio can contribute further parameters on the composition of the crust (Christensen, 1996). For example, alteration processes such as serpentinization or the distribution of predominantly mafic and felsic rocks can be constrained. We calculated the Poisson's ratio for every velocity node of the P- and S-wave models and gridded their distribution. Since the S-wave model has a sparser resolution than the P-wave model, it limits the resolution of the Poisson's ratio model. For AWI-20120100, the calculated Poisson's ratio is not presented due to the poor resolution of this profile.

### 5.3.3 Modeling of gravity data

As shipborne gravity data were not collected, we relied on free-air gravity anomaly records extracted from the global satellite-derived gravity anomaly grid by Sandwell and Smith (1997 (V.23)) with values extracted along our seismic profiles. In a starting model using the forward modeling software IGMAS (Götze *et al.*, 2002), we incorporated the layer boundaries of the P-wave velocity-depth model and converted the P-wave velocities to rock densities using the relationships by Hamilton (1978) and Barton (1986). We assigned rock densities to P-wave velocity clusters representing the different crustal layers of the P-wave velocity models (Tab. 5.2). As this 2-D approach turned out to be affected by large-amplitude anomaly features offline, a perfect fit could not be achieved by retaining realistic model parameters such as the seafloor topography. In several iterations, the model parameters were altered to generate a best fit to the observed gravity anomalies and the P- and S-wave models.

Layer	AWI-20120100	AWI-20120200
sediments	2050	2050
low velocity upper crust	2400	not present
upper crust	2650	2800
upper middle crust	2800	2900
middle crust	2900	not present
lower middle crust	2950	2950
lower crust	3130	3150
mantle	3300	3300

**Table 5.2:** Rock densities [ $\text{kg/m}^3$ ] Barton (1986); Hamilton (1978) used for specific layers in the gravity anomaly model

## 5.4 Results of data analysis and modeling

### 5.4.1 Bathymetric and sedimentary features

The two seismic refraction/wide-angle reflection profiles allow a comparison of the two main provinces of the Manihiki Plateau. Profile AWI-20120100 crosses the Western Plateaus from the northwest to the southeast (Fig. 5.1). The water depth ranges from 4800 m in the Tokelau Basin to 3800 m on the Western Plateaus. The deepest areas of the profile are the Danger Islands Troughs with a maximum depth of 4900 m. A small part of the westernmost High Plateau is also covered by the eastern part of this profile. Bathymetric and seismic reflection data reveal a rough seafloor topography with multiple faults and graben systems along with local seamounts (Fig. 5.6). Sedimentary cover is mainly restricted to the basins between the numerous basement highs (Uenzelmann-Neben, 2012; Winterer et al., 1974). Profile AWI-20120200 images the High Plateau of the Manihiki Plateau in a west to east section (Fig. 5.1). The water depth ranges from 5100 m in the Samoan Basin and Penrhyn Basin to a mean depth of the High Plateau of 2500 m with a relatively smooth seafloor. The Manihiki Scarp in the east and the margin towards the Samoan Basin in the west form sharp flanks bordering the sub-province. Seismic reflection data reveal an approximately 800 m thick sedimentary cover and several basement highs on the central plateau. Sedimentation appears to be restricted to pockets and small basins between basement highs on the margins of the High Plateau (Ai et al., 2008; Beiersdorf et al., 1995b; Winterer et al., 1974).

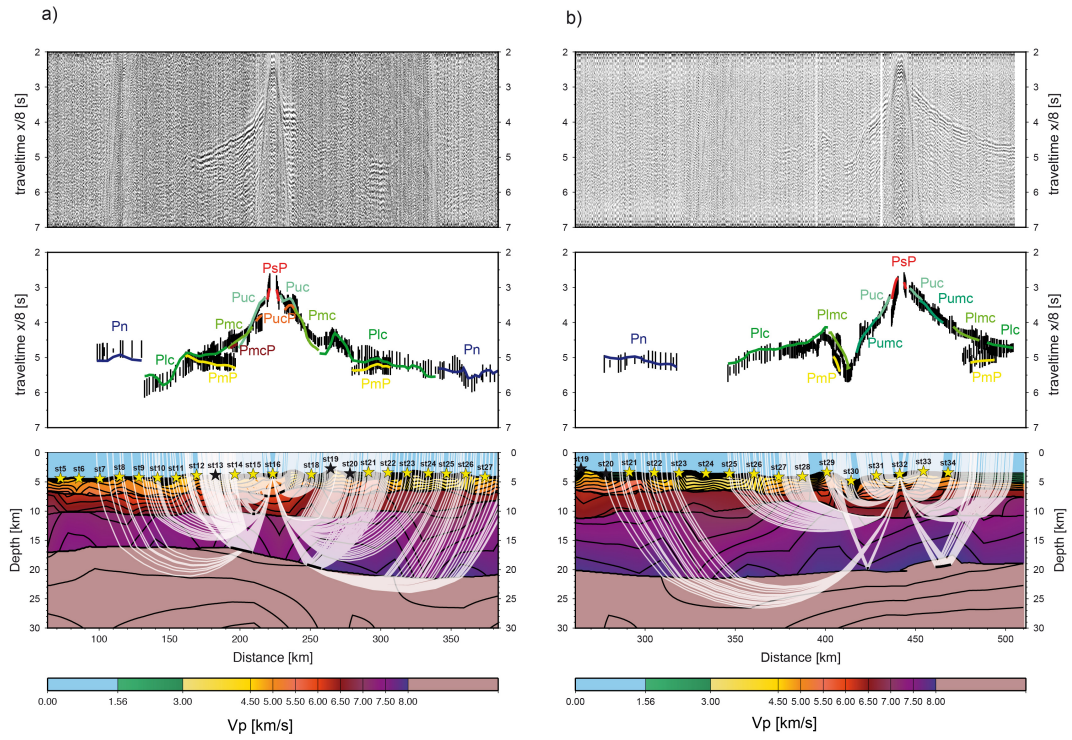


**Figure 5.2:** Data examples for P-wave arrivals (AWI-20120100) at a) st16 representing the central Western Plateaus and b) st32 representing the Danger Islands Troughs area

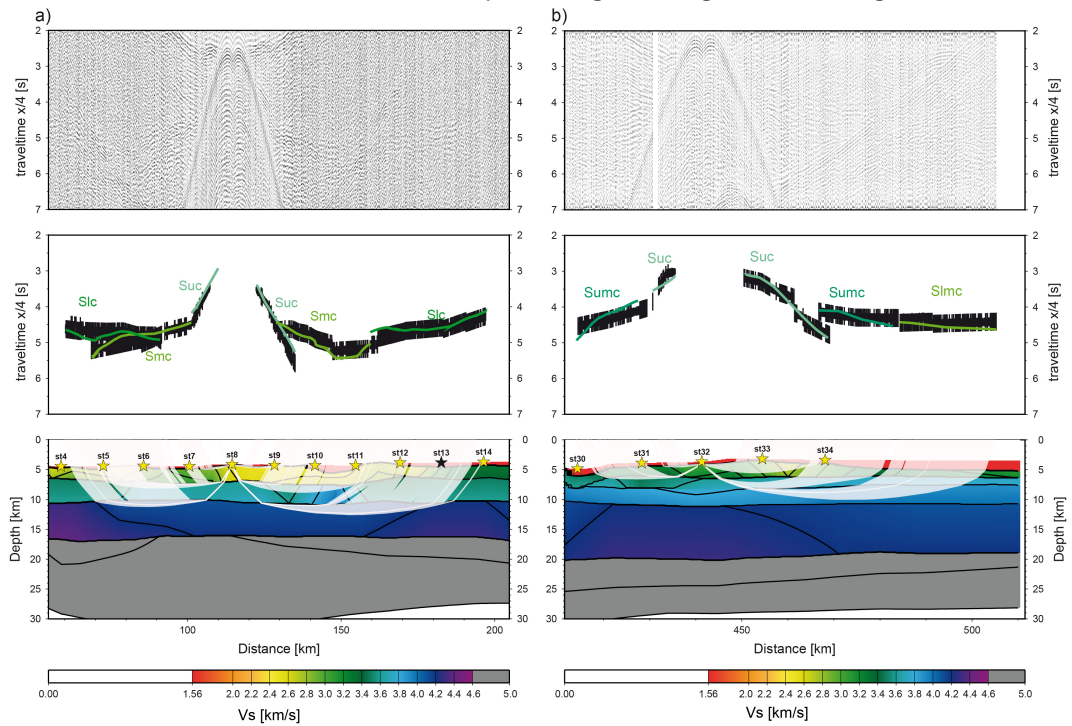


**Figure 5.3:** Data examples for S-wave arrivals (AWI-20120100) at a) st08 representing the western part of the Western Plateaus and b) st32 representing the Danger Islands Troughs area

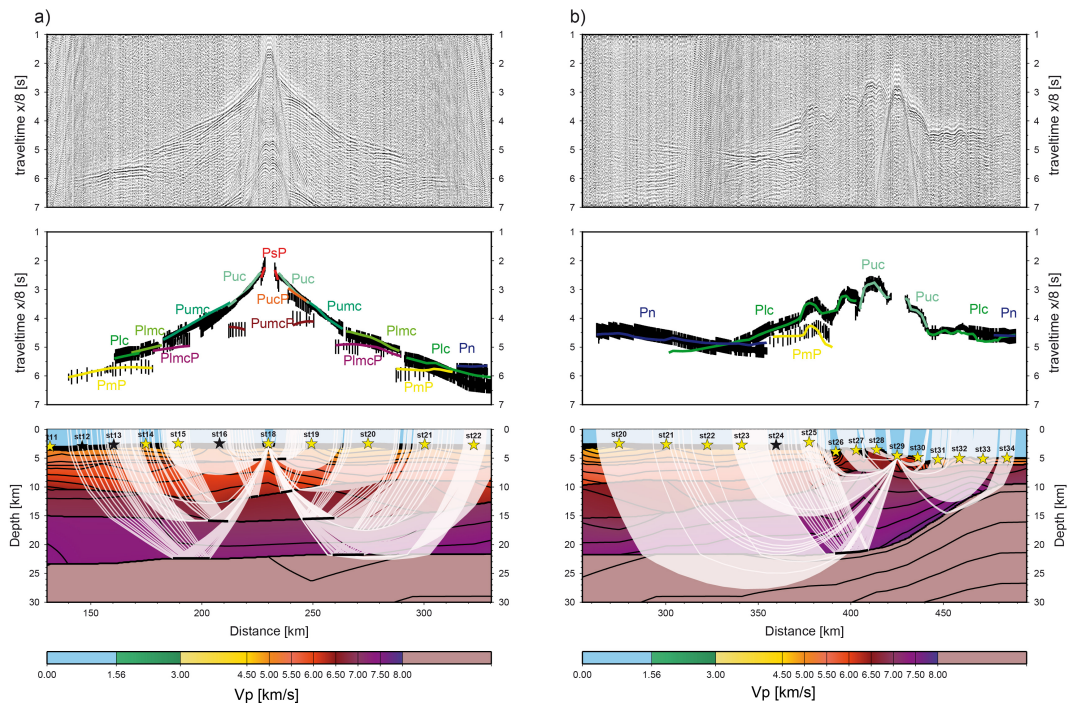


**Figure 5.4:** Data examples for P-wave arrivals (AWI-20120200) at a) st18 representing the central High Plateau and b) st29 representing the Manihiki Scarp area

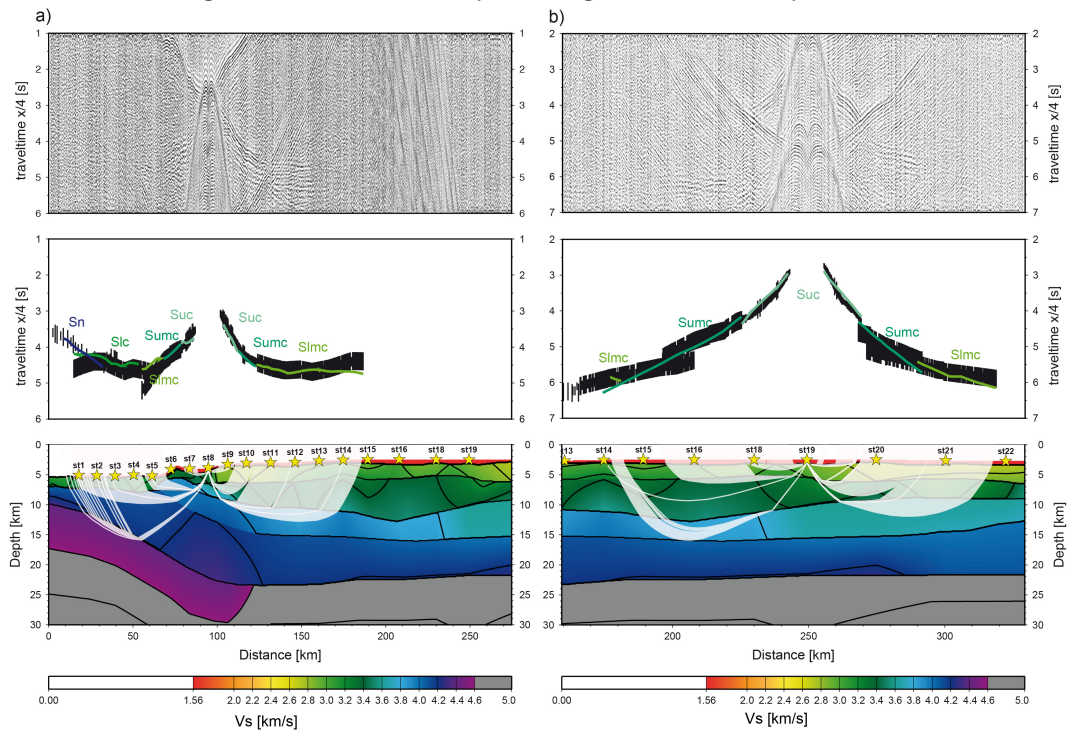


**Figure 5.5:** Data examples for S-wave arrivals (AWI-20120200) at a) st08 representing the western margin of the High Plateau and b) st19 representing the central High Plateau



### 5.4.2 Upper crustal layers

The upper crustal layer of the Western Plateaus and the High Plateau include the acoustic basement of the seismic reflection data and are represented by the refracted phases ( $P_{uc}/S_{uc}$ ) and constrained by the wide-angle reflections at the upper layer boundary  $P_sP$  and  $P_{uc}P$  at the base of the layer (Figs. 5.2, 5.3, 5.4 and 5.5).

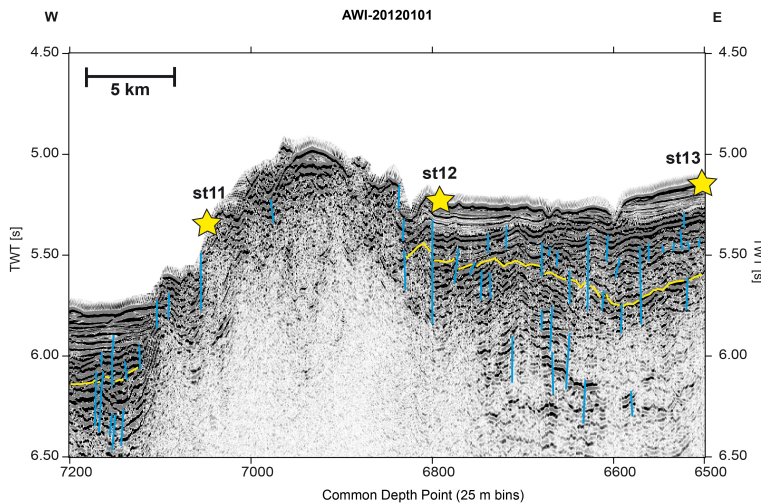


**Figure 5.6:** Seismic reflection data from AWI-20120100 between OBS-station 11 and OBS-station 13, the blue lines indicate fault systems; the yellow reflector indicates the top of basalt. The faults were identified in an enlarged section.

On the Western Plateaus, the upper crust is characterized by a rough basement topography and a widely variable velocity field. The western 50 km of the profile consist of an upper crustal layer with P-wave velocities between 5.2 and 5.5 km/s (Fig. 5.7). Between 50 km and 300 km profile distance, P-wave velocities decrease to 4.5 km/s with small patches of lower velocities (3.8 km/s). It is important to note that due to the malfunction of two neighbouring stations (st19,

st20) the ray coverage is not ideal in this area. Between 300 and 370 km profile distance, unusual low velocities ranging from 3.0 to 4.3 km/s are present. S-wave velocities show a block-like structure (Fig. 5.8) rather than a continuous change. From 0 to 100 km, S-wave velocities range from 2.9 to 3.2 km/s. Velocities decrease to 2.5 to 2.8 km/s between st8 and st12 (110 km to 170 km). From 180 km to 250 km profile distance, S-wave velocities from 2.9 to 3.3 km/s are common. This block is followed by an area of unusual high S-wave velocities, which corresponds to higher velocities in the middle crust (3.7 to 4.3 km/s). The Danger Islands Troughs area lacks a visible upper crust (Figs. 5.2b and 5.7).

The High Plateau shows higher and more homogenous P-wave velocities between 4.7 and 5.6 km/s (Figs. 5.4 and 5.9) and S-wave velocities between 2.7 and 3.2 km/s (Figs. 5.5 and 5.10). Several extrusive and intrusive magmatic features can be identified in the seismic reflection data (Pietsch and Uenzelmann-Neben, 2015). Those magmatic centres can be connected to areas of higher P-wave velocities (e.g. at st21) in the P-wave velocity model.

The upper crust of the surrounding ocean basins close to the margins of the Manihiki Plateau, the Penrhyn Basin and the Samoan Basin show P-wave velocities between 5.2 and 5.8 km/s (Fig. 5.9). S-wave velocities range from 3.3 km/s in the Samoan Basin to 2.9 km/s in the Penrhyn Basin (Fig. 5.10). Whereas the Samoan Basin shows Poisson's ratio values of around 0.25, which can be related to basalt (Christensen, 1996), the Penrhyn Basin on the other hand

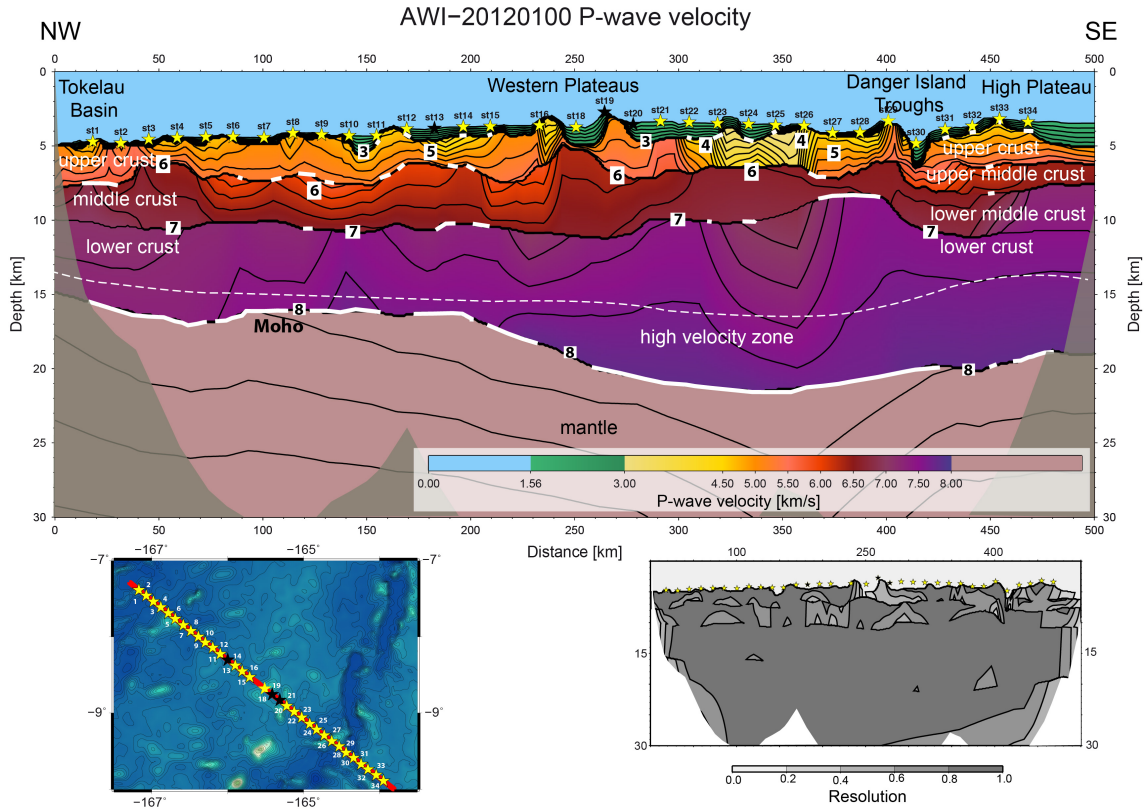


**Figure 5.7:** P-wave velocity model of AWI-20120100; the grey transparent areas are not covered by rays. White layer boundaries are constraint by wide-angle reflections. The location of OBS stations is indicated with the yellow (functioning station) and black (malfunctioning station) stars. The resolution calculated for the velocity nodes is shown in the lower right corner. The RMS-value of this model is 0.189 and the  $\chi^2$  is 1.552. The vertical exaggeration is 7:1.

shows high Poisson's ratio values of over 0.30 (Fig. 5.11), which is typical for basalts and partly serpentinized basalts in the uppermost crust.

### 5.4.3 Middle crustal layers

The middle crustal layers of the Manihiki Plateau consist of two layers ( $P_{umc}/S_{umc}$  from upper-middle crust and  $P_{lmc}/S_{lmc}$  from lower-middle crust) on the High Plateau (Figs. 5.4 and 5.5) and one layer on the Western Plateaus ( $P_{mc}/S_{mc}$ ) (Figs. 5.4 and 5.5). On the Western Plateaus, the P-wave velocity structure of the middle crust is homogeneous and ranges between 5.8 and 6.8 km/s (Fig. 5.7). In between the ridge-like structures at 230 and 270 km profile distance, the upper crustal layer is absent and the top of the middle crustal layer represents the acoustic basement. This feature is also present in the gravity anomaly model (Fig. 5.12). The S-wave velocity model shows more variation in the middle crust, with values ranging from 3.6 to 4.0 km/s in the west to very high S-wave velocities of up to 4.3 km/s at st22 (Fig. 5.8). S-wave velocities decrease to 3.8 to 4.0 km/s towards the Danger Islands Troughs. The middle crust is present at the Danger Islands Troughs. East of the troughs, the middle crust is divided into two separate crustal layers, the upper-middle crust and the lower-middle crust (Figs. 5.2b and 5.7).

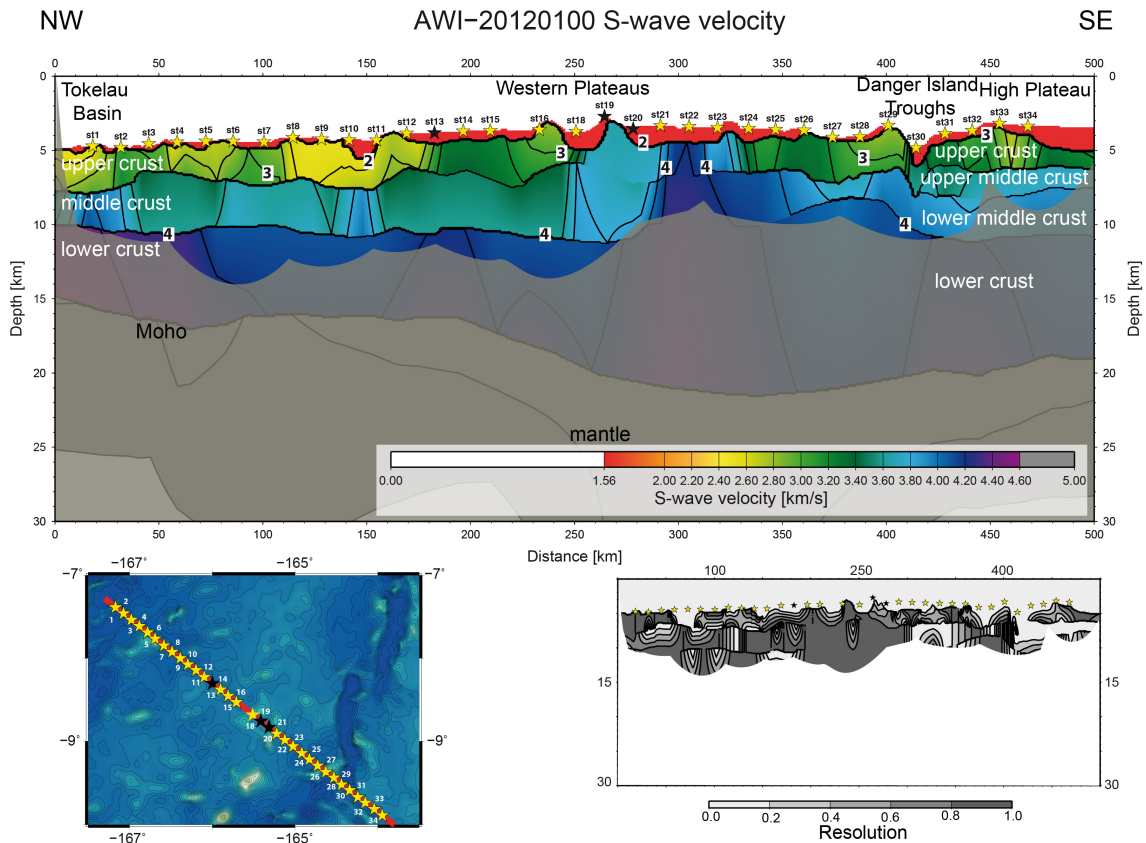


**Figure 5.8:** S-wave velocity model of AWI-20120100; the grey transparent areas are not covered by rays. The locations of OBS stations are indicated with the yellow (functioning station) and black (malfunctioning station) stars. The resolution calculated for the velocity nodes is shown in the lower right corner. The RMS-value of this model is 0.280 and the  $\chi^2$  is 2.751. The vertical exaggeration is 7:1.

The upper-middle crust shows P-wave velocities between 5.4 and 6.4 km/s (Fig. 5.7) and S-wave velocities between 3.0 and 3.6 km/s (Fig. 5.8). This crustal layer is thicker in the western part of the High Plateau. The lower-middle crust presents relatively high P-wave velocities (6.7 to 6.9 km/s) and S-wave velocities between 4.0 and 4.3 km/s (Figs. 5.9 and 5.10). The lower-middle crustal layer crops out at the seafloor at the Manihiki Scarp. Here, S-wave velocities up to 4.65 km/s are present. The Poisson's ratio shows three distinct areas of higher values ( $> 0.26$ ) below the central plateau (Fig. 5.11). Those can be connected to areas of higher P-wave velocities and therefore the magmatic structures within the upper crust. Middle crustal layers are not present in the adjacent oceanic basins.

#### 5.4.4 Lower crustal layers

The lower crust of most LIPs consists of a zone of high P-wave velocities ( $> 7.3$  km/s), a so called high-velocity zone (HVZ) (Coffin and Eldholm, 1994; Ridley and Richards, 2010). On the Manihiki Plateau, we observe this HVZ on both sub-provinces within the lower crust ( $P_{lc}/S_{lc}$ ). The HVZ is also present in the lower crust of the Tokelau Basin and extends into the Samoan Basin. At

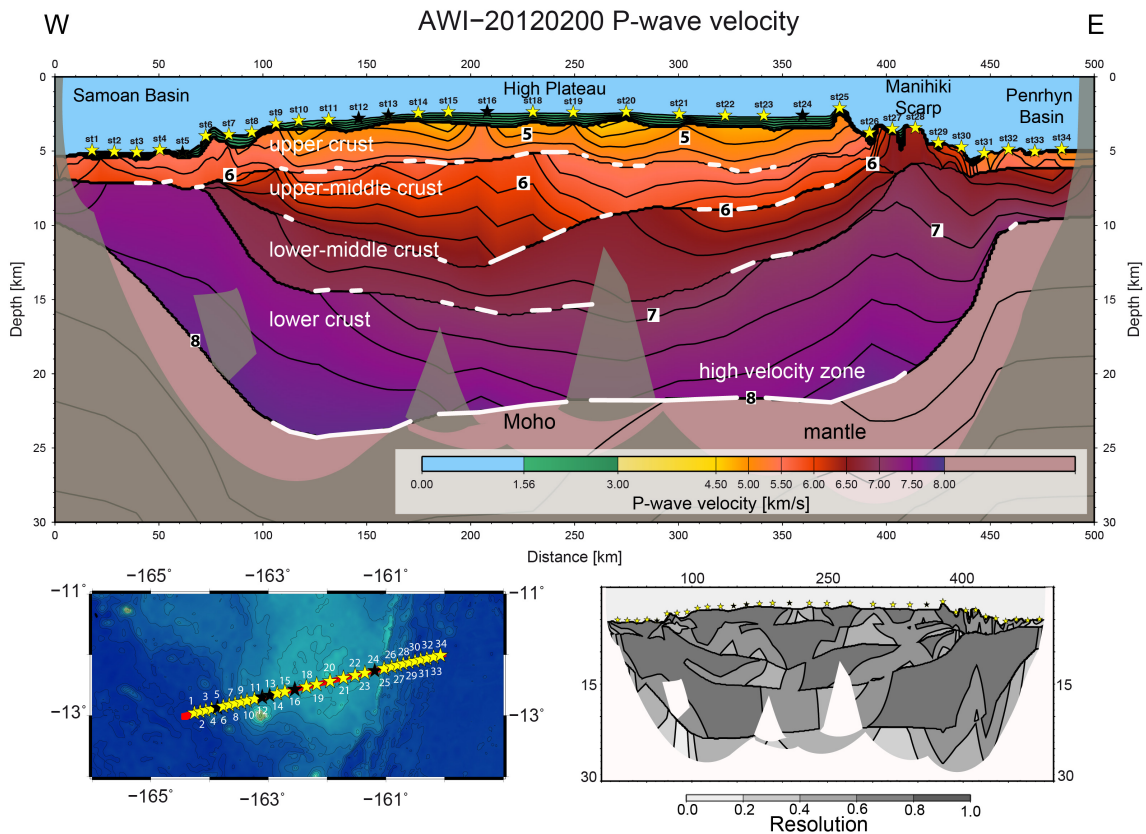


**Figure 5.9:** P-wave velocity model of AWI-20120200; the grey transparent areas are not covered by rays. White layer boundaries are constrained by wide-angle reflections. The locations of OBS stations are indicated with the yellow (functioning station) and black (malfunctioning station) stars. The resolution calculated for the velocity nodes is shown in the lower right corner. The RMS-value of this model is 0.186 and the  $\chi^2$  is 1.674. The vertical exaggeration is 7:1.

the Manihiki Scarp, the HVZ terminates abruptly. P-wave velocities range between 6.8 and 7.8 km/s on the Western Plateaus (Fig. 5.7) and 7.0 to 7.8 km/s on the High Plateau (Fig. 5.9). The ray-coverage of S-waves is poor on the High Plateau and only a few interpretable signals were returned for the lower crust of the Western Plateaus. S-wave velocities range between 4.1 and 4.3 km/s on the Western Plateaus (Fig. 5.8). At the western margin of the High Plateau, S-wave velocities reach 4.4 km/s and at the Manihiki Scarp values of 4.7 km/s are present (Fig. 5.10).

#### 5.4.5 Crust-mantle boundary and mantle

The boundary between the crystalline crust and the mantle (Moho) can be constrained by refracted phases from the uppermost mantle ( $P_n$ ) as well as reflections at the Moho itself ( $P_mP$ ) (Figs. 5.2 and 5.7). On the High Plateau, the Moho is visible in the data throughout the central plateau at a depth of 20 km below the seafloor (Figs. 5.9 and 5.13). In the Samoan Basin and the Penrhyn Basin the crustal thickness, the combined thickness of the sedimentary column



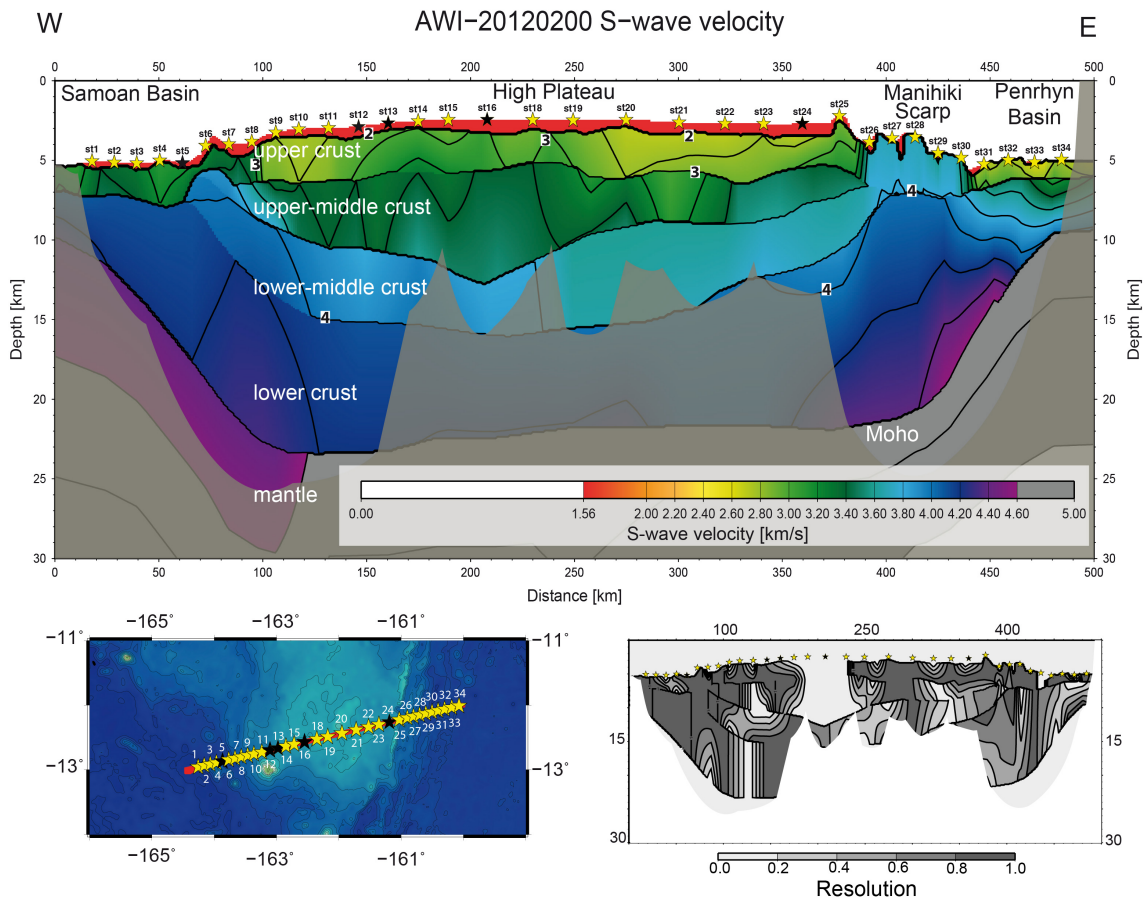


**Figure 5.10:** S-wave velocity model of AWI-20120200; the grey transparent areas are not covered by rays. The locations of OBS stations are indicated with the yellow (functioning station) and black (malfunctioning station) stars. The resolution calculated for the velocity nodes is shown in the lower right corner. The RMS-value of this model is 0.223 and the  $\chi^2$  is 2.11. The vertical exaggeration is 7:1.

and the igneous crust, changes rather abruptly to only 5 km. Those depths for the crust-mantle boundary are also consistent with gravity anomaly modeling (Fig. 5.13). The nature of the upper mantle can be inferred from Pn refraction phases. The uppermost mantle shows normal mantle P-wave velocities of 8.1 km/s. The P-wave velocities of the mantle below the Western Plateaus are slightly higher with 8.2 km/s. The crustal thickness of the Western Plateaus ranges between 9.3 km in the Tokelau Basin to 17.2 km west of the Danger Islands Troughs (Figs. 5.7 and 5.12).

#### 5.4.6 Two different magmatic and tectonic regimes on the Manihiki Plateau

In general, the crust of the Manihiki Plateau is severely faulted at its margins and by the troughs intersecting the plateau (Ai *et al.*, 2008; Pietsch and Uenzelmann-Neben, 2015; Winterer *et al.*, 1974) likely due to plate-tectonic reorganization of the Pacific Ocean during the Cretaceous Normal Superchron. In previous works, the Western Plateaus were assumed to be of a similar structure as the High Plateau (Hussong *et al.*, 1979; Viso *et al.*, 2005) due to the lack of data from

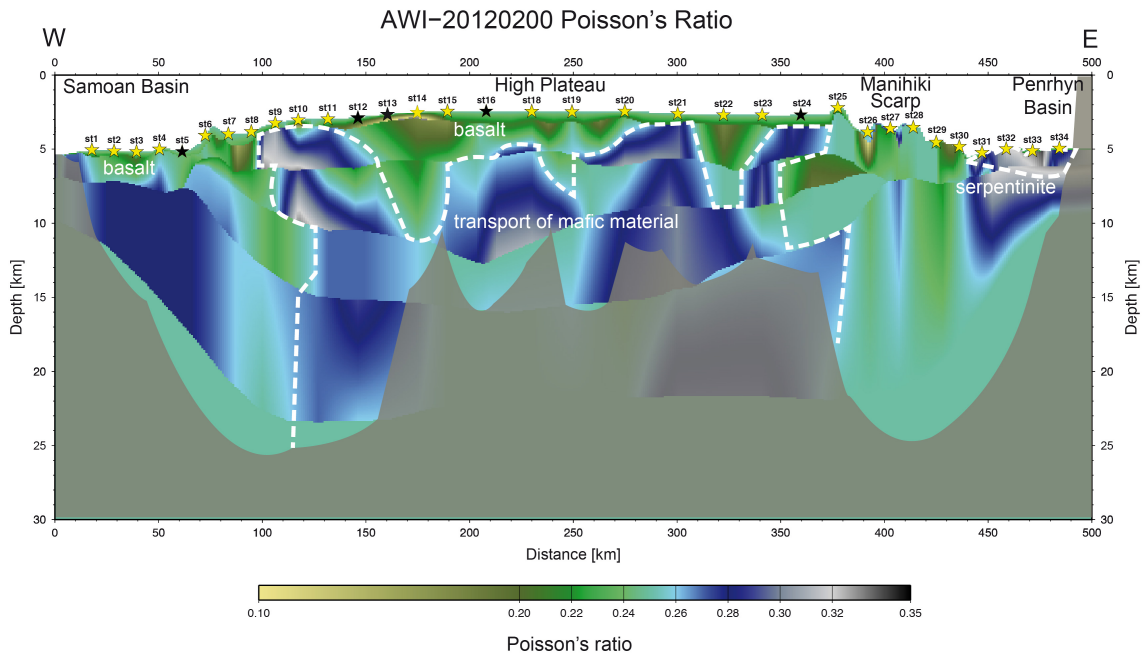


**Figure 5.11:** Calculated Poisson's ratio of AWI-20120200; grey shaded areas are not covered by rays in the S-wave model and therefore cannot return reliable values for the Poisson's ratio. White dashed lines indicate areas of higher Poisson's ratio. The locations of OBS stations are indicated with the yellow (functioning station) and black (malfunctioning station) stars. The vertical exaggeration is 7:1.

deep crustal layers. By interpreting our P- and S-wave velocity and gravity models along with the Poisson's ratio model, the crustal structure of the different sub-provinces as well as their individual margins and adjacent ocean basins can be further constrained. Both sub-provinces exhibit a HVZ in the lower crust. These HVZs with velocities higher than 7.3 km/s are also common at other oceanic LIPs (Coffin and Eldholm, 1994; Coffin et al., 2006; Richards et al., 2013; Ridley and Richards, 2010) and can be related to the presence of gabbros as well as the olivine and pyroxene cumulates (Karlstrom and Richards, 2011; Ridley and Richards, 2010) (Figs. 5.14 and 5.15). The crustal thicknesses of the Western Plateaus and the High Plateau differ. Whereas the High Plateau shows a constant crustal thickness of 20 km, which is comparable to other oceanic LIPs such as the Agulhas Plateau and southern Mozambique Ridge (Gohl and Uenzelmann-Neben, 2001; Gohl et al., 2011; Uenzelmann-Neben et al., 1999) with steep boundaries towards the adjacent oceanic basins, the Western Plateaus show a gradual decrease in the crustal thickness from 17.2 km in the east to 9 km in the west. A clear boundary between normal oceanic crust in the Tokelau Basin and the oceanic LIP cannot be identified because the HVZ is still present below the Tokelau Basin.

The middle crust of both sub-provinces shows similarities in the P- and S-wave velocity structure. The middle crust of the Western Plateaus has a velocity field, which is comparable to the lower-middle crust of the High Plateau. This velocity and density distribution can be associated with gabbroic intrusions (Christensen, 1996; Coffin and Eldholm, 1994; Richards et al., 2013; Rid-

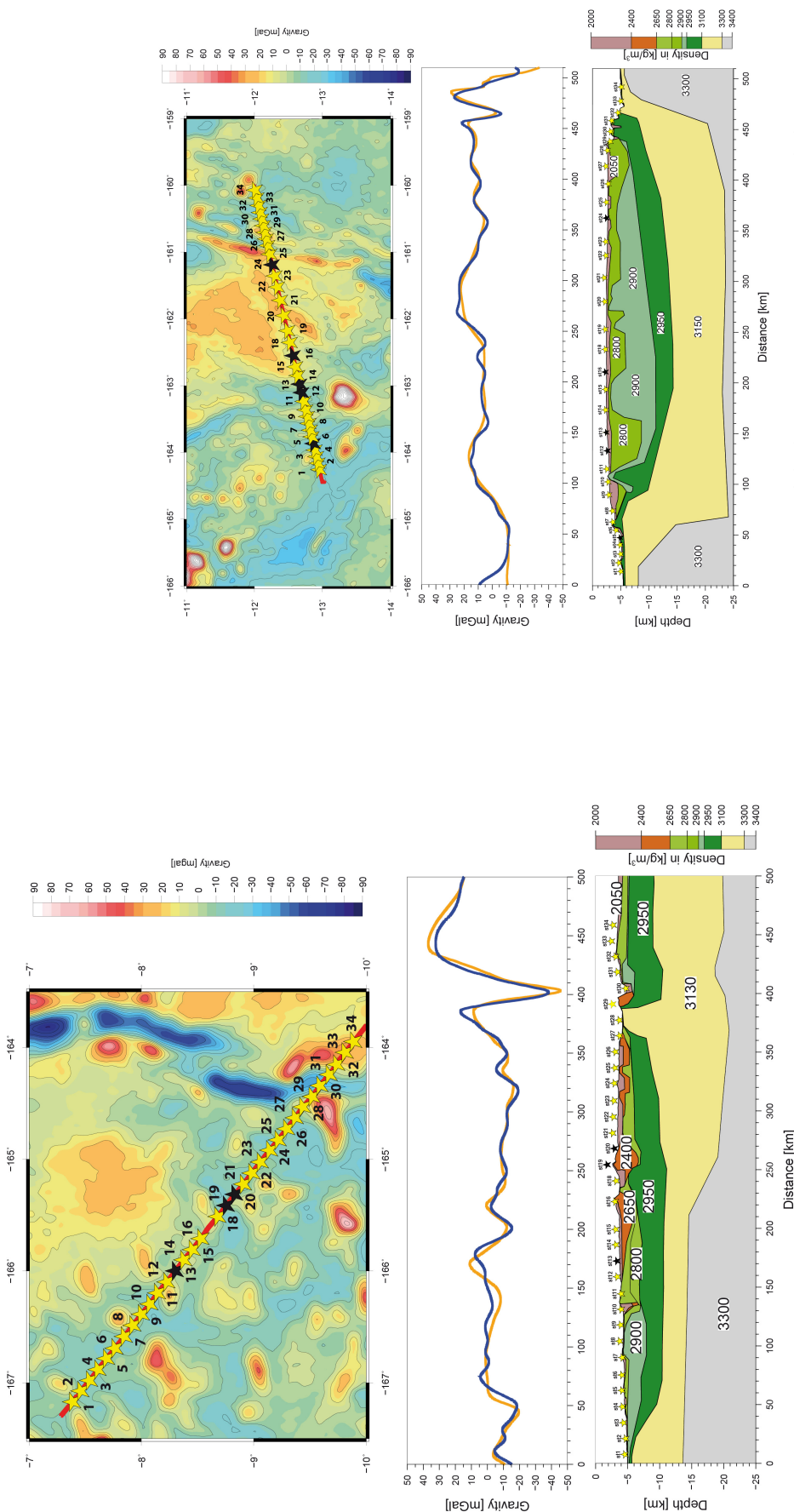


**Figure 5.12:** Gravity model of AWI-20120100 upper panel: free-air gravity anomaly in blue calculated anomaly in orange, middle panel: measured gravity model for AWI-20120100. The locations of OBS stations are indicated with the yellow (functioning station) and black (malfunctioning station) stars. The mean residual value for this model is 3.6 mgal. The largest misfits are created by magmatic features, which lay off profile (e.g. st20 to st22 and st28).

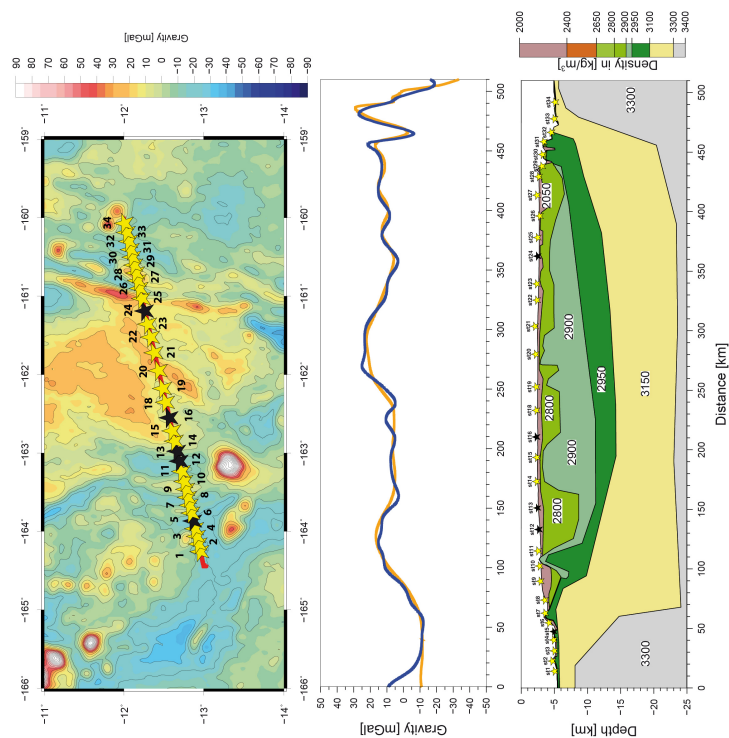


**Figure 5.13:** Gravity model of AWI-20120200 upper panel: free-air gravity anomaly in blue calculated anomaly in orange, middle panel: measured gravity model for AWI-20120200. The locations of OBS stations are indicated with the yellow (functioning station) and black (malfunctioning station) stars. The mean residual value for this model is 5.8 mgal (mean residual value of 2.6 mgal between 40 and 490 km). The largest misfits are created by magmatic features, which lay off profile (e.g. st18 to st20).

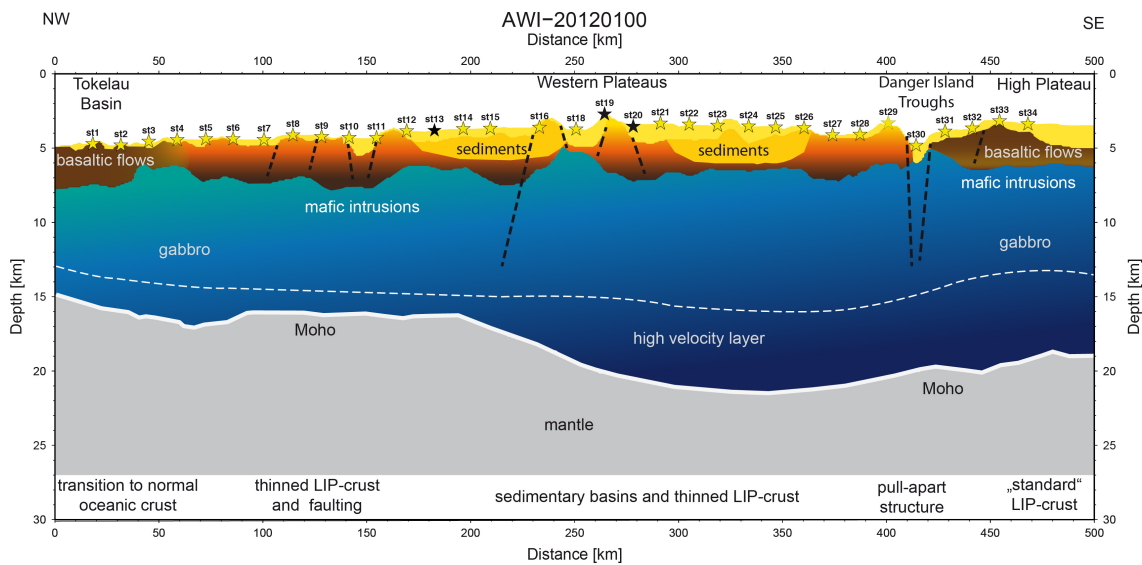


**Figure 5.14:** Sketch of geological interpretation of AWI-20120100, black dashed lines indicate fault systems, the white dashed lines indicate the presence of the HVZ. The vertical exaggeration is 7:1.

ley and Richards, 2010). On the High Plateau, the upper-middle crust shows a slightly different velocity field and a small decrease in density (Tab. 5.1). Such a transitional layer is not present in the Western Plateaus. Additionally, the middle crust underlying the central High Plateau exhibits three large areas of high Poisson's ratio, which correspond to magmatic centres observed in the seismic reflection data (Fig. 5.11) (Pietsch and Uenzelmann-Neben, 2015). These zones mark former magmatic pathways towards the seafloor of the High Plateau, possibly during a later magmatic stage (Fig. 5.15) (Pietsch and Uenzelmann-Neben, 2015). Karlstrom and Richards (2011) published a model of LIP crustal magma transport, which indicates the formation of individual upward migrating sills during later stages of magmatic activity. Similar structures as e.g. magmatic centres and massive basaltic flow units cannot be observed on the Western Plateaus. The secondary (or late stage) magmatic activity on the Western Plateaus is restricted to low volume seamount volcanism and to small volume magmatic activity along fault zones (Fig. 5.6).

The upper crust of the two sub-provinces differs significantly. The High Plateau consists of countless volcanic centres, which are partly eroded and covered and interbedded by volcanoclastic and pelagic sedimentary rocks (Ai et al., 2008; Beiersdorf et al., 1995b). Thus, the upper crust consists of basaltic flow units as well as subvolcanic intrusions (Karlstrom and Richards, 2011), possibly interlayering each other as a result of the multiple stages of secondary magmatism. Massive fault systems are only present at the margins of the High Plateau (Fig. 5.15) (Ai et al., 2008; Viso et al., 2005; Winterer et al., 1974). At the Manihiki Scarp, deeper crustal layers, most likely consistent with the lower-middle crust, crop out at the seafloor in multiple ridges. Based on gravity data, Viso et al. (2005) postulated that the upper crust was serpentinized in this area. We can further support this assumption by high values in the Poisson's ratio (Fig. 5.11)



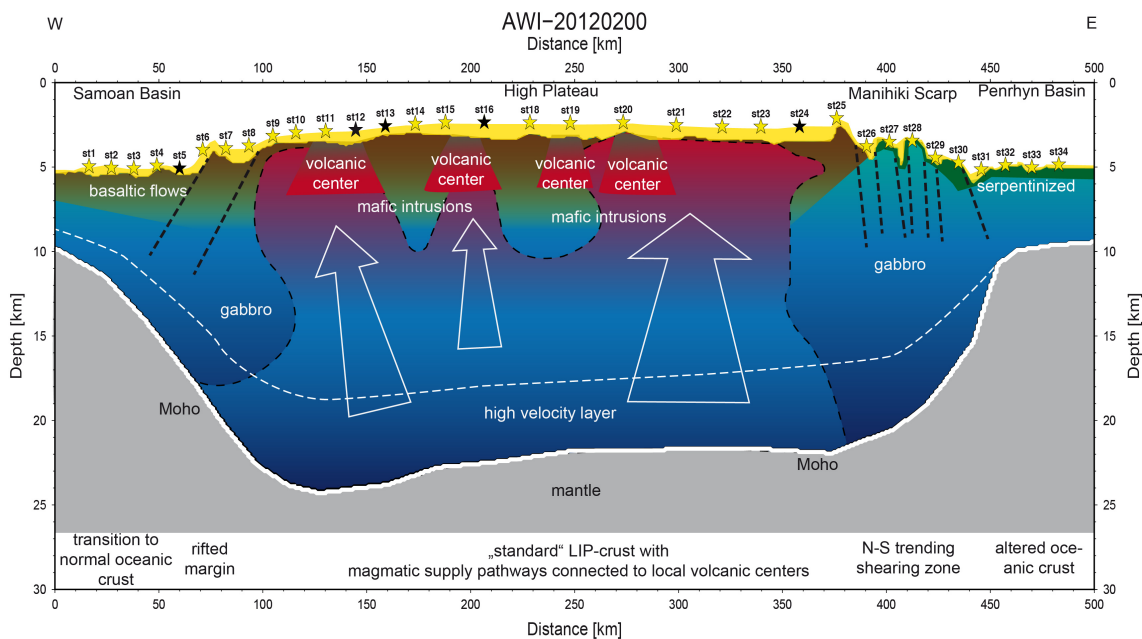


**Figure 5.15:** Sketch of geological interpretation of AWI-20120200, white arrows indicate areas of magmatic upwelling, black dashed lines indicate fault systems, dashed white lines indicate the presence of the HVZ. The vertical exaggeration is 7:1.

and lower densities (Fig. 5.13) at the Manihiki Scarp and the Penrhyn Basin and interpret mafic material, which has been partly serpentinized in this area. The margins towards the Samoan Basin and the Samoan Basin themselves show basaltic flow units and have no indications for large-scale serpentinization in this area. Whereas the High Plateau shows clear indications for multiple magmatic phases within its upper crust, the data from the Western Plateaus present possible basaltic flow units interlayered with mafic intrusions comparable to the upper crust of the High Plateau only in the Tokelau Basin.

Reflection seismic data reveal multiple basement highs interlayered by sedimentary basins and various normal faults (Fig. 5.6). The magmatic activity is limited to low-volume seamount magmatism and the emplacement of magmatic material along weakened zones such as numerous faults (Fig. 5.6). P- and S-wave modeling, as well as gravity anomaly modeling reveal the presence of diverse rock types ranging between igneous rocks and sedimentary rocks. It can be debated whether the upper crust consists of volcanoclastic deposits or even massive carbonate banks (Grevenmeyer *et al.*, 2001). The crust of the Western Plateaus thins step-wise towards the Tokelau Basin. The thinning of the crust of the Western Plateaus could be due to its greater distance from the centre of emplacement of the plateau. On the Ontong Java Plateau, this mode of crustal thinning can be observed at its northern boundaries. The local bathymetry indicates a relative smooth and constant lowering towards the oceanic basin, consistent with basaltic flow patterns (Mochizuki *et al.*, 2005). On the Western Plateaus the gradual decrease of crustal thickness is stepwise. This could not have been achieved by the

lack of magmatic material. An alternative model for this reduction of the crustal thickness could be extensional processes due to tectonic activity. Since the tectonic mechanisms of the spreading at the Nova Canton Trough and the opening of the Ellice Basin are still debated, a clear distinction between tectonic thinning and the lack of magmatic material cannot be drawn on the basis of the current data and plate tectonic reconstructions. Volcanic extrusions, e.g. the occurrence of basaltic flows, can only be interpreted for the Tokelau Basin and are only locally present on the Western Plateaus (Fig. 5.14), mainly at already weakened structures along faults. The southern Western Plateaus are fringed by seamounts which can be related to a phase of magmatic reactivation within the late Cretaceous (*Hoernle et al.*, 2009) and/or < 45 Myr, similar to the islands and prominent seamounts on the High Plateau (*Pietsch and Uenzelmann-Neben*, submitted). The Danger Islands Troughs dissect the Manihiki Plateau into the two main sub-provinces. The troughs are characterized by the absence of typical upper crustal material (Fig. 5.14). The lower crustal layers as well as the crust-mantle boundary show only few relicts of former tectonic activity such as an updoming of the mantle at this position or a thinning of the lower crust. In the middle crust, the Danger Islands Troughs mark the distinct change over between a single layer middle crust on the Western Plateaus and the upper-middle crust and lower-middle crust of the High Plateau (Figs. 5.2b and 5.14). The thinning of the upper crustal material and the lack of an updoming of the mantle suggest, that the Danger Islands Troughs are formed as a series of pull-apart basins. The previously suggested formation as an initial rift system (*Taylor*, 2006; *Winterer et al.*, 1974) seems unlikely since upper crustal material is thinned and fault systems indicate a shearing component (*Nakanishi et al.*, 2015). Additionally the Danger Islands Troughs seem to separate two areas of the Manihiki Plateaus with different crustal properties within their upper and middle crust, the magmatically highly active central High Plateau, which exposes tectonic activity mainly at its margins and the Western Plateaus, which underwent smaller magmatic alteration and shows a thinning of the crust.

## **5.5 Discussion: Western Plateaus vs. High Plateau – two different crustal environments of the Manihiki Plateau**

This paper presents the first comprehensive insight into the crustal structure of the two major sub-provinces of the Manihiki Plateau. The results of our analyses revise earlier models. The Western Plateaus and the High Plateau of the Manihiki Plateau exhibit similar features, such as a continuous HVZ within the lower crust, but also show large differences, especially in the upper crustal layers and the crustal thicknesses.

### **5.5.1 Comparison with other oceanic LIPs**

By comparing the Western Plateaus and the High Plateau with other oceanic LIPs, the crustal thickness and velocity-depth distribution of the High Plateau resembles those of the Kerguelen Plateau (*Charvis and Operto*, 1999), Broken Ridge (*Francis and Raitt*, 1967), Agulhas Plateau (*Gohl and Uenzelmann-Neben*, 2001; *Parsieglä et al.*, 2008) and Mozambique Ridge (*Gohl et al.*,

2011) (Fig. 5.16). The proportional velocity-depth distribution is also similar to that of the southern Ontong Java Plateau (Miura *et al.*, 2004), but the Ontong Java Plateau exhibits up to twice the crustal thickness at various locations (Furumoto *et al.*, 1976; Gladchenko *et al.*, 1997; Klosko *et al.*, 2001; Richardson *et al.*, 2000). A dominant feature of all oceanic LIPs is the HVZ of the lower crust with P-wave velocities ranging between 7.3 and 7.7 km/s (Fig. 5.16) (Coffin and Eldholm, 1994; Ridley and Richards, 2010). Both the Western Plateaus and the High Plateau show such high P-wave velocities in the lower crust. The HVZ is also continuous between the two sub-provinces in the Danger Island Troughs area. High velocities are also present in the lower middle crust (P-wave velocities between 6.3 and 7.0 km/s). The continuous presence of the HVZ suggests a process, in which today's Manihiki Plateau was emplaced as a single continuous and larger LIP ("Greater Manihiki Plateau") during a first magmatic phase possibly connected to the Hikurangi Plateau and the Ontong Java Plateau.

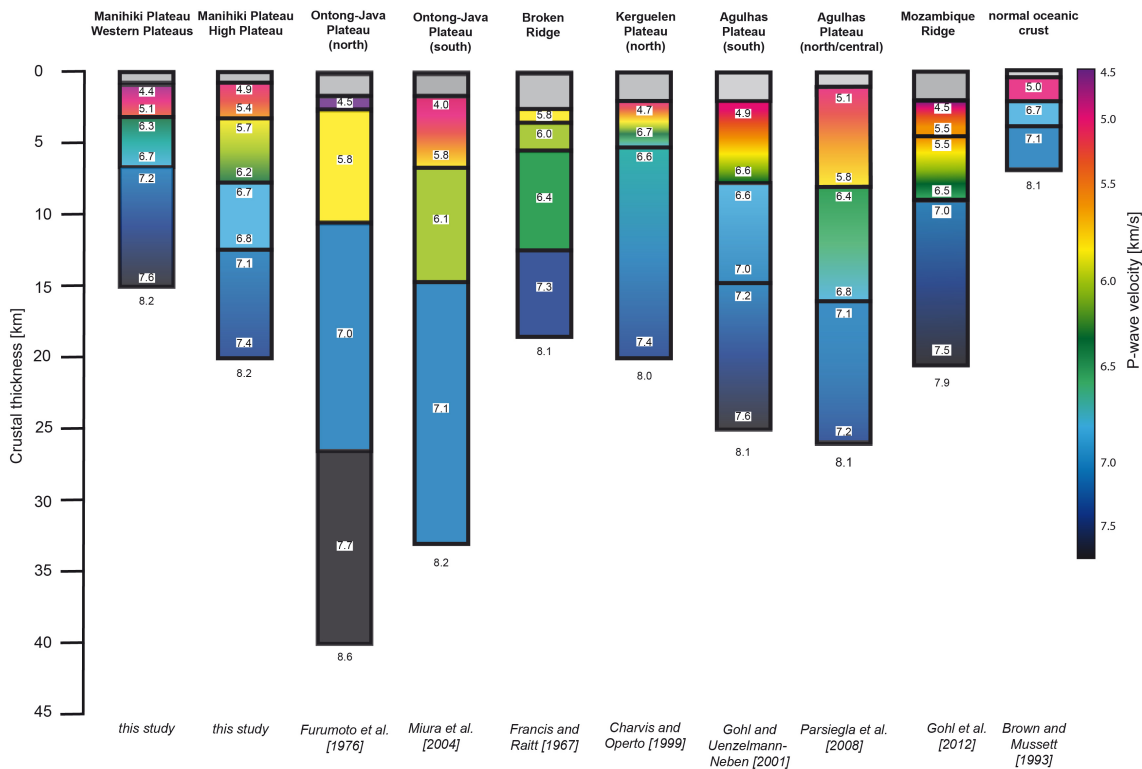


**Figure 5.16:** Comparison of the crustal structure of the Western Plateaus and the High Plateau with other oceanic LIPs; The grey shaded areas represent the sedimentary cover. The high velocity zone of the lower crust is represented in the dark blue colours. The transitional crustal layer is depicted in the yellow and orange colours.

The High Plateau along with other oceanic LIPs has an upper middle crustal layer of P-wave velocities 5.0 to 5.8 km/s (yellow to orange colours in Fig. 5.16). This layer is present on all previously presented LIPs as part of the middle crust but is not always resolved as an individual crustal unit constrained by intracrustal reflections. Surprisingly, this transitional layer with its specific velocity range is not present on the Western Plateaus (Fig. 5.16) leaving a large gap in

the relative continuous P-wave velocity distribution within the igneous crust of a LIP. Therefore the Western Plateaus are not presenting a substantial crustal layer present in all other oceanic LIPs, a layer associated with mafic intrusions formed during later stages of magmatic activity (*Karlstrom and Richards, 2011*). This provides an important indication that the magmatism on the Western Plateaus might differ from the magmatic activity of the High Plateau during secondary magmatic stages. The uppermost crust of oceanic LIPs mainly consists of basaltic flow units interlayered with pillow lavas and possibly volcanoclastic layers formed by regional secondary volcanic phases (*Hoernle et al., 2010; Inoue et al., 2008; Timm et al., 2011*). The High Plateau shows local volcanic centres, which have been the outlets of extrusive volcanism during secondary magmatic phases, similar as observed on the Ontong Java Plateau (*Inoue et al., 2008*) or the Hikurangi Plateau (*Davy and Wood, 1994; Davy et al., 2008; Hoernle et al., 2010*). Extrusive and intrusive magmatic activity is also visible in seismic reflection data throughout the High Plateau (*Pietsch and Uenzelmann-Neben, 2015*). Buried seamount chains can also be located in gravity anomaly grids on the High Plateau of the Manihiki Plateau (Fig. 5.13). On the contrary, the upper crust of the Western Plateaus consist of several areas of very low velocities and low rock densities that are associated with volcanoclastic sedimentation and carbonate banks rather than with igneous rocks (*Grevenmeyer et al., 2001*). Seamounts and seamounts are mainly located at the margins and result from later magmatic reactivation phases in the late Cretaceous and/or from the overriding of the Tahiti and Society Islands hotspots during the Eocene. Neither the seismic refraction/wide-angle reflection data nor the multichannel seismic reflection data acquired on the central Western Plateaus indicate extensive secondary magmatism such as the massive and wide-ranged emplacement of basaltic flow units. Short wavelength gravity anomalies are mainly attributed to basement highs and the local occurrence of seamounts (Figs. 5.6 and 5.12). Basaltic flow units cropping out at the seafloor are only present in the Tokelau Basin. On the central Western Plateaus, deep basins of lower velocities are imbedded into igneous material. We can therefore distinguish the two sub-provinces of the Manihiki Plateau by their middle and upper crust. A wide variety of rock types are included in the upper crust of the Western Plateaus, whereas the upper crust of the High Plateau consists of basaltic flow units and volcanoclastic and/or carbonate successions. The lower and lower-middle crust of the High Plateau and the Western Plateaus are similar to previously described oceanic LIPs. The two main sub-provinces of the Manihiki Plateau hence must have undergone a different magmatic evolution after their initial emplacement phase.

### **5.5.2 The role of the HVZ in the lower crust of the Manihiki Plateau**

The HVZ in the lower crust is a key component of a LIP (*Coffin and Eldholm, 1994; Ridley and Richards, 2010*). The HVZ is a result of the upwelling of very hot mantle material and consists of an olivine and pyroxene crystal fraction captured above the Moho (*Karlstrom and Richards, 2011; Ridley and Richards, 2010*). The presence and absence of the HVZ within the lower crust can be seen as an indicator for the emplacement mechanism of the igneous volume and allows the distinction between LIP – related crust and oceanic crust created by seafloor-spreading



processes. On the Manihiki Plateau, the HVZ is present within the whole lower crust and is not intersected at the Danger Islands Troughs (Fig. 5.14). This suggests that the Manihiki Plateau was emplaced as a single crustal unit, and that the formation of different sub-provinces is restricted to the upper and middle crustal layers. Furthermore, the HVZ indicates various tectonic forces acting on the margins of the Manihiki Plateau. Our data cover three different margins, the Manihiki Scarp, the margins towards the Samoan Basin and the Tokelau Basin. At the Manihiki Scarp, the HVZ rather terminates abruptly (Figs. 5.9 and 5.15). The Penrhyn Basin does not show high P-wave velocities in its lower crust. Tectonically, the Manihiki Scarp is a strike-slip zone (*Larson et al.*, 2002; *Viso et al.*, 2005), where a subducted fragment of the Manihiki Plateau was emplaced. The sudden termination of the HVZ illustrates this razor-sharp boundary between the LIP and the adjacent Penrhyn basin. This clear distinction between LIP-related crust and surrounding oceanic basins can neither be seen in the Samoan Basin nor in the Tokelau Basin. The Samoan Basin shows a thin HVZ (Figs. 5.9 and 5.15). Therefore, the margin of the High Plateau and the adjacent ocean basin experienced a plume/hotspot-influence after the break-up between the Manihiki Plateau and the Hikurangi Plateau by the formation of the Osborn Trough. On the Western Plateaus, the Tokelau Basin shows a clear HVZ in its lower crust (Figs. 5.7 and 5.14). This implies that the crust present in the Tokelau Basin is in fact still part of the Manihiki Plateau and was not produced as a part of the “normal” oceanic seafloor spreading in the Ellice Basin. By close evaluation of the measured and modelled P- and S-wave velocities, we can compare our findings to the results of Richards et al. (2013). The authors modelled multiple batch melting processes recreating the high-velocity, ultramafic, intrusive body below hotspot tracks. These intrusive features are – at smaller scale – similar to a HVZ below an oceanic LIP. Applying the calculations by Richards et al. (2013), our P- and S- wave velocities suggest an emplacement scenario for the HVZ below the High Plateau with a 30% liquid melt fraction of a MgO portion of 15-20 wt%. This would result in a potential melting temperature of 1850 °K, which is in accordance with new geochemical data from the area (*Golowin et al.*, 2014; *Timm et al.*, 2011).

### 5.5.3 Emplacement scenario of the Manihiki Plateau and its two major sub-provinces

The initial magmatic event of a LIP emplaces approximately 75% of the total igneous volume of the igneous province (*Bryan and Ernst*, 2008; *Karlstrom and Richards*, 2011). Therefore the lower and middle crustal layers of the two sub-provinces of the Manihiki Plateau show similar attributes such as their density and P- and S-wave distribution. The lower and middle crust are suggested to have been emplaced during the “Greater Ontong Java Nui event” creating the LIPs of the southwestern Pacific Ocean (*Chandler et al.*, 2012, 2013; *Taylor*, 2006). As a previously presumed process, the initial emplacement of the “Greater Manihiki Plateau” took place as a single crustal block, which included all present sub-provinces as well as later subducted fragments. To the south, the Hikurangi Plateau was emplaced simultaneously. The High Plateau of the Manihiki Plateau was emplaced at subaerial level or close to sea level (*Ai et al.*, 2008; *Schlanger et al.*, 1976; *Simoneit et al.*, 2014). *Pietsch and Uenzelmann-Neben* (2015) report

intra-basalt reflections representing areas of a possible subaerial exposition, which correspond to the upper boundary of the upper-middle crust on the High Plateau. Strong wide-angle reflections throughout the High Plateau (Figs. 5.4 and 5.9) support the presence of subaerial lava flows, possibly interbedded with volcanoclastic sediments emplaced during the initial plateau formation. At this stage, two geochemically different types of tholeiitic basalts have been formed at the Manihiki Plateau. The first group shows EM I (enriched mantle I) type signatures and is similar to basement lavas of the Ontong Java Plateau. The second group, on the other hand comprises tholeiitic basalts with a U-shaped incompatible element patterns and unusually low abundances of several elements (Golowin *et al.*, 2014; Ingle *et al.*, 2007; Timm *et al.*, 2011). Basalts showing this composition, have not been reported on other parts of the “Greater-Ontong-Java event” related LIPs so far. Ingle *et al.* (2007) propose a formation of these magmas in a subduction zone setting by extensive melting of a depleted mantle wedge material and addition of subducted, possibly ocean island derived volcanoclastic sediments. This hypothesis, however, is not consistent with our seismic data, which do not show any evidence of abnormalities, such as lateral velocity and density changes within the mantle beneath the Manihiki Plateau. Alternative models, being in better accordance with our data, have been presented by Timm *et al.* (2011) and Golowin *et al.* (2014). These authors explain the formation of the unusual basaltic compositions by hot melting of a depleted mantle source and mixing with an enriched HIMU (high  $\mu$ : high  $^{238}\text{U}/^{204}\text{Pb}$ -ratio) component being similar to the source of late-stage magmatism of all “Greater-Ontong-Java event” related plateaus. This scenario supports our findings of a continuous HVZ on the Manihiki Plateau as an indicator of massive upwelling of hot mantle material.

The fragmentation of the “Greater Manihiki Plateau” followed this first magmatic phase (Chandler *et al.*, 2012, 2013; Hoernle *et al.*, 2004a, 2010; Taylor, 2006; Timm *et al.*, 2011; Worthington *et al.*, 2006) (Fig. 5.17). The Danger Island Troughs, which separate the High and the Western Plateau, formed during this time (Ingle *et al.*, 2007; Nakanishi *et al.*, 2015; Timm *et al.*, 2011). Faulting occurred throughout the Manihiki Plateau, especially at its margins such as the Manihiki Scarp, where a transform fault developed (Larson *et al.*, 2002; Viso *et al.*, 2005). If the joined emplacement of the Manihiki Plateau and the Ontong Java Plateau is a testable hypothesis, it can be assumed that, after the initial emplacement, clock-wise rotational motion (Chandler *et al.*, 2013) acted as well on the adjacent Western Plateaus. Such a rotation is indicated by a series of pull-apart basins in the Danger Islands Troughs (Nakanishi *et al.*, 2015). To the south, the Hikurangi Plateau rifted away from the High Plateau of the Manihiki Plateau with the development of the Osborn Trough spreading centre (Billen and Stock, 2000; Davy *et al.*, 2008; Worthington *et al.*, 2006). During and after the establishment of seafloor spreading encircling the Manihiki Plateau, a secondary magmatic stage started, resulting in seamount volcanism and the emplacement of basaltic flows (Ai *et al.*, 2008; Pietsch and Uenzelmann-Neben, 2015; Winterer *et al.*, 1974) (Fig. 5.17). Secondary magmatism formed the upper crust of the Manihiki Plateau by intrusions and extrusive volcanism mainly of alkalic composition (Clague, 1976; Hoernle *et al.*, 2010; Ingle *et al.*, 2007; Timm *et al.*, 2011). We interpret relicts of volcanic centers as

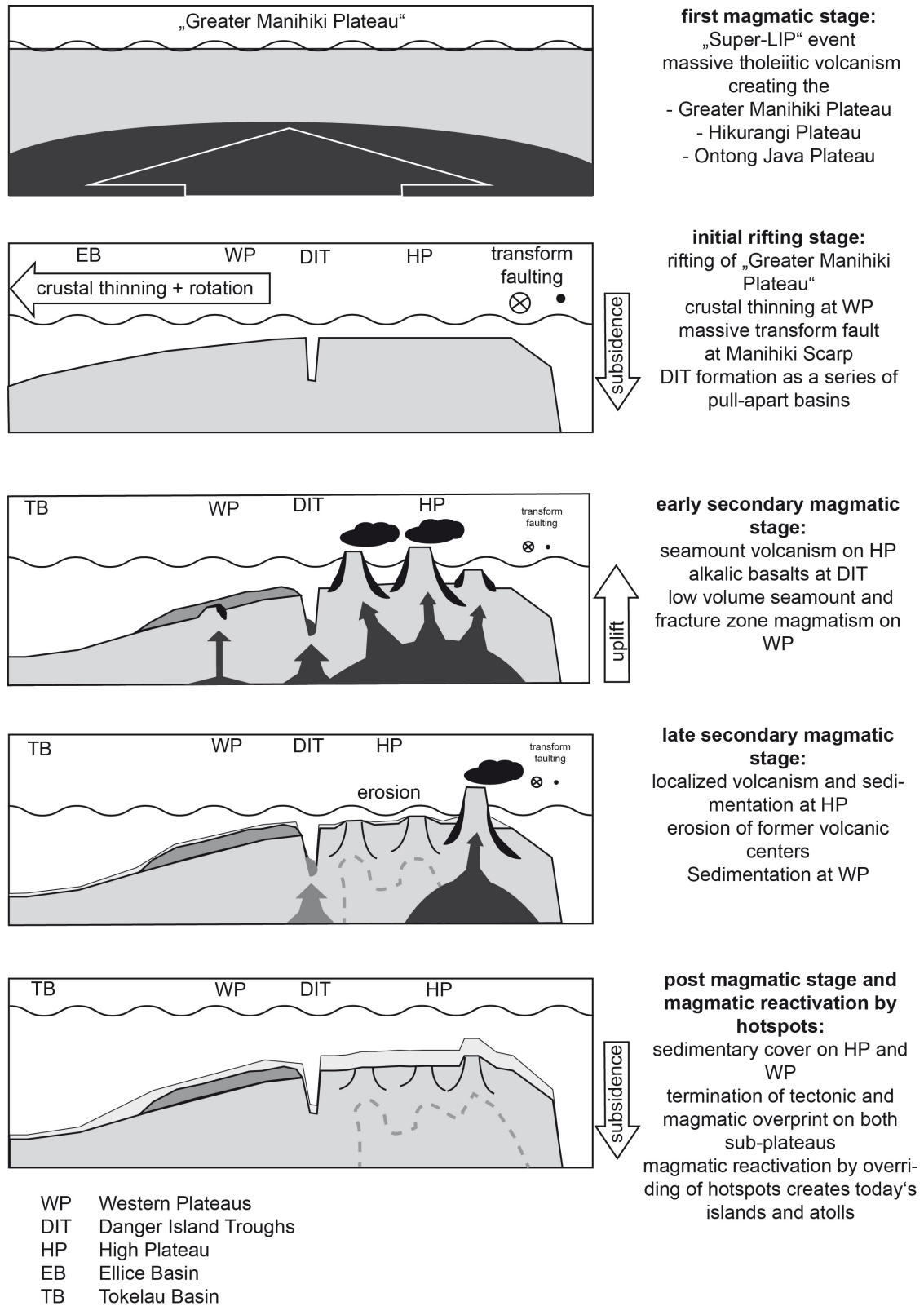


**Figure 5.17:** Sketch of the evolution of the Manihiki Plateau with special focus on the High Plateau and the Western Plateaus from the early Cretaceous to the current setting

well as magmatic pathways within the crust of the High Plateau from our data. At the Danger Islands Troughs, alkaline lavas with a strong enrichment in light rare earth and large-ion lithophile elements were emplaced (*Ingle et al.*, 2007). A comparable amount of igneous material could not be identified in our data from the Western Plateaus, where only low-volume magmatic activity is concentrated along fault systems and localized seamounts. On the High Plateau secondary magmatic phases (>65 Ma) resulted in smoothing of the basement by the emplacement of volcanoclastic sedimentation and basaltic flows (*Pietsch and Uenzelmann-Neben*, 2015). The basement of the Western Plateaus is rough and sedimentation is restricted to pockets between basement highs. Upper crustal layers created during secondary magmatic stages could have been certainly eroded as they were close to the sea surface. In this case, erosion should have been very effective, and magmatic pathways and late stage mafic intrusions should be visible in the middle crustal layers of the presented models (Figs. 5.14 and 5.15). On the High Plateau, weathering products of the volcanic edifices formed during secondary volcanic stages are incorporated into the volcanoclastic sedimentation (*Schlanger et al.*, 1976), which leads to the build up of about 200 m thick volcanoclastic units (*Ai et al.*, 2008; *Pietsch and Uenzelmann-Neben*, 2015). Comparable strata cannot be found on the Western Plateaus, where it is not possible to distinguish between different secondary magmatic phases within the reflection seismic data (*Pietsch and Uenzelmann-Neben*, 2015). Also, the unusual low velocities of parts of the acoustic basement infer that volcanoclastic and/or carbonate sedimentation occurred within tectonic pockets on the Western Plateaus (Fig. 5.14). As no rock samples from the central Western Plateaus are available for ground-truthing, we rely only on geophysical parameters. Carbonate sedimentation, e.g. the build-up of carbonate platforms, is likely, since the Manihiki Plateau did not reside below the Carbonate Compensation Depth (*Van Andel*, 1975) during its entire lifespan. As the upper crust, consisting of sedimentary rocks, thins towards the west, and magmatic rocks become present again, it is likely that this portion of the Western Plateaus had already subsided deeper and was farther away from the source region of volcanoclastic sedimentation. Therefore, the western Western Plateaus, towards the Tokelau Basin experienced less sedimentation, and magmatic rocks are exposed in the upper crust. During a later stage of secondary magmatism, its activity on the High Plateau weakened and moved its activity centre to the east and towards the margins, as eastern volcanic structures are better preserved and early deformed sedimentary layers are visible in seismic reflection data (*Ai et al.*, 2008) (Fig. 5.17). Older volcanic edifices are eroded, leading to an almost smooth acoustic basement in the seismic reflection data (*Pietsch and Uenzelmann-Neben*, 2015). After the last main magmatic pulse ceased, further pelagic sedimentation covered most of the volcanic relicts and the faults and ridges generated by tectonic motion. The Manihiki Plateau subsided to the current water-depth of 2600 m for the High Plateau and 4000-3600 m for the Western Plateaus (Fig. 5.17).

In summary, the different sub-plateaus of the Manihiki Plateau experienced multiple stages of magmatic emplacement. The initial emplacement was a rapid subaerial emplacement of massive amounts of igneous material. Later volcanic stages differ between the two main sub-

provinces. Whereas the High Plateau experienced multiple phases of massive secondary magmatism, the magmatism on the Western Plateaus was restricted to pre-weakened fault zones and low-volume seamount volcanism. The Danger Islands Troughs, a series of pull-apart basins, form the prominent dissection between those two sub-provinces and their different evolution after the initial emplacement of the Manihiki Plateau.

### 5.6 Conclusions

We present the first seismic refraction/wide-angle reflection P-wave and S-wave models of the two main sub-provinces – the Western Plateaus and the High Plateau – of the Manihiki Plateau. From the newly gained information on the crustal structure of the sub-provinces, the tectonic and magmatic evolution of this oceanic LIP can be further illuminated. Additionally we gain insight into the relationship between the sub-provinces, which have been treated as a single crustal block in previous studies. The High Plateau shows key features of a LIP such as a HVZ in the lower crust and basaltic flow units in the upper crust. The crustal thickness presents a constant 20 km throughout the southern High Plateau. Eruptive centers of secondary magmatic phases are visible in the upper crust and major magmatic pathways can be traced in the middle and lower crust of the LIP throughout the High Plateau. The Western Plateaus, on the other hand show a stepwise decrease in crustal thickness from 17.3 km in the east to 9.2 km in the west. The presence of the HVZ within the lower crust indicates a joined emplacement with the High Plateau during an initial magmatic stage. The upper crust of the Western Plateaus does not consist of major basaltic flow units and massive amounts of volcanoclastics such as the upper crust of the High Plateau. Therefore we propose an individual development of the two main sub-provinces of the Manihiki Plateau after the initial emplacement of the LIP. The two sub-provinces show a clear distinction between later magmatic stages, which has not been reported for any other oceanic LIP so far.

### Acknowledgements

We thank Ernst Flüh and Jörg Bialas of GEOMAR for providing the OBS and OBH systems. We also thank Cpt. L. Mallon and his crew of RV Sonne for their support and assistance during the cruise SO-224. This project contributes to the Workpackage 3.2 of the AWI Research Programm PACES-II. This project has been funded through a grant by the German Federal Ministry of Education and Research (BMBF) under project number O3G0224A and by institutional resources of the AWI.

# 6 Playing jigsaw with Large Igneous Provinces - a plate tectonic reconstruction of Ontong Java Nui

K. Hochmuth<sup>1</sup>, K. Gohl<sup>1</sup> and G. Uenzelmann-Neben<sup>1</sup>

<sup>1</sup>Alfred-Wegener Institut Helmholtz-Zentrum für Polar- und Meeresforschung

## Keypoints

- new plate kinematic reconstruction of the western Pacific during the Cretaceous
- detailed break-up scenario of the “Super” Large Igneous Province Ontong Java Nui
- Ontong Java Nui “Super” - Large Igneous Province as result of plume-ridge interaction

## Abstract

The three largest Large Igneous Provinces (LIP) of the western Pacific – Ontong Java, Manihiki and Hikurangi plateaus – were emplaced during the Cretaceous Normal Superchron and show strong similarities in their geochemistry and petrology. The plate tectonic relationship between those LIPs, herein referred to as Ontong Java Nui, is uncertain, but a joined emplacement was proposed by *Taylor (2006)*. Since this hypothesis is still highly debated and struggles to explain features such as the strong differences in crustal thickness between the different plateaus, we revisited the joined emplacement of Ontong Java Nui in light of new data from the Manihiki Plateau. By evaluating seismic refraction/wide-angle reflection data along with seismic reflection records of the margins of the proposed “Super”-LIP, a detailed scenario for the emplacement and the initial phase of break-up has been developed. The LIP is a result of an interaction of the arriving plume head with the Phoenix-Pacific spreading ridge in the early Cretaceous. The break-up of the LIP shows a complicated interplay between multiple microplates and tectonic forces such as rifting, shearing and rotation. Our plate kinematic model of the western Pacific incorporates new evidence from the break-up margins of the LIPs, the tectonic fabric of the seafloor as well as previously published tectonic concepts such as the

rotation of the LIPs. The updated rotation poles of the western Pacific allow a detailed plate tectonic reconstruction of the region during the Cretaceous Normal Superchron and highlights the important role of LIPs in the plate tectonic framework.

**Keywords:**

Large Igneous Provinces, Manihiki Plateau, Ontong Java Nui, plate kinematic reconstruction, western Pacific

**Index Terms:**

3040 Plate tectonics

3038 Oceanic plateaus and microcontinents

8137 Hotspots, large igneous provinces and flood basalt volcanism

8415 Intraplate processes

## 6.1 Introduction

The plate tectonic set-up of the central and western Pacific since the Cretaceous is a mosaic of multiple small and short-lived oceanic plates and continental fragments. Plate kinematic reconstructions (e.g. by *Chandler et al.*, 2012; *Davy et al.*, 2008; *Seton et al.*, 2012) struggle to explain all the features of the difficult interplay between Large Igneous Provinces (LIP), relict spreading centers, subduction and hotspot volcanism overprinting the area. As the generation of most of the oceanic crust of the Western Pacific takes place during the Cretaceous Normal Superchron (CNS), no magnetic seafloor-spreading anomalies constrain the plate tectonic reconstructions (Fig. 6.1). The remnants of the proposed “Super”-LIP (Ontong Java Nui) emplacement during the early Cretaceous (*Chandler et al.*, 2012, 2013; *Taylor*, 2006) play an important role in this set-up, since two former components of this Super-“LIP” - the Ontong Java Plateau and the Hikurangi Plateau - interact with subduction trenches bordering the Australian Plate (Fig. 6.1) and were possibly individual oceanic plates during the Cretaceous. We suggest that the termination of the subduction at the eastern Gondwana margin is caused by the arrival of the Hikurangi Plateau at the subduction zone (*Billen and Stock*, 2000; *Davy*, 2014; *Davy and Wood*, 1994; *Davy et al.*, 2008, 2012; *Luyendyk*, 1995; *Matthews et al.*, 2012; *Reyners*, 2013; *Timm et al.*, 2014). This process initiated a global plate reorganization event (*Matthews et al.*, 2012). The third major LIP component, the Manihiki Plateau, has currently no direct interaction with active plate boundaries, but tectonic deformation at its margins, due to the possible break-up of Ontong Java Nui and internal fragmentation must have occurred during the Cretaceous (*Winterer et al.*, 1974). The internal fragmentation and partitioning of the Manihiki Plateau into three sub-provinces has previously been ignored by all published plate tectonic reconstructions. Recent findings reveal distinct differences in the tectonic and magmatic evolution between the main two sub-provinces the Western Plateaus and the High Plateau (*Hochmuth et al.*, in review;

*Pietsch and Uenzelmann-Neben, 2015*). In this paper, we analyze the role of the Ontong Java Nui LIPs in the plate tectonic framework of the western Pacific Ocean and revisit the hypothesis of the coupled emplacement of the major LIPs of the western Pacific as proposed by Taylor [2006] and Chandler et al. [2012]. By re-examining available seismic refraction/wide-angle reflection data along with seismic reflection records and global gravity and bathymetry grids, we present a more detailed reconstruction of the emplacement of the western Pacific's LIPs, possible break-up scenarios and the role of internal fragmentation of the Manihiki Plateau.

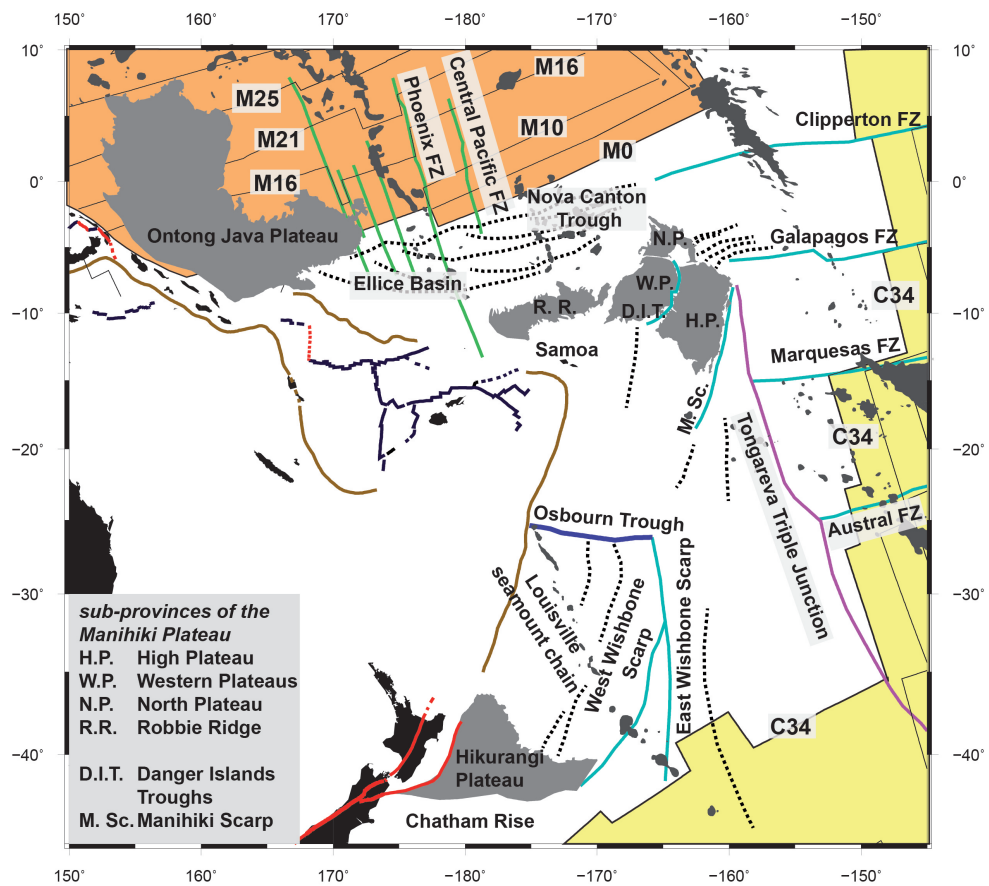


**Figure 6.1:** Current plate tectonic set-up of the western Pacific Ocean; active subduction zones are shown in brown, transform faults in red and mid-ocean ridges in black. Black dashed lines are tectonic lineations tracked from magnetic anomaly maps (*Maus et al., 2009*) and gravity anomaly maps (*Sandwell et al., 2014*). Green and turquoise lines indicate fault zones within Jurassic seafloor (*Nakanishi et al., 1992*) and Cretaceous seafloor respectively. The former spreading center at the Osbourn Trough is marked in blue and the Tongareva Triple Junction Trace is marked in magenta. Isochrons (thin black lines) are taken from *Seton et al. (2012)* and are shaded in orange for the M-Series and in yellow for the C-Series on the Pacific Plate. Pacific seafloor emplaced during the CNS is shown in white.



## 6.2 Geological Setting

### 6.2.1 The Large Igneous Provinces of the western Pacific

The crustal structure and geodynamic development of LIPs differ greatly from those of normal oceanic crust. Although the igneous material (basalt in the upper crust, gabbros in the lower crust) is the same, the crust of LIPs is three times thicker on average than that of normal oceanic crust (Coffin and Eldholm, 1994; Ridley and Richards, 2010).

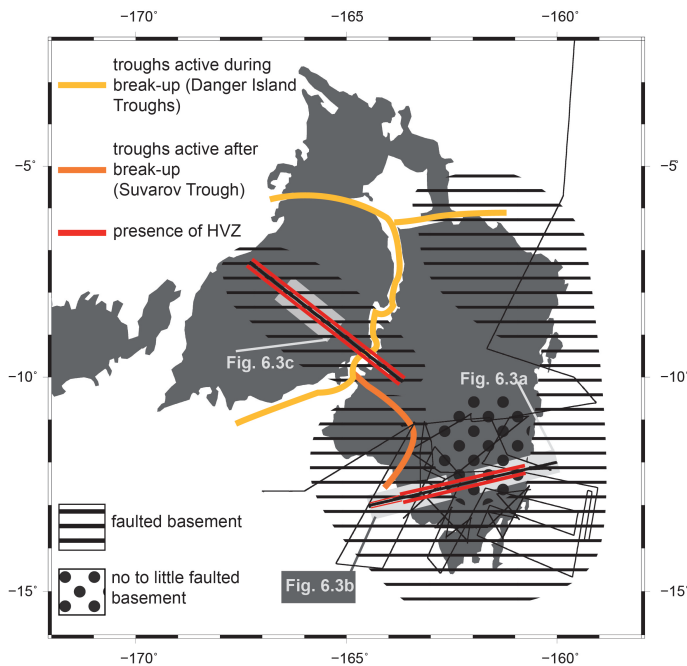


**Figure 6.2:** Relicts of tectonic alteration on the Manihiki Plateau as seen in seismic reflection lines from So-224 and KIWI-12 (thin black lines) and seismic refraction lines (thick black lines) from So-224. Dashed areas indicate faulted basement. The dotted areas show little to no faulting within the basement. The yellow line indicates a series of troughs (e.g. Danger Islands Troughs) active during the supposed break-up of Ontong Java Nui. The orange line marks the Suvarov Trough, which was active after the initial break-up. The red lines on the seismic refraction profiles indicate the presence and thickness of the High Velocity Zone (HVZ), within the P-wave velocity models. The position of the seismic refraction profiles shown in Fig. 6.3 is indicated by the light grey boxes.

The Ontong Java Plateau has a crustal thickness of  $>30$  km (Furumoto *et al.*, 1976; Miura *et al.*, 2004). Crustal thickness of the High Plateau of Manihiki Plateau is about 20 km (Hochmuth *et al.*, in review). The Western Plateaus of the Manihiki Plateau show a crust that thins from a maximum crustal thickness of 17 km in the east to 9 km in the west (Hochmuth *et al.*, in review). The crustal thickness of the Hikurangi Plateau is inferred to be approximately between 17 km and 23 km from gravity modeling (Davy *et al.*, 2008). All these LIPs experienced phases of secondary magmatic and volcanic activity, which partly overprinted tectonic sutures (Davy *et al.*, 2008; Hoernle *et al.*, 2010; Inoue *et al.*, 2008; Pietsch and Uenzelmann-Neben, 2015).

An important key feature of LIPs is the high velocity zone (HVZ) with P-wave velocities between 7.3 and 7.7 km/s within its lower crust. The HVZ is believed to consist of olivine and pyroxene crystal fractionation, which is trapped above

the crust-mantle boundary (Moho) (Karlstrom and Richards, 2011; Ridley and Richards, 2010). The presence of the HVZ indicates the influence of hot mantle upwelling, e.g. due to the presence of a hotspot or a mantle plume. The configuration of the HVZ along LIP margins allows

	Latitude	Longitude	Age	Paleolatitude	Reference:
ODP Leg 130 - 807	3.6000	156.620	122.3	$-17.9 \pm 3.3$	(Mahoney et al., 1993)
ODP Leg 192 -1183	-1.177	157.015	121	$-27.9 \pm 7.2$	(Riisager et al., 2003)
ODP Leg 192 -1184	-5.011	164.223	123.5	$-34.4 \pm 5$	(Chambers et al., 2004)
ODP Leg 192 -1185	-0.358	161.668	121	$-23.3 \pm 2.2$	(Riisager et al., 2003)
ODP Leg 192 -1186	-0.680	159.844	121	$-25.2 \pm 3.5$	(Riisager et al., 2003)
ODP Leg 192 -1187	0.943	161.451	121	$-22.2 \pm 2.3$	(Riisager et al., 2003)
DSDP Leg 33 - 317	-11.0015	-165.263	116.8	-47.5	(Cockerham and Jarrard, 1976)
So-168 DR55	-40.7508	-160.916	115	-	(Mortimer et al., 2006)
Malaita	-8.772	160.916	160	-	(Ishikawa et al., 2005)

**Table 6.1:** Additional dated locations and paleo-latitude data used as constraints for the plate kinematic reconstruction

an insight into tectonic alteration as well as LIP formation processes (Fig. 6.2). HVZs have been derived from seismic refraction/wide-angle reflection experiments, which have been carried out on the Ontong Java Plateau (Furumoto et al., 1976; Miura et al., 2004) and on the Manihiki Plateau (Figs. 6.2 and 6.3) (Hochmuth et al., in review; Winterer et al., 1974). In addition to the LIPs of the western Pacific, numerous active and former hotspot tracks, such as the Louisville seamount chain and the Samoa Hotspot characterize the area (Fig. 6.1). The omnipresence of volcanically altered oceanic crust has an important impact on the plate tectonic mechanisms of the western Pacific. For example, buoyancy calculations by Cloos (1993) predict that oceanic plateaus as thick as 17 km can be subducted. Orogenesis by subducting oceanic plateaus requires a broad volcanic feature (>100 km long and 50 km wide) with a crustal thickness of 30 km (Cloos, 1993). These calculations indicate that LIPs can play a significant role in the plate tectonic framework, especially in the Pacific Ocean, since it is surrounded by subduction zones. LIPs influence the behavior of oceanic plates by volcanic arc polarity reversal (e.g. Mann and Taira, 2004; Musgrave, 1990) or altering subduction patterns (e.g. Gutscher et al., 1999; Liu et al., 2010).

### 6.2.2 The plate tectonic framework of the Pacific during the Cretaceous

The plate kinematics of the Cretaceous Pacific area include countless microplates and past subducted plates (e.g. *Seton et al.*, 2012). During the Jurassic, the so-called Pacific Triangle developed, which is the birthplace of today's Pacific Plate. The Pacific Triangle was formed by the Izanagi Plate in the northwest, the Farallon Plate in the northeast and the Phoenix Plate in the south, which were connected by triple junctions. Magnetic seafloor spreading anomalies can be identified from M27 (155 Ma) to MO (120 Ma) within the Phoenix lineation northeast of the Ontong Java Plateau (*Nakanishi et al.*, 1992) (Fig. 6.1). After the CNS, magnetic seafloor spreading anomalies can be traced from C34n (83 Ma) to C1 (0.8 Ma) to the east of the Manihiki Plateau (Fig. 6.1). The whole tectonic re-organization of the Ontong Java Nui LIPs occurred during a time of a relatively stable magnetic field, which does not allow to trace the motion of individual plates by polarity reversals of the magnetic field. In this case, the plate motion can be traced either by fracture zones (*Matthews et al.*, 2012), which act as motion paths, or by the variations of the strength of the magnetic field (*Granot et al.*, 2012). We introduce two competing models deciphering this time period presented in the literature, and will re-examine these models in the light of newly acquired data from the Manihiki Plateau: The “Super”-LIP Ontong Java Nui and the separated formation of the Ontong Java Plateau with a coupled emplacement of Manihiki and Hikurangi.

#### The Ontong Java Nui hypothesis

*Taylor* (2006) hypothesized that the three major LIPs of the western Pacific Plate were emplaced as a single “Super” Large Igneous Province. This “Super”-LIP Ontong Java Nui was formed in the vicinity of the Farallon-Phoenix-Pacific triple junction approximately at 125 Ma (*Timm et al.*, 2011). The trace of this triple junction is imprinted on today's Pacific Plate by a gravity anomaly called the Tongareva Triple Junction Trace, which is trackable from the Manihiki Plateau to the Pacific-Antarctic Ridge striking NW-SE (*Larson et al.*, 2002; *Viso et al.*, 2005) (Fig. 6.1). The break-up of Ontong Java Nui was initiated at all margins of the Manihiki Plateau between 120 Ma and 118 Ma. To the south, the Osborn Trough developed as a spreading center, separating the Hikurangi Plateau from Manihiki (*Billen and Stock*, 2000; *Davy et al.*, 2008; *Worthington et al.*, 2006). The Ontong Java Plateau drifted away to the west by spreading at the Nova Canton Trough (*Chandler et al.*, 2012; *Taylor*, 2006). The northeastern fragment of the Manihiki Plateau rifted northeastwards on the Farallon Plate and the eastern part of the Manihiki Plateau was integrated into the Phoenix Plate in a southward direction (*Larson et al.*, 2002; *Viso et al.*, 2005). The motion between the Hikurangi Plateau and the Manihiki Plateau stopped at 100 Ma with the Hikurangi Plateau jamming into the subduction zone at the Chatham Rise followed by cessation of spreading at the Osborn Trough (*Davy*, 2014; *Davy et al.*, 2008). Other authors (e.g. *Billen and Stock*, 2000; *Sutherland and Hollis*, 2001; *Worthington et al.*, 2006) argue for a longer lifespan of the Osborn Trough, but all agree that the cessation of spreading occurred within the CNS (120–83 Ma). At around 80 Ma, spreading in the Nova Canton Trough

between the Ontong Java Plateau and the Manihiki Plateau terminated (*Taylor, 2006*), although the Ontong Java Plateau was not subducting at the Solomon Trench at that time. The opening at the Nova Canton Trough included a rotational component (*Chandler et al., 2013*) between  $37^\circ$  and  $52^\circ$  obtained from paleomagnetic reconstructions. This rotation requires either a decoupling of the Ontong Java Plateau from the Pacific Plate or a yet unrecognized large-scale rotation of the Pacific Plate between 125 and 83 Ma. The main objections towards this coupled emplacement of the three LIPs include the different crustal thicknesses between the Ontong Java Plateau ( $> 30$  km of crust) (*Furumoto et al., 1976; Gladchenko et al., 1997; Klosko et al., 2001; Miura et al., 2004; Richardson et al., 2000*) and the conjugate margin at the Manihiki Plateau, the Western Plateaus, which present a gradual decrease of crustal thickness from 17 km to 9 km towards the Nova Canton Trough (*Hochmuth et al., in review*). If the emplacement was coupled the Western Plateaus should have a similar crustal thickness as its conjugate plateau. Additionally, the tectonic fit between the two plateaus cannot be achieved easily since secondary volcanism and tectonic activity altered the plateaus margins (*Pietsch and Uenzelmann-Neben, 2015*). A further complication of the plate kinematic reconstruction is that the Nova Canton Trough does not show a clear spreading axis, but seems to consist of multiple small ridges and fracture zones, which point to a scissor-like opening of the basin (*Chandler et al., 2012; Taylor, 2006*).

#### **Individual emplacement of Ontong Java and Manihiki-Hikurangi**

Whereas the coupled emplacement of the Hikurangi Plateau and the Manihiki Plateau seems to be a well-established factor in the plate kinematics of the western Pacific, the fit between the Ontong Java Plateau and the Manihiki Plateau is still under debate for the reasons mentioned above. Therefore, we give an overview of published scenarios, which do not include a coupled emplacement between the Ontong Java Plateau and the Manihiki and Hikurangi Plateaus. *Larson and Chase (1972)* and *Winterer et al. (1974)* propose a plate tectonic set-up, where the oceanic plateaus of Ontong Java Nui are situated on the spreading axis between the Pacific and the Antarctic Plate. The different sub-provinces of the Manihiki Plateau are created by a spreading segment jump (*Winterer et al., 1974*) or the presence of the Farallon-Antarctic spreading on the High Plateau (*Larson and Chase, 1972*). *Larson (1997)* propose that individual plumes created the Manihiki Plateau and the Ontong Java Plateau. The Pacific-Phoenix spreading ridge separated these plumes. The present Nova Canton Trough was created after the primary magmatism by reheating and extension of the young lithosphere. This concept highlights the importance of a possible ridge-plume interaction creating the LIPs of the western Pacific.

### **6.3 Overview on published and additional data**

Before we re-evaluate emplacement mechanisms and tectonic activity, a condensed overview on the relevant data, which is currently available in the western Pacific region, is presented. The

main phase of tectonic evolution within this region occurs during the CNS. Small variations within the magnetic field strength during this time period have been detected in the Atlantic Ocean offshore North Africa (*Granot et al.*, 2012), but unfortunately these variations cannot be recognized within the western Pacific. The Nova Canton Trough shows no clear spreading axis, and the Osbourn Trough is magmatically overprinted by the Louisville Hotspot in the south and the smaller Austral-Cook and MacDonald Hotspots in the north (*Billen and Stock*, 2000). Therefore, the intensity variations cannot help to reconstruct the plate re-organization, magnetic data can only be used to frame the crust, which was emplaced during the CNS. *Chandler et al.* (2013) compiled all available paleolatitude data from Deep Sea Drilling Project (DSDP), Ocean Drilling Project (ODP) and International Ocean Drilling Project (IODP) cores on the Ontong Java Plateau (Table 6.1). Their findings point to an emplacement latitude of the Ontong Java Plateau between 17°S and 33°S with a clock-wise rotation of the plateau of between 37° and 52°. This rotation is currently not integrated in any plate kinematic reconstructions and may indicate a large-scale rotation of the Pacific Plate or an individual motion of the Ontong Java Plateau during the Cretaceous.

Drilled cores reaching the crystalline basement are sparse in the area, and only a very small number have published basement ages. But along with dredges, e.g. from the Wishbone Scarp (*Mortimer et al.*, 2006) or the Danger Islands Troughs (*Ingle et al.*, 2007), and rocks outcropping on islands, e.g. Malaita (*Ishikawa et al.*, 2005, 2007; *Musgrave*, 2013), they can be used as a valuable references for the timing of local tectonic events (Table 6.1). Further constraints to be considered include tectonic lineations trackable in satellite gravity anomaly maps and bathymetric maps. Large-scale anomalies such as the Tongareva Triple Junction trace (*Larson et al.*, 2002), the East and West Wishbone Scarps (*Mortimer et al.*, 2006) and the Manihiki Scarp (*Viso et al.*, 2005) are relicts of former plate boundaries (Fig. 6.1). Additional information of the plate motion can be extracted from intraplate fracture zones. *Taylor* (2006) and *Chandler et al.* (2012) examined the fracture zones within the Ellice Basin (Nova Canton Trough), which strike in an East-West direction. North-south striking fracture zones can be observed north and south of the Osbourn Trough (Fig. 6.1). Fracture zones dissect the Ellice Basin and the Phoenix lineations (*Nakanishi et al.*, 1992). The large Pacific Fracture zones, e.g. Galapagos Fracture Zone or the Clipperton Fracture Zone, further constrain the evolution of the Pacific Plate and the Pacific-Farallon spreading center. The LIP itself provides important constraints for the plate reconstruction of the Cretaceous western Pacific. The current state of these magmatic bodies has been altered by tectonic deformation and volcanism of later magmatic stages and does not necessarily resemble the LIP at its emplacement. In our reconstruction, we account for crustal extension due to crustal stretching or massive emplacement of magmatic material as well as for “lost” fragments to the east and north of the Manihiki Plateau (*Larson et al.*, 2002; *Pietsch and Uenzelmann-Neben*, 2015; *Viso et al.*, 2005).

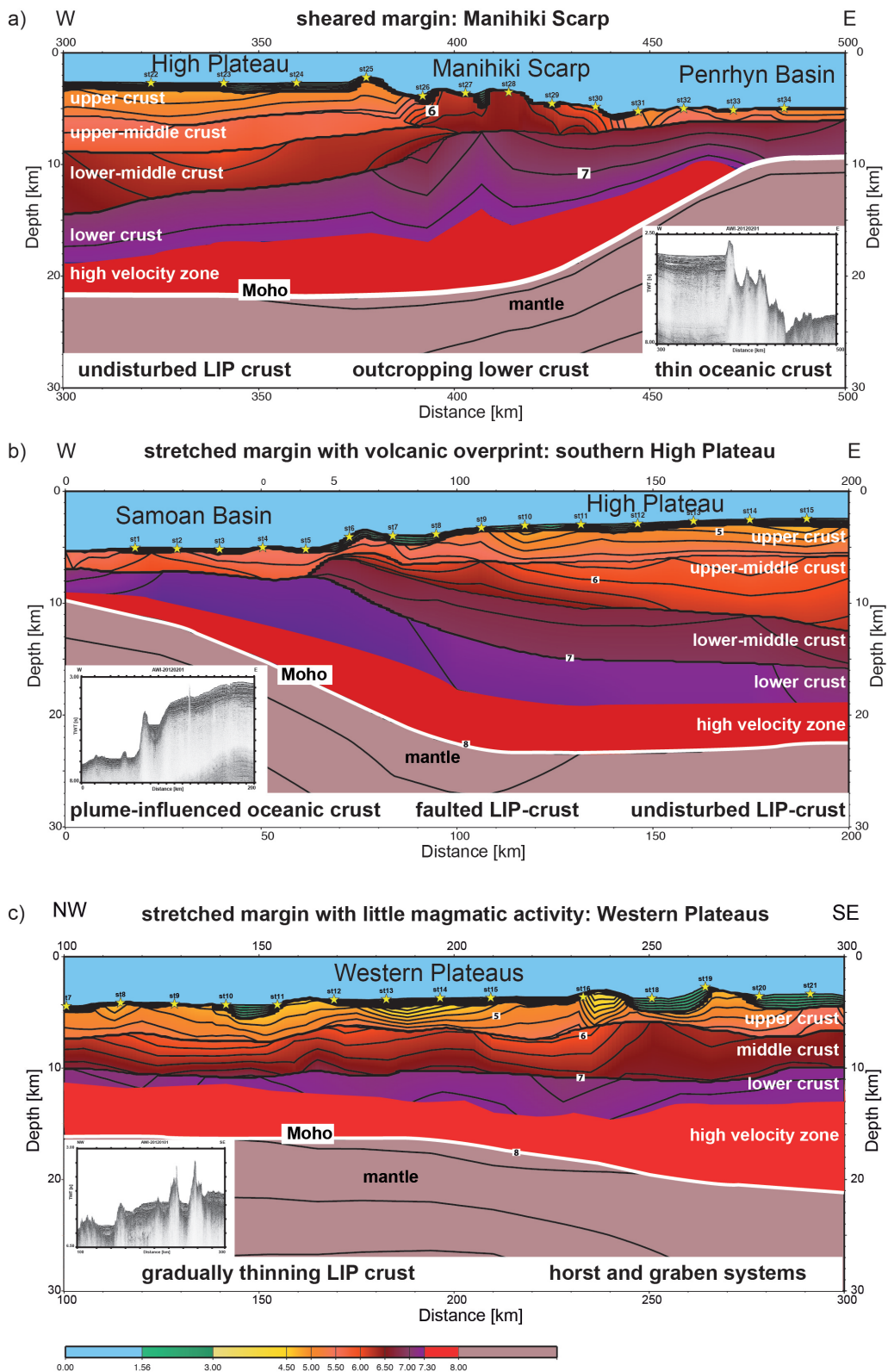


**Figure 6.3:** Examples for P-wave velocity models crossing the different margins of the Manihiki Plateau. The position of the different profiles is indicated in Fig. 6.2. (a) shows the Manihiki Scarp - a sheared margin, (b) shows the southern High Plateau - a stretched margin with volcanic overprint and (c) shows a part of the Western Plateaus - a stretched margin with little magmatic activity; The small insets depict the corresponding reflection seismic data of the shown profile

## 6.4 Possible break-up mechanisms on the Manihiki Plateau

The Manihiki Plateau plays an important role in the plate tectonic setup of the Pacific during the Cretaceous, since it potentially exposes break-up margins towards the other LIPs of the region and the seafloor emplaced during the CNS. A close examination of the crustal structure along with the magmatic and tectonic activity displayed in high-resolution seismic reflection data (*Pietsch and Uenzelmann-Neben, 2015*) and seismic refraction/wide-angle reflection data (*Hochmuth et al., in review*) acquired in 2012 (*Uenzelmann-Neben, 2012*) allows us to identify possible break-up mechanisms on the Manihiki Plateau. Additionally it is important for further reconstructions to incorporate the amount of crustal growth created by later magmatic stages and tectonic strain (Fig. 6.2). The Manihiki Plateau was created by a first phase of extrusive volcanism with an approximated minimum age of 125 Ma (*Timm et al., 2011*). Later magmatic stages (<65 Ma) differ between low-volume secondary magmatism on the Western Plateaus and high volume emplacement at the High Plateau (*Hochmuth et al., in review; Pietsch and Uenzelmann-Neben, 2015*). A more important factor for assessing the extension of the crust after the initial emplacement of the LIP is the tectonic alteration (Fig. 6.2), which is visible by countless faults (e.g. High Plateau) and the decrease of crustal thickness (e.g. Western Plateaus) (*Ai et al., 2008; Hochmuth et al., in review; Pietsch and Uenzelmann-Neben, 2015*). The potential overlap ( $o$ ) between the two plateaus can be calculated by the stretching coefficient ( $\beta$ ) and the width of the stretched crust ( $w$ ) with the following formula:  $o = w * (\beta - 1) / \beta$ . Additional information on the extent of the LIP influenced crust can be derived from the presence of a HVZ with P-wave velocities above 7.3 km/s in the lower crust of the plateaus (*Hochmuth et al., in review*) (Fig. 6.3).

We identify four different areas of tectonic characteristics on the Manihiki Plateau. On the central High Plateau, tectonic activity is low and mainly induced by magmatism (*Pietsch and Uenzelmann-Neben, 2015*) (Fig. 6.2). The eastern flank of the High Plateau, the Manihiki Scarp, exhibits a north-south trending sheared margin (*Hochmuth et al., in review; Larson et al., 2002; Pietsch and Uenzelmann-Neben, 2015; Viso et al., 2005*) with up to eight basement ridges exposing lower crust (Fig. 6.3a). The HVZ terminates below the basement ridges, and crustal thickness decreases from 15 to 4.5 km within 60 km lateral distance (Fig. 6.3a). Additional crustal material seems to be emplaced by the exposure of lower crustal material and not by stretching processes. The southern High Plateau shows multiple normal fault systems, which can be related to rifting activity during the Cretaceous and later tectonic stress (40-1.8 Ma) (*Pietsch and Uenzelmann-Neben, 2015*) (Fig. 6.2). This area has also been influenced by secondary magmatic stages (>65 Ma) and even younger magmatic activity (23-10 Ma). The HVZ in the lower crust of the Manihiki Plateau stretches into the Samoan Basin (Fig. 6.3b). Crustal stretching ( $\beta$ ) is evident but relatively small ( $\beta=1.26$ ). The western High Plateau and the Western Plateaus show low-volume secondary magmatism (*Hochmuth et al., in review; Pietsch and Uenzelmann-Neben, 2015*). In seismic refraction/wide-angle reflection data from the Western Plateaus, we observe a constant presence of the HVZ and a decrease in crustal thickness

from 18 km in the East to 9 km in the West ( $\beta=2$ ) over 400 km distance (Fig. 6.3c). This indicates a potential overlap with a conjugate margin of 200 km. Small and large offset faults are present throughout the sub-province (Figs. 6.2 and 6.3). Other significant features of the Manihiki Plateau are its internal troughs, the N-S trending Danger Islands Troughs and the NE-SW trending Suvarov Trough (Fig. 6.2). Seismic reflection data indicates that the Suvarov Trough is younger than 65 Ma and can therefore not be a result of the initial tectonic activity within the CNS (*Pietsch and Uenzelmann-Neben*, submitted). Seismic refraction/wide-angle reflection data reveal the lack of typical upper crustal material within the Danger Island Troughs, but a relatively undisturbed lower and middle crust (*Hochmuth et al.*, in review). The Danger Islands Troughs mark, as a series of pull-apart basins a significant border between the two magmatic and tectonic regimes of the High Plateau and the Western Plateaus. By tracing the exposed fault systems in bathymetry (*Weatherall et al.*, 2015) and global satellite gravity anomaly maps (*Sandwell et al.*, 2014) a rotational component from NNE-SSW striking features in the North to NNW-SSE striking features in the South can be observed (*Nakanishi et al.*, 2015). This supports the hypothesis that the Western Plateaus and the High Plateau acted as individual tectonic plates during part of the Cretaceous. Similar margin features as described above can be seen on the Ontong Java Plateau and the Hikurangi Plateau (Tab. 6.2 and Fig. 6.4). We extrapolated our classification of the break-up margins across these plateaus by including published seismic reflection and refraction data along with gravity models, gravity anomaly maps and bathymetric measurements. In addition to the margins encountered on the Manihiki Plateau, a tectonically inactive margin and subducting margins are present on the Ontong Java Plateau and the Hikurangi Plateau (Fig. 6.4). The Rapuhia Scarp of the western Hikurangi Plateau shows a very narrow transition zone between LIP crust and normal oceanic crust (*Davy and Collot*, 2000) and introduces a fourth mode of rifting within the system.

## 6.5 Plate tectonic reconstruction of the Cretaceous western Pacific

The regional plate kinematic reconstruction presented here uses the global plate tectonic GPlates model of *Seton et al.* (2012) as its basis. We additionally use the hotspot reference frame W&K08-D by *Wessel and Kroenke* (2008) and *Chandler et al.* (2012). The model comprises the time frame from 125 Ma to 80 Ma and translates directly into the model by *Seton et al.* (2012) for the development after the CNS. An overview on the modeled tectonic events is provided in Table 6.3.

### 6.5.1 The emplacement of Ontong Java Nui – plume-ridge interaction and single “Super”-plume head

The published data indicates that at least two main eruptive centers were present, on the High Plateau of the Manihiki Plateau and on the High Plateau of the Ontong Java Plateau, during the initial emplacement of the LIP (*Furumoto et al.*, 1976; *Hochmuth et al.*, in review; *Miura et al.*, 2004). The presence of the thinner Western Plateaus (Fig. 6.3c) and possible eastern Ontong



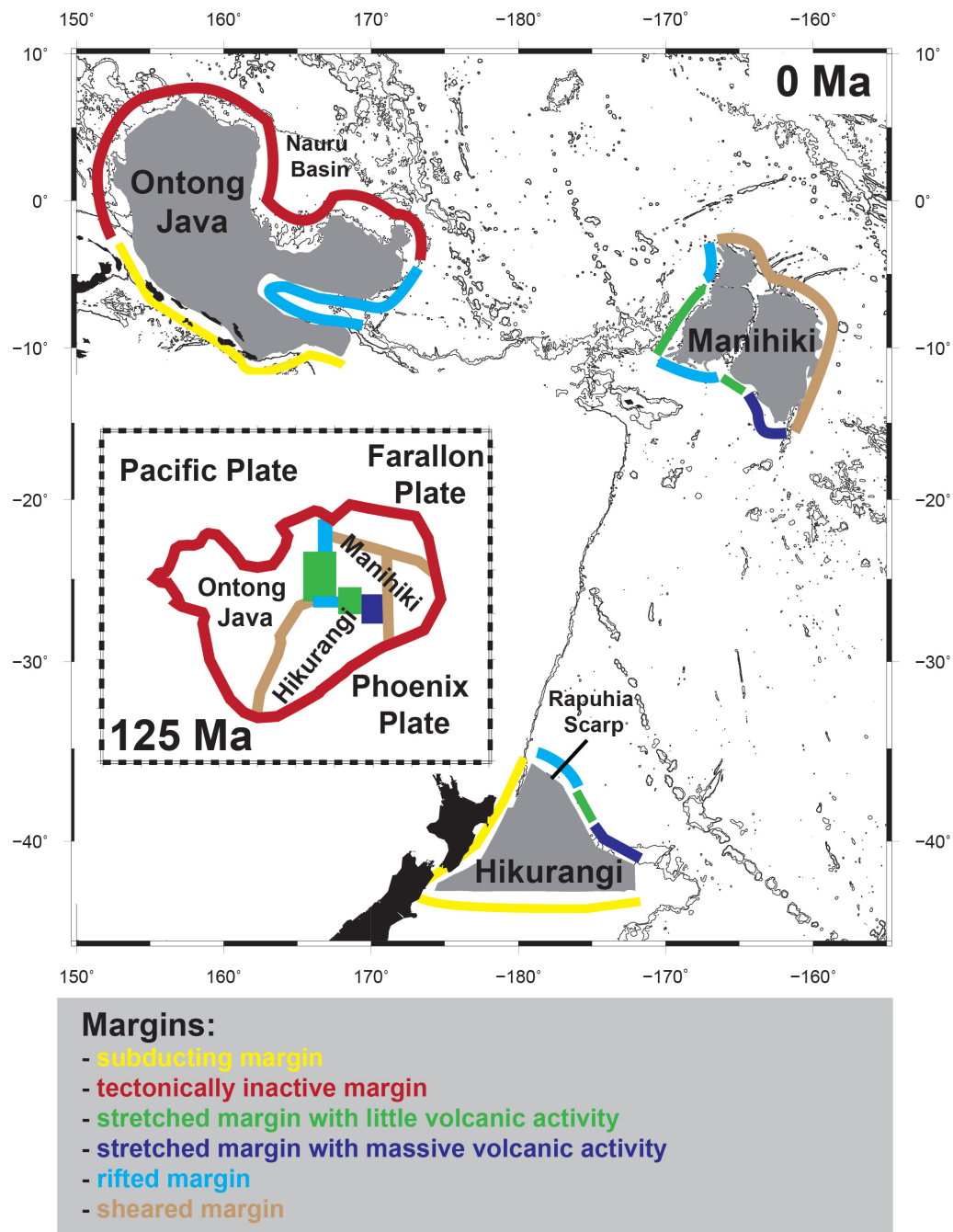
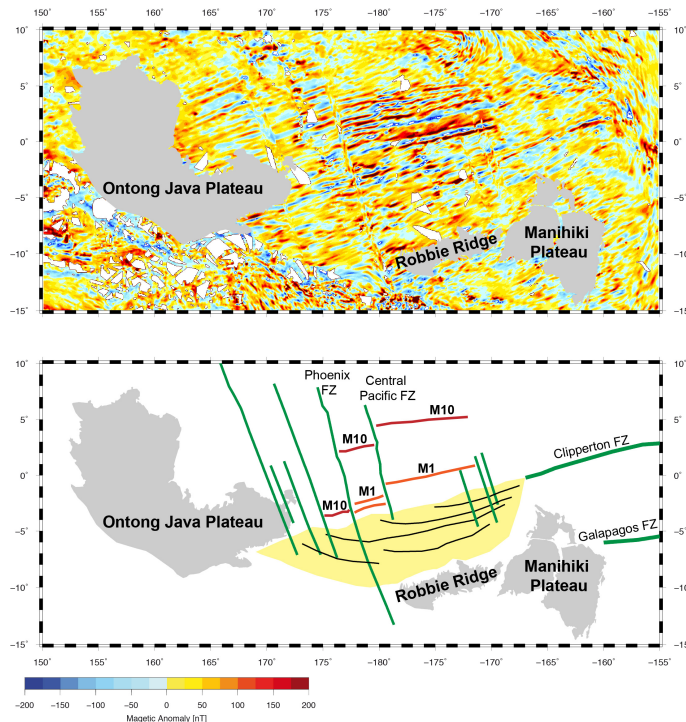


Figure 6.4: Classification of the margins of Ontong Java Nui in their current setting (main figure) and during their emplacement (inlet figure).

margin	characteristica	regional example	reference	interfered from
tectonically inactive margin	slow decrease in depth, basalt flows into the oceanic basin, dip angle < 0.1 degrees	northern Ontong Java Plateau	(Mochizuki et al., 2005)	seismic reflection, bathymetry, gravity anomaly
subducting margin	subduction of LLP crust	Ontong Java Plateau – Solomon Trench Hikurangi – Chatham Rise	(Day, 2014; Day et al., 2008; Miura et al., 2004)	seismic refraction, reflection seismic, bathymetry, gravity anomaly
sheared margin	rough topography with multiple ridges exposing lower crustal layers, sudden termination of HVZ	Manihiki Scarp	(Ai et al., 2008; Hochmuth et al., in review; Larson et al., 2002; Pietsch and Uenzelmann-Neben, 2015; Viso et al., 2005)	seismic reflection, refractions seismic, bathymetry, gravity anomaly
stretched margin with little magmatic activity	countless large and small offset faults, low volume secondary magmatism, constant HVZ, massive crustal stretching	Western Plateaus (Manihiki Plateau), Rekohu Embayment (Hikurangi Plateau)	(Day et al., 2008; Hochmuth et al., in review)	refraction seismic, reflection seismic, bathymetry, gravity anomaly
stretched margin with magmatic overprint	multiple fault systems, massive magmatic activity during later magmatic stages, small amount of crustal stretching	southern Manihiki Plateau, Southeast High Plateau (Hikurangi Plateau)	(Day et al., 2008; Hochmuth et al., in review; Pietsch and Uenzelmann-Neben, 2015)	refraction seismic, seismic reflection data, gravity anomaly, bathymetry
rifted margin	short LLP - ocean basin transition area, sharp boundary, sudden depth decrease dip angle > 5 degrees	Rapuhia Scarp (Hikurangi Plateau)	(Day and Collat, 2000; Day et al., 2008)	seismic reflection, bathymetry, gravity anomaly

Table 6.2: Overview on the different margins of Ontong Java Nui and their individual features

Java Plateau makes the scenario of a single “Super”-plume (Taylor, 2006) surfacing in the area unlikely, since this should create a crust of comparable crustal thickness. Larson (1997) proposed that the oceanic LIPs of the region originated by two individual plume heads rising at both sides of the Pacific-Phoenix spreading center. Individual plumes would explain the significant differences in crustal thickness. The Nova Canton Trough, which separates the Ontong Java Plateau and the Manihiki Plateau, shows a reorientation of the spreading orientation in comparison to its predecessor the Pacific-Phoenix Ridge from E-W to NE-SW (Fig. 6.5).



**Figure 6.5:** (a) magnetic anomaly map of the Nova Canton Trough after Maus *et al.* (2009), grey areas indicate the oceanic LIPs (b) tectonic interpretation with major fracture zones in green from Nakanishi *et al.* (1992) for the Phoenix lineations and additional smaller fracture zones at the convergence between the Nova Canton Trough and the Clipperton FZ, fracture zones within the Nova Canton Trough (yellow area) after Taylor (2006) in black and the magnetic isochrones of M10 (red) and M1 (orange) within the Phoenix lineations (Nakanishi *et al.*, 1992).

Even though a clear spreading axis is not detectable (Chandler *et al.*, 2012; Taylor, 2006), it can be inferred that the oblique spreading in the Nova Canton Trough cross-cuts the magnetic spreading anomaly M-Series at M10 in the vicinity of the Ontong Java Plateau and leaves the M1 spreading center visible northeast of the Manihiki Plateau (Fig. 6.5) (Nakanishi *et al.*, 1992). Therefore, the spreading in the Nova Canton Trough is distinct from the earlier spreading in the area and is not caused by an overprinting of a former spreading center during the CNS as suggested by Larson (1997). In addition, the possible presence of three areas of mantle upwelling within such a confined area – an Ontong Java Plume, a Manihiki/Hikurangi Plume and the Pacific-Phoenix ridge – seems geodynamically unrealistic. However, the concept of the interaction between plumes and the Pacific-Phoenix spreading center appears to be an important factor in the emplacement of Ontong Java Nui.

hiki/Hikurangi Plume and the Pacific-Phoenix ridge – seems geodynamically unrealistic. However, the concept of the interaction between plumes and the Pacific-Phoenix spreading center appears to be an important factor in the emplacement of Ontong Java Nui.

A ridge-centered hotspot can currently be observed for example on Iceland (e.g. Darbyshire *et al.*, 1998; Ito *et al.*, 1996) and the interaction between a hotspot and a spreading-ridge is present, for example, at the Galapagos hotspot (e.g. Kokfelt *et al.*, 2005; Sinton *et al.*, 2003).

Modeling of these interactions reveals that the plume-ridge interaction is mainly influenced by the spreading rate at the ridge and the plume flux (*Albers and Christensen, 2001*). Therefore, multiple pulses and the spreading at the ridge between the pulses can create areas of variable crustal thickness. The nature of the plume-ridge interaction—whether centered or off-axis—also influences the emplacement process. Off-axis plumes have to penetrate a thicker and older lithosphere and have an up-slope flow towards the ridge (*Ito et al., 1996, 2003; Ribe, 1996; Ribe and Delattre, 1998; Ribe et al., 1995*). To explore the result of a possible interaction of an arriving plume head at the Pacific-Phoenix ridge, models of hotspot-ridge interactions (e.g. *Dyment et al., 2007*) and models of plume-ridge interactions (e.g. *Whittaker et al., 2015*) can be used. These scenarios differ mostly in the volume of the emplaced igneous material, which is far larger for a plume scenario. It has also been proposed that plume-ridge interaction causes asymmetric seafloor spreading (*Müller et al., 1998*). When a spreading system approaches a hotspot, the magmatic flow is channeled towards the ridge resulting in an additional production of seamounts. An increased steady magma supply would possibly generate an oceanic plateau (Fig. 6.6). The main emplacement of the LIP would occur during a phase of a ridge-centered plume with massive volcanic outpourings and intrusions within the lower crust. As soon as the ridge passes the area of the plume, the emplacement of igneous material decreases, but channeling towards the ridge is still present, possibly resulting in an area of thinner, but still over-thickened oceanic crust. The former main emplacement area with its large crustal thickness is rifting away from the ridge (Fig. 6.6). The interplay between ridge dynamics and a plume might help to understand the observation of the large differences in crustal thickness across the LIP. On the Manihiki Plateau, a strong seismic intra-basement reflection is traceable (*Pietsch and Uenzelmann-Neben, 2015*), which can be interpreted to represent an initial formation stage of the plateau. Strong intra-crustal seismic wide-angle reflections (*Hochmuth et al., in review*) can also be attributed to this layer. The strong reflections within the crust in both datasets might be the result of the overprinting between an early arrival of the plume and the main emplacement phase during the time of a ridge-centered plume. A similar set-up of pulsating volcanic activity has been reported for the Southeast African LIP, where the Transkai Rise separates, analog the Western Plateaus of the Manihiki Plateau, two areas of thicker LIP crust, the Agulhas Plateau and the Mozambique Ridge (*Gohl et al., 2011*). Since the data indicate a tectonic connection, within the crust of the Western Plateaus between the Ontong Java Plateau and the Manihiki Plateau and the presented emplacement mechanism does not oppose such a scenario, we attempt our reconstruction with the re-assemblage of Ontong Java Nui, by accounting for rotational components (*Chandler et al., 2013; Davy, 2014*), the growth of the LIP after break-up by either crustal stretching or secondary magmatism and incorporating for the characteristics of the break-up margins. Subducted fragments are added. Here, we use the traceable slab of the Hikurangi Plateau below New Zealand (*Reyners, 2013*) and the estimated extension of the Ontong Java Plateau by *Musgrave (2013)*. Since the northeastern and the eastern fragment of the Manihiki Plateau were subducted, we estimated the extent of these fragments under the assumption that the emplacement mechanism is similar to that of the northern Ontong Java

Plateau, where basalt flows limit the extent of the Nauru Basin (*Mochizuki et al.*, 2005) (Fig. 6.4). These assumptions result in an initial size of Ontong Java Nui to be 1.1% of the Earth's surface, which is larger than previously anticipated. By comparing the reassembled LIP with recent global plate tectonic models (e.g. *Seton et al.*, 2012) and magnetic lineations (*Nakanishi et al.*, 1992), the paleo-latitudes calculated for the Ontong Java Plateau are approximately 400 km farther north than the reconstructed position of the Ontong Java Plateau (Fig. 6.7). Even though only a few paleolatitude calculations exist, implying a large error margin, we investigate further possible factors for this significant offset. The mismatch between the reconstructed and the magnetic lineations is partly due to the complicated spreading at the Pacific – Phoenix – Farallon Triple Junction, where the presence of multiple microplates and jumping spreading centers is proposed (*Seton et al.*, 2012). The Phoenix lineations show multiple fracture zones (FZ) within their sequence (*Nakanishi et al.*, 1992) including the Phoenix FZ and the Central Pacific FZ (Figs. 6.5 and 6.7). These induce a considerable offset between the magnetic lineations in the vicinity of the Ontong Java Plateau and are, along with other smaller FZ, traceable within the eastern Nova Canton Trough (*Maus et al.*, 2009; *Sandwell et al.*, 2014) (Fig. 6.5). The crust of the Nova Canton Trough was emplaced after the oceanic LIPs, which allows an emplacement of the LIP farther north with later, post-emplacement movement towards the south. From asynchronous bends in the seamount chains of the Gilbert Ridge and the Tokelau seamounts, *Koppers and Staudigel* (2005) inferred two short extensional phases within the Nova Canton Trough (67 Ma and 57 Ma), which might be related to a re-activation of the trough or to the activity of fracture zones. If these fracture zones were active after the Cretaceous spreading in the Nova Canton Trough, they can at least partly account for the offset between reconstructed and calculated paleo-latitudes (Fig. 6.7). We, therefore, infer an emplacement of Ontong Java Nui between 18° and 40° S (Fig. 6.8a).

The absolute plate motion of the Pacific Plate during the Cretaceous is vaguely constrained by direct measurements from basaltic flows, but a hook-like shape of the

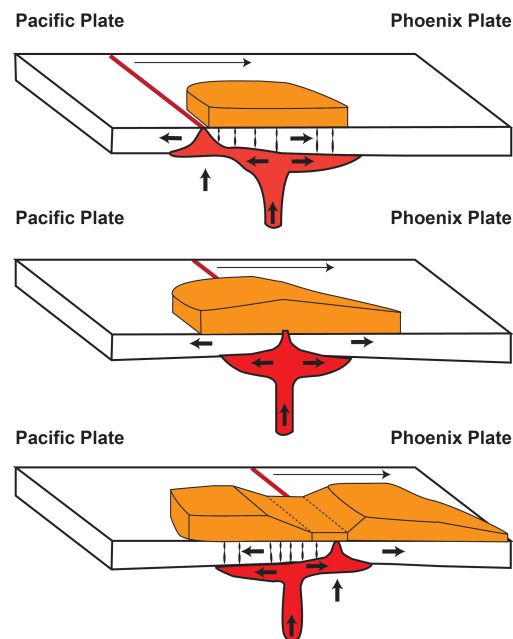


**Figure 6.6:** Sketch of possible plume-ridge interaction at the Pacific-Phoenix ridge, upper panel: surfacing of a plume head in vicinity of the Phoenix-Pacific spreading ridge; middle panel: plume head at the ridge creating a thicker plateau; lower panel: spreading center moved away from the plume creating rifting of the thick plateau and emplaces a thinner oceanic plateau between the previously emplaced parts

absolute polar wander path is proposed (Sager, 2006; Wessel and Kroenke, 2008). Unfortunately, the data from the Ontong Java Plateau do not fit this path. Sager (2006) suggests a decoupling of the northern and southern Pacific Plate – including the Ontong Java Plateau – during the Cretaceous. Paleo-plate boundaries are not observed within the Jurassic Pacific Plate, which makes this uncoupling rather unlikely. If the Pacific Plate and the Ontong Java Plateau were coupled during the early Cretaceous, we can infer that the rotation of the Ontong Java Plateau was at least partly also performed by the Pacific Plate. It is also important to account for the possible Neogene intraplate motion, which occurred at the Nova Canton Trough (Koppers and Staudigel, 2005). Unfortunately, the data needed to distinguish between these scenarios are not available. In addition, the southern hemisphere Pacific is underrepresented in the calculations of the rotation poles (Sager, 2006), which might be a cause for an underestimate of possible rotations. To be able to constrain the motion of the Pacific Plate before its connection to the global plate tectonic circuit, it is necessary to obtain a better insight in the internal plate motion of the Pacific Plate and a closer grid of basement samples from both hemispheres. In our reconstruction, we assume a rotation of the Pacific Plate along with the Ontong Java Plateau based on Chandler *et al.* (2013).

### **6.5.2 The initial break-up of Ontong Java Nui – evaluation of the break-up mechanisms on oceanic LIPs (120-116 Ma)**

The development of break-up margins can be traced along all margins of the Manihiki Plateau. The initial break-up of the “Super”-LIP was rather complex and included multiple tectonic deformations such as shearing and crustal stretching before the establishment of clear spreading centers (Fig. 6.8b). The relicts of these first movements between the oceanic LIPs and within the Manihiki Plateau are imprinted in the nature of the different margins (Fig. 6.3). The magmatic activity was still strong on the plateaus (Hoernle *et al.*, 2010; Inoue *et al.*, 2008; Pietsch and Uenzelmann-Neben, 2015), leading to alteration and magmatic overprinting of the tectonic sutures. We present the tectonic mechanisms initiating the break-up of Ontong Java Nui and the fragmentation of the Manihiki Plateau in an anti-clockwise fashion beginning in the south, where the Osbourn Trough is located (Fig. 6.1) (Billen and Stock, 2000; Downey *et al.*, 2007; Worthington *et al.*, 2006). The first motion between the Hikurangi Plateau and the Manihiki Plateau occurred at the southern Western Plateaus and the conjugate Rapuhia Scarp, where a rifted margin was identified (Fig. 6.4). This rapid separation was followed by a phase of crustal stretching at the southern High Plateau and the eastern Hikurangi Plateau, possibly including an anti-clockwise motion (Fig. 6.8b). Normal faults are identified in seismic reflection data (Pietsch and Uenzelmann-Neben, 2015). The presence of a HVZ within the Samoa Basin can be attributed to the later overprint of the presence of the Tahiti-Society Islands hotspot at the Manihiki Plateau (Pietsch and Uenzelmann-Neben, submitted) (Fig. 6.3b) and is not a relict of the “Super”-LIP break-up. To the east, the Osbourn Trough intersects with the Manihiki Scarp. This shearing zone (Fig. 6.3a) can be traced along the eastern High Plateau and established itself as the eastern plate boundary of the Manihiki Plateau (Fig. 6.1). As Larson *et al.* (2002)

proposed, the triple junction between the Pacific, Farallon and Phoenix Plates jumped to the northeastern corner of the Manihiki Plateau, the northern end of the Tongareva Triple Junction Trace (Figs. 6.1 and 6.8). This gravity anomaly trace is the relict of the southward motion of the triple junction.

Seton *et al.* (2012) in their model divided the Farallon Plate in a northern Farallon Plate north of the Clipperton FZ and a southern Farallon Plate called the Chasca Plate. The Phoenix Plate is called Catequil Plate in their reconstruction. To allow a better comparison between those reconstructions we also separate between a northern and a southern Farallon Plate (Figs. 6.8b and 6.9a-c). The eastern fragment of the Manihiki Plateau is incorporated into the Phoenix Plate along the Manihiki Scarp and moves southwards (Figs. 6.8b and 6.9a-c). The northeastern fragment of the Manihiki Plateau becomes part of the southern Farallon Plate (Chasca Plate). The northern margin of the Manihiki Plateau is mostly unsurveyed, but bathymetry (Nakanishi *et al.*, 2015) and gravity data (Sandwell *et al.*, 2014) indicate the presence of massive tectonic activity, possibly related to shearing processes. We propose a fast clock-wise rotation of the northeastern fragment of the Manihiki Plateau, resulting in multiple ridges (Fig. 6.1) and the possible extension of the crust on the northern High Plateau (Fig. 6.2).

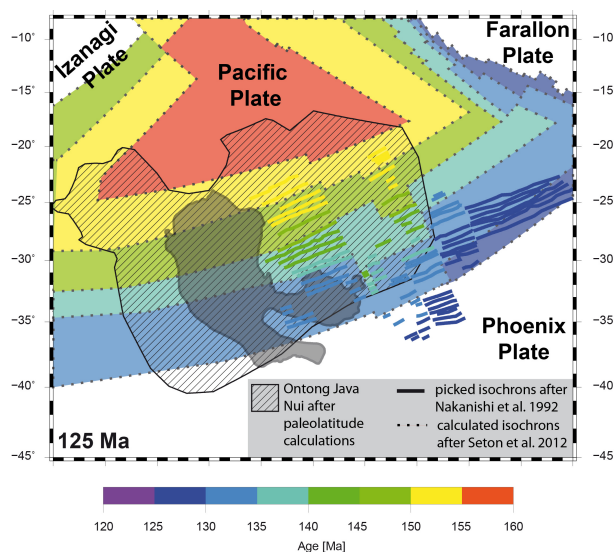


**Figure 6.7:** Comparison of paleo-latitude data (hatched area of possible emplacement of Ontong Java Nui), calculated isochrones (dashed lines) (Seton *et al.*, 2012) and magnetic anomaly picks (continuous lines) (Nakanishi *et al.*, 1992). The grey area indicates the Ontong Java Plateau in relation to the magnetic anomaly picks.

Additional to these major break-up scenarios, the Manihiki Plateau is fragmented into its sub-provinces. At the Danger Islands Troughs, the division into the Western Plateaus and the High Plateau is manifested by a series of pull-apart basins (Hochmuth *et al.*, in review), which show a similar rotation as proposed for the Ontong Java Plateau. The Western Plateaus seem to have moved with the Ontong Java Plateau during the initial phase of break-up (Fig. 6.8b), leading to faulting and stretching of the crust. Therefore the thinner crust of the Western Plateaus (Fig. 6.3c) can result from a combination of the emplacement mechanism and tectonic stress during the break-up of Ontong Java Nui (Figs. 6.6 and

6.8b). The Hikurangi Plateau and Ontong Java Plateau are separated by the former spreading center between the Pacific and Phoenix Plate, which possibly developed a transform motion



(Figs. 6.8b and 6.9a). The reconstruction in this area is very difficult and can only be achieved by crude assumptions of the subducted seafloor. *Musgrave* (2013) proposed an additional triple junction in this area to account for the so-called Malaita Terranes. In his study, *Musgrave* (2013) omits the rotation of the Ontong Java Plateau (*Chandler et al.*, 2013). This rotation enables to reconstruct the Malaita terranes, which lay on 160 Ma old crust, without additional plate boundaries.

### 6.5.3 Dispersal of Ontong Java Nui over the Pacific Ocean

After the initial break-up, which involved a tremendous (up to 200 km at the Western Plateaus) amount of crustal stretching, short-lived spreading centers and rotational forces, the plate boundaries stabilized (Fig. 6.9a). The timing of the stabilization correlates with the fading of massive volcanic activity on the Manihiki Plateau (*Pietsch and Uenzelmann-Neben*, 2015). Therefore, the influence of the plume ceased and secondary phases of magmatic stages show a clearly weaker and more localized volcanic emplacement. The Osbourn Trough developed a spreading half-rate of 10 cm/a (116-100 Ma) and significantly slows down the production of new crust after the soft-docking of the Hikurangi Plateau at the Chatham Rise (*Davy*, 2014; *Davy et al.*, 2008) (Fig. 6.9b). The interaction with the Chatham Rise also introduces a rotation of the Hikurangi Plate, which can also be observed in the change in orientation of the Osbourn Trough (Fig. 6.9b) (*Davy*, 2014). The morphology of the Osbourn Trough resembles a slow-spreading ridge (*Billen and Stock*, 2000; *Downey et al.*, 2007). Therefore, we propose a change in orientation from NW-SE to W-E after the soft-docking of the LIP crust at the continental Chatham Rise and a slowing of the spreading rate to 3 cm/a, which is consistent with previous publications calculating spreading rates (*Billen and Stock*, 2000; *Downey et al.*, 2007). The Hikurangi Plate partly subducted beneath the Gondwana Margin at the location of the Chatham Rise (Fig. 6.9a). This docking event has a great impact on the whole western Pacific and led *Matthews et al.* (2012) to propose that kinks within fracture zones can be correlated and dated to this event. In our reconstruction, we also link re-orientations of fracture zones observed on the Hikurangi Plate and Manihiki Plate to this time frame (Fig. 6.1). To the East, the Wishbone Scarp a short-lived interoceanic subduction zone develops (*Mortimer et al.*, 2006), representing the plate boundary between the Phoenix (Catequil) Plate and the Hikurangi Plate (Fig. 6.9b). The Hikurangi Plate subducts below the Phoenix Plate at this location. The shape of the Wishbone Scarp gives further indication of a clockwise rotation of the Hikurangi Plate after the initial collision with the Chatham Rise (Fig. 6.1). The Manihiki Plateau was decoupled from the Pacific Plate by the Clipperton Fracture Zone and moved eastwards (Fig. 6.9a). The motion at the Danger Islands Troughs stopped at around 110 Ma due to the establishment of an oblique spreading within the Nova Canton Trough (Figs. 6.9a and 6.9b). This indicates, that the different sub-provinces of the Manihiki Plateau acted as individual plates for a short time, but still inherited significant differences within their crustal structure during the initial break-up of Ontong Java Nui. For the Nova Canton Trough, a scissor-like opening was proposed by *Taylor* (2006) and *Chandler et al.* (2012), separating the Ontong Java Plateau from the Manihiki



	Manihiki Plateau	Ontong Java Nui	Pacific
<b>prior to 125 Ma</b>	- subaerial emplacement as a single crustal unit by massive volcanic outpourings	- emplacement by massive volcanic outpourings with multiple main centers of activity - result of plume-ridge interaction	-formation of the Pacific Triangle (180 Ma) -seafloor spreading at multiple triple junctions
<b>120 Ma</b>	-high magmatic activity on the High Plateau -limited magmatic activity on the Western Plateaus	-initial motion between Manihiki and Hikurangi rotation and crustal stretching	
<b>118 Ma</b>	-initiation of the fragmentation of the Manihiki Plateau -creation of the Manihiki Scarp, spreading north of the High Plateau -creation of the Danger Islands Troughs -initiation of crustal stretching at the Western Plateaus	-development of the Osbourn spreading center between Manihiki and Hikurangi -rotation of the Ontong Java Plateau along with the Western Plateaus	-Triple Junction jump (PAC-FAR-PHO) (Tongareva Triple Junction), -reorganization of plate tectonic framework -possible initiation of the rotation of the Pacific Plate -southward migration of Farallon Phoenix spreading along Tongareva Triple Junction trace
<b>115 Ma</b>	- incorporation of NE – Manihiki into Farallon Plate -incorporation or E-Manihiki into Phoenix Plate	-initiation of spreading at Nova Canton Trough	-initiation of ocean – ocean subduction at West Wishbone Scarp
<b>110 Ma</b>		-first interaction between Hikurangi Plateau and Chatham Rise -rotation of Osbourn Trough -soft – docking of Hikurangi Plateau with Chatham Rise	
<b>100 Ma</b>	-final development of the Danger Islands Troughs	-establishment of oblique spreading at Nova Canton Trough	
<b>95-83 Ma</b>		-cessation of southwards subduction of Hikurangi Plateau -cessation of spreading at Nova Canton Trough -incorporation into Pacific Plate	-full establishment of spreading within the Bellingshausen Sea -cessation of subduction at West Wishbone Scarp

**Table 6.3:** Overview on the tectonic events in the western Pacific from >125 to 83 Ma

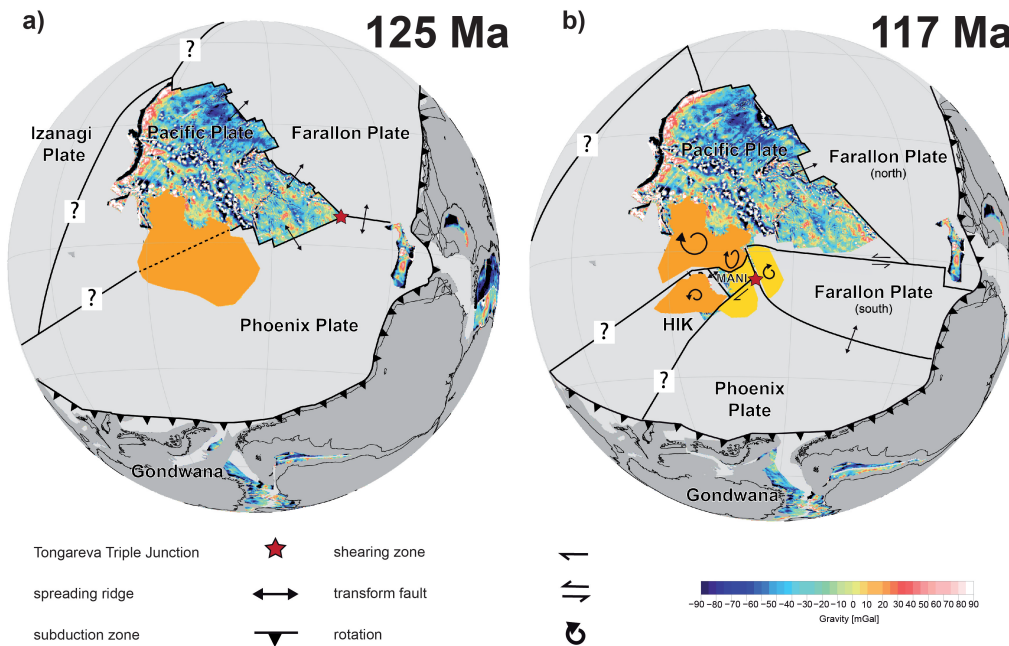


**Figure 6.8:** Tectonic evolution of the Western Pacific during the CNS. The model shows the plate kinematic model of *Seton et al.* (2012) with updated rotation poles for the Western Pacific region obtained in this study. The fixed plate is the Pacific Plate; gravity anomaly map taken from *Sandwell et al.* (2014); plate boundaries (relevant for the reconstruction) are marked in black, continental fragments are shown in grey with today's coast lines in black for better orientation; light grey areas shows seafloor, which has been subducted; Ontong Java Nui related LIPs are marked in orange and yellow for the Manihiki Plateau; the red star indicates the position of the Tongareva Triple Junction; MANI = Manihiki Plate, HIK = Hikurangi Plate (a) 125 Ma (b) 117 Ma

Plateau with an additional rotational component (Figs. 6.9a and 6.9b). After the hard-docking of the Hikurangi Plateau with the Chatham Rise, subduction at the Gondwana margin ceased, leading to one of the largest re-organizations within the plate tectonic framework of the Pacific (e.g. *Luyendyk*, 1995). Seafloor spreading ceased around the Manihiki Plateau and between the different fragments of Ontong Java Nui (Fig. 6.9c). With the establishment of the spreading in the Bellingshausen Sea (e.g. *Eagles et al.*, 2004; *Wobbe et al.*, 2012) the different plateaus are firmly integrated into the Pacific Plate. Younger tectonic activity can mainly be related to hotspot volcanism. *Koppers and Staudigel* (2005) identified tectonic activity within the area of the Nova Canton Trough at 67 and 57 Ma leading to the re-orientation of the Gilbert Ridge and the Tokelau seamount chain, respectively. Multiple fracture zones are identified at the junction between the Nova Canton Trough and the Clipperton FZ as well as at the central Nova Canton Trough (Fig. 6.5). This motion may have been responsible for the southward motion of the Ontong Java Plateau and the re-activation of the Nova Canton Trough as well as the creation of the Suvarov Trough on the Manihiki Plateau (*Pietsch and Uenzelmann-Neben*, submitted). In summary, we updated rotation poles (Tab. 6.4) for the different plates of the western Pacific by considering and incorporating concepts such as the rotation of the Ontong Java Plateau and the Hikurangi Plateau and the presence of a subduction zone at the Wishbone Scarp, which

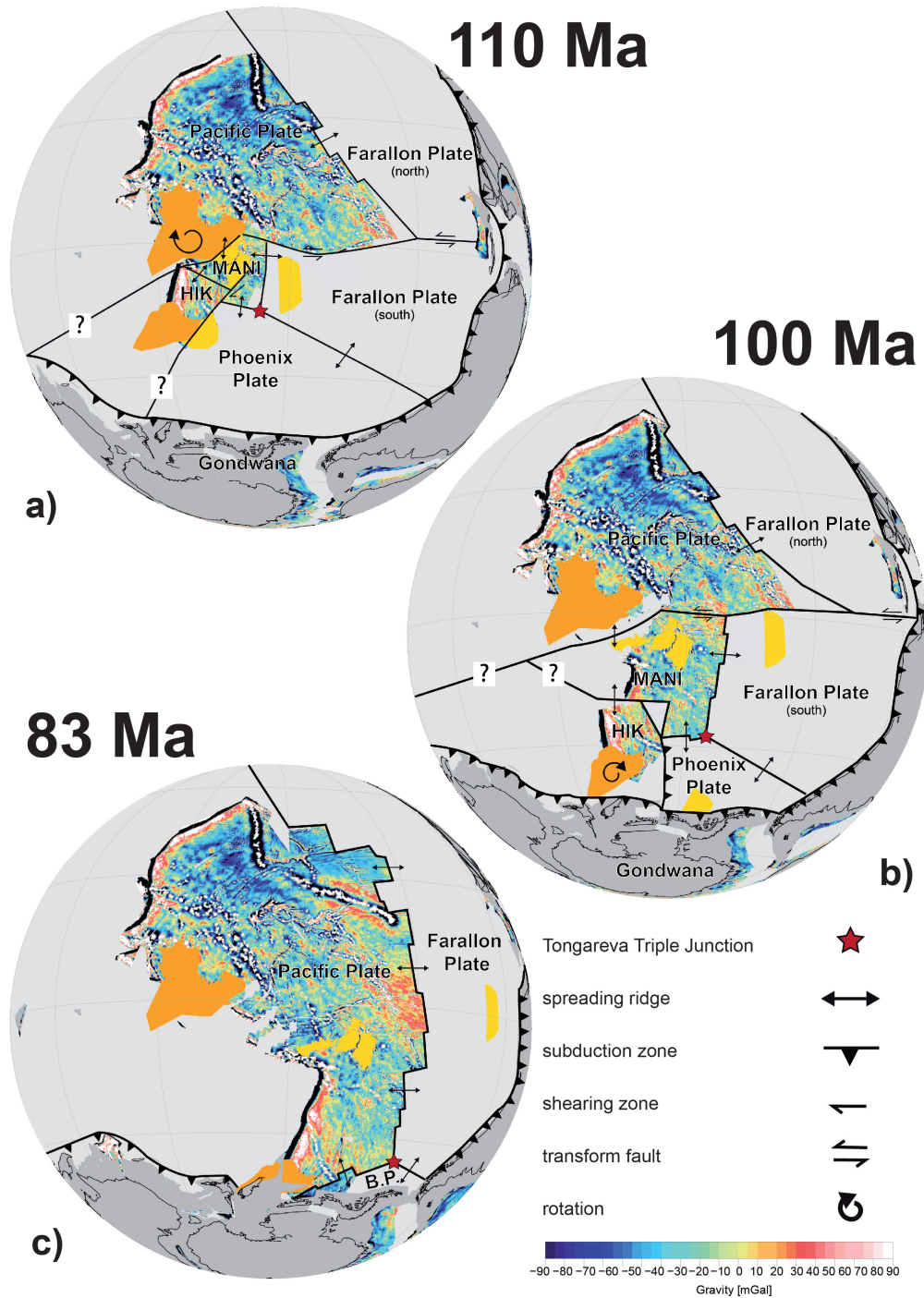


**Figure 6.9:** Tectonic evolution of the Western Pacific during the CNS. The model shows the plate kinematic model of *Seton et al. (2012)* with updated rotation poles for the Western Pacific region obtained in this study. The fixed plate is the Pacific Plate; gravity anomaly map taken from *Sandwell et al. (2014)*; plate boundaries (relevant for the reconstruction) are marked in black, continental fragments are shown in grey with today's coast lines in black for better orientation; light grey areas shows seafloor, which has been subducted; Ontong Java Nui related LIPs are marked in orange and yellow for the Manihiki Plateau; the red star indicates the position of the Tongareva Triple Junction; MANI = Manihiki Plate, HIK = Hikurangi Plate, B.P. = Bellingshausen Plate (a) 110 Ma (b) 100 Ma (c) 83 Ma

	t1 [Ma]	t2 [Ma]	Latitude	Longitude	$\omega$
High Plateau	118	100	-33.72	-4.34	35.28°
	100	90	-45.48	-32.98	16.99°
Western Plateaus	110	100	-47.78	-7.77	28.91°
	100	95	-45.48	-32.98	16.99°
Northeastern Fragment	118	110	-70.61	-18.19	129.52°
Eastern Fragment	118	105	-18.07	-24.77	49.50°
Hikurangi Plateau	120	118	-24.97	52.50	32.53°
	118	100	-77.54	100.71	33.83°
	100	95	-25.38	-65.41	10.96°

**Table 6.4:** relative stage rotations of the Ontong Java Nui related LIPs to the Ontong Java Plateau (fixed to Pacific Plate), while acting as individual plates

have previously not been modeled in a plate kinematic context. Our reconstruction is based on the presence of the LIPs in the western Pacific and gives a detailed history of the early stages of break-up as visible at the plateaus margins. We additionally present evidence for post-Cretaceous tectonic activity in the area of the Nova Canton Trough, which possibly allows the reconciliation between the reconstructed latitudes and paleolatitudes obtained from rock samples.

## 6.6 Conclusions

The Large Igneous Provinces of the western Pacific play an important role within the plate tectonic framework of the region. By evaluating possible emplacement scenarios of a joined emplacement of the Ontong Java Nui related LIPs, an interaction between an arriving plume head and the Pacific-Phoenix ridge can explain the individual crustal structure of the oceanic plateaus. Seismic refraction and reflection data, along with bathymetry and gravity measurements shed light on the multi-faced break-up mechanisms of the “Super”-LIP. The initial break-up includes short-lived spreading centers to the north and east of the Manihiki Plateau, crustal stretching at the Western Plateaus and the southern High Plateau and shearing forces along the Manihiki Scarp. The sub-provinces of the Manihiki Plateau acted as individual plates. Whereas the Western Plateaus rotated along with the Ontong Java Plateau resulting in the pull-apart basins of the Danger Islands Troughs, the High Plateau shows clear break-up margins to all parts of Ontong Java Nui. The updated version of rotational parameters for the Western Pacific includes the individual plates of the Manihiki Plateau as well as the rotation of the Ontong Java Plateau and the Hikurangi Plateau, which have so far been excluded from plate kinematic reconstructions. Late Cretaceous and early Paleocene tectonic activity within the Nova Canton Trough allows the reconciliation between the paleolatitudes from rock samples and the

modeled latitudes.

### **Acknowledgements**

We thank Ernst Flüh and Jörg Bialas of GEOMAR for providing the OBS and OBH systems. We also thank Cpt. L. Mallon and his crew of RV Sonne for their support and assistance during the cruise So-224. We also thank Joann Stock and Bruce Luyendyk for providing access to the seismic data collected during R/V Revelle cruise Kiwi Leg 12 via <http://www.ig.utexas.edu.sdc> and the reviewer, who chose to remain anonymous for his/her comments and suggestions, which improved the manuscript. This project contributes to the Workpackage 3.2 of the AWI Research Programm PACES-II. This project has been funded through a grant by the German Federal Ministry of Education and Research (BMBF) under project number O3GO224A and by institutional resources of the AWI. GPlates 1.5 by the EarthByte Group (University of Sydney, Australia) was used for the plate kinematic reconstruction. Most figures were prepared with GMT4. The data will be available to the public over PANGEA ([www.pangea.de](http://www.pangea.de)) after the completion of the dissertation of K. Hochmuth.

# 7 From the western Pacific to the Andes and Antarctica: The Manihiki Plateau on the move

K. Hochmuth<sup>1</sup> and K. Gohl<sup>1</sup>

<sup>1</sup>*Alfred-Wegener Institut Helmholtz-Zentrum für Polar- und Meeresforschung*

## Abstract

The continents encircling the Pacific Ocean are fringed with terranes of which some are of oceanic origin. Finding the original location of these volcanic terranes in the context of their larger emplacement realm has remained a challenge. The present Manihiki Plateau, a Large Igneous Province (LIP), was emplaced in the early Cretaceous originally with additional fragments to the Northeast and East. Plate kinematic reconstructions suggest the capturing of these fragments by the Farallon Plate and the Phoenix Plate, respectively. By tracing these fragments, we report a Palaeocene collision of the northeastern Manihiki Plateau fragment with the northern South American craton. The northern Andes exhibit multiple terranes of LIP origin. We infer that the Piñón formation consist of lower crustal units of the former Manihiki Plateau. A mid-Cretaceous collision of the eastern Manihiki Plateau fragment can be reconstructed for West Antarctica. The complete subduction of this fragment in the Palmer Land region initiated two collisional stages and a flattening of the subduction slab. The association between present LIPs of the western Pacific, their possible remnants and across-Pacific collision zones allows an insight to the complicated interplay between LIPs, the plate tectonic framework, and modifications of subduction margins from a new angle.

## Keywords:

Large Igneous Provinces, Ontong Java Nui, Plate Tectonics, Pacific Ocean, Interaction oceanic plateau-subduction zone, Manihiki Plateau

## 7.1 Introduction: Large Igneous Provinces in the plate circuit

Oceanic plateaus and oceanic Large Igneous Provinces (LIP) (Coffin and Eldholm, 1994) (Fig. 7.1) play an important role in the plate tectonic circuit, since they alter or radically transform the behavior of the oceanic plate and its boundaries. In the Pacific realm, a wide variety of interaction of oceanic plateaus with subduction zones can be observed, which range from the accretion of terranes (e.g. Malaita terranes) (Ishikawa *et al.*, 2005; Musgrave, 1990) and subsequent blocking of the subduction zone at the Ontong Java Plateau (Coleman and Kroenke, 1981; Mann and Taira, 2004; Miura *et al.*, 2004; Petterson *et al.*, 1999; Taira *et al.*, 2004) to the complete subduction of the oceanic plateau below the Americas (Gutscher *et al.*, 1999; Liu *et al.*, 2010) (Fig. 7.1). Furthermore, the collision of LIPs with continental margins have been associated with the evolution of mountain ranges such as the Laramide orogeny (Liu *et al.*, 2010), or the southern Alps of New Zealand (Reyners *et al.*, 2011). The Pacific subduction margins of North and South America illustrate the interaction with oceanic plateaus in various stages and time frames. Oceanic plateaus, which subducted beneath North America include the conjugate of the Shatsky Rise in the middle Cretaceous (Liu *et al.*, 2010) and the conjugate of the Hess Rise in the late Cretaceous (Fig. 7.1) (Liu *et al.*, 2010). The Inca Plateau influenced the subduction at the South American trench during the Miocene (Gutscher *et al.*, 1999) and the Nazca Ridge within recent times (Fig. 7.1). The Iquique Plateau is currently approaching the subduction zone. Overthickened oceanic crust is often invoked as the origin of accreted mafic terranes (e.g. Mamberti *et al.*, 2003; Tejada *et al.*, 1996), but their emplacement location along with possible remnants is not well constrained. The main challenges for connecting onshore terranes of oceanic plateau origin with their marine conjugates are the great distance between the emplacement areas of the LIP and today's location, considering uncertainties of plate tectonic reconstructions and the alteration and overprint that these terranes experienced during the accretionary process. We use a detailed new plate kinematic model of the Cretaceous western Pacific (Hochmuth *et al.*, 2015) which focuses on the break-up and subsequent dispersal of the Ontong Java Nui "Super"-LIP. This LIP was emplaced during the early Cretaceous (Taylor, 2006) and rifted apart during the Cretaceous Normal Superchron (CNS) (120–83 Ma) (Davy *et al.*, 2008; Taylor, 2006). Previous studies focused only on the main units and sub-plateaus of Ontong Java Nui, omitting smaller fragments. We trace the plate tectonic motion of these fragments and provide insight in projected regions of their subduction and terrane accretion. This allows an insight into deeper crustal layers of oceanic plateaus, possibly revealing emplacement mechanisms of LIPs. A detailed reconstruction also sheds light on the role of LIP fragments and terranes in the plate circuit of the Pacific Ocean.



**Figure 7.1:** Overview on the LIPs of the Pacific Ocean and their subducted remnants. Present LIPs are marked in red, areas of subduction are in light blue. The dark blue areas indicate the possible areas of subducted former northeastern (NE) and eastern (E) fragments of the Manihiki Plateau at the northwestern South America and West Antarctica margins. Previously identified joinedly emplaced LIPs are connected by dashed lines. Present plate boundaries are marked with grey lines. The insert map shows the different sub-provinces of the Manihiki Plateau and the position of the parts of Ontong Java Nui encircling the Manihiki Plateau.

## 7.2 Geological setting: Ontong Java Nui and its remnants

Taylor (2006) proposed the emplacement of the three major LIPs of the western Pacific region (Fig 7.1) – Ontong Java Plateau, Manihiki Plateau and Hikurangi Plateau – as a single “Super”-LIP, named Ontong Java Nui. Shortly after its emplacement within the early Cretaceous (Hoernle *et al.*, 2010; Timm *et al.*, 2011) this “Super”-LIP breaks apart (Davy *et al.*, 2008; Hochmuth *et al.*, 2015; Taylor, 2006; Viso *et al.*, 2005). Crustal models from seismic reflection and refraction data allow a detailed study of this “Super”-LIP break-up (Hochmuth *et al.*, 2015). Whereas the Manihiki Plateau experienced mainly internal fragmentation and has no direct interaction with recent plate boundaries, the Hikurangi Plateau and the Ontong Java Plateau have interacted with the Kermadec-Tonga-Solomon Trench of the Australian Plate boundary. The Hikurangi Plateau collided with and partially subducted below the Chatham Rise within the early Creta-



ceous (Davy *et al.*, 2008; Reyners *et al.*, 2011; Timm *et al.*, 2014) (Fig 7.1). The Ontong Java Plateau blocks the subduction of the Pacific Plate below the Australian Plate and caused a change in subduction direction (e.g. Coleman and Kroenke, 1981; Mann and Taira, 2004; Miura *et al.*, 2004; Petterson *et al.*, 1999; Taira *et al.*, 2004). Prior to the cessation of subduction, multiple small fragments have been obducted as part of the island arc such as the Malaita terranes (Muscgrave, 1990). In addition to the three largest parts of Ontong Java Nui, smaller fragments to the northeast and the east of the Manihiki Plateau have been proposed (Fig 7.1) (Hochmuth *et al.*, 2015; Larson *et al.*, 2002; Pietsch and Uenzelmann-Neben, 2015; Viso *et al.*, 2005). The true size of these fragments can only be estimated by comparison with areas of similar emplacement history such as the northern Ontong Java Plateau (Mochizuki *et al.*, 2005) or the subducted parts of the Hikurangi Plateau (Reyners *et al.*, 2011). In these regions, the undisturbed transition between overthickened LIP crust, which would correspond to the High Plateau and normal oceanic crust, in this case the Phoenix Plate can be observed. Pietsch and Uenzelmann-Neben (2015) show a continuation of intra-basalt seismic reflector bands towards the eastern High Plateau of the Manihiki Plateau, which terminates at the Manihiki Scarp. Deeper layers indicate also the former presence of overthickened crust by the sudden termination of the high velocity zone above the Moho below the Manihiki Scarp (Hochmuth *et al.*, 2015). We infer an approximated emplacement area with a radius of 500 km of the fragments (Fig 7.1) by the initial crustal thickness obtained from seismic refraction data (20 km) and the undisturbed leveling to normal oceanic crust within the overlying basaltic units as seen on the northern Ontong Java Plateau. The true magmatic volume of the fragments cannot be calculated from the available datasets. The current locations of the northeastern and eastern fragments of the Manihiki Plateau can be derived by carefully reconstructing their plate kinematic paths across the Pacific region and by geophysical and geological observations from their predicted present locations.

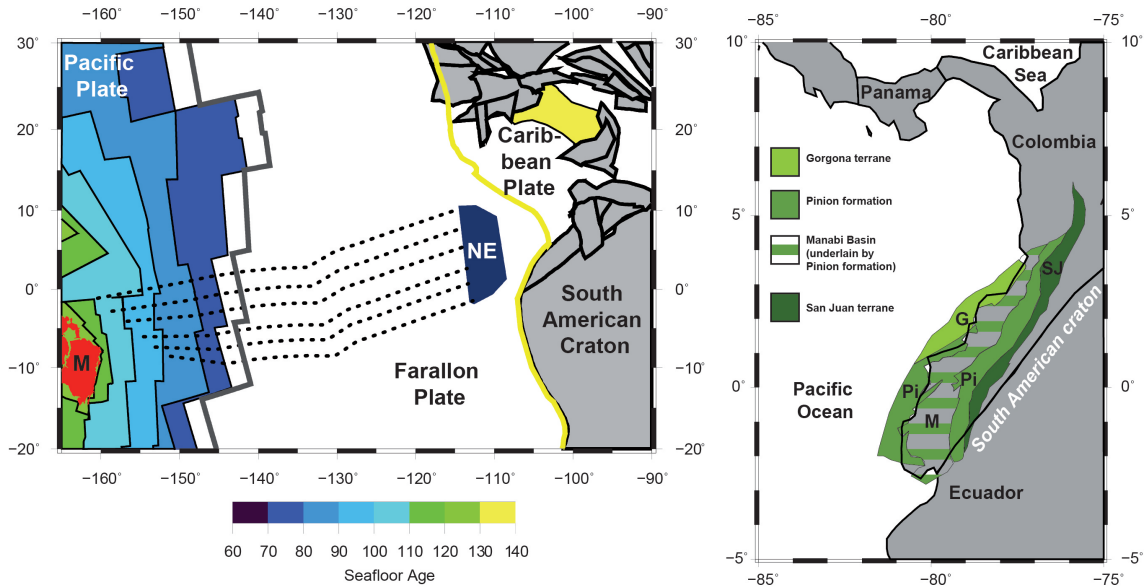
### **7.3 Results of plate kinematic modeling of the Pacific Ocean (Cretaceous – Paleogene)**

Our presented plate kinematic model of the Pacific is based on the global reconstruction by Seton *et al.* (2012) for the time after the CNS and the reconstruction of the initial break-up of Ontong Java Nui for the time of the initial emplacement until chron C34 (83 Ma) by Hochmuth *et al.* (2015).

#### **7.3.1 Northeastern Manihiki Plateau fragment**

A former northeastern continuation of the Manihiki Plateau beyond its present extent has been proposed from bathymetric and gravimetric observations by multiple authors (Larson *et al.*, 2002; Viso *et al.*, 2005). Its size is constrained by the presence of the Clipperton Fracture Zone (FZ) to the North. The northeastern fragment was separated from the Manihiki Plateau by a fast clockwise rotation and captured by the Farallon Plate shortly after the break-up of Ontong Java Nui (Hochmuth *et al.*, 2015; Viso *et al.*, 2005). Its motion across the Pacific is confined by the

spreading rate between the Pacific Plate and Farallon Plate (Seton *et al.*, 2012) (Fig 7.2a). The plateau fragment was trapped between the Clipperton FZ and the Galapagos FZ, which allow tracing its motion. It was transported towards the South American craton, where it arrived during the Paleocene at today's northern Andes of Ecuador and Colombia (Fig 7.2).



a) 60 Ma

b) geological map at 0 Ma

**Figure 7.2:** Paleocene collision of the northeastern fragment of the Manihiki Plateau (NE) with the South American craton: a) plate tectonic setting at 60 Ma with the motion path of the fragment (dotted lines), subduction trench (yellow) and Pacific-Farallon spreading (dark grey line); b) simplified geological map of the northern Andes after Mamberti *et al.* (2004) and Cedié *et al.* (2003) with marked Cretaceous LIP remnants

### 7.3.2 Eastern Manihiki Plateau fragment

Seismic reflection and refraction seismic data show strong evidence of the former presence of an eastern fragment of the Manihiki Plateau (Hochmuth *et al.*, in review; Pietsch and Uenzelmann-Neben, 2015). The break-up between the High Plateau of the Manihiki Plateau and the eastern fragment involved a large shearing zone at the Manihiki Scarp (Fig. 7.1) and short-lived spreading centers (Hochmuth *et al.*, 2015; Larson *et al.*, 2002; Viso *et al.*, 2005). The plate boundary between the Manihiki Plateau and the Phoenix Plate is defined by the Tongareva Triple Junction trace (Fig. 7.3a). We can, therefore, limit the possible collision area between the eastern fragment and the eastern Gondwana margin of present West Antarctica to the area west of the Tongareva Triple Junction and east of the Chatham Rise where the Hikurangi Plateau subducted (Fig. 7.3). The entire motion between the eastern fragment and the Manihiki Plateau took place during the CNS. Since magnetic spreading anomalies are absent during this time period, we constrain the motion by seafloor fabric such as fault systems as well as major tectonic events (Fig. 7.3a). The Hikurangi Plateau hard-docked to the Chatham Rise approximately

between 105 and 100 Ma (Davy, 2014), ceasing the southward subduction. We predict a similar timeframe for the interaction of the eastern fragment with the subduction zone along the present Bellingshausen Sea margin of West Antarctica. Collision and subduction must have occurred within the Alexander Island and Palmer Land region (Figs. 7.3b,c).

## 7.4 The Manihiki Plateau on the move

### 7.4.1 Oceanic terranes of the northern Andes: Resting place of Manihiki Plateau fragment

The northern Andes and the adjacent Caribbean region, the projected area of collision of the northeastern Manihiki Plateau fragment during the Paleocene, are a mosaic of countless terranes of oceanic and continental origin (see e.g. *Boschman et al.*, 2014, and references therein for an overview) (Fig. 7.2b). The Caribbean Large Igneous Province (CLIP) emplaced at about 90 Ma and can be attributed to the Galapagos hotspot (e.g. *Hill*, 1993). *Hoernle et al.* (2004b) identified evidence of earlier plume activity in the region and argue for multiple magmatic episodes spanning 70 million years. After the main emplacement phase of the CLIP, very young and, therefore, still buoyant LIP crust collided with the South American craton, resulting in terrane aggregation (*Jaillard et al.*, 2009; *Kerr and Tarney*, 2005; *Mamberti et al.*, 2003). Other terranes of the region are older than the CLIP event, dating in the early Cretaceous, such as the San Juan terranes and the Piñón formation in Ecuador and Columbia (Fig. 7.2b) (*Jaillard et al.*, 2009; *Mamberti et al.*, 2003; *Reynaud et al.*, 1999) and the Chortis Block in Costa Rica (*Hoernle et al.*, 2004b), making them possible candidates to be remnants of the Manihiki Plateau fragment. The Gorgona Plateau, which is obducted at Gorgona Island, shows an emplacement age of 90 Ma, comparable to that of the CLIP, but was accreted to the South American craton in the Paleocene (*Kerr and Tarney*, 2005). Paleolatitude calculations provide an emplacement latitude between 26 °S and 30 °S (*Kerr and Tarney*, 2005), which is also the emplacement latitude of the northern Manihiki Plateau (*Cockerham and Jarrard*, 1976; *Hochmuth et al.*, 2015). The age of the accreted overthickened LIP crust plays, along with the igneous volume and the crustal thickness, a crucial role for the interaction with the subduction zone (*Cloos*, 1993). Whereas a young LIP resists subduction due to its buoyancy, older LIPs are less buoyant and can be subducted. The northeastern fragment of the Manihiki Plateau has a maximum crustal thickness of 20 km and arrived 60 Myrs after its emplacement at the subduction zone, according to our plate kinematic model. A possible analog for this interaction is the subduction of the counterpart of the Shatsky Rise below southern California, which led to a flattening of the subduction slab and triggered, after the basalt-eclogite transformation, the build-up of the Laramide orogen (*Liu et al.*, 2010). Another similar set-up can be observed at the Inca Plateau in the Peruvian Andes (Fig. 7.1), where a flat subduction slab is present (*Gutscher et al.*, 1999). The counterpart of the Inca Plateau, the Marquesas Plateau, shows a similar crustal thickness of 17 km (*Caress et al.*, 1995) as the Manihiki Plateau. But can a flattening of the subduction slab also be observed in the northern Andes? The northern Andes are an amagmatic arc between

140 Ma and 40 Ma (Jaillard *et al.*, 2009). Therefore, subduction mechanisms differ from the magmatic-arc central Andes including a north-south trending shearing component. This might lead to the presence of oceanic plateau slivers such as the San Juan terranes or the Piñón formation within the northern Andes (Fig. 7.2b). The Piñón formation shows strong geochemical similarities to the Ontong Java Plateau formation, is dated at 123 Ma (Reynaud *et al.*, 1999) and was obducted during a secondary large accretional event within the Paleocene. The San Juan formation is of the same age, is also attributed to a LIP event (Mamberti *et al.*, 2003; Reynaud *et al.*, 1999), but was accreted to the South American craton in the early Campanian during a first major accretion phase (Reynaud *et al.*, 1999). Therefore, we suggest from the available data that the Piñón formation is the most likely remnant of the northeastern fragment of the Manihiki Plateau. Seismic refraction studies by Graindorge (2004) indicate P-wave velocities of 6.1 km/s to 7.0 km/s, which is comparable to those of the middle and lower crust of the Manihiki Plateau. A high velocity zone (P-wave velocities >7.3 km/s), as present in the lower crust of the Manihiki Plateau (Hochmuth *et al.*, 2015, in review), could not be resolved in the presented data. The Piñón formation is severely faulted and overlain by Cenozoic to recent sediments of the Manabí Basin (Mamberti *et al.*, 2004). By comparing the estimated size of the northeastern fragment and the oceanic terranes within the northern Andes, we infer that parts of the plateau, probably those of thinner crustal thickness, and most of the lowermost crust have been subducted in this region. Paleolatitude calculations provide strong indications for the ophiolites of Gorgona Island to have been a part of the Manihiki Plateau. They were dated to be about 90 Ma old and therefore not emplaced during the initial Ontong Java Nui event within the early Cretaceous (Kerr and Tarney, 2005). This age correlates to the secondary magmatic phases of the Manihiki Plateau (Hochmuth *et al.*, in review; Pietsch and Uenzelmann-Neben, 2015), but it is uncertain whether this magmatic phase occurred on all fragments, although both the Hikurangi Plateau and the Ontong Java Plateau experienced multiple phases of magmatic activity (Hoernle *et al.*, 2010; Inoue *et al.*, 2008). The northeastern fragment of the Manihiki Plateau could also have experienced further fragmentation and alteration during the accretionary process, breaking the plateau into allochthon terranes comparable to the Ontong Java Plateau at the Solomon Islands (Mann and Taira, 2004; Musgrave, 1990; Petterson *et al.*, 1999). The presence of the LIP remnant as an accreted terrane within the northern Andes allows an insight into the lower crust of the present Manihiki Plateau, which cannot be sampled in its marine setting. For instance, physical, petrological and geochemical properties of the lower crust and the high velocity zone above the Moho, which is a key characteristics in LIP identifications (Coffin and Eldholm, 1994; Ridley and Richards, 2010), or even of the Moho can be tested in such an in-situ like situation. The unique amagmatic setting of the South American subduction zone in the northern Andes allows the preservation of migrated LIP fragments, which would otherwise have been subducted such as those of the conjugate Hess Rise and the Inca Plateau.

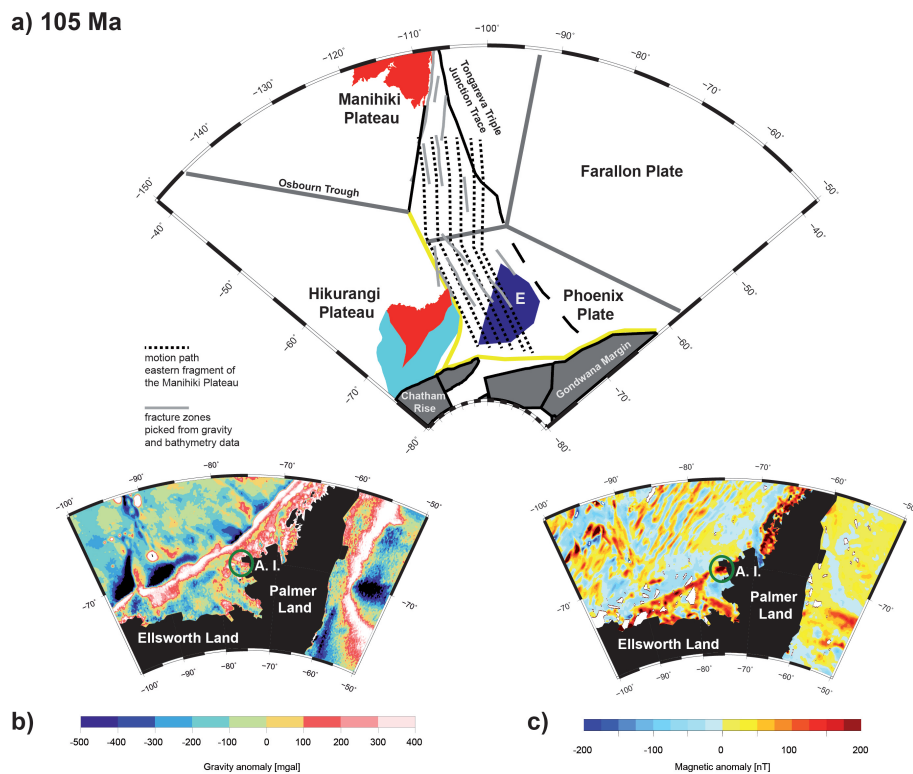


**Figure 7.3:** Mid-Cretaceous collision of the eastern fragment of the Manihiki Plateau (E) with the Gondwana margin of West Antarctica: a) plate tectonic setting at 105 Ma; dotted lines mark the motion path of the eastern fragment along mapped fracture zones (light grey). Dark grey lines indicate spreading centers, yellow lines indicate subduction zones. b) Marine gravity anomaly map after *Sandwell et al.* (2014) c) Magnetic anomaly map after *Maus et al.* (2009). The green circle in both figures marks the position of the Charcot magnetic anomaly and Charcot Island west of Alexander Island (A.I.).

#### 7.4.2 Palmer Land events: initiated by LIP subduction?

As opposed to the identification of possible remnants of the Manihiki Plateau within the northern Andes, which can be based on a wide variety of fieldwork and published data, the prospected collision site of the eastern fragment of the Manihiki Plateau within the Bellingshausen Sea and Palmer Land of present West Antarctica has been only scarcely investigated and mapped due to ice coverage. Rock outcrops are few and extremely difficult to access and sample. The identification of possible LIP fragments is based on the few available rock samples and geophysical data from the area (Fig. 7.3b,c). The presence of a flattened subduction slab analog to the Inca Plateau cannot be used as an indicator for LIP subduction, as the plate tectonic setting changed dramatically from an active subduction to a passive margin since the Cretaceous. The Pacific realm of West Antarctica has been described as a mosaic of different terranes – similar to the northern Andes – which were accreted since the establishment of the eastern Gondwana subduction margin (e.g. *Ferraccioli et al.*, 2006). The subduction was supposedly stopped by the hard-docking of the Hikurangi Plateau, part of former Ontong Java Nui, at the Chatham Rise of Zealandia (conjugate of present Marie Byrd Land sector of Antarctica) at 105-100 Ma (Fig.

7.3a) (Davy, 2014; Davy *et al.*, 2008). Unlike the Hikurangi Plateau, the eastern fragment of the Manihiki Plateau, which is also about 25 m.y. old by its arrival at the subduction zone, seems to have subducted completely. Along with age and the subduction mode, the crustal thickness is the main factor that determines whether an oceanic plateau is subducted or not (Cloos, 1993). The crustal thickness of the Hikurangi Plateau has been derived from gravity anomaly modeling to be between 15 km (Davy and Wood, 1994) and 23–25 km (Davy *et al.*, 2008). The larger thickness is comparable to that of the Manihiki Plateau (20 km for High Plateau) (Hochmuth *et al.*, in review) and the Ontong Java Plateau (>30 km) (Miura *et al.*, 2004). The eastern Manihiki Plateau fragment must have had a maximum crustal thickness of 20 km at its break-up margin at the Manihiki Scarp with decreasing thickness towards its outer margins at the fringe of Ontong Java Nui. It is, therefore, comparable to the subducted thinner part of the Hikurangi Plateau (Reyners *et al.*, 2011). We suggest that the complete subduction of the eastern Manihiki Plateau fragment was possible due to its smaller crustal thickness in comparison to that of the Hikurangi Plateau. Our study suggests that the break-up between Zealandia and West Antarctica, which occurred after the hard-docking of the Hikurangi Plateau in the mid-Cretaceous (e.g. Eagles and Vaughan, 2009; Larter *et al.*, 2002), was preceded by the subduction of the eastern fragment of the Manihiki Plateau. The presence of relatively young buoyant LIP crust could cause a the flattening of the subducting slab (Gutscher *et al.*, 1999, 2000). A flattened slab leads to the emplacement of adakites within the volcanic arc (Gutscher *et al.*, 2000). In the Palmer Land region, adakitic rocks crop out (Wareham *et al.*, 1997) and point to a mixing of different magmatic sources including a young (< 25 M. yr.) oceanic component, which corresponds to the age of the LIP fragment. Vaughan *et al.* (2012) identified two distinct kinematic phases in the Palmer Land region they called the Palmer Land Events with phase 1 (about 107 Ma) and phase 2 (about 103 Ma). Both events fall into the projected collision time of the eastern fragment of the Manihiki Plateau with the margin. Whether the two distinct phases can be associated with soft- and hard-docking events or rotation of the fragment comparable to that of the Hikurangi Plateau (Davy, 2014) cannot be distinguished from our reconstruction. But as the geological evidence indicates two different paleo-strain axes (Vaughan *et al.*, 2012), a modification of the collision pattern such as a rotation analog to the Hikurangi Plateau (Davy, 2014) seems plausible. A possible candidate to host remnants of the eastern fragment of the Manihiki Plateau may be the yet unexplained, strong Charcot magnetic anomaly, which lies at the continental margin of the Palmer Land Event orogen west of Alexander Island (Fig. 7.3b,c). Petrological samples from Alexander Island point to multiple phases of northward moving magmatic activity related to the subduction of young oceanic crust, which may be related to the subduction of the colliding Pacific-Phoenix oceanic spreading ridge (McCarron and Larter, 1998) or to presence of an oceanic plateau fragment, although the composition of dykes does not change in this time frame (Scarrow *et al.*, 1998). The presence of an oceanic LIP fragment in the area of Palmer Land and Alexander Island seems plausible, although the exact area and impact of the collision or subduction cannot be better constrained. However, the presence of adakitic rocks indicate a slab flattening induced by the subduction of an oceanic plateau. The identification

of LIP fragments within West Antarctica enhances the understanding of the tectonic and geodynamic evolution this region, which is a crucial piece towards consistent global plate tectonic models and the connection between the Pacific and Atlantic/Indian plate circuit.

### **7.5 Conclusions: The impact of Ontong Java Nui on the Pacific evolution**

Ontong Java Nui emplaced during the Early Cretaceous and disintegrated into multiple fragments within a relative short period of time. Whereas the Manihiki Plateau – as its centerpiece – is located far from any present plate boundaries, all other fragments interacted with the circum-Pacific subduction zones. By blocking the subduction at the Solomon Trench, the Ontong Java Plateau initiated a subduction polarity reversal. The Hikurangi Plateau subducted below the Chatham Rise and the South Island of New Zealand, leading to a cessation of the subduction in this area of the eastern Gondwana margin. We trace the motions of northeastern and eastern fragments of the Manihiki Plateau across the Pacific Ocean to locations where they collided at the subduction margins of in the northern Andes and of West Antarctica, respectively. We propose, based on geophysical, petrological and plate kinematic evidence, that the Piñón formation represents the remnant of the Manihiki Plateau within the northern Andes. The aggregation and partial subduction below the South American craton occurred during the Paleocene. The eastern fragment of the Manihiki Plateau was completely subducted in the area of Palmer Land of the southern Antarctic Peninsula in the middle Cretaceous, analogue to the subducted part of the Hikurangi Plateau.

### **Acknowledgements**

This project contributes to the Workpackage 3.2 of the AWI Research Programm PACES-II. This project has been funded through a grant by the German Federal Ministry of Education and Research (BMBF) under project number O3GO224A, associated with the RV Sonne cruise SO-224 to the Manihiki Plateau led by Gabriele Uenzelmann-Neben. Additional funds were provided by institutional resources of the AWI. We thank Graeme Eagles and Robert Larter for their helpful discussion input to this paper. GPlates 1.5 by the EarthByte Group (University of Sydney, Australia) was used for the plate kinematic reconstruction. Most figures were prepared with GMT4.

## 8 Conclusions

The aim of this thesis was to improve our knowledge of the crustal and upper mantle structure of the Manihiki Plateau, as well as its role in the plate kinematic setting of the proposed "Super"-LIP Ontong Java Nui and the Pacific Ocean. In the following, I will summarize my findings, as presented in the previous chapters and relate them to the research questions raised in Chapter 2. For convenience, Fig. 8.1 shows the major geographical locations of the western Pacific, that are discussed in this dissertation.

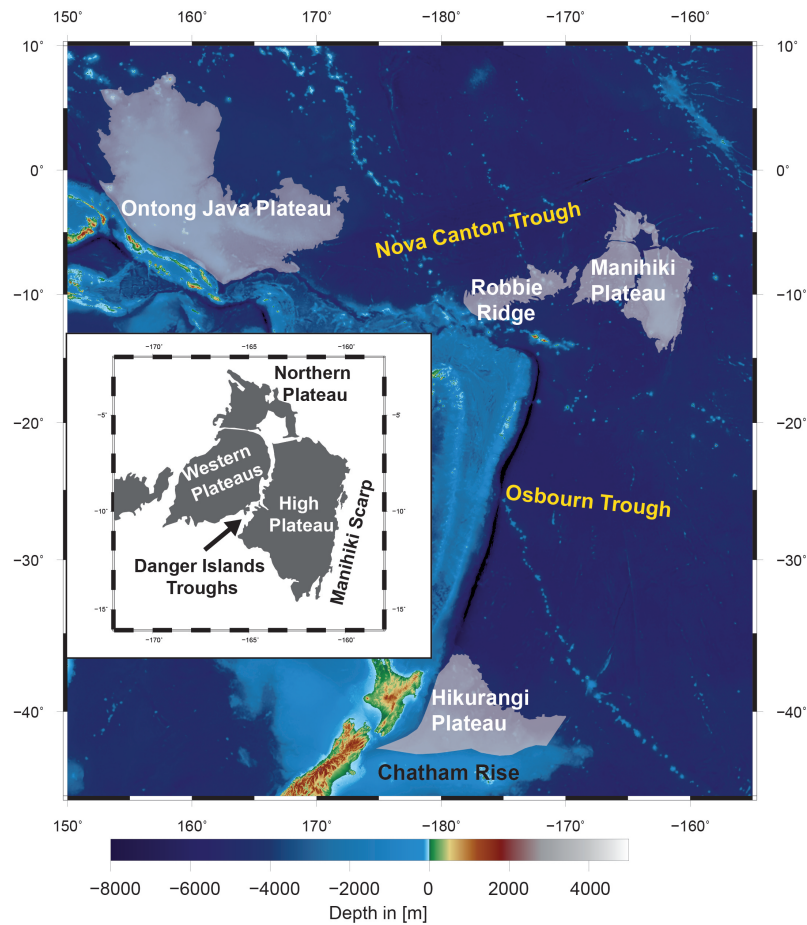


**Figure 8.1:** Bathymetric map of the western Pacific, LIPs of Ontong Java Nui are shaded in white, former spreading centers are marked in yellow, the inlet figure shows a close-up of the Manihiki Plateau



## **Crustal and upper mantle structure of the Manihiki Plateau (Chapter 5)**

Refraction/wide-angle reflection seismic profiling revealed the crustal structure of the two main sub-provinces of the Manihiki Plateau (Fig. 8.1), the High Plateau and the Western Plateaus, for the first time. The total crustal thickness of the High Plateau is 20 km, which is comparable to previously studied LIPs. A HVZ is present in the lower layers of the whole plateau. This points to the emplacement by a hot mantle source. The upper crust of the High Plateau consists of basaltic flow units of multiple volcanic phases. The eruptive centers of the secondary magmatic phase are visible in the upper crust and can be connected to major magmatic pathways in the middle and lower crust. The Western Plateaus show more variation in the crustal thickness, which decreases from 17.3 km in the East to 9.2 km in the West. Analog to the High Plateau, a HVZ is present throughout the profile within the lower crust of the sub-province. The crust is structured by multiple normal fault systems. The secondary volcanism on the Western Plateaus is a low-volume seamount volcanism and lacks the massive emplacement of basaltic flow units during secondary volcanic phases. Subsequently, the sub-provinces of the Manihiki Plateau were initially emplaced as one crustal structure, but later magmatic stages differ significantly. This magmatic and tectonic setting has not been reported from any other LIP so far.

## **The internal fragmentation of the Manihiki Plateau (Chapter 5)**

The fragmentation of the Manihiki Plateau into multiple sub-provinces (Fig. 8.1) with different magmatic and tectonic histories is a unique setting inherited by the plate tectonic reorganization of the Pacific Ocean during the early Cretaceous. The Manihiki Plateau also experienced tectonic deformation at all its margins.

The refraction/wide-angle reflection seismic profiles revealed the structure of the margins of the plateau and of the Danger Islands Troughs, which separate the two main sub-provinces of the Manihiki Plateau. The Danger Islands Troughs mark the border between the two tectonic and magmatic regimes of the Manihiki Plateau. The High Plateau experienced marginal tectonic activity and massive magmatic emplacement during secondary magmatic stages. The Western Plateaus are tectonically altered and show only low-volume secondary volcanism. The troughs developed shortly after the initial emplacement phase of the LIP and lack upper crustal layers, a typical feature of pull-apart basins. The pull-apart basins of the Danger Islands Troughs are the result of the rotation of the Ontong Java Plateau and the Western Plateaus prior to the initiation of spreading at the Nova Canton Trough. Therefore, the fragmentation of the Manihiki Plateau is a result of the individual motion of the different sub-provinces during the initial break-up of Ontong Java Nui.

Further fragments of the Manihiki Plateau were previously proposed to the East and the Northeast of the High Plateau. The HVZ in the lower crust of the High Plateau terminates rather abruptly at the Manihiki Scarp, a North-South trending shearing zone, where lower crustal layers are exposed at the seafloor. This indicates that the Manihiki Plateau had an eastward con-

tinuation. This is in agreement with intrabasaltic reflections visible within the seismic reflection data from the High Plateau (*Pietsch and Uenzelmann-Neben, 2015*). Gravimetry and bathymetry data of the area proposes the presence of an northeastern fragment north of the High Plateau, but there is no seismic data available yet from this area to support or disprove this hypothesis.

### **The Manihiki Plateau and the proposed "Super" - LIP Ontong Java Nui (Chapter 6)**

The question, if the three largest LIPs of the western Pacific emplaced as one single "Super"-LIP is still highly debated in the scientific community. The Manihiki Plateau would expose break-up margins to all parts of the proposed "Super"-LIP. The joined emplacement between the Manihiki Plateau and the Hikurangi Plateau is well constrained by the former spreading center at the Osbourn Trough (Fig. 8.1). The Nova Canton Trough, however, lacks a clear spreading center between the Western Plateaus and the Ontong Java Plateau (Fig. 8.1). The data from the Western Plateaus shows multiple deep reaching normal fault sequences, which are in agreement with crustal stretching and rifting structures. The omnipresence of a HVZ in the lower crust of the Manihiki Plateau also indicates a prolongation of the initial plateau to the West. The direction of the pull-apart basins of the Danger Islands Troughs is consistent with the rotation proposed for the Ontong Java Plateau after the emplacement (*Chandler et al., 2013*). This points to a partial rotation of the Western Plateaus and Ontong Java as a single crustal block and therefore a joined emplacement of the Manihiki Plateau and the Ontong Java Plateau.

For reconstructing Ontong Java Nui, a variety of different tectonic and magmatic features need to be considered. Therefore, I mapped the structure of the margins of the Manihiki Plateau and calculated the possible overlap between the different sub-provinces due to tectonic stretching and secondary magmatic overprint. By extrapolating this classification of the margin to the other LIPs, Ontong Java Nui can be reassembled. Subducted fragments can be added from the literature (*Musgrave, 2013; Reyners et al., 2011*) and by the extrapolation of basalt flow patterns to the East and the North of the Manihiki Plateau. This leads to an initial size of Ontong Java Nui of 1.1 % of the Earth's surface, which is approximately twice the size of Argentina. The different crustal thicknesses of Ontong Java Nui can be explained by a pulsating plume, which interacted with the Pacific-Phoenix spreading center during the emplacement of the LIP. The HVZ within the lower crust shows the extent of the initial magmatic emplacement area of Ontong Java Nui.

### **Plate-tectonic reconstruction of the western Pacific for the Cretaceous Normal Superchron (Chapters 6 and 7)**

The Manihiki Plateau lays at the center of Ontong Java Nui, exposing break-up margins to all parts of the "Super"-LIP. Since no seafloor spreading anomalies are present during the CNS, plate motion has been traced for example by fracture zones, which act as motion paths of the tectonic plate and traces of former plate boundaries such as the Tongareva triple junction trace. Before the spreading centers at the Osbourn Trough (Manihiki - Hikurangi) and at the

Nova Canton Trough (Ontong Java - Manihiki) were established at 118 Ma and 100 Ma respectively, the break-up of Ontong Java Nui was a mosaic of rifting, transform and rotational forces. The eastern and northeastern fragment were captured by the Phoenix and Farallon Plates, respectively. The soft-docking of the Hikurangi Plateau and the Chatham Rise initiated a rotation of the plateau (105 Ma). The southward subduction at the Chatham Rise ceased at 95 Ma. At the end of the CNS, the spreading between all LIP fragments stopped and the fragments were integrated into the Pacific Plate. Neogene and Paleogene tectonic motion can be reported from the Nova Canton Trough area and also from the Manihiki Plateau, where the Suvarov Trough is created.

The northeastern and eastern fragments of the Manihiki Plateau have so far been omitted in plate tectonic reconstructions. By tracing their motion along with the Farallon Plate and the Phoenix Plate, possible areas of subduction can be identified. The northeastern fragment of the Manihiki Plateau reached the Andean subduction zone in the region of today's Ecuador and Colombia at 60 Ma. The northern Andes are an amagmatic arc, with a North-South trending shearing component at the time, leading to the aggregation of oceanic plateaus. By comparing petrological, geochemical and geophysical data, the Piñón formation (northern Andes) can be identified as a possible remnant of the Manihiki Plateau.

The eastern fragment of the Manihiki Plateau moved southwards arriving at the eastern Gondwana subduction zone at 100 Ma. In the Palmer Land area of western Antarctica, a two-phased collision by a mafic block has been proposed during this time. The presence of adakitic rocks points to a flattened subduction zone initiated by the presence of an oceanic plateau in the area, which subducted completely. A possible relict of the eastern fragment is the Charcot anomaly offshore Alexander Island within the Bellingshausen Sea.

## 9 Outlook and further research

The cruise So-224 and the subsequent processing and interpretation of the acquired data increased our understanding of the crustal structure of the Manihiki Plateau, its role within Ontong Java Nui and the plate tectonic framework of the western Pacific Ocean. But several new questions arose, which calls for further investigation.

### 9.1 Crustal structure of the Manihiki Plateau and its margins

I modeled the crustal structure of the two main sub-provinces of the Manihiki Plateau. The highly variable structure and thickness of the crust is a so far unreported feature of LIPs. To be able to fully understand the break-up of Ontong Java Nui, the fragmentation of the Manihiki Plateau and grasp the total magmatic volume of the LIP emplacement, additional surveying with reflection seismic and refraction/wide-angle reflection data across the so far unsurveyed margins of the Manihiki Plateau is needed (Fig. 9.1).

The crustal structure of the North Plateau and its northern margins is unknown. For a better understanding of the break-up of Ontong Java Nui and the fragmentation of the Manihiki Plateau, refraction seismic and seismic reflection data needs to be acquired from this area. Additionally, there are only few age constraints on the trough separating the North Plateau from the Western Plateaus, although this area has been sampled extensively (*Werner et al.*, 2013). Profile A-A' could clarify, if the trough is an extension of the Danger Islands Troughs or the result of Neogene tectonic reactivation. This profile crosses the potentially thickest part of the Western Plateau, as inferred from gravity anomaly maps (Fig. 9.1) (*Sandwell et al.*, 2014), and the margin towards the Samoan Basin. The crustal structure of the southern Western Plateaus is characterized by strong tectonic deformation and low-volume-seamount-magmatism (*Hochmuth et al.*, in review), but gravity anomaly maps possibly indicate strong variations within the sub-province, which could be accessed further by this profile. The southern margin towards the Samoan Basin has not been surveyed so far. It could give further indications of the separation between the Manihiki Plateau, as the potential conjugate to the Rapuhia Scarp of the Hikurangi Plateau and the evolution of the Samoan Basin.

Profile B-B' could clarify the crustal nature of the North Plateau and its relationship to the Ontong Java Plateau (Fig. 9.1). Furthermore, with additional data from the Tokelau Basin the

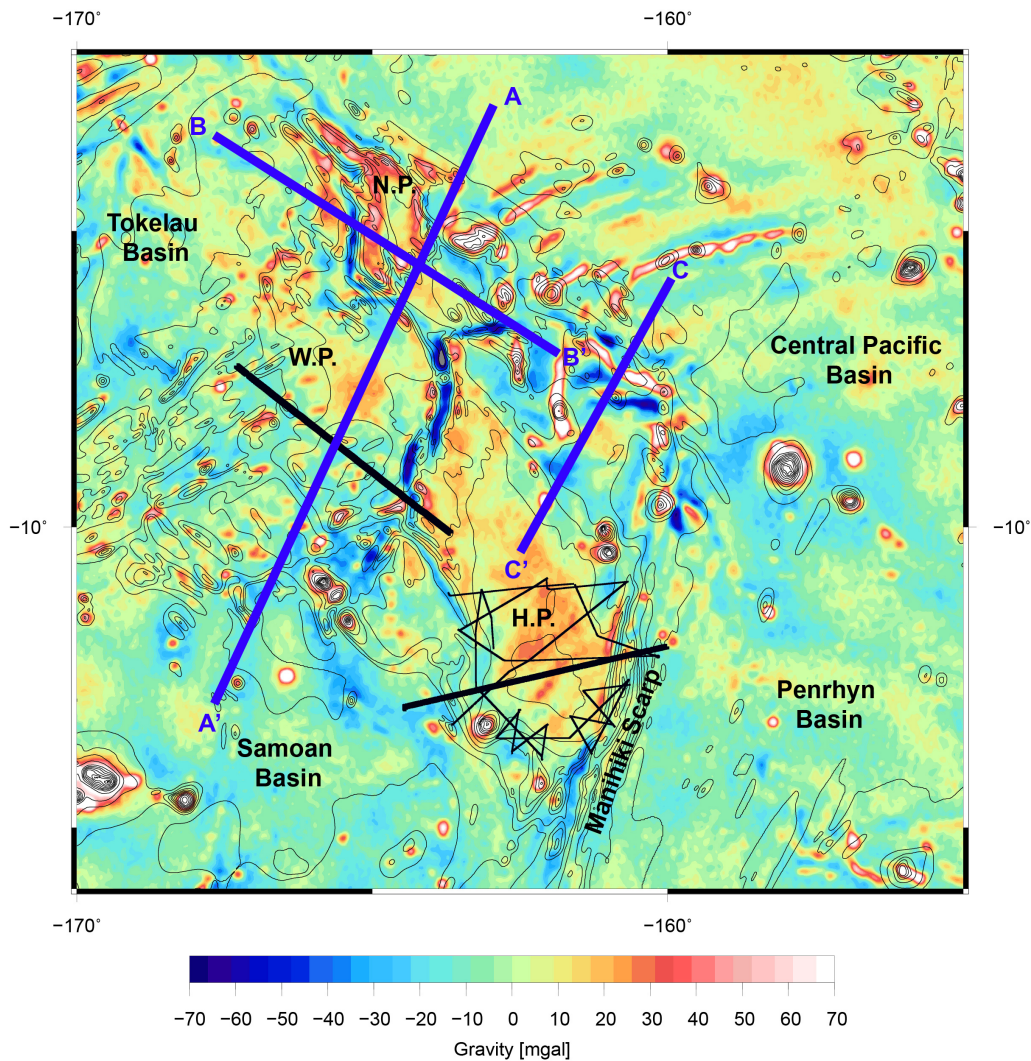


**Figure 9.1:** Gravity anomaly map of the Manihiki Plateau (Sandwell *et al.*, 2014) illustrating the position of proposed additional refraction/wide-angle reflection profiles (blue), H.P. = High Plateau. N.P. = North Plateau, W.P. = Western Plateaus, the data collected during So-224 is shown in black

transition between LIP crust and normal oceanic crust could be identified. The current data set (AWI-20120100) unfortunately fails to cross the transition zone, which is apparently further to the West within the Tokelau Basin. This would further constrain the amount of crust emplaced during the Ontong Java Nui event.

Finally, a profile C-C' would help to understand the different signature of the gravity anomaly of the northern High Plateau, which is rather comparable to the Western Plateaus (Fig. 9.1). The proposed northeastern fragment of the Manihiki Plateau was emplaced here. Additional refraction/wide-angle reflection seismic data could provide further indications of its existence and its separation mechanism during the break-up of Ontong Java Nui.

## 9.2 Enhancement of plate tectonic reconstructions

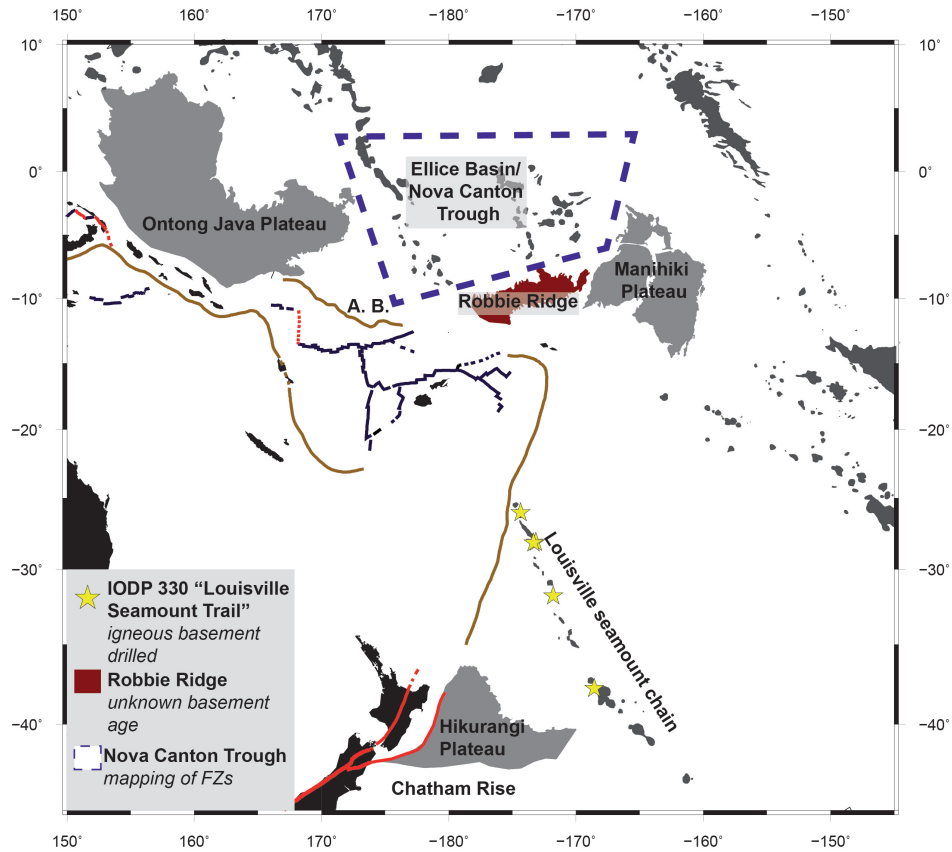


**Figure 9.2:** Additional data for plate kinematic reconstruction of the Western Pacific: stars indicate the drilled igneous basement at the Louisville hotspot chain; the Robbie Ridge is marked in red; the blue dashed line encircles the Ellice Basin/ Nova Canton Trough; the position of the Alexa Bank is marked by A. B.. Active subduction zones are marked in brown, transform faults in red and mid-ocean ridges in black.

Plate tectonic reconstruction in the time of the CNS is complicated and evokes a large error margin. To constrain plate motion during this time it is necessary to use all available dated locations (see Chapter 6 Tab. 6.1). The main features that used in this dissertation to trace the plate motion are fracture zones and the margins of the LIPs. They can give good indications of the plate motion, but dating remains very critical. In 2011, IODP expedition 330 "Louisville Seamount Trail" drilled a section of age progressing seamounts of the Louisville seamount chain, which crosscuts the former Hikurangi Plate (*Expedition 330 Scientists, 2011*) (Fig. 9.2). One of the main goals of this expedition was dating the underlying igneous basement formed at the Osborn Trough. Unfortunately, the resulting data are not published yet. Dating the Hikurangi Plate is crucial for the reconstruction of the plate motion between the Manihiki Plateau and the Hikurangi Plateau. A better constrain on the cessation of spreading at the Osborn Trough could clarify the timing of the soft- and haddocking events of the Hikurangi Plateau at the continental Chatham Rise (Fig. 9.2). The crustal thickness of the Hikurangi

Plateau is also of great interest, since it has so far only been inferred by gravity modeling (Davy and Wood, 1994). The upcoming RV Sonne cruise So-246 to the Chatham Rise, aims to provide further insight into the interaction between the Hikurangi Plateau and the Chatham Rise as well as of its role in the separation between Zealandia and Antarctica by acquiring refraction and reflection seismic data along with potential field and petrological data. Their results will certainly improve our understanding of the eastern Gondwana margin during the CNS.

Furthermore, plate tectonic reconstructions would benefit from dated rock samples of the Nova Canton Trough. Additional bathymetric and gravimetric surveying in this area would enable the mapping of relict spreading centers and fault systems. This would improve our knowledge of the plate motion between the Manihiki Plateau and the Ontong Java Plateau and also clarify the role of the Phoenix FZ and Central Pacific FZ during the proposed Neogene and Paleogene reactivation of the Nova Canton Trough (Fig. 9.2).

The Robbie Ridge, located south of the Nova Canton Trough is still an enigma in the plate tectonic framework (Fig. 9.2). Winterer *et al.* (1974) attribute the ridge to spreading center volcanism and speculate about a genetic connection to the Alexa Bank (Fig. 9.2). The Alexa Bank is of Oligocene age (Johnson *et al.*, 1986) and therefore not related to the Ontong Java Nui event. Thus, the question remains: Was the Robbie Ridge emplaced as part of the Manihiki Plateau and is it a further fragment of Ontong Java Nui? Or was the volcanism building-up Robbie Ridge completely unrelated to Ontong Java Nui? An assessment of the evolution of Robbie Ridge would improve the understanding of this region and could possibly provide information on the evolution of the Nova Canton Trough during the CNS.

### 9.3 Presence of fragments of the Manihiki Plateau in western Antarctica

The plate tectonic reconstruction indicates the presence of a fragment of the Manihiki Plateau within the Bellingshausen Sea, western Antarctica. So far, this is only a hypothesis based on plate kinematic calculations and geophysical evidence is needed for verification. A refraction/wide-angle seismic profile (D-D') covering the shelf area of the Bellingshausen Sea, crossing the Charcot anomaly and possibly parts of Palmer Land would help to identify possible remnants of the eastern fragment of the Manihiki Plateau in the area (Fig. 9.3). Additionally, this data would provide insight into the tectonic framework of the western Antarctic margin by revealing for example the continent-ocean transition zone and different terranes. Due to environmental restrictions by the Umweltbundesamt refraction/wide-angle seismic reflection data acquisition in the area of Charcot Island seems unlikely to take place in the near future. Heavy sea ice conditions are also a limiting factor for ship borne operations in the area.

A more feasible scenario to test the hypothesis of the presence of a fragment of the Manihiki Plateau within Palmer Land would be airborne magnetic and gravimetric profiling or conducting a passive seismic survey using for example receiver functions and ambient noise correlation.

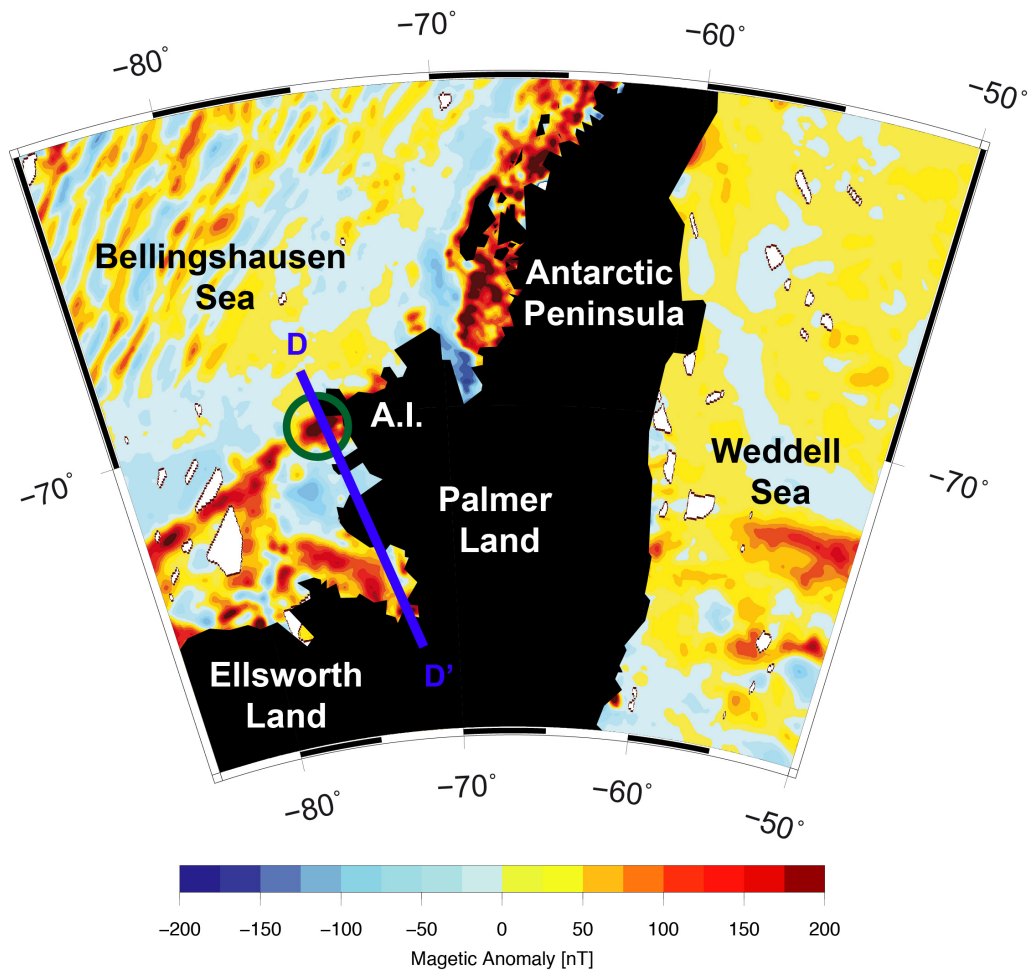


**Figure 9.3:** Magnetic anomaly map (Maus *et al.*, 2009) of eastern Bellingshausen Sea and Palmer Land illustrating the position of a proposed additional refraction/wide-angle reflection profile (blue). The green circle marks the position of the Charcot magnetic anomaly and Charcot Island west of Alexander Island (A.I.)

Additionally, the re-examination of the few rock samples from the area with particular attention to rare element concentrations related to LIPs such as the chalcophile and siderophile elements could provide further evidence to the presence of a LIP fragment within western Antarctica.



# Bibliography

- Achterberg, E. P., C. M. Moore, S. A. Henson, S. Steigenberger, A. Stohl, S. Eckhardt, L. C. Aven-  
dano, M. Cassidy, D. Hembury, J. K. Klar, M. I. Lucas, A. I. Macey, C. M. Marsay, and T. J. Ryan-  
Keogh (2013), Natural iron fertilization by the Eyjafjallajökull volcanic eruption, *Geophysical  
Research Letters*, 40(5), 921–926, doi:10.1002/grl.50221.
- Ai, H.-A., J. M. Stock, R. Clayton, and B. Luyendyk (2008), Vertical tectonics of the High Plateau  
region, Manihiki Plateau, Western Pacific, from seismic stratigraphy, *Marine Geophysical Re-  
search*, 29(1), 13–26, doi:10.1007/s11001-008-9042-0.
- Albers, M., and U. R. Christensen (2001), Channeling of plume flow beneath mid-ocean ridges,  
*Earth and Planetary Science Letters*, 187(1-2), 207–220, doi:10.1016/s0012-821x(01)00276-x.
- Altenbernd, T., W. Jokat, I. Heyde, and V. Damm (2014), A crustal model for northern Melville  
Bay, Baffin Bay, *Journal of Geophysical Research-Solid Earth*, 119(12), 8610–8632, doi:10.1002/  
2014JB011559.
- Barton, P. J. (1986), The relationship between seismic velocity and density in the continental  
crust – a useful constraint?, *Geophysical Journal International*, 87(1), 195–208, doi:10.1111/j.  
1365-246X.1986.tb04553.x.
- Beiersdorf, H., W. Bach, R. A. Duncan, J. Erzinger, and W. Weiss (1995a), New evidence for  
the production of EM-type ocean island basalts and large volumes of volcanoclastites dur-  
ing the early history of the Manihiki Plateau, *Marine Geology*, 122(3), 181–205, doi:10.1016/  
0025-3227(94)00107-V.
- Beiersdorf, H., T. Bickert, P. Cepek, J. Fenner, N. Petersen, J. Schönfeld, W. Weiss, and M. Z. Won  
(1995b), High-resolution stratigraphy and the response of biota to Late Cenozoic environ-  
mental changes in the central equatorial Pacific Ocean (Manihiki Plateau), *Marine Geology*,  
125(1), 29–59, doi:10.1016/0025-3227(95)00021-P.
- Billen, M. I., and J. Stock (2000), Morphology and origin of the Osbourn Trough, *Journal of Geo-  
physical Research: Solid Earth*, 105(B6), 13,481–13,489, doi:10.1029/2000JB900035.
- Boschman, L. M., D. van Hinsbergen, T. H. Torsvik, W. Spakman, and J. L. Pindell (2014), Kine-  
matic reconstruction of the Caribbean region since the Early Jurassic, *Earth-Science Reviews*,  
138, 102–136, doi:10.1016/j.earscirev.2014.08.007.

- Boyden, J. A., R. D. Müller, M. Gurnis, T. H. Torsvik, J. A. Clark, M. Turner, H. Ivey-Law, R. J. Watson, and J. S. Cannon (2011), Next-generation plate-tectonic reconstructions using GPlates, *Geoinformatics: cyberinfrastructure for the solid earth sciences*, pp. 95–114.
- Briffa, K. R., P. D. Jones, F. H. Schweingruber, and T. J. Osborn (1998), Influence of volcanic eruptions on Northern Hemisphere summer temperature over the past 600 years, *Nature*, 393(6684), 450–455, doi:10.1038/30943.
- Bryan, S. E., and R. E. Ernst (2008), Revised definition of large igneous provinces (LIPs), *Earth-Science Reviews*, 86(1-4), 175–202, doi:10.1016/j.earscirev.2007.08.008.
- Bryan, S. E., and L. Ferrari (2013), Large igneous provinces and silicic large igneous provinces: Progress in our understanding over the last 25 years, *Geological Society of America Bulletin*, 125(7-8), 1053–1078, doi:10.1130/B30820.1.
- Caress, D. W., M. K. McNutt, R. S. Detrick, and J. C. Mutter (1995), Seismic imaging of hotspot-related crustal underplating beneath the Marquesas Islands, *Nature*, doi:10.1038/373600a0.
- Cediel, F., R. P. Shaw, and C. Caceres (2003), Tectonic assembly of the northern Andean Block, *AAPG Memoir*.
- Chambers, L. M., M. S. Pringle, and J. G. Fitton (2004), Phreatomagmatic eruptions on the Ontong Java Plateau: an Aptian 40Ar/39Ar age for volcanoclastic rocks at ODP Site 1184, *Geological Society*, 229, 325–331, doi:10.1144/GSL.SP.2004.229.01.18.
- Chandler, M. T., P. Wessel, B. Taylor, M. Seton, S.-S. Kim, and K. Hyeong (2012), Reconstructing Ontong Java Nui: Implications for Pacific absolute plate motion, hotspot drift and true polar wander, *Earth and Planetary Science Letters*, 331–332, 140–151, doi:10.1016/j.epsl.2012.03.017.
- Chandler, M. T., P. Wessel, and W. W. Sager (2013), Analysis of Ontong Java Plateau palaeolatitudes: evidence for large-scale rotation since 123 Ma?, *Geophysical Journal International*, 194(1), 18–29, doi:10.1093/gji/ggt075.
- Charvis, P., and S. Operto (1999), Structure of the Cretaceous Kerguelen Volcanic Province (southern Indian Ocean) from wide-angle seismic data., *Journal of Geodynamics*, 28(1), 51–71, doi:10.1016/S0264-3707(98)00029-5.
- Christensen, N. I. (1996), Poisson's ratio and crustal seismology, *Journal of Geophysical Research: Solid Earth*, 101(B2), 3139–3156, doi:10.1029/95JB03446.
- Church, J. A., N. J. White, and J. M. Arblaster (2005), Significant decadal-scale impact of volcanic eruptions on sea level and ocean heat content, *Nature*, 438(7064), 74–77, doi:10.1038/nature04237.
- Clague, D. A. (1976), Petrology of basaltic and gabbroic rocks dredged from the Danger Island Troughs, Manihiki Plateau, *Initial Reports of the Deep Sea Drilling Project*, 33, 891–911.

## BIBLIOGRAPHY

---

- Cloos, M. (1993), Lithospheric buoyancy and collisional orogenesis: Subduction of oceanic plateaus, continental margins, island arcs, spreading ridges, and seamounts, *Geological Society of America Bulletin*, 105(6), 715–737, doi:10.1130/0016-7606(1993)105<0715:LBACOS>2.3.CO;2.
- Cockerham, R. S., and R. D. Jarrard (1976), Paleomagnetism of some leg 33 sediments and basalts, *Initial Reports of the Deep Sea Drilling Project*, 33, 631–647, doi:10.2973/dsdp.proc.33.1976.
- Coffin, M. F., and O. Eldholm (1993), Scratching the surface: Estimating dimensions of large igneous provinces, *Geology*, 21(6), 515–518, doi:10.1130/0091-7613(1993)021<0515:STSEDO>2.3.CO;2.
- Coffin, M. F., and O. Eldholm (1994), Large igneous provinces: crustal structure, dimensions, and external consequences, *Reviews of Geophysics and Space Physics*, 32, 1–36, doi:10.1029/93RG02508.
- Coffin, M. F., M. S. Pringle, R. A. Duncan, T. Gladchenko, M. Storey, R. D. Müller, and L. M. Gahagan (2002), Kerguelen hotspot magma output since 130 Ma, *Journal of Petrology*, 43(7), 1121–1137, doi:10.1093/petrology/43.7.1121.
- Coffin, M. F., R. A. Duncan, O. Eldholm, J. G. Fitton, F. A. Frey, H. C. Larsen, J. J. Mahoney, A. D. Saunders, R. Schlich, and P. J. Wallace (2006), Large igneous provinces and scientific ocean drilling: Status quo and a look ahead, *Oceanography*, 19(4), 150–160, doi:10.5670/oceanog.2006.13.
- Coleman, P. J., and L. W. Kroenke (1981), Subduction without volcanism in the Solomon Islands arc, *Geo-Marine Letters*, 1(2), 129–134, doi:10.1007/BF02463330.
- Coulbourn, W. T., and P. J. Hill (1991), A field of volcanoes on the Manihiki Plateau: Mud or lava?, *Marine Geology*, 98(2–4), 367–388, doi:10.1016/0025-3227(91)90111-G.
- Courtillot, V., C. Jaupart, I. Manighetti, P. Tapponnier, and J. Besse (1999), On causal links between flood basalts and continental breakup, *Earth and Planetary Science Letters*, 166(3), 177–195, doi:10.1016/S0012-821X(98)00282-9.
- Darbyshire, F. A., I. T. Bjarnason, R. S. White, and Ó. G. Flóvenz (1998), Crustal structure above the Iceland mantle plume imaged by the ICEMELT refraction profile, *Geophysical Journal International*, 135(3), 1131–1149, doi:10.1046/j.1365-246X.1998.00701.x.
- Davy, B. (2014), Rotation and offset of the Gondwana convergent margin in the New Zealand region following Cretaceous jamming of Hikurangi Plateau large igneous province subduction, *Tectonics*, doi:10.1002/2014TC003629.

- Davy, B., and J. Y. Collot (2000), The Rapuhia Scarp (northern Hikurangi Plateau) – its nature and subduction effects on the Kermadec Trench, *Tectonophysics*, 328(3-4), 269–295, doi:10.1016/S0040-1951(00)00211-0.
- Davy, B., and R. Wood (1994), Gravity and magnetic modelling of the Hikurangi Plateau, *Marine Geology*, 118(1-2), 139–151, doi:10.1016/0025-3227(94)90117-1.
- Davy, B., K. Hoernle, and R. Werner (2008), Hikurangi Plateau: Crustal structure, rifted formation, and Gondwana subduction history, *Geochemistry Geophysics Geosystems*, doi:10.1029/2007GC001855.
- Davy, B., V. Stagpoole, D. Barker, and J. Yu (2012), Subsurface structure of the Canterbury region interpreted from gravity and aeromagnetic data, *New Zealand Journal of Geology and Geophysics*, doi:10.1080/00288306.2012.690765.
- De Silva, S. L., and G. A. Zielinski (1998), Global influence of the AD 1600 eruption of Huaynaputina, Peru, *Nature*, 393(6684), 455–458, doi:10.1038/30948.
- Dobrovine, P. V., and B. Steinberger (2012), Absolute plate motions in a reference frame defined by moving hot spots in the Pacific, Atlantic, and Indian oceans, *Journal of Geophysical Research: Solid Earth*, 117, doi:10.1029/2011JB009072.
- Dobrovine, P. V., and J. A. Tarduno (2008), A revised kinematic model for the relative motion between Pacific oceanic plates and North America since the Late Cretaceous, *Journal of Geophysical Research: Solid Earth*, 113(B12), B12,101, doi:10.1029/2008JB005585.
- Downey, N. J., J. M. Stock, R. W. Clayton, and S. C. Cande (2007), History of the Cretaceous Osborn spreading center, *Journal of Geophysical Research: Solid Earth* (1978–2012), 112(B4), B04,102, doi:10.1029/2006JB004550.
- Dyment, J., J. Lin, and E. T. Baker (2007), Ridge-hotspot interactions: What mid-ocean ridges tell us about deep Earth processes, *Oceanography*, doi:10.1038/322137a0.
- Eagles, G., and A. P. M. Vaughan (2009), Gondwana breakup and plate kinematics: Business as usual, *Geophysical Research Letters*, 36(10), L10,302, doi:10.1029/2009GL037552.
- Eagles, G., K. Gohl, and R. D. Larter (2004), High-resolution animated tectonic reconstruction of the South Pacific and West Antarctic Margin, *Geochemistry Geophysics Geosystems*, 5(7), 1–21, doi:10.1029/2003GC000657.
- Expedition 330 Scientists (2011), *IODP Preliminary Report*, IODP Preliminary Report, Integrated Ocean Drilling Program, doi:10.2204/iodp.pr.330.2011.
- Ferraccioli, F., Jones, P. C., A. P. M. Vaughan, and P. T. Leat (2006), New aerogeophysical view of the Antarctic Peninsula: More pieces, less puzzle, *Geophysical Research Letters*, 33(5), doi:10.1029/2005GL024636.

## BIBLIOGRAPHY

---

- Francis, T. J. G., and R. W. Raitt (1967), Seismic refraction measurements in the southern Indian Ocean, *Journal of Geophysical Research: Solid Earth*, 72(12), 3015–3041, doi:10.1029/JZ072i012p03015.
- Fromm, T. (2012), AWIForge > Projects > PRay > Home.
- Fromm, T., L. Planert, W. Jokat, T. Ryberg, J. H. Behrmann, M. H. Weber, and C. Haberland (2015), South Atlantic opening: A plume-induced breakup?, *Geology*, doi:10.1130/G36936.1.
- Furumoto, A. S., J. P. Webb, M. E. Odegard, and D. M. Hussong (1976), Seismic studies on the Ontong Java plateau, 1970, *Tectonophysics*, doi:10.1016/0040-1951(76)90177-3.
- Gee, J. S., and D. V. Kent (2007), Source of oceanic magnetic anomalies and the geomagnetic polarity time scale, *Treatise on Geophysics, vol. 5: Geomagnetism*, pp. 455–507, doi:10.1016/B978-044452748-6.00097-3.
- Gladchenko, T., M. F. Coffin, and O. Eldholm (1997), Crustal structure of the Ontong Java Plateau: modeling of new gravity and existing seismic data, *Journal of Geophysical Research: Solid Earth*, 102, 22,711–22,729, doi:10.1029/97JB01636.
- Gohl, K., and G. Uenzelmann-Neben (2001), The crustal role of the Agulhas Plateau, southwest Indian Ocean: evidence from seismic profiling, *Geophysical Journal International*, 144(3), 632–646, doi:10.1046/j.1365-246X.2001.01368.x.
- Gohl, K., G. Uenzelmann-Neben, and N. Grobys (2011), Growth and dispersal of a Southeast African large igneous province, *South African Journal of Geology*, doi:10.2113/gssaig.114.3-4.379.
- Golwin, R., K. Hoernle, M. Portnyagin, F. Hauff, A. Gurenko, D. Garbe-Schönberg, and R. Werner (2014), Mantle in the Manihiki Plateau source with ultra-depleted incompatible element abundances but FOZO-like isotopic signature, in *AGU Fall Meeting 2014*, San Francisco, USA.
- Götze, H. J., S. Schmidt, B. Lahmeyer, G. Goltz, M. Alvers, C. Klesper, M. Schneider, and J. Schulte (2002), IGMAS - Interactive Gravity and Magnetic Application System.
- Graindorge, D. (2004), Deep structures of the Ecuador convergent margin and the Carnegie Ridge, possible consequence on great earthquakes recurrence interval, *Geophysical Research Letters*, 31(4), L04,603–5, doi:10.1029/2003GL018803.
- Granot, R., J. Dyment, and Y. Gallet (2012), Geomagnetic field variability during the Cretaceous Normal Superchron, *Nature Geoscience*, 5(3), 220–223, doi:10.1038/ngeo1404.
- Grevemeyer, I., W. Weigel, S. Schüssler, and F. Avedik (2001), Crustal and upper mantle seismic structure and lithospheric flexure along the Society Island hotspot chain, *Geophysical Journal International*, 147(1), 123–140, doi:10.1046/j.0956-540x.2001.01521.x.

- Griffiths, R. W., and I. H. Campbell (1990), Stirring and structure in mantle starting plumes, *Earth and Planetary Science Letters*, 99(1), 66–78.
- Grobys, J. W. G., K. Gohl, B. Davy, G. Uenzelmann-Neben, T. Deen, and D. Barker (2007), Is the Bounty Trough off eastern New Zealand an aborted rift?, *Journal of Geophysical Research: Solid Earth*, 112(B3), B03,103, doi:10.1029/2005JB004229.
- Gudmundsson, M. T., T. Thordarson, Á. Höskuldsson, G. Larson, H. Björnsson, F. J. Prata, B. Oddsson, E. Magnússon, T. Högnadóttir, G. N. Petersen, C. L. Hayward, J. A. Stevenson, and I. Jónsdóttir (2012), Ash generation and distribution from the April-May 2010 eruption of Eyjafjallajökull, Iceland, *Scientific Reports*, doi:10.1038/srep00572.
- Gurnis, M., M. Turner, S. Zahirovic, L. DiCaprio, S. Spasojevic, R. D. Müller, J. Boyden, M. Seton, V. C. Manea, and D. J. Bower (2012), Plate tectonic reconstructions with continuously closing plates, *Computers & Geosciences*, 38(1), 35–42, doi:10.1016/j.cageo.2011.04.014.
- Gutscher, M. A., J. L. Olivet, D. Aslanian, J. P. Eissen, and R. Maury (1999), The “lost Inca Plateau”: cause of flat subduction beneath Peru?, *Earth and Planetary Science Letters*, 171(3), 335–341, doi:10.1016/S0012-821X(99)00153-3.
- Gutscher, M.-A., R. Maury, J.-P. Eissen, and E. Bourdon (2000), Can slab melting be caused by flat subduction?, *Geology*, 28(6), 535–538, doi:10.1130/0091-7613(2000)28<535:CSMBCB>2.0.CO;2.
- Hamilton, E. L. (1978), Sound velocity–density relations in sea-floor sediments and rocks, *The journal of the Acoustical Society of America*, 63(2), 366–377, doi:10.1121/1.381747.
- Hill, R. I. (1993), Mantle plumes and continental tectonics, *Lithos*, doi:10.1016/0024-4937(93)90035-B.
- Hochmuth, K., K. Gohl, and G. Uenzelmann-Neben (2015), Playing jigsaw with Large Igneous Provinces—A plate tectonic reconstruction of Ontong Java Nui, West Pacific, *Geochemistry Geophysics Geosystems*, 16, 1–19, doi:10.1002/2015GC006036.
- Hochmuth, K., K. Gohl, G. Uenzelmann-Neben, and R. Werner (in review), Multiphase magmatic and tectonic evolution of a large igneous province – evidence from the crustal structure of the Manihiki Plateau, western Pacific, *Geophysical Journal International*, pp. 1–56.
- Hoernle, K., F. Hauff, R. Werner, and N. Mortimer (2004a), New insights into the origin and evolution of the Hikurangi oceanic plateau, *Eos, Transactions American Geophysical Union*, 85(41), 401–408, doi:10.1029/2004EO410001.
- Hoernle, K., F. Hauff, and P. van den Bogaard (2004b), 70 m.y. history (139–69 Ma) for the Caribbean large igneous province, *Geology*, 32(8), 697, doi:10.1130/G20574.1.

## BIBLIOGRAPHY

---

- Hoernle, K., C. Timm, F. Hauff, L. Rüpke, R. Werner, P. van den Bogaard, P. Michael, M. F. Coffin, N. Mortimer, and B. Davy (2009), New Results for the Multi-stage Geochemical Evolution of the Manihiki and Hikurangi Plateaus, in *Eos Trans. AGU*, pp. 1–24.
- Hoernle, K., F. Hauff, P. van den Bogaard, R. Werner, N. Mortimer, J. Geldmacher, D. Garbe-Schönberg, and B. Davy (2010), Age and geochemistry of volcanic rocks from the Hikurangi and Manihiki oceanic Plateaus, *GEOCHIMICA ET COSMOCHIMICA ACTA*, **74**, 1–24, doi:10.1016/j.gca.2010.09.030.
- Hussong, D. M., L. K. Wipperfurth, and L. W. Kroenke (1979), The Crustal Structure of the Ontong Java and Manihiki Oceanic Plateaus, *Journal of Geophysical Research: Solid Earth*, **84**(B11), 6003–6010, doi:10.1029/JB084iB11p06003.
- Ingle, S. P., J. J. Mahoney, H. Sato, M. F. Coffin, J.-I. Kimura, N. Hirano, and M. Nakanishi (2007), Depleted mantle wedge and sediment fingerprint in unusual basalts from the Manihiki Plateau, central Pacific Ocean, *Geology*, **35**(7), 595, doi:10.1130/G23741A.1.
- Inoue, H., M. F. Coffin, Y. Nakamura, K. Mochizuki, and L. W. Kroenke (2008), Intrabasement reflections of the Ontong Java Plateau: Implications for plateau construction, *Geochemistry Geophysics Geosystems*, **9**(4), 1–19, doi:10.1029/2007GC001780.
- Ishikawa, A., E. Nakamura, and J. J. Mahoney (2005), Jurassic oceanic lithosphere beneath the southern Ontong Java Plateau: Evidence from xenoliths in alnöite, Malaita, Solomon Islands, *Geology*, **33**(5), 393–396, doi:10.1130/G21205.1.
- Ishikawa, A., T. Kuritani, A. Makishima, and E. Nakamura (2007), Ancient recycled crust beneath the Ontong Java Plateau: Isotopic evidence from the garnet clinopyroxenite xenoliths, Malaita, Solomon Islands, *Earth and Planetary Science Letters*, **259**(1–2), 134–148, doi:10.1016/j.epsl.2007.04.034.
- Ito, G., J. Lin, and C. W. Gable (1996), Dynamics of mantle flow and melting at a ridge-centered hotspot: Iceland and the Mid-Atlantic Ridge, *Earth and Planetary Science Letters*, **144**(1–2), 53–74, doi:10.1016/0012-821X(96)00151-3.
- Ito, G., J. Lin, and D. Graham (2003), Observational and theoretical studies of the dynamics of mantle plume–mid-ocean ridge interaction, *Reviews of Geophysics and Space Physics*, doi:10.1029/2002RG000117.
- Jaillard, E., H. Lapierre, M. Ordoñez, J. T. Álava, A. Amórtégui, and J. Vanmelle (2009), Accreted oceanic terranes in Ecuador: southern edge of the Caribbean Plate?, *Geological Society, London, Special Publications*, **328**(1), 469–485, doi:10.1144/SP328.19.
- Johnson, K. T. M., J. M. Sinton, and R. C. Price (1986), Petrology of seamounts northwest of Samoa and their relation to Samoan volcanism, *Bulletin of Volcanology*, **48**(4), 225–235, doi:10.1007/BF01087676.

- Karlstrom, L., and M. A. Richards (2011), On the evolution of large ultramafic magma chambers and timescales for flood basalt eruptions, *Journal of Geophysical Research: Solid Earth*, 116(B8), B08216, doi:10.1029/2010JB008159.
- Kerr, A. C., and J. Tarney (2005), Tectonic evolution of the Caribbean and northwestern South America: The case for accretion of two Late Cretaceous oceanic plateaus, *Geology*, 33(4), 269–272, doi:10.1130/G21109.1.
- Klosko, E. R., R. M. Russo, E. A. Okal, and W. P. Richardson (2001), Evidence for a rheologically strong chemical mantle root beneath the Ontong–Java Plateau, *Earth and Planetary Science Letters*, 186(3), 347–361, doi:10.1016/S0012-821X(01)00235-7.
- Kokfelt, T. F., C. Lundstrom, K. Hoernle, and F. Hauff (2005), Plume–ridge interaction studied at the Galápagos spreading center: Evidence from 226 Ra–230 Th–238 U and 231 Pa–235 U isotopic disequilibria, *Earth and Planetary Science Letters*, doi:10.1016/j.epsl.2005.02.031.
- Koppers, A. A. P., and H. Staudigel (2005), Asynchronous bends in Pacific seamount trails: a case for extensional volcanism?, *Science*, 307, doi:10.1126/science.1107260.
- Korenaga, J. (2005), Why did not the Ontong Java Plateau form subaerially?, *Earth and Planetary Science Letters*, 234(3), 385–399, doi:10.1016/j.epsl.2005.03.011.
- Langmann, B., A. Folch, M. Hensch, and V. Matthias (2012), Volcanic ash over Europe during the eruption of Eyjafjallajökull on Iceland, April–May 2010, *Atmospheric Environment*, 48, 1–8, doi:10.1016/j.atmosenv.2011.03.054.
- Larson, R. L. (1997), Superplumes and ridge interactions between Ontong Java and Manihiki Plateaus and the Nova-Canton Trough, *Geology*, 25(9), 779–782, doi:10.1130/0091-7613(1997)025<0779:SARIBO>2.3.CO;2.
- Larson, R. L., and C. Chase (1972), Late Mesozoic Evolution of the Western Pacific Ocean, *Geological Society of America Bulletin*, 83(12), 3627, doi:10.1130/0016-7606(1972)83[3627:LMEOTW]2.0.CO;2.
- Larson, R. L., and E. Erba (1999), Onset of the Mid-Cretaceous greenhouse in the Barremian–Aptian: Igneous events and the biological, sedimentary, and geochemical responses, *Paleoceanography*, 14(6), 663–678, doi:10.1029/1999PA900040.
- Larson, R. L., R. A. Pockalny, R. Viso, E. Erba, L. Abrams, B. Luyendyk, J. Stock, and R. Clayton (2002), Mid-Cretaceous tectonic evolution of the Tongareva triple junction in the southwestern Pacific Basin, *Geology*, 90, 67–70, doi:10.1130/0091-7613(2002)030<0067:MCTEOT>2.0.CO;2.
- Larter, R. D., A. Cunningham, P. Barker, K. Gohl, and F. O. Nitsche (2002), Tectonic evolution of the Pacific margin of Antarctica 1. Late Cretaceous tectonic reconstructions, *Journal of Geophysical Research: Solid Earth*, 107(B12), 2345, doi:10.1029/2000JB000052.



## BIBLIOGRAPHY

---

- Liu, L., M. Gurnis, M. Seton, J. Saleeby, R. D. Müller, and J. M. Jackson (2010), The role of oceanic plateau subduction in the Laramide orogeny, *Nature Geoscience*, *3*(5), 353–357, doi:10.1038/ngeo829.
- Luyendyk, B. (1995), Hypothesis for Cretaceous Rifting of East Gondwana Caused by Subducted Slab Capture, *Geology*, *23*(4), 373–376.
- Mahoney, J. J., and K. J. Spencer (1991), Isotopic Evidence for the Origin of the Manihiki and Ontong Java Oceanic Plateaus, *Earth and Planetary Science Letters*, *104*, 196–210, doi:10.1016/0012-821X(91)90204-U.
- Mahoney, J. J., M. Storey, R. A. Duncan, K. J. Spencer, and M. S. Pringle (1993), Geochemistry and geochronology of Leg 130 basement lavas: nature and origin of the Ontong Java Plateau, *Proceedings of the Ocean Drilling Program, Scientific Results*, *130*, 3–22, doi:10.2973/odp.proc.sr.130.040.1993.
- Mamberti, M., H. Lapierre, D. Bosch, E. Jaillard, and R. Ethien (2003), Accreted fragments of the late cretaceous Caribbean-Colombian plateau in Ecuador, *Lithos*, *66*(3–4), 173–199, doi:10.1016/S0024-4937(02)00218-9.
- Mamberti, M., H. Lapierre, and D. Bosch (2004), The Early Cretaceous San Juan Plutonic Suite, Ecuador: a magma chamber in an oceanic plateau?, *Canadian Journal of Earth Sciences*, doi:10.1139/e04-060.
- Mann, P., and A. Taira (2004), Global tectonic significance of the Solomon Islands and Ontong Java Plateau convergent zone, *Tectonophysics*, *389*(3–4), 137–190, doi:10.1016/j.tecto.2003.10.024.
- Matthews, K. J., R. D. Müller, P. Wessel, and J. M. Whittaker (2011), The tectonic fabric of the ocean basins, *Journal of Geophysical Research: Solid Earth* (1978–2012), *116*(B12).
- Matthews, K. J., M. Seton, and R. D. Müller (2012), Earth and Planetary Science Letters, *Earth and Planetary Science Letters*, *355–356*(c), 283–298, doi:10.1016/j.epsl.2012.08.023.
- Maus, S., U. Barckhausen, and H. Berkenbosch (2009), EMAG2: A 2-arc min resolution Earth Magnetic Anomaly Grid compiled from satellite, airborne, and marine magnetic measurements, *Geochemistry Geophysics Geosystems*, doi:10.1029/DanaInfo=dx.doi.org+2009GC002471.
- McCarron, J. J., and R. D. Larter (1998), Late Cretaceous to early Tertiary subduction history of the Antarctic Peninsula, *Journal of the Geological Society*, *155*(2), 255–268, doi:10.1144/gsjgs.155.2.0255.
- McNutt, M. K. (2006), Another nail in the plume coffin?, *Science*, *313*(5792), 1394, doi:10.1126/science.1131298.

- Mechie, J., K. Abu-Ayyash, Z. Ben-Avraham, R. El-Kelani, I. Qabbani, and M. Weber (2009), Crustal structure of the southern Dead Sea basin derived from project DESIRE wide-angle seismic data, *Geophysical Journal International*, 178(1), 457–478, doi:10.1111/j.1365-246x.2009.04161.x.
- Miura, S., K. Suyehiro, M. Shinohara, N. Takahashi, E. Araki, and A. Taira (2004), Seismological structure and implications of collision between the Ontong Java Plateau and Solomon Island Arc from ocean bottom seismometer–airgun data, *Tectonophysics*, 389(3–4), 191–220, doi:10.1016/j.tecto.2003.09.029.
- Mjelde, R. (2005), Continent-ocean transition on the Vøring Plateau, NE Atlantic, derived from densely sampled ocean bottom seismometer data, *Journal of Geophysical Research: Solid Earth*, 110(B5), B05101, doi:10.1029/2004JB003026.
- Mjelde, R., P. Digranes, M. Van Schaack, H. Shimamura, H. Shiobara, S. Kodaira, O. Naess, N. Sørensen, and E. Vågnes (2001), Crustal structure of the outer Vøring Plateau, offshore Norway, from ocean bottom seismic and gravity data, *Journal of Geophysical Research: Solid Earth* (1978–2012), 106(B4), 6769–6791.
- Mochizuki, K., M. F. Coffin, O. Eldholm, and A. Taira (2005), Massive Early Cretaceous volcanic activity in the Nauru Basin related to emplacement of the Ontong Java Plateau, *Geochemistry Geophysics Geosystems*, 6(10), 1–19, doi:10.1029/2004GC000867.
- Morgan, W. J. (1971), Convection Plumes in the Lower Mantle, *Nature*, 230(5288), 42–43, doi:10.1038/230042a0.
- Mortimer, N., K. Hoernle, F. Hauff, J. M. Palin, W. J. Dunlap, R. Werner, and K. Faure (2006), New constraints on the age and evolution of the Wishbone Ridge, southwest Pacific Cretaceous microplates, and Zealandia–West Antarctica breakup, *Geology*, 34(3), 185–188, doi:10.1130/G22168.1.
- Müller, R. D., W. R. Roest, and J. Y. Royer (1998), Asymmetric sea-floor spreading caused by ridge–plume interactions, *Nature*, doi:10.1038/24850.
- Musgrave, R. J. (1990), Paleomagnetism and tectonics of Malaita, Solomon Islands, *Tectonics*, 9(4), 735–759, doi:10.1029/TC009i004p00735.
- Musgrave, R. J. (2013), Evidence for Late Eocene emplacement of the Malaita Terrane, Solomon Islands: Implications for an even larger Ontong Java Nui oceanic plateau, *Journal of Geophysical Research-Solid Earth*, doi:10.1002/jgrb.50153.
- Nakanishi, M., K. Tamaki, and K. Kobayashi (1992), A new Mesozoic isochron chart of the north-western Pacific Ocean: Paleomagnetic and tectonic implications, *Geophysical Research Letters*, 19(7), 693–696, doi:10.1029/92GL00022.

## BIBLIOGRAPHY

---

- Nakanishi, M., Y. Nakamura, M. F. Coffin, K. A. Hoernle, and R. Werner (2015), Topographic expression of the Danger Islands Troughs and implications for the tectonic evolution of the Manihiki Plateau, western equatorial Pacific Ocean, *GSA Special Papers*, **511**, doi:10.1130/2015.2511(11).
- Neal, C. R., M. F. Coffin, N. T. Arndt, R. A. Duncan, O. Eldholm, E. Erba, C. Farnetani, J. G. Fitton, S. P. Ingle, and N. Ohkouchi (2008), Investigating large igneous province formation and associated paleoenvironmental events: A white paper for scientific drilling, *Scientific Drilling*, **6**, 4–18.
- O'Neill, C., D. Müller, and B. Steinberger (2005), On the uncertainties in hot spot reconstructions and the significance of moving hot spot reference frames, *Geochemistry Geophysics Geosystems*, **6**(4), doi:10.1029/2004GC000784.
- Parsiegla, N., K. Gohl, and G. Uenzelmann-Neben (2008), The Agulhas Plateau: Structure and evolution of a large igneous province, *Geophysical Journal International*, **174**(1), 336–350, doi:10.1111/j.1365-246X.2008.03808.x.
- Petterson, M. G., T. Babbs, C. R. Neal, J. J. Mahoney, A. D. Saunders, R. A. Duncan, D. Tolia, R. Magu, C. Qopoto, H. Mahoa, and D. Natogga (1999), Geological–tectonic framework of Solomon Islands, SW Pacific: crustal accretion and growth within an intra-oceanic setting, *Tectonophysics*, **301**(1–2), 35–60, doi:10.1016/s0040-1951(98)00214-5.
- Pietsch, R., and G. Uenzelmann-Neben (2015), The Manihiki Plateau—A multistage volcanic emplacement history, *Geochemistry Geophysics Geosystems*, doi:10.1002/2015GC005852.
- Pietsch, R., and G. Uenzelmann-Neben (submitted), The Manihiki Plateau - A key to missing hotspot tracks?, *Geophysical Journal International*.
- Pyle, D. M. (1998), Volcanoes: How did the summer go?, *Nature*, **393**(6684), 415–417, doi:10.1038/30848.
- Reynaud, C., E. Jaillard, H. Lapierre, M. Mamberti, and G. H. Mascle (1999), Oceanic plateau and island arcs of southwestern Ecuador: their place in the geodynamic evolution of northwestern South America, *Tectonophysics*, **307**(3–4), 235–254, doi:10.1016/S0040-1951(99)00099-2.
- Reyners, M. (2013), The central role of the Hikurangi Plateau in the Cenozoic tectonics of New Zealand and the Southwest Pacific, *Earth and Planetary Science Letters*, **361**, 460–468, doi:10.1016/j.epsl.2012.11.010.
- Reyners, M., D. Eberhart-Phillips, and S. Bannister (2011), Tracking repeated subduction of the Hikurangi Plateau beneath New Zealand, *Earth and Planetary Science Letters*, **311**(1–2), 165–171, doi:10.1016/j.epsl.2011.09.011.

- Ribe, N. M. (1996), The dynamics of plume-ridge interaction: 2. Off-ridge plumes, *Journal of Geophysical Research: Solid Earth (1978–2012)*, *101*(B7), 16,195–16,204, doi:10.1029/96JB01187.
- Ribe, N. M., and W. L. Delattre (1998), The dynamics of plume-ridge interaction—III. The effects of ridge migration, *Geophysical Journal International*, *133*(3), 511–518, doi:10.1046/j.1365-246X.1998.00476.x.
- Ribe, N. M., U. R. Christensen, and J. Theissing (1995), The dynamics of plume-ridge interaction, 1: Ridge-centered plumes, *Earth and Planetary Science Letters*, *134*(1–2), 155–168, doi:10.1016/0012-821X(95)00116-T.
- Richards, M. A., R. A. Duncan, and V. E. Courtillot (1989), Flood Basalts and Hot-Spot Tracks: Plume Heads and Tails, *Science*, *246*(4926), 103–107, doi:10.1126/science.246.4926.103.
- Richards, M. A., E. Contreras-Reyes, C. Lithgow-Bertelloni, M. Ghiorso, and L. Stixrude (2013), Petrological interpretation of deep crustal intrusive bodies beneath oceanic hotspot provinces, *Geochemistry Geophysics Geosystems*, *14*, 604–619, doi:10.1029/2012GC004448.
- Richardson, W. P., E. A. Okal, and S. Van der Lee (2000), Rayleigh-wave tomography of the Ontong-Java Plateau, *Physics of the Earth and Planetary Interiors*, *118*(1), 29–51, doi:10.1016/S0031-9201(99)00122-3.
- Ridley, V. A., and M. A. Richards (2010), Deep crustal structure beneath large igneous provinces and the petrologic evolution of flood basalts, *Geochemistry Geophysics Geosystems*, *11*(9), doi:10.1029/2009GC002935.
- Riisager, P., J. Riisager, X. Zhao, and R. S. Coe (2003), Cretaceous geomagnetic paleointensities: Thellier experiments on Pillow lavas and Submarine basaltic glass from the Ontong Java Plateau, *Geochemistry Geophysics Geosystems*, *4*(12), doi:10.1029/2003GC000611.
- Rosenbaum, G., D. Giles, M. Saxon, P. G. Betts, R. F. Weinberg, and C. Duboz (2005), Subduction of the Nazca Ridge and the Inca Plateau: Insights into the formation of ore deposits in Peru, *Earth and Planetary Science Letters*, *239*(1–2), 18–32, doi:10.1016/j.epsl.2005.08.003.
- Sadler, J. P., and J. P. Grattan (1999), Volcanoes as agents of past environmental change, *Global and Planetary Change*, *21*(1–3), 181–196, doi:10.1016/S0921-8181(99)00014-4.
- Sager, W. W. (2006), Cretaceous paleomagnetic apparent polar wander path for the Pacific plate calculated from Deep Sea Drilling Project and Ocean Drilling Program basalt cores, *Physics of the Earth and Planetary Interiors*, *156*(3–4), 329–349, doi:10.1016/j.pepi.2005.09.014.
- Sandwell, D. T., R. D. Müller, W. H. F. Smith, E. Garcia, and R. Francis (2014), New global marine gravity model from CryoSat-2 and Jason-1 reveals buried tectonic structure, *Science*, *346*(6205), 65–67, doi:10.1126/science.1258213.

- Scarrow, J. H., P. T. Leat, C. D. Wareham, and I. L. Millar (1998), Geochemistry of mafic dykes in the Antarctic Peninsula continental-margin batholith: a record of arc evolution, *Contributions to Mineralogy and Petrology*, 131(2-3), 289–305, doi:10.1007/s004100050394.
- Schlanger, S. O., E. Jackson, R. E. Boyce, H. Cook, H. C. Jenkyns, D. Johnson, A. Kaneps, K. Kelts, E. Martini, C. McNulty, and E. L. Winterer (1976), Initial Report of the Deep Sea Drilling Project, *Initial Reports of the Deep Sea Drilling Project*, 33, 1–354, doi:doi:10.2973/dsdp.proc.33.101.1976.
- Schmincke, H. U. (2004), *Vulkanismus*, Wissenschaftliche Buchgesellschaft, Darmstadt.
- Self, S., R. Gertisser, T. Thordarson, M. Rampino, and J. Wolff (2004), Magma volume, volatile emissions, and stratospheric aerosols from the 1815 eruption of Tambora, *Geophysical Research Letters*, doi:10.1029/2004GL020925.
- Seton, M., R. D. Müller, S. Zahirovic, C. Gaina, T. Torsvik, G. Shephard, A. Talsma, M. Gurnis, M. Turner, S. Maus, and M. Chandler (2012), Global continental and ocean basin reconstructions since 200Ma, *Earth-Science Reviews*, 113(3-4), 212–270, doi:10.1016/j.earscirev.2012.03.002.
- Seton, M., J. M. Whittaker, P. Wessel, R. D. Müller, C. DeMets, S. Merkouriev, S. Cande, C. Gaina, G. Eagles, R. Granot, J. Stock, N. Wright, and S. E. Williams (2014), Community infrastructure and repository for marine magnetic identifications, *Geochemistry Geophysics Geosystems*, 15(4), 1629–1641, doi:10.1002/2013GC005176.
- Simoneit, B., D. R. Oros, and P. M. Medeiros (2014), Organic matter provenance and paleoenvironment in the Cretaceous on the Manihiki Plateau, South Pacific, *Palaeogeography*, 409, 48–56, doi:10.1016/j.palaeo.2014.05.002.
- Sinton, J., R. Detrick, J. P. Canales, G. Ito, and M. Behn (2003), Morphology and segmentation of the western Galápagos Spreading Center, 90.5°–98°W: Plume-ridge interaction at an intermediate spreading ridge, *Geochemistry Geophysics Geosystems*, 4(12), doi:10.1029/2003GC000609.
- Sobolev, S. V., A. V. Sobolev, D. V. Kuzmin, N. A. Krivolutsкая, A. G. Petrunin, N. T. Arndt, V. A. Radko, and Y. R. Vasiliev (2011), Linking mantle plumes, large igneous provinces and environmental catastrophes, *Nature*, 477(7364), 312–316, doi:10.1038/nature10385.
- Sutherland, R., and C. Hollis (2001), Cretaceous demise of the Moa plate and strike-slip motion at the Gondwana margin, *Geology*, 29(3), 279, doi:10.1130/0091-7613(2001)029<0279:CDOTMP>2.0.CO;2.
- Taira, A., P. Mann, and R. Rahardiawan (2004), Incipient subduction of the Ontong Java Plateau along the North Solomon trench, *Tectonophysics*, 389(3-4), 247–266, doi:10.1016/j.tecto.2004.07.052.

- Taylor, B. (2006), The single largest oceanic plateau: Ontong Java-Manihiki-Hikurangi, *Earth and Planetary Science Letters*, 241, 372–380, doi:10.1016/j.epsl.2005.11.049.
- Tejada, M. L. G., J. J. Mahoney, R. A. Duncan, and M. P. Hawkins (1996), Age and Geochemistry of Basement and Alkaline Rocks of Malaita and Santa Isabel, Solomon Islands, Southern Margin of Ontong Java Plateau, *Journal of Petrology*, 37(2), 361–394, doi:10.1093/petrology/37.2.361.
- Tejada, M. L. G., K. Suzuki, J. Kuroda, R. Coccioni, J. J. Mahoney, N. Ohkouchi, T. Sakamoto, and Y. Tatsumi (2009), Ontong Java Plateau eruption as a trigger for the early Aptian oceanic anoxic event, *Geology*, 37(9), 855–858, doi:10.1130/G25763A.1.
- Timm, C., K. Hoernle, R. Werner, F. Haufl, P. van den Bogaard, P. Michael, M. F. Coffin, and A. A. P. Koppers (2011), Age and geochemistry of the oceanic Manihiki Plateau, SW Pacific: New evidence for a plume origin, *Earth and Planetary Science Letters*, 304, 135–146, doi:10.1016/j.epsl.2011.01.025.
- Timm, C., B. Davy, K. Haase, K. A. Hoernle, I. J. Graham, C. E. J. de Ronde, J. Woodhead, D. Bassett, F. Haufl, N. Mortimer, H. C. Seebeck, R. J. Wysoczanski, F. Caratori-Tontini, and J. A. Gamble (2014), Subduction of the oceanic Hikurangi Plateau and its impact on the Kermadec arc, *Nature Communications*, 5, 4923, doi:10.1038/ncomms5923.
- Torsvik, T. H., R. D. Müller, R. van der Voo, B. Steinberger, and C. Gaina (2008), Global plate motion frames: Toward a unified model, *Reviews of Geophysics and Space Physics*, 46(3), RG3004, doi:10.1029/2007RG000227.
- Uenzelmann-Neben, G. (2012), The expedition of the research vessel "Sonne" to the Manihiki Plateau in 2012 (So 224), *EPIC3 Berichte zur Polar- und Meeresforschung = Reports on polar and marine research, Bremerhaven, Alfred Wegener Institute for Polar and Marine Research*, 672, 111 p., ISSN: 1866-3192.
- Uenzelmann-Neben, G., K. Gohl, A. Ehrhardt, and M. Seargent (1999), Agulhas Plateau, SW Indian Ocean: New evidence for excessive volcanism, *Geophysical Research Letters*, 26(13), 1941–1944, doi:10.1029/1999GL900391.
- Van Andel, T. H. (1975), Mesozoic/Cenozoic calcite compensation depth and the global distribution of calcareous sediments, *Earth and Planetary Science Letters*, 26(2), 187–194, doi:10.1016/0012-821X(75)90086-2.
- Vaughan, A., G. Eagles, and M. J. Flowerdew (2012), Evidence for a two-phase Palmer Land event from crosscutting structural relationships and emplacement timing of the Lassiter Coast Intrusive Suite, Antarctic ..., *Tectonics*, pp. 1–19, doi:10.1029/2011TC003006.
- Viso, R., R. L. Larson, and R. A. Pockalny (2005), Tectonic evolution of the Pacific-Phoenix-Farallon triple junction in the South Pacific Ocean, *Earth and Planetary Science Letters*, 233(1–2), 179–194, doi:10.1016/j.epsl.2005.02.004.

- Wareham, C. D., I. L. Millar, and A. P. M. Vaughan (1997), The generation of sodic granite magmas, western Palmer Land, Antarctic Peninsula, *Contributions to Mineralogy and Petrology*, 128(1), 81–96, doi:10.1007/s004100050295.
- Weatherall, P., K. M. Marks, M. Jakobsson, T. Schmitt, S. Tani, J.-E. Arndt, M. Rovere, D. Chayes, V. Ferrini, and R. Wigley (2015), A New Digital Bathymetric Model of the World's Oceans, *Earth and Space Science*, doi:10.1002/2015EA000107.
- Werner, R., and F. Hauff (2007), FS Sonne, Fahrtbericht/Cruise Report SO193 MANIHIKI: Temporal, Spatial, and Tectonic Evolution of Oceanic Plateaus, *IFM-Geomar Reports*.
- Werner, R., D. Nürnberg, and F. Hauff (2013), RV SONNE Fahrtbericht/Cruise Report SO225, Manihiki II Leg 2, The Manihiki Plateau-Origin, structure and effects of oceanic plateaus and Pleistocene dynamic of the West Pacific Warm Water Pool, *Geomar Reports*, doi:10.3289/GEOMAR\_REP\_NS\_6\_2013.
- Wessel, P., and L. W. Kroenke (2008), Pacific absolute plate motion since 145 Ma: An assessment of the fixed hot spot hypothesis, *Journal of Geophysical Research: Solid Earth*, 113(B6), B06101, doi:10.1029/2007JB005499.
- White, R. S., and D. McKenzie (1995), Mantle plumes and flood basalts, *Journal of Geophysical Research: Solid Earth*, 100(B9), 17,543–17,585, doi:10.1029/95JB01585.
- Whittaker, J. M., J. C. Afonso, S. Masterton, R. D. Müller, P. Wessel, S. E. Williams, and M. Seton (2015), Long-term interaction between mid-ocean ridges and mantle plumes, *Nature Geoscience*, 8(6), 479–483, doi:10.1038/ngeo2437.
- Wignall, P. (2005), The Link between Large Igneous Province Eruptions and Mass Extinctions, *Elements*, 1(5), 293–297, doi:10.2113/gselements.1.5.293.
- Wignall, P. B. (2001), Large igneous provinces and mass extinctions, *Earth-Science Reviews*, 53(1–2), 1–33, doi:10.1016/S0012-8252(00)00037-4.
- Wilson, J. T. (1965), Evidence from Ocean Islands Suggesting Movement in the Earth, *Philosophical Transactions of the Royal Society A: Mathematical, Physical and Engineering Sciences*, 258(1088), 145–167, doi:10.1098/rsta.1965.0029.
- Winterer, E. L., P. L. Lonsdale, J. L. Matthews, and B. R. Rosendahl (1974), Structure and acoustic stratigraphy of the Manihiki Plateau, *Deep Sea Research and Oceanographic Abstracts*, 21(10), 793–813, doi:10.1029/JB084iB11p06003.
- Wobbe, F., K. Gohl, A. Chambord, and R. Sutherland (2012), Structure and breakup history of the rifted margin of West Antarctica in relation to Cretaceous separation from Zealandia and Bellingshausen plate motion, *Geochemistry Geophysics Geosystems*, 13(4), 1–19, doi:10.1029/2011GC003742.

Worthington, T. J., R. Hekinian, P. Stoffers, T. Kuhn, and F. Hauff (2006), Osbourn Trough: Structure, geochemistry and implications of a mid-Cretaceous paleosspreading ridge in the South Pacific, *Earth and Planetary Science Letters*, 245(3-4), 685-701, doi:10.1016/j.epsl.2006.03.018.

Zelt, B. (2004), zp - Software for plotting & picking SEG-Y seismic refraction data.

Zelt, C. A., and R. B. Smith (1992), Seismic traveltime inversion for 2-D crustal velocity structure, *Geophysical Journal International*, 108(1), 16-34, doi:10.1111/j.1365-246X.1992.tb00836.x/abstract.



# Danksagung

Wissenschaftliches Arbeiten ist ein Teamsport. Während der letzten drei Jahre in denen ich mich intensiv mit dem Manihiki Plateau und den weiteren Large Igneous Provinces im westlichen Pazifik beschäftigt habe, erfuhr ich viel Unterstützung, Interesse an meiner Arbeit und Wertschätzung. Dafür möchte ich mich bei euch allen bedanken.

Zuerst möchte ich meinem Betreuer Karsten Gohl von Herzen danken. Vielen Dank, dass deine Tür immer für Fragen offen steht und du es verstehst, in guten Gesprächen neue Perspektiven und Interpretationen aufzuzeigen. Außerdem konnte ich mir deiner Unterstützung immer sicher sein, auch wenn ich dich mit meiner these-those Schwäche bestimmt zur Weißglut getrieben habe. Des Weiteren möchte ich meinen beiden Gutachtern Wilfried Jokat und Wolfgang Bach danken, dass sie sich bereit erklärt haben diese Arbeit zu bewerten. Wilfried Jokat gebührt außerdem großer Dank für sämtliche Unterschriften auf allen erdenklichen bürokratischen Formularen und für sein jederzeit offenes Ohr für Probleme und Nöte. Gabi Uenzelmann-Neben danke ich für ihre Unterstützung und viele guten Ratschläge.

Für Korrekturdienste rund um diese Arbeit gebührt Tabea, Tanja, Jan und Teresa ein großer Dank.

Im Rahmen meiner Doktorandenzeit hatte ich das große Glück zwei spannende und großartige Expeditionen miterleben zu dürfen. Hierbei möchte ich "meinem" OBS-Team, Karsten, Jürgen, Thomas, Jude, und Tobi von So-224 danken, die durch ihren großartigen Einsatz die Datengrundlage für diese Arbeit geschaffen haben. ANT29/8 war eine wunderbare Erfahrung und ich durfte meine ersten (wenn auch sehr kleinen) Eisberge bewundern. Hier danke ich Vera Schlindwein, dass sie mich ins "Team OBS" geholt hat.

Manchmal ist man als Doktorandin eine Einzelkämpferin. Ich hatte das große Glück viele Mitkämpfer im Boot zu haben. Hier danke ich meinen lieben Mitdoktoranden und allen weiteren Mitarbeitern und Mitarbeiterinnen in der Sektion Geophysik. Meine Bürokollegen Michael und Ricarda sind die besten "Mitbewohner", die ich mir wünschen konnte. Vielen Dank für die vielen Gespräche (wissenschaftlich oder eben auch nicht), die Unterstützung bei großen und kleinen Sorgen und die Gabe mich auch in den schwierigen Zeiten zum Lachen bringen zu können. Antje, Tanja, Tabea, Jude, Jan, Michael, Ricarda, Flo, Maren, Claudia, Patricia und wie ihr alle heißt, vielen Dank für unsere vielen gemeinsamen Stunden beim Kochen, Backen, Grillen, Fussballgucken, DiscGolf spielen, Äpfelverarbeiten, Klönen... Ein besonderer Bonus waren auch unsere großen und kleinen gemeinsamen Konferenz- und Expeditionsreisen. Zusammen haben wir viele schöne Orte entdeckt, viel erfahren und ganz wichtig immer gut gegessen.

Meine Familie und Freunde haben mich von Anfang an bis zur Zielgrade unterstützt. Auch wenn ich vielleicht etwas genervt oder aufbrausend war, ihr steht immer hinter mir und erträgt den Sturm mehr oder weniger gelassen. Das betrifft vor allem meinen Adrian, der am meisten von euch allen an meiner zeitweisen Abwesenheit gelitten hat und daran, dass sich unsere verschiedenen Welten immer weiter von einander entfernt haben. Danke für dein Verständnis und deine Unterstützung, ohne dich wäre einiges sicher schwerer gewesen.

# Appendix

# A OBS/OBH data of So-224

## A.1 Map of deployment locations

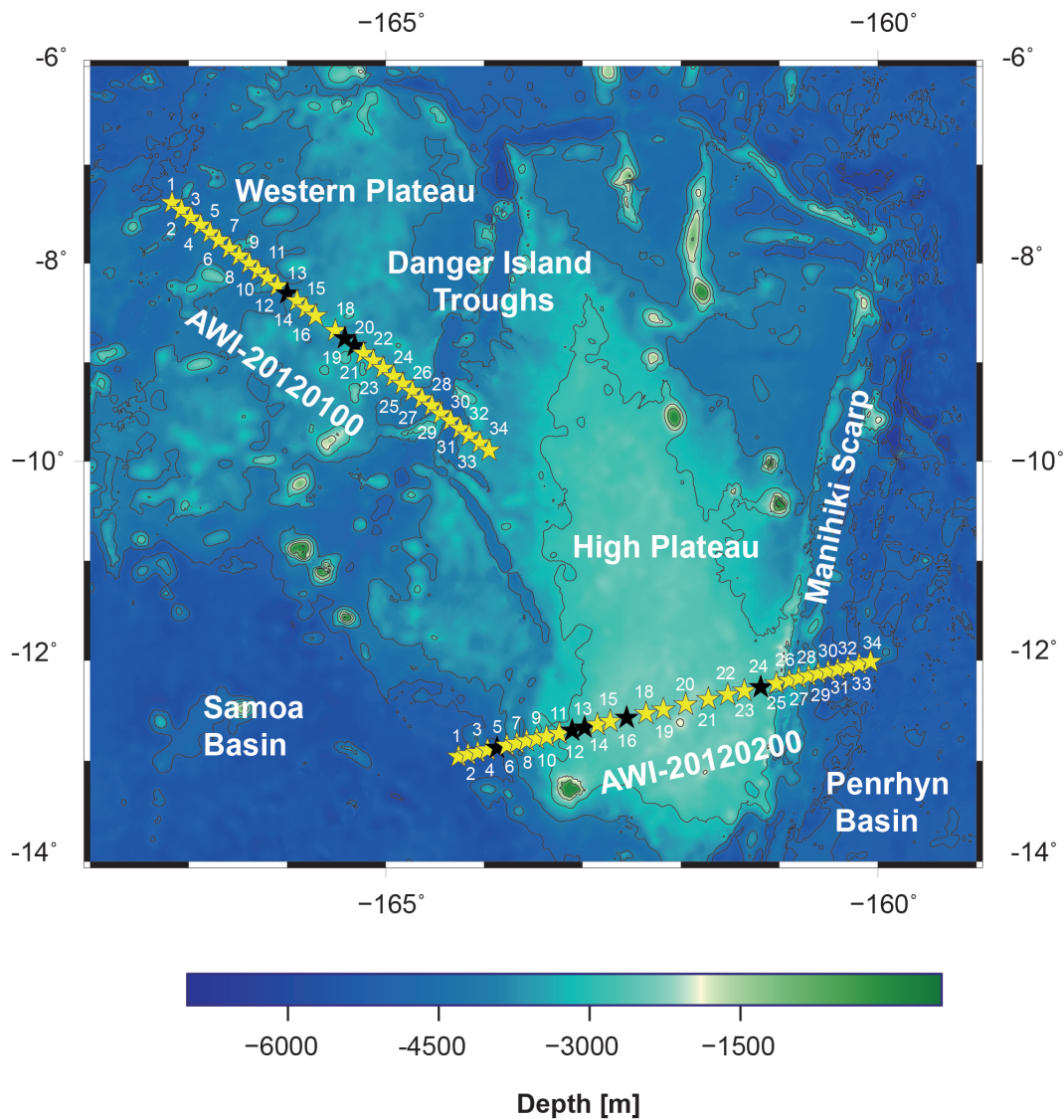


**Figure A.1:** Deployment positions of OBS/OBH stations during So-224; positions are marked with yellow stars black stars indicate stations, which did not return any data, underlying bathymetry is taken from GEBCO (*Weatherall et al., 2015*)

## A.2 Performance of OBS/OBH-stations

### A.2.1 AWI-20120100

station		H	X	Y	Z
1	OBS	1	2	2	2
2	OBS	2	3	3	3
3	OBS	1	3	3	3
4	OBS	2	2	1-2	1-2
5	OBS	1-2	2	1	1
6	OBS	1	2	2	3
7	OBS	2	3	3	3
8	OBS	2	3	3	1-2
9	OBH	1	-	-	-
10	OBS	1	3	3-4	3
11	OBS	1-2	2-3	3-4	3
12	OBS	1-2	3	2-3	2-3
13	OBS	4	4	4	4
14	OBS	2	3-4	3	3
15	OBS	2	3	3-4	1-2
16	OBH	2	-	-	-
18	OBS	1-2	2-3	2-3	3
19	OBS	4	3-4	3-4	3-4
20	OBS	4	4	4	4
21	OBS	1	3	3	2
22	OBH	1	-	-	-
23	OBS	1-2	3	2-3	3
24	OBS	1-2	3	1-2	2
25	OBS	2	2-3	4	4
26	OBH	2-3	-	-	-
27	OBS	1	3	3	3
28	OBS	2	2-3	3	3-4
29	OBH	1-2	-	-	-
30	OBS	1-2	4	4	3
31	OBS	1-2	4	4	4
32	OBS	1	-	-	-
33	OBS	1	4	4	4
34	OBS	4	1-2	2	1-2

**Table A.1:** Performance of OBS/OBH-stations on profile AWI-20120100, the different channels are labeled as follows: H hydrophone, X and Y horizontal geophones, Z vertical geophone, ranking: 1 = very good data, 2 = good data, 3 = usable data, 4 = recording failed or no usable data; completely failed stations are shaded in grey

## A.2.2 AWI-20120200

station		H	X	Y	Z
1	OBS	1	1	1	1
2	OBS	2	2	2-3	2-3
3	OBS	1	3	2-3	2
4	OBS	1-2	3	3	3
5	OBS	4	4	4	4
6	OBS	1	1-2	2	3
7	OBS	1	3	2-3	2-3
8	OBS	1	2	2	2
9	OBH	1	-	-	-
10	OBS	1	2	1-2	2
11	OBS	1	2	1-2	1-2
12	OBS	4	4	4	4
13	OBS	4	4	4	4
14	OBS	1	2	1	1
15	OBS	1	1-2	1	1
16	OBH	4	-	-	-
18	OBS	1	2	1-2	1
19	OBS	1	2-3	1-2	2
20	OBS	1	2	1-2	1-2
21	OBS	3	1-2	2	3
22	OBH	1	-	-	-
23	OBS	1	2-3	3	1-2
24	OBS	4	4	4	4
25	OBH	1	-	-	-
26	OBS	1	2-3	2	2-3
27	OBS	1	3	3-4	3
28	OBS	1	1-2	1-2	1-2
29	OBH	1	-	-	-
30	OBS	1-2	2-3	2-3	2-3
31	OBS	4	1-2	1-2	1
32	OBS	1	3-4	3	2
33	OBS	1	3-4	2-3	2
34	OBS	1	3	1-2	1-2

**Table A.2:** Performance of OBS/OBH-stations on profile AWI-20120200, the different channels are labeled as follows: H hydrophone, X and Y horizontal geophones, Z vertical geophone, ranking: 1 = very good data, 2 = good data, 3 = usable data, 4 = recording failed or no usable data

### A.3 OBS/OBH stations of AWI-20120100

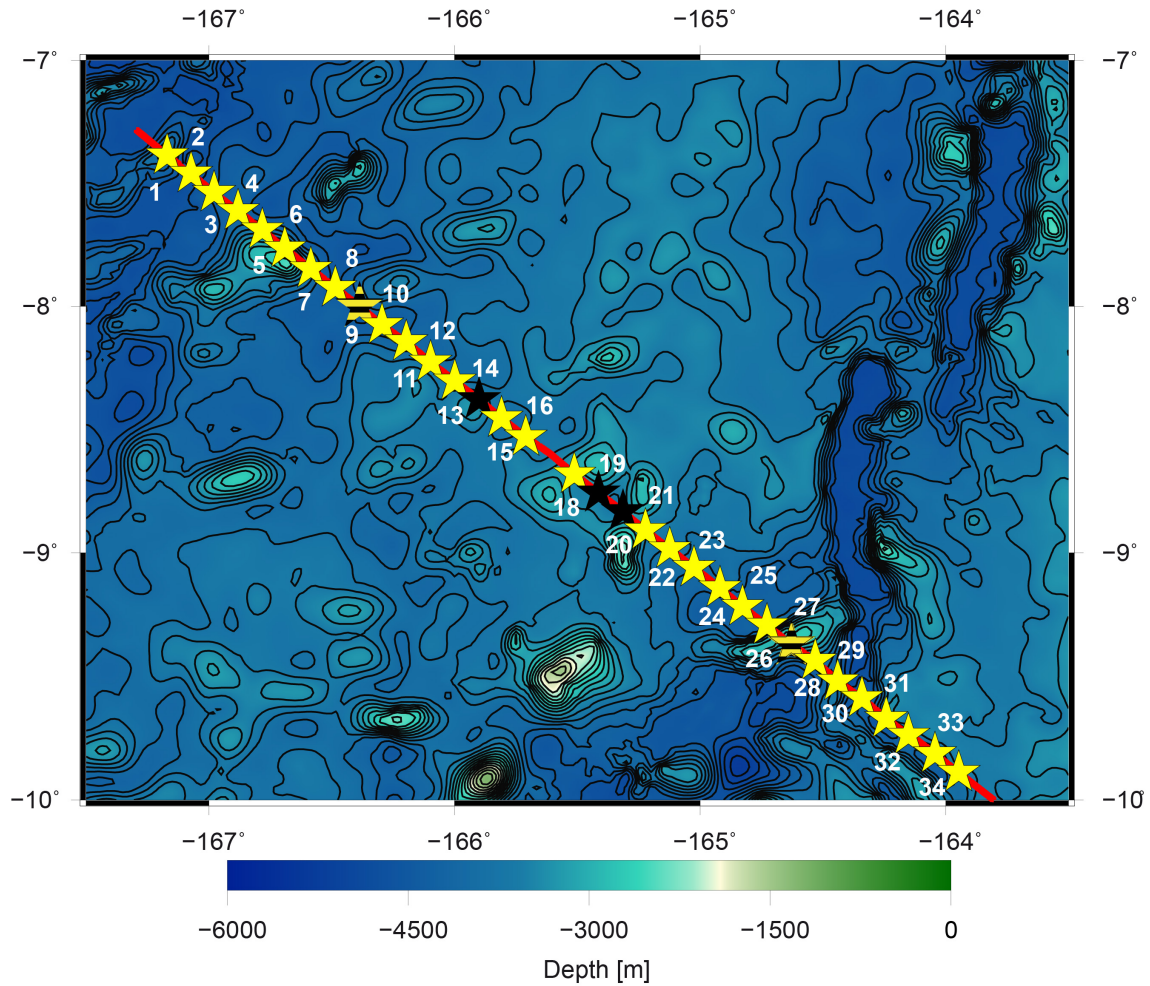


**Figure A.2:** Bathymetric map of AWI-20120100 across the Western Plateaus of the Manihiki Plateau, yellow stars indicate stations, which provided P- and S-wave data, black stars indicate stations

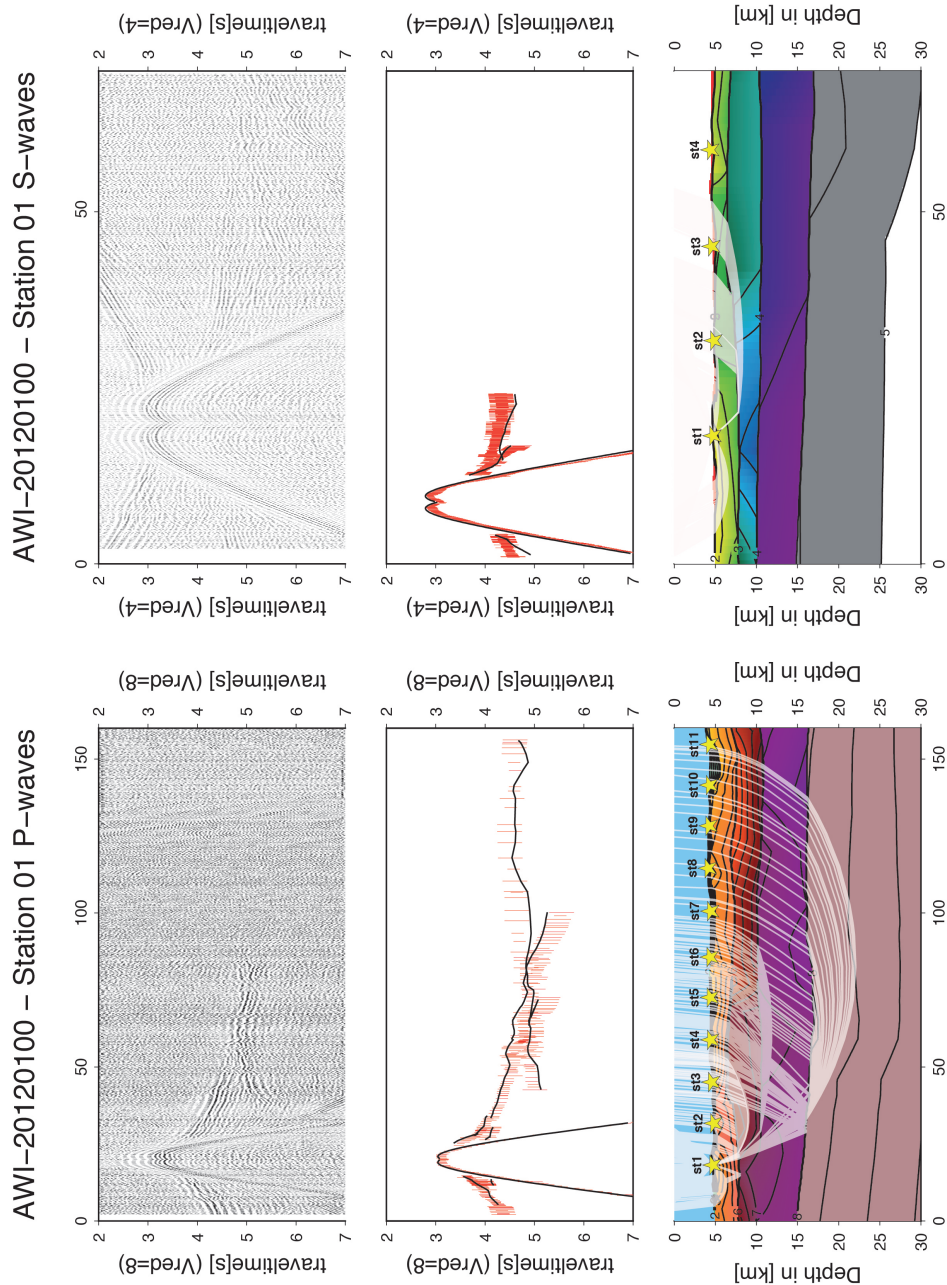
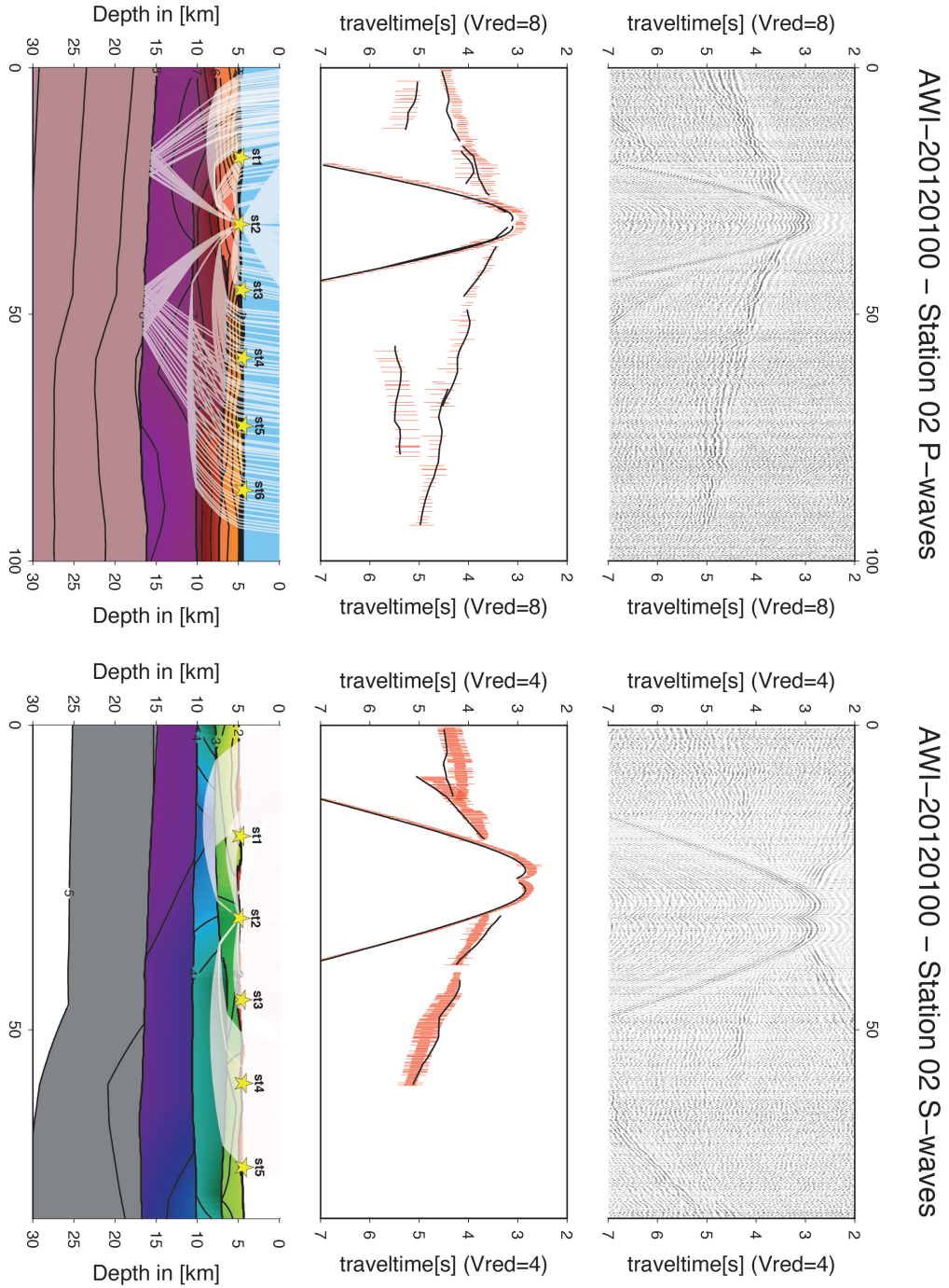


Figure A.3: P- and S-wave station 100st01 upper panel: seismogram, middle panel: picked and modeled arrival times, lower panel: resulting velocity model





**Figure A.4:** P- and S-waves station 100st02 upper panel: seismogram, middle panel: picked and modeled arrival times, lower panel: resulting velocity model



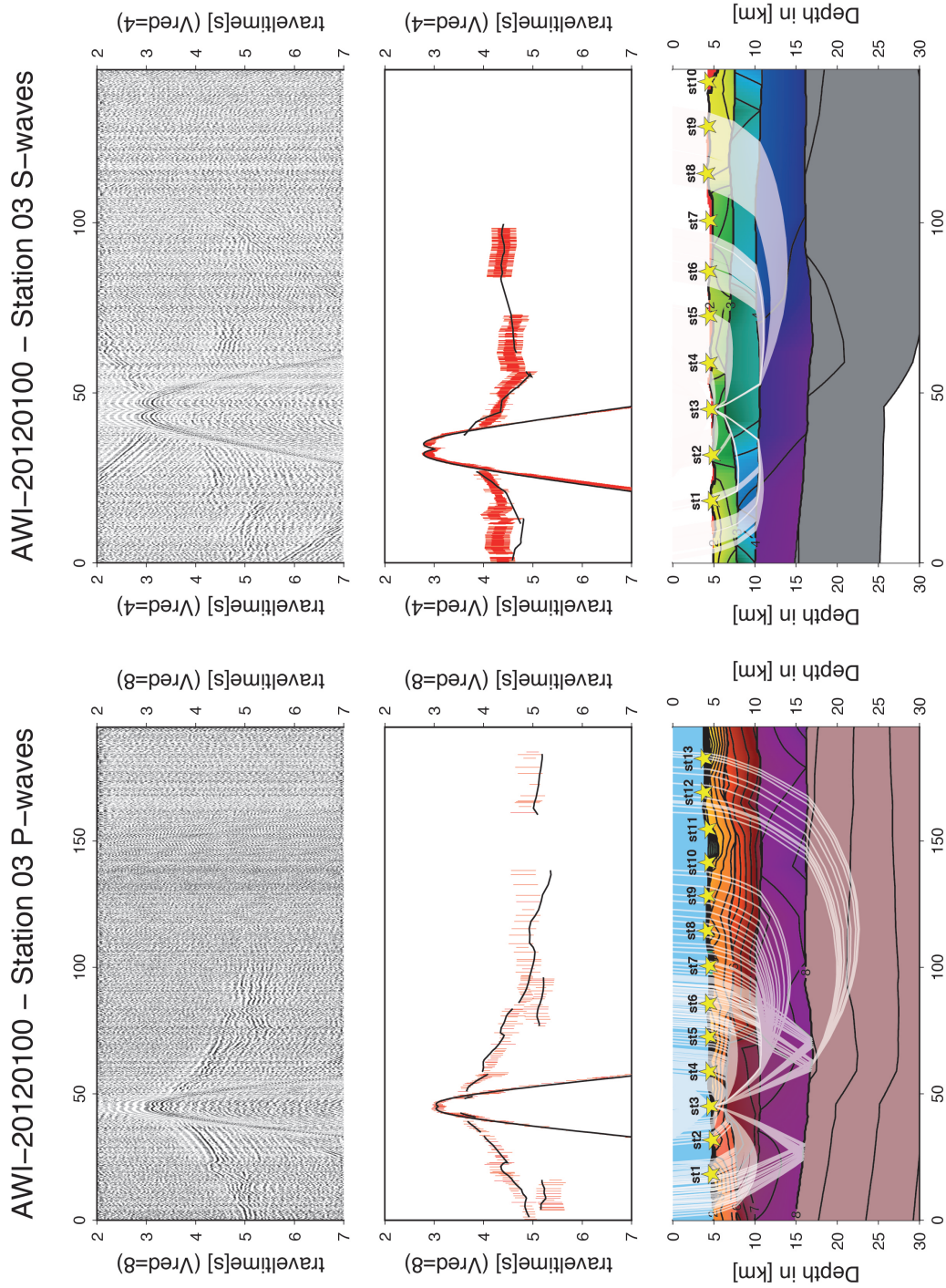
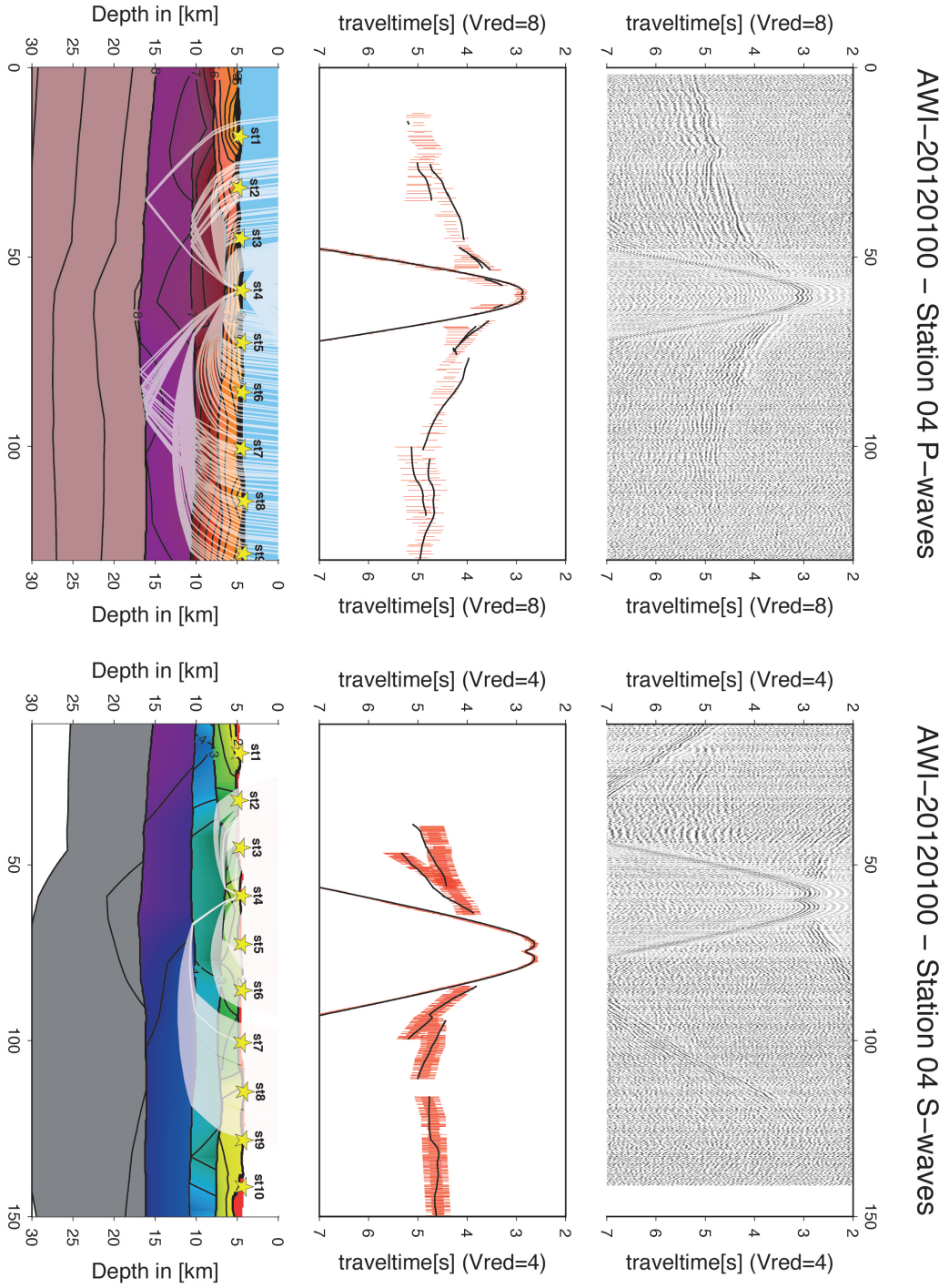


Figure A.5: P- and S-waves station 100st03 upper panel: seismogram, middle panel: picked and modeled arrival times, lower panel: resulting velocity model



**Figure A.6:** P- and S-waves station 100st04 upper panel: seismogram, middle panel: picked and modeled arrival times, lower panel: resulting velocity model

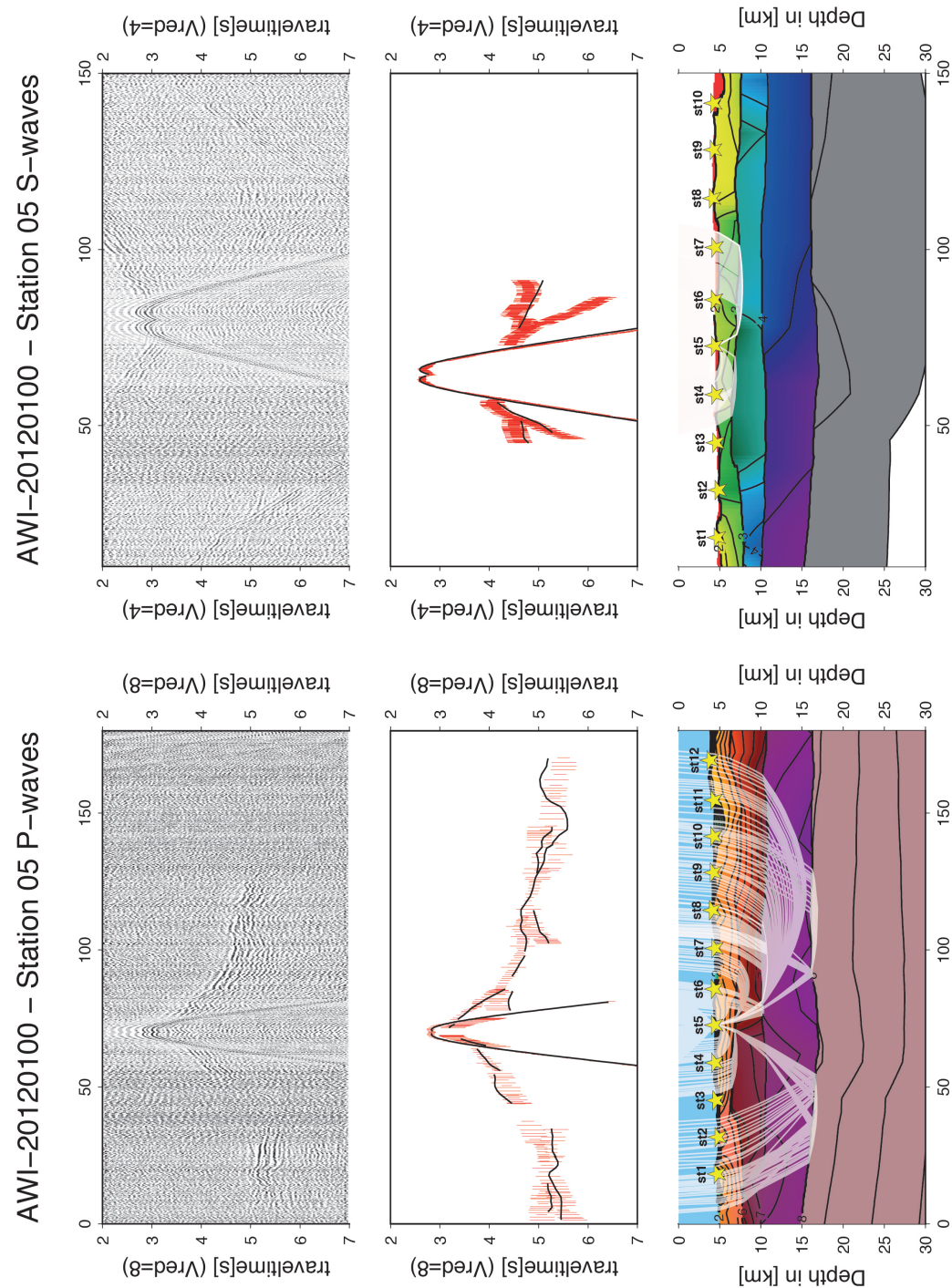
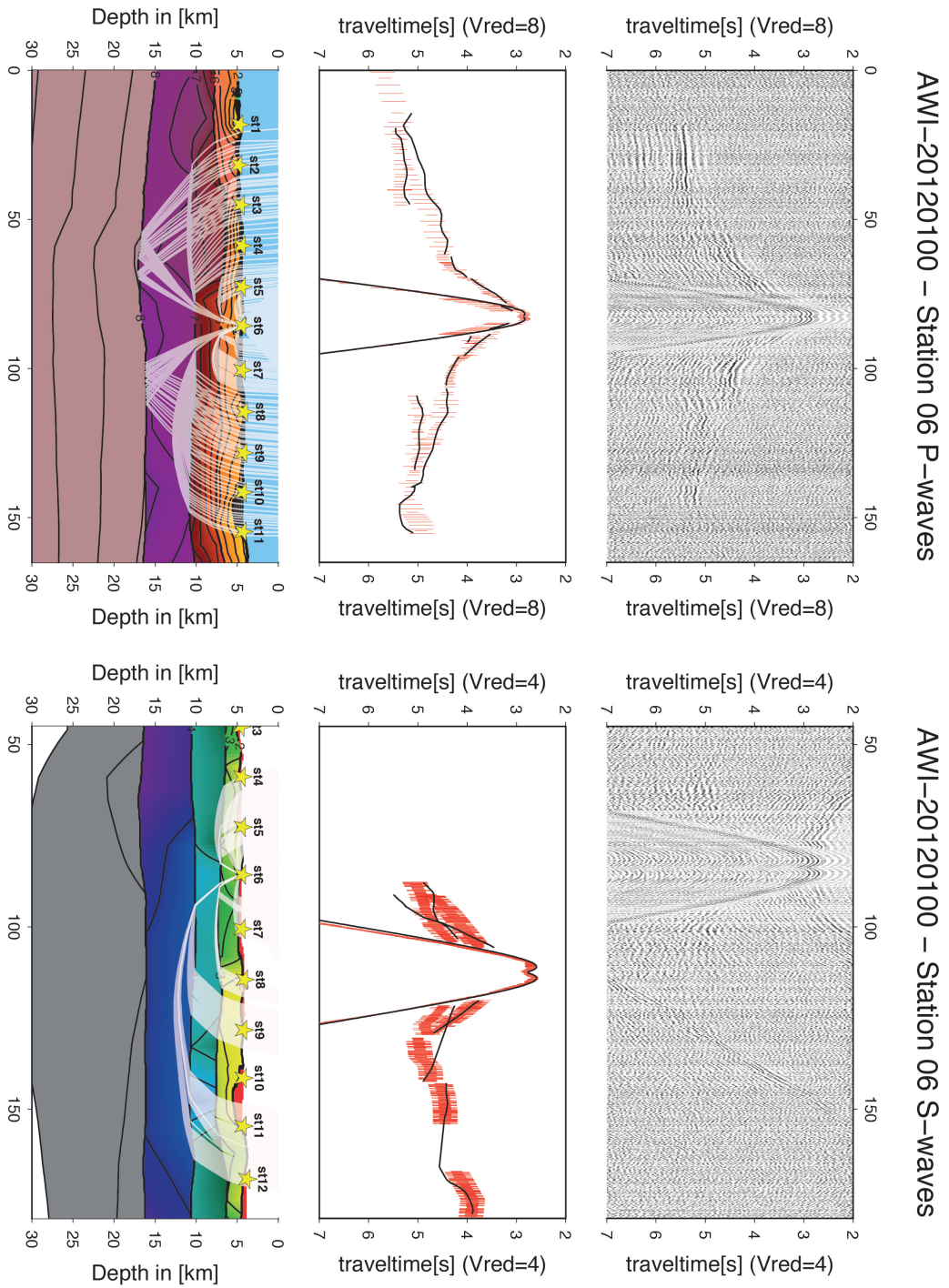
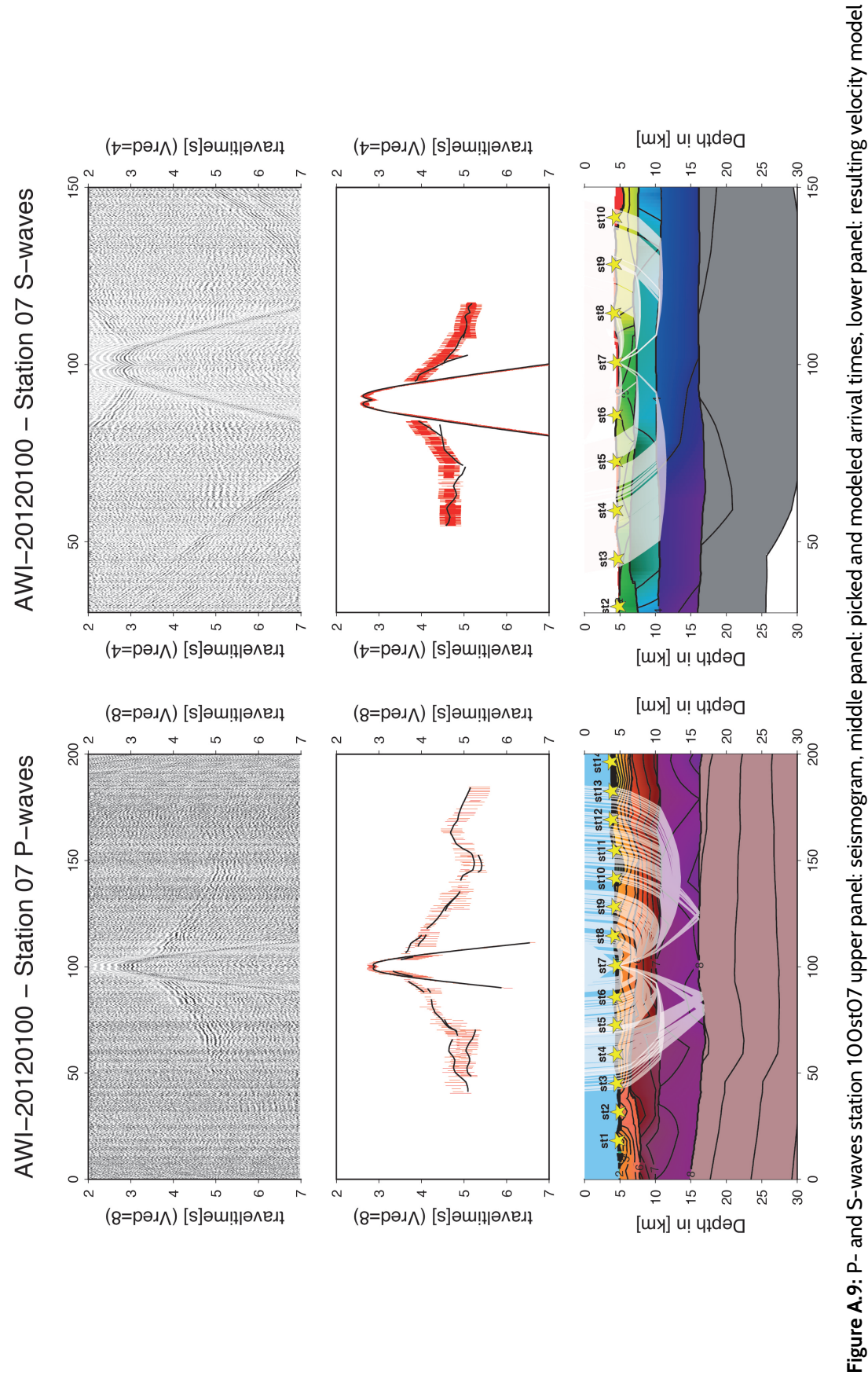


Figure A.7: P- and S-wave station 10Ost05 upper panel: seismogram, middle panel: picked and modeled arrival times, lower panel: resulting velocity model



**Figure A.8:** P- and S-waves station 10Ost06 upper panel: seismogram, middle panel: picked and modeled arrival times, lower panel: resulting velocity model





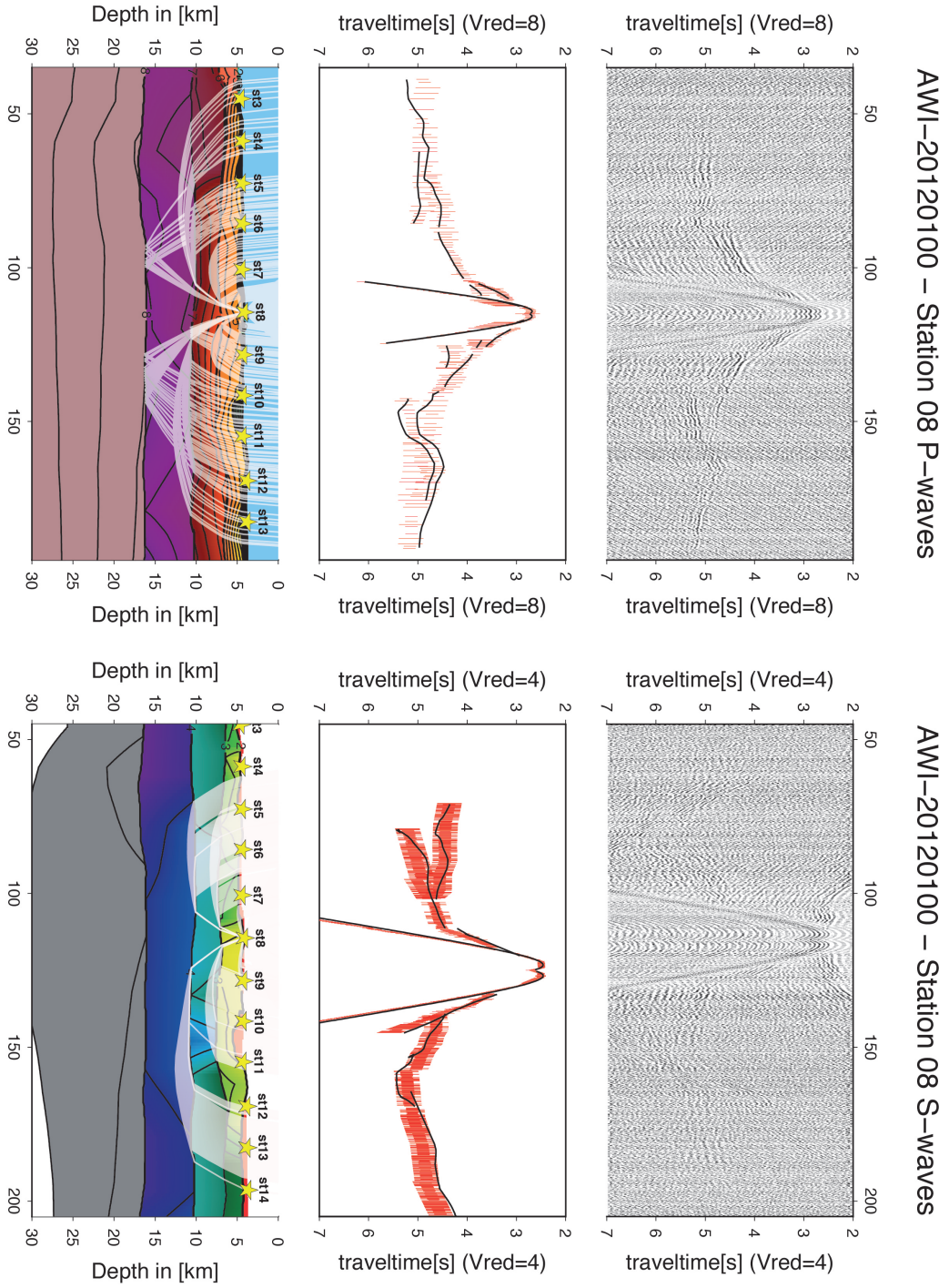


**Figure A.10:** P- and S-waves station 100Ost08 upper panel: seismogram, middle panel: picked and modeled arrival times, lower panel: resulting velocity model



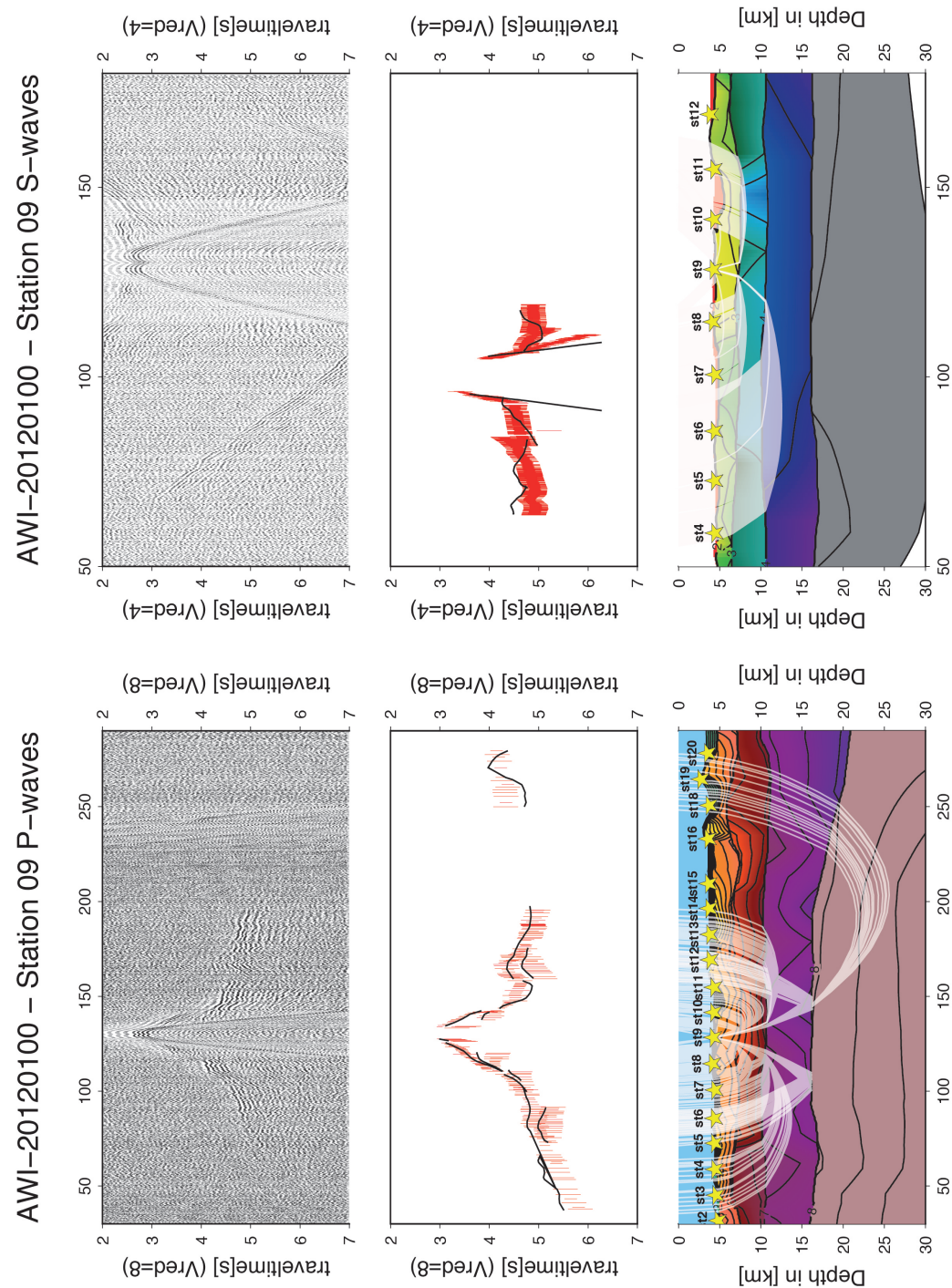
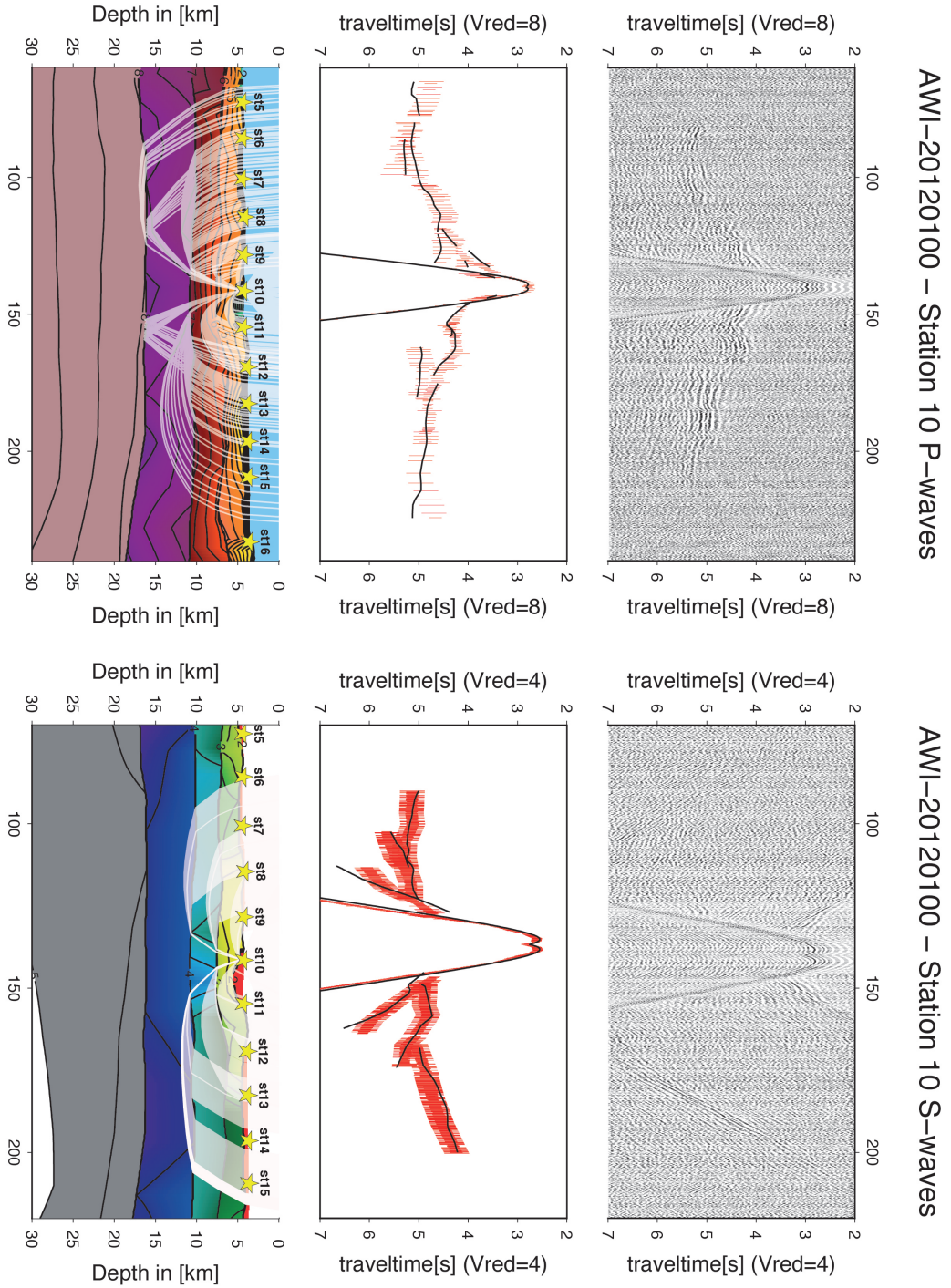


Figure A.11: P- and S-waves station 100st09 upper panel: seismogram, middle panel: picked and modeled arrival times, lower panel: resulting velocity model



**Figure A.12:** P- and S-waves station 100st10 upper panel: seismogram, middle panel: picked and modeled arrival times, lower panel: resulting velocity model



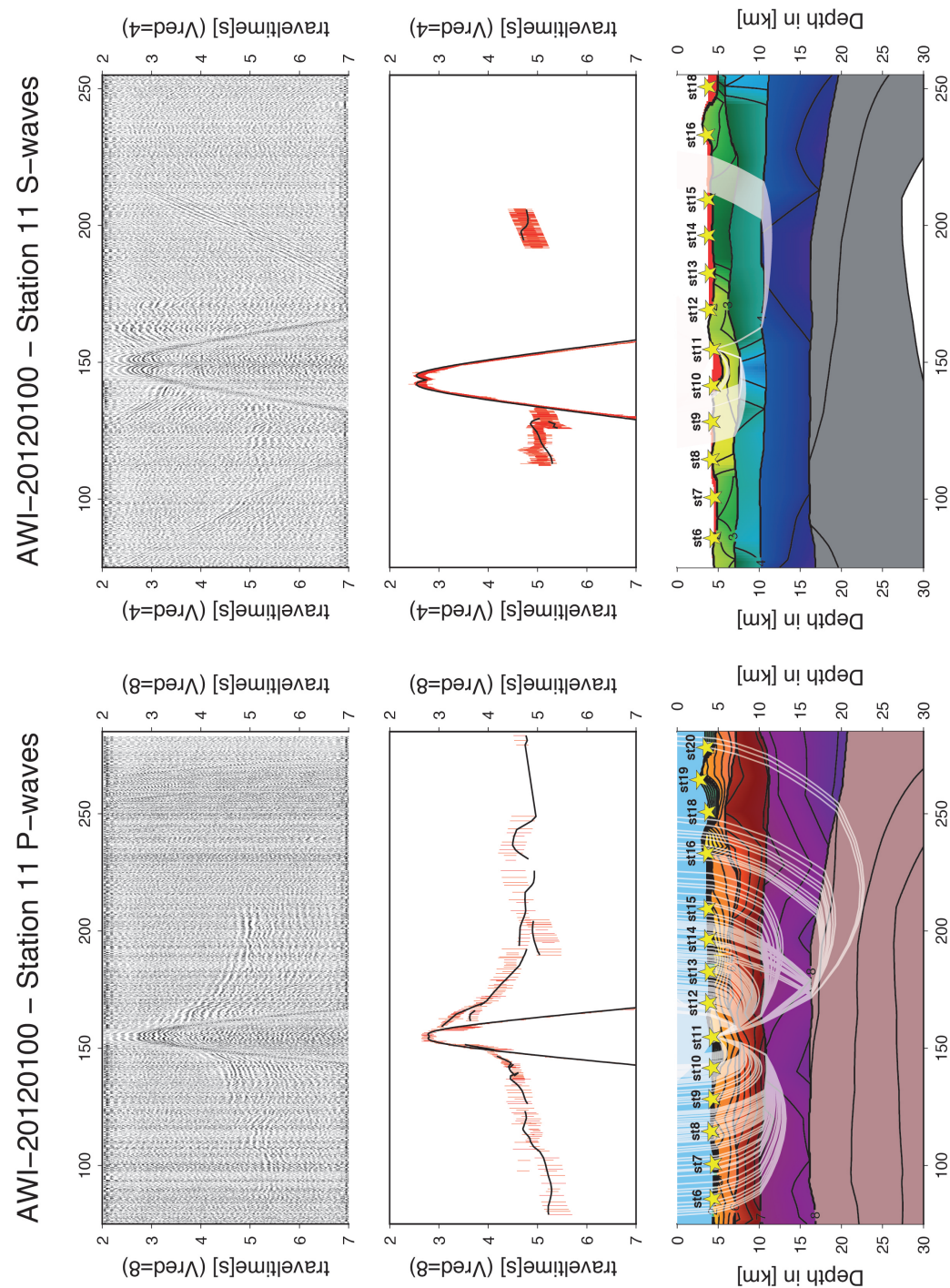
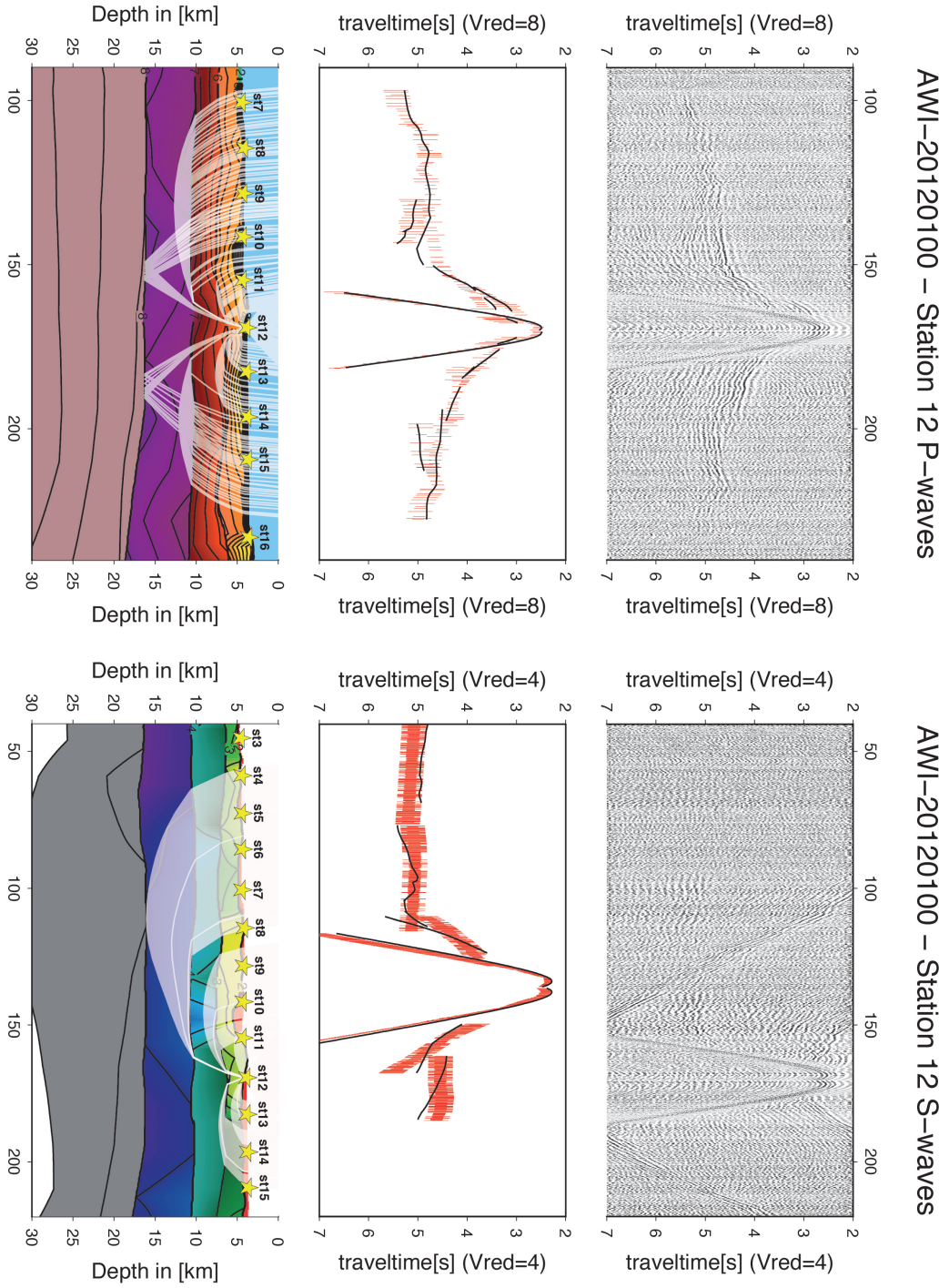


Figure A.13: P- and S-waves station 100st11 upper panel: seismogram, middle panel: picked and modeled arrival times, lower panel: resulting velocity model



**Figure A.14:** P- and S-waves station 100st12 upper panel: seismogram, middle panel: picked and modeled arrival times, lower panel: resulting velocity model

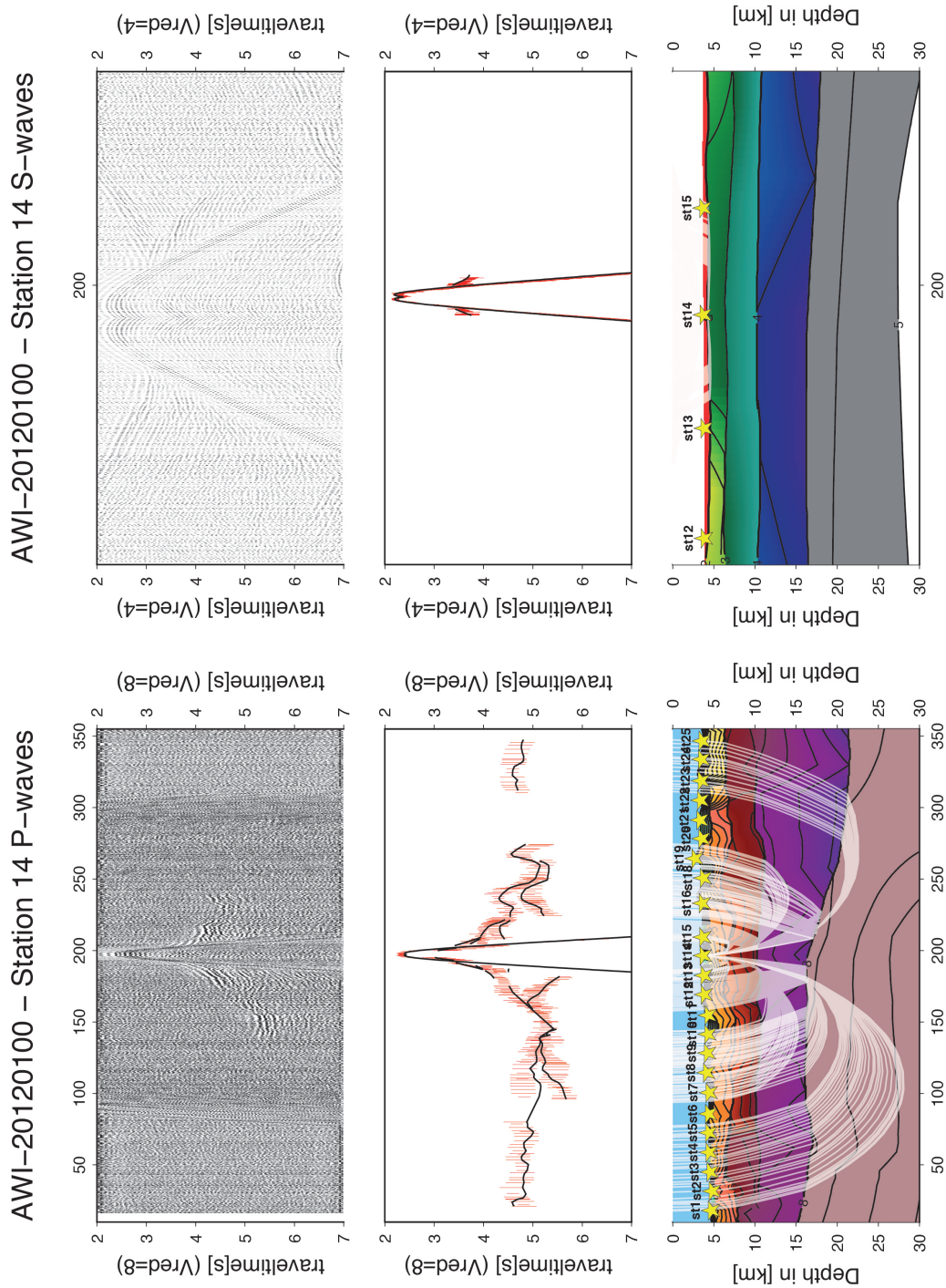


Figure A.15: P- and S-waves station 100st14 upper panel: seismogram, middle panel: picked and modeled arrival times, lower panel: resulting velocity model



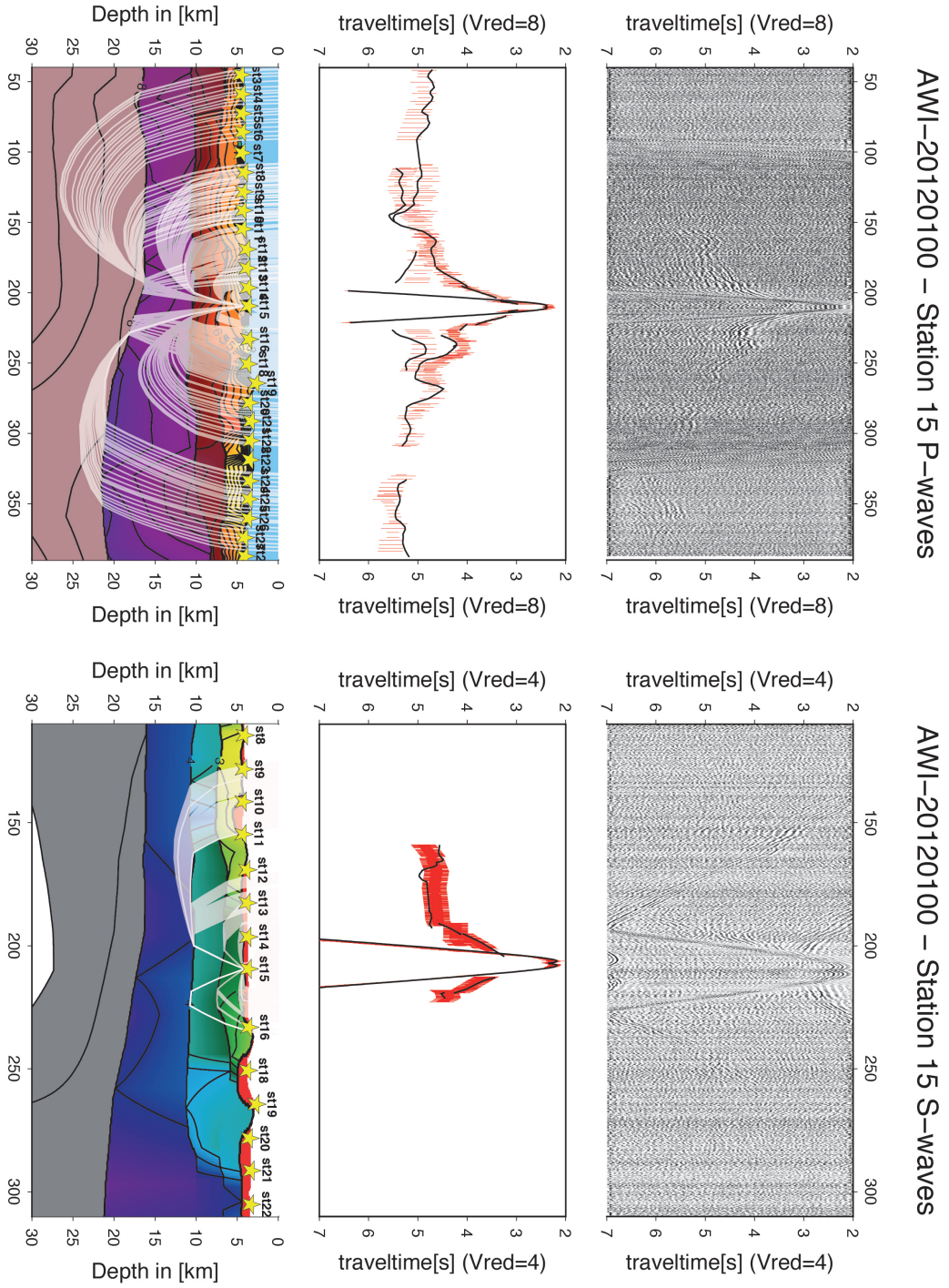
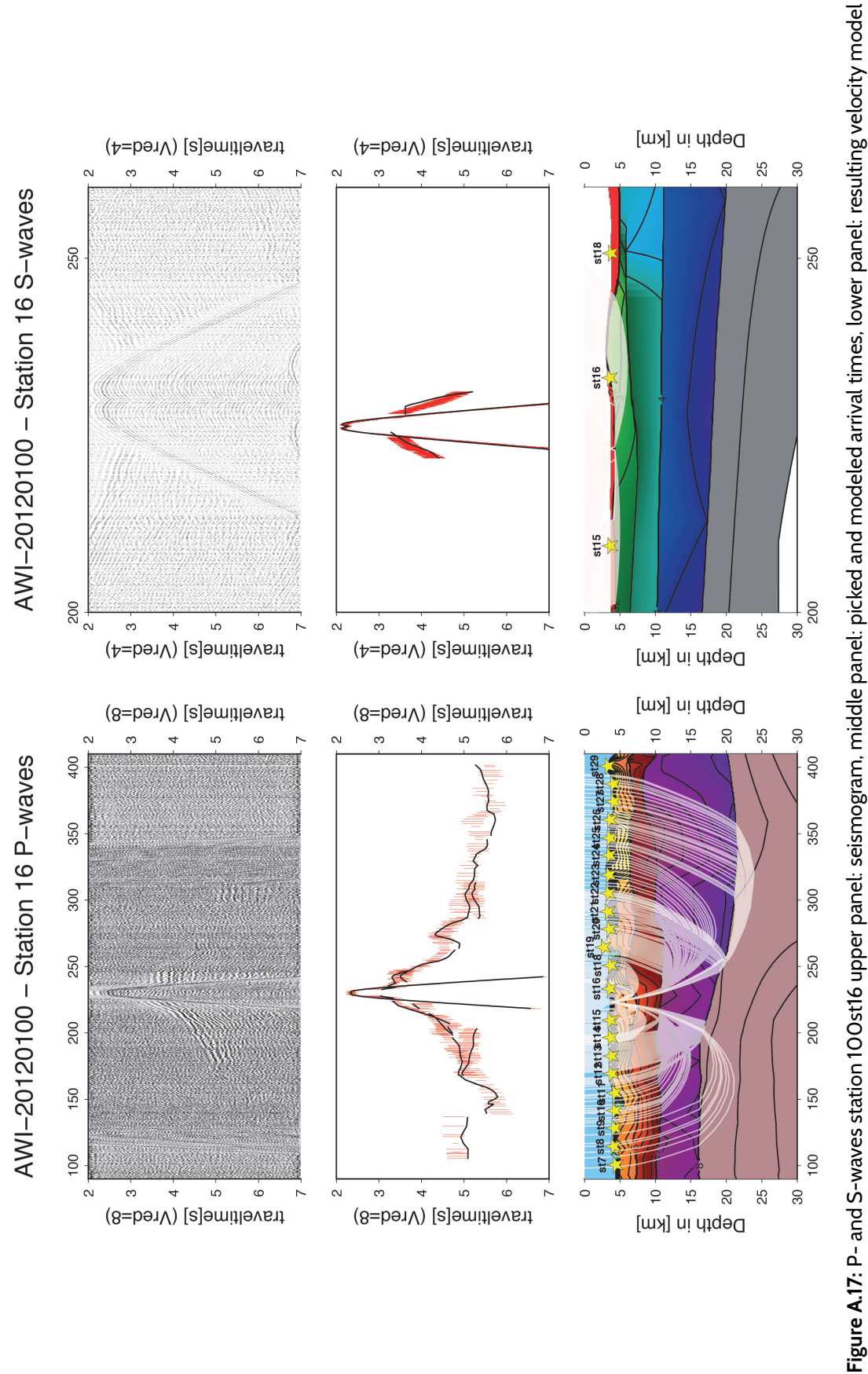
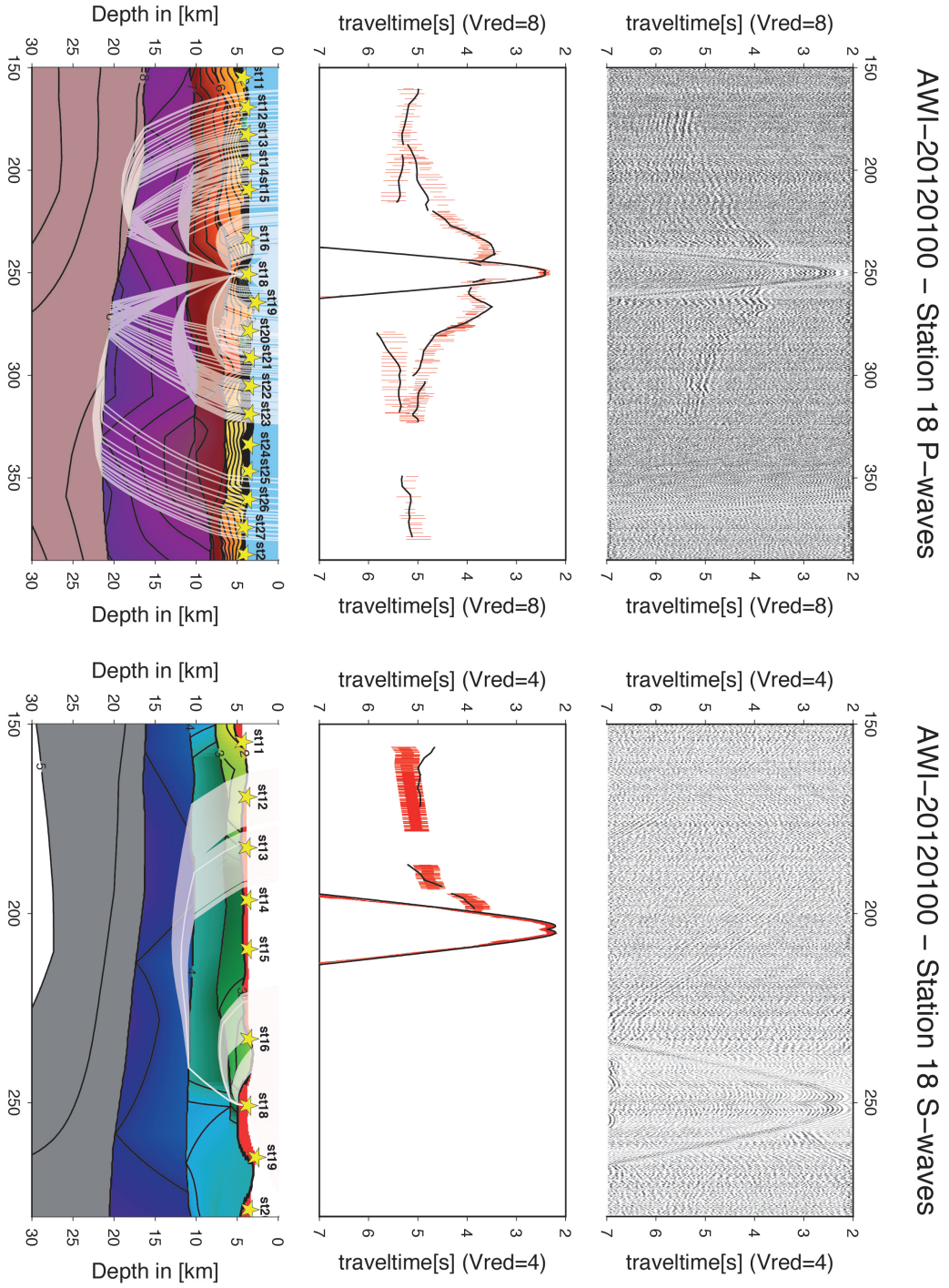


Figure A.16: P- and S-waves station 100st15 upper panel: seismogram, middle panel: picked and modeled arrival times, lower panel: resulting velocity model







**Figure A.18:** P- and S-waves station 100st18 upper panel: seismogram, middle panel: picked and modeled arrival times, lower panel: resulting velocity model

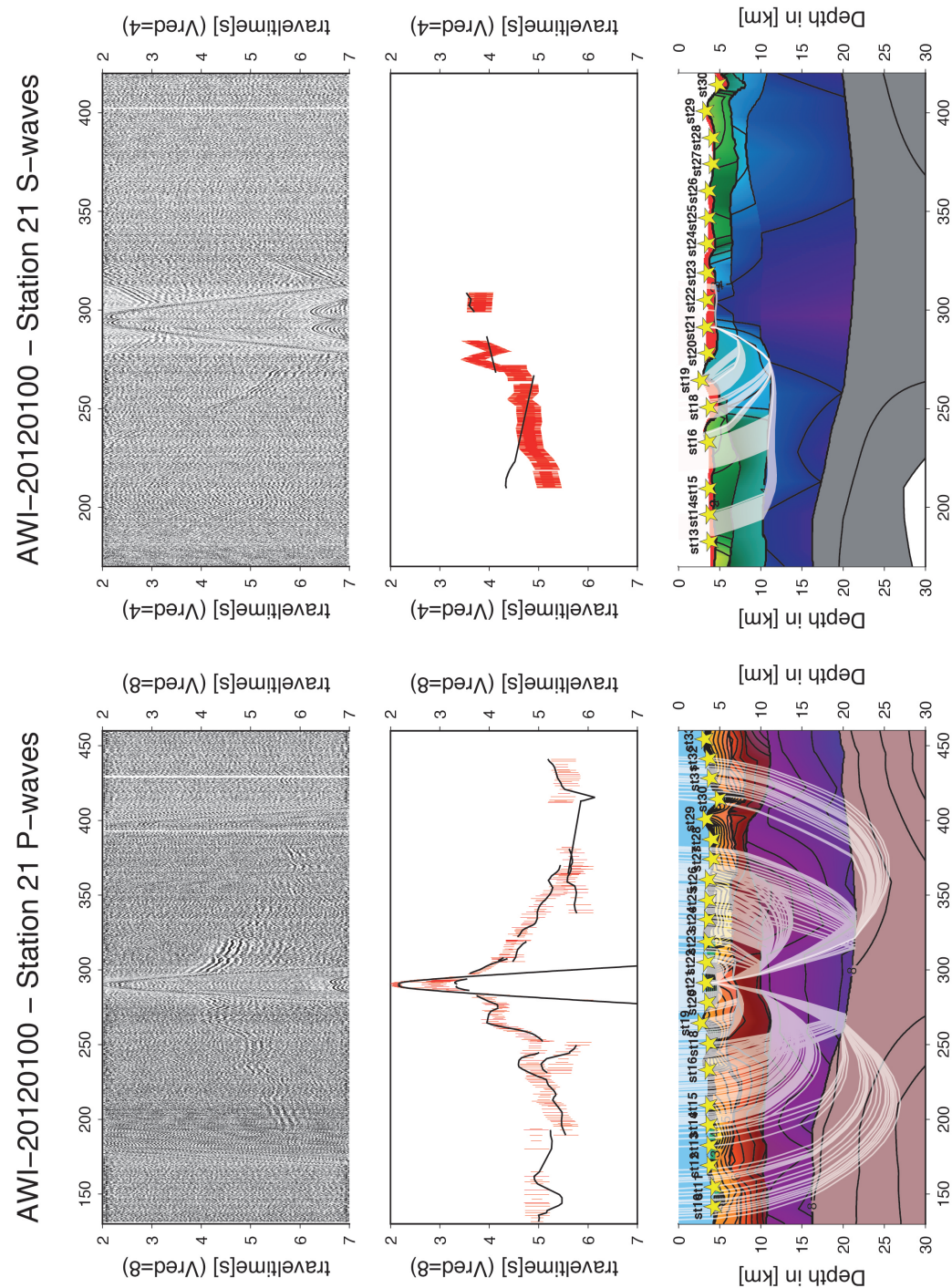


Figure A.19: P- and S-wave station 100st21 upper panel: seismogram, middle panel: picked and modeled arrival times, lower panel: resulting velocity model



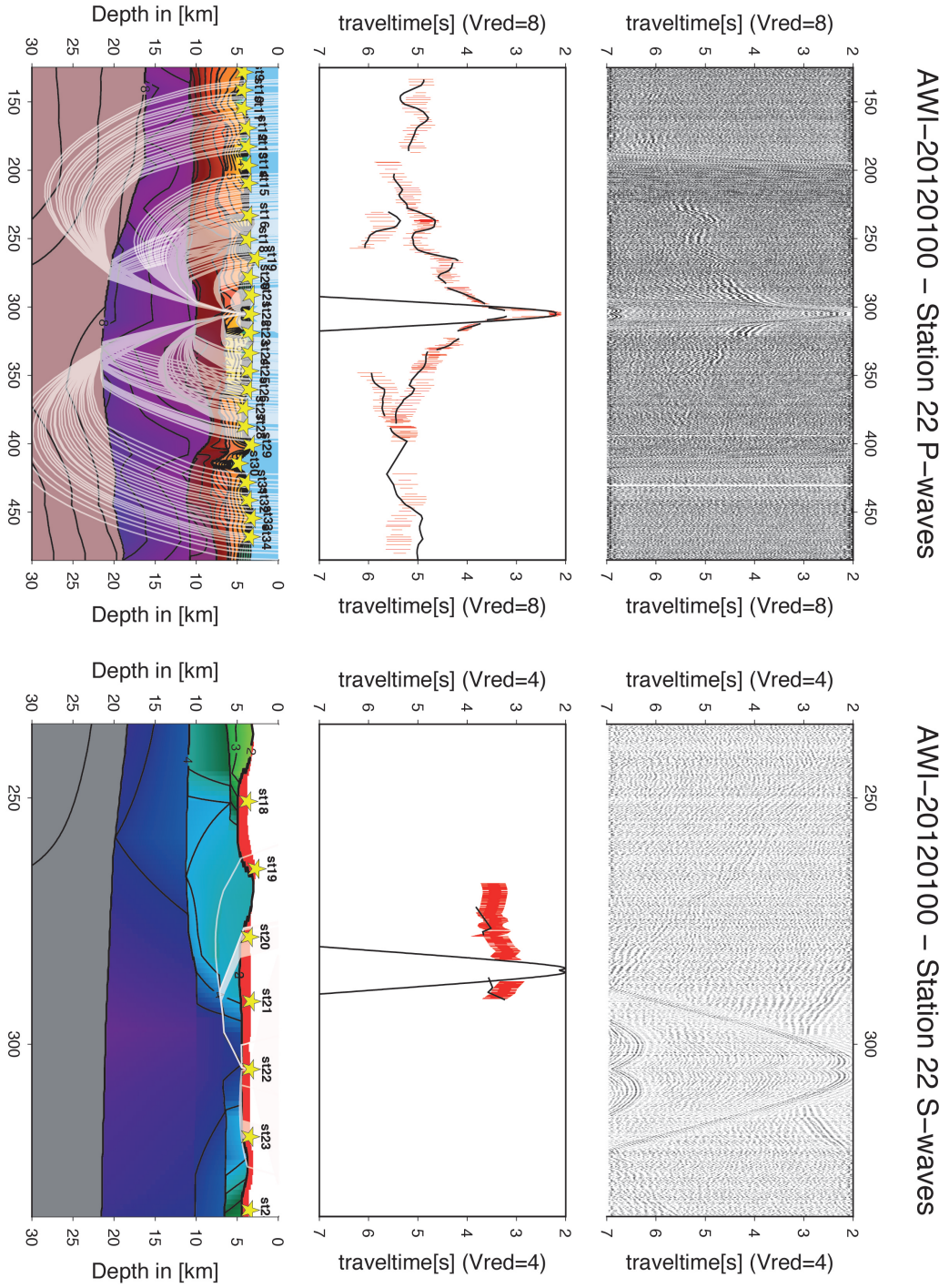


Figure A.20: P- and S-waves station 100st22 upper panel: seismogram, middle panel: picked and modeled arrival times, lower panel: resulting velocity model



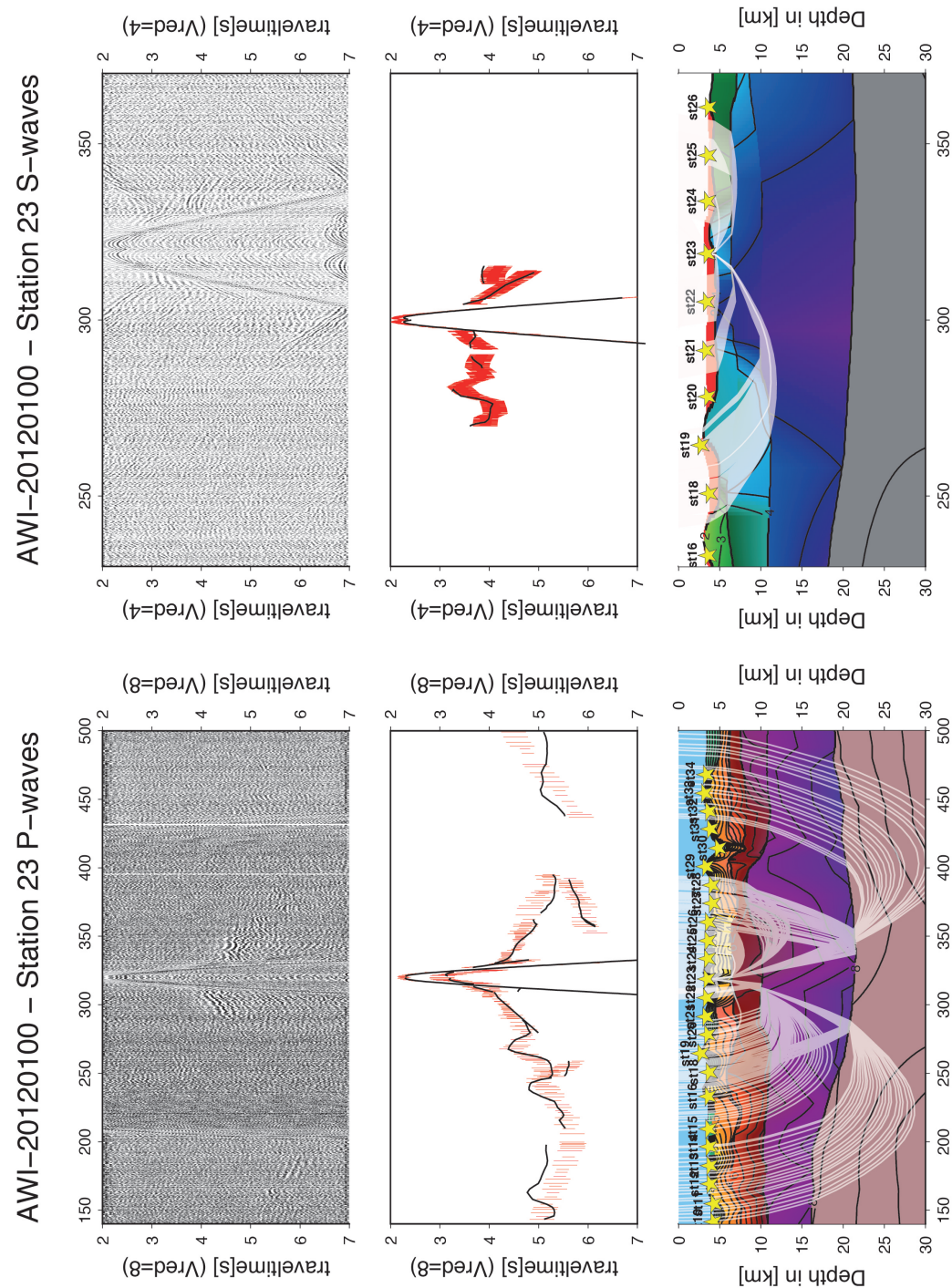
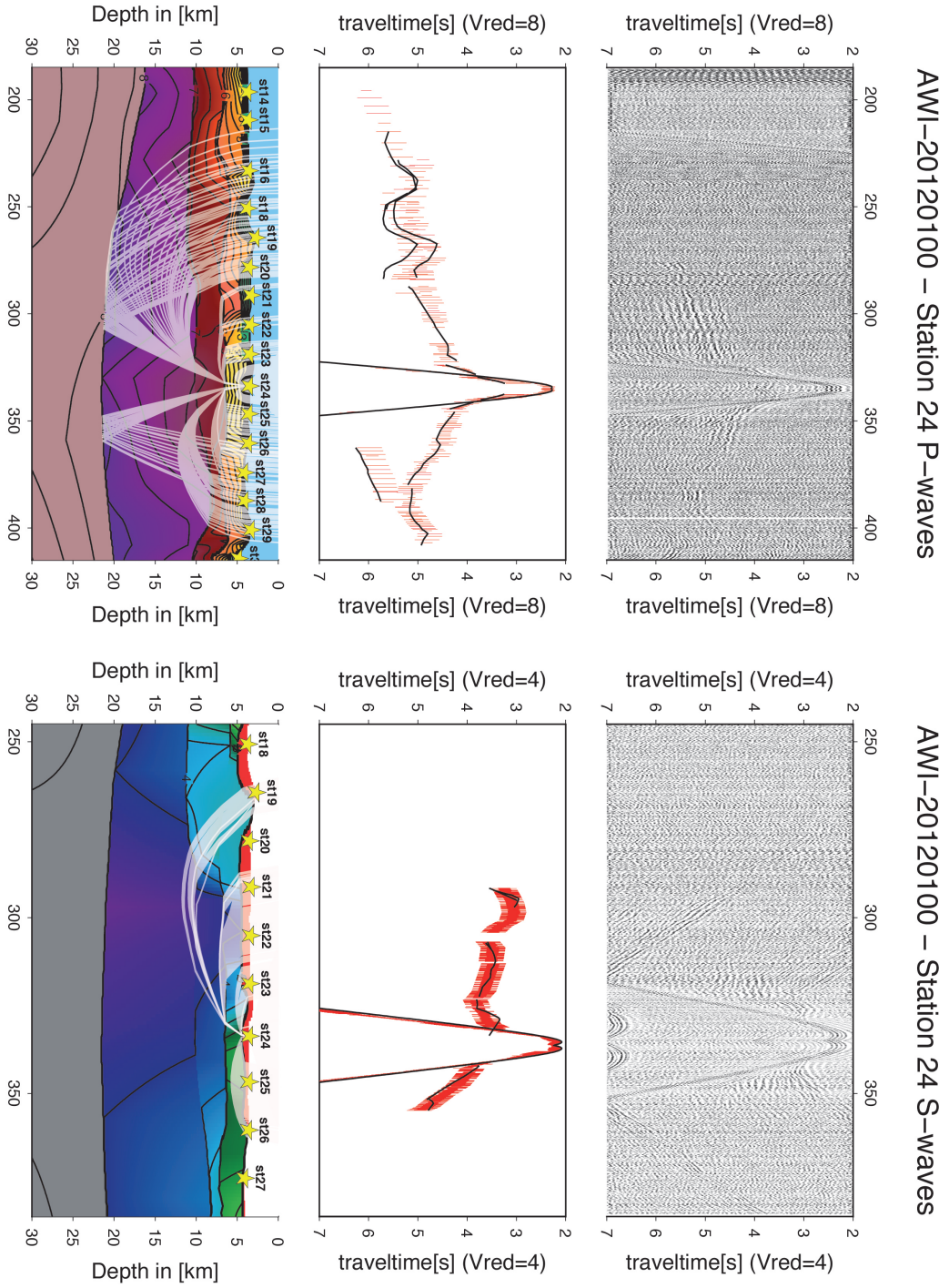


Figure A.21: P- and S-wave station 100st23 upper panel: seismogram, middle panel: picked and modeled arrival times, lower panel: resulting velocity model



**Figure A.22:** P- and S-waves station 100st24 upper panel: seismogram, middle panel: picked and modeled arrival times, lower panel: resulting velocity model



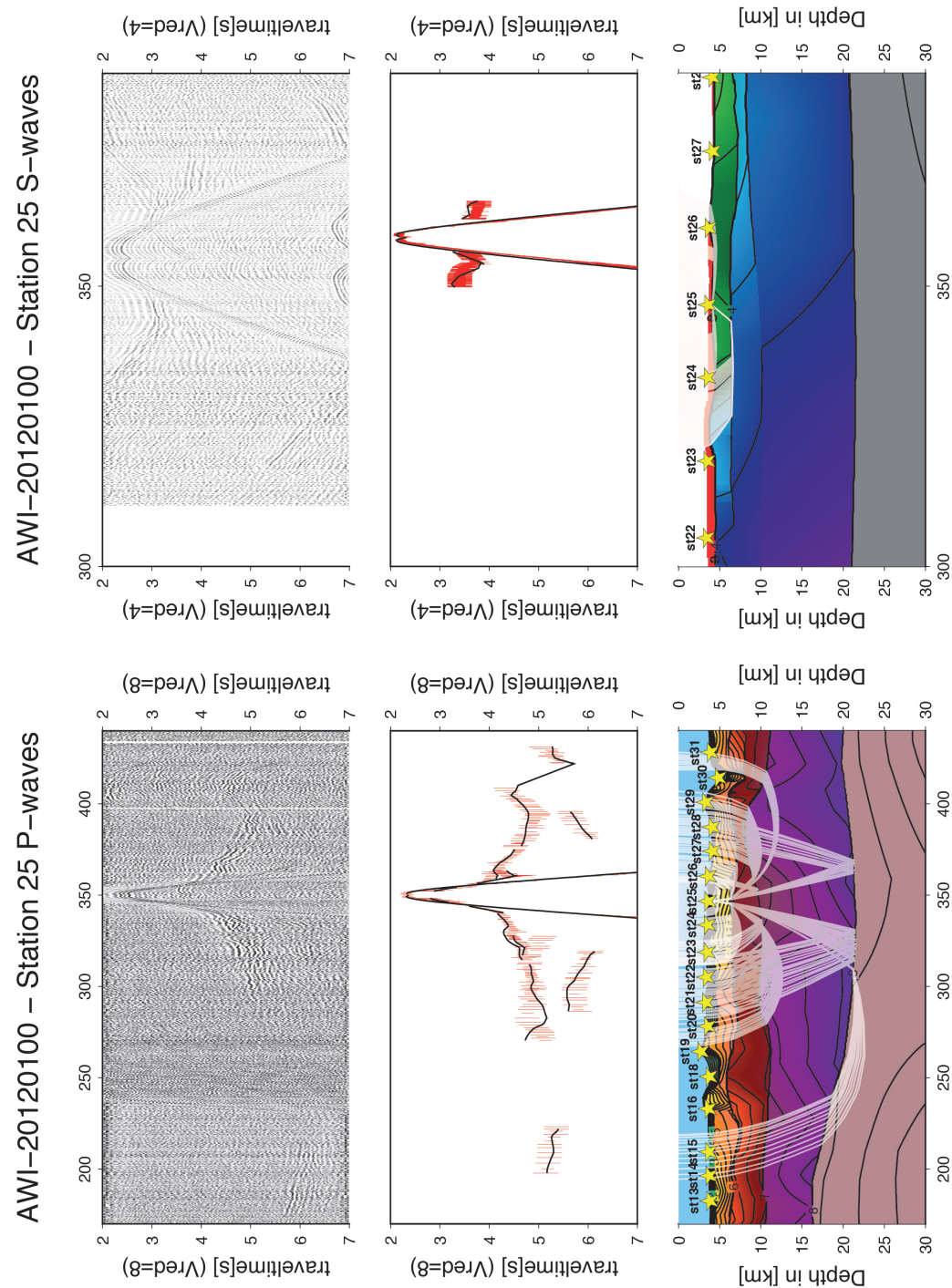
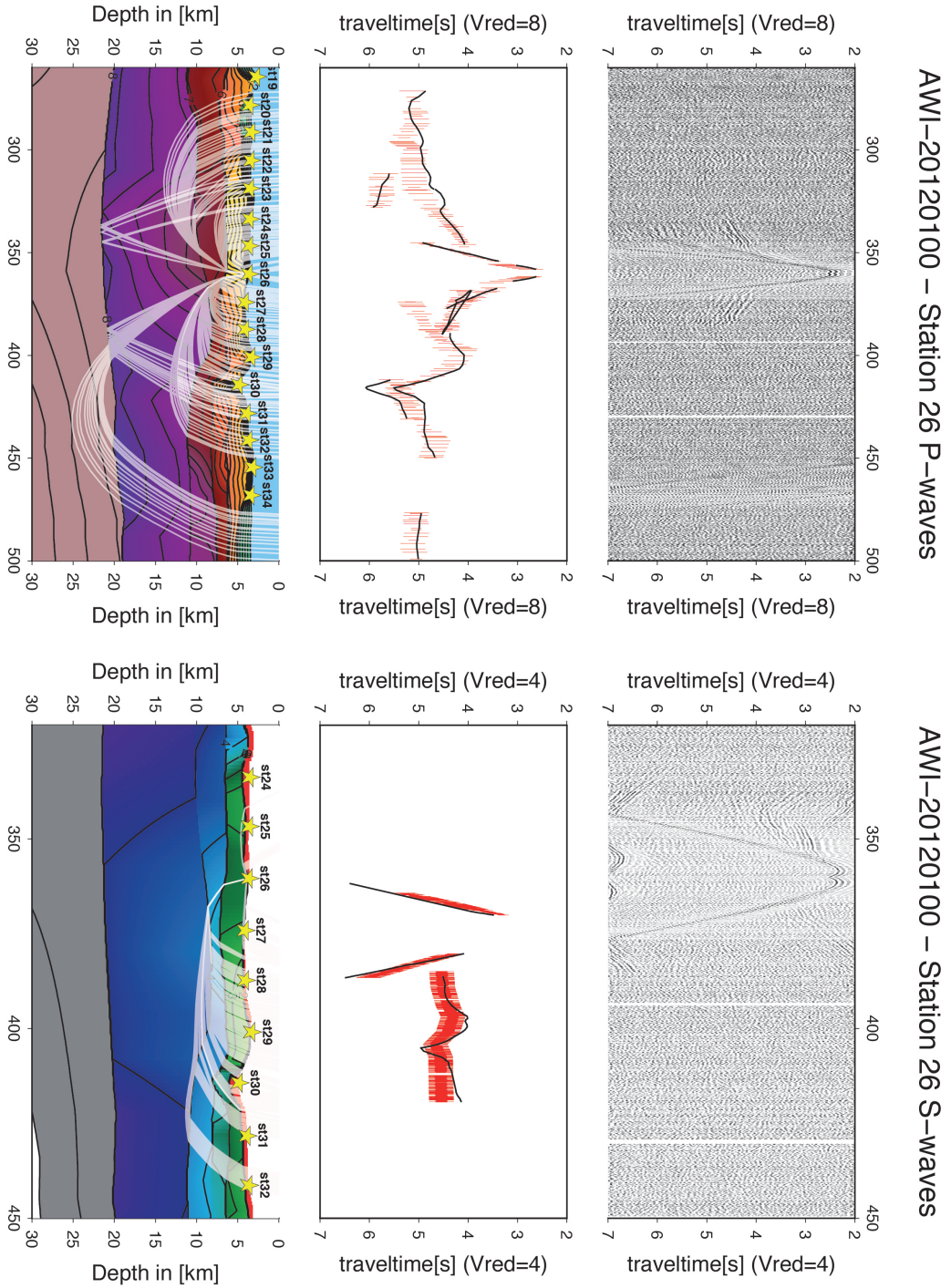


Figure A.23: P- and S-wave station 100st25 upper panel: seismogram, middle panel: picked and modeled arrival times, lower panel: resulting velocity model



**Figure A.24:** P- and S-waves station 100st26 upper panel: seismogram, middle panel: picked and modeled arrival times, lower panel: resulting velocity model

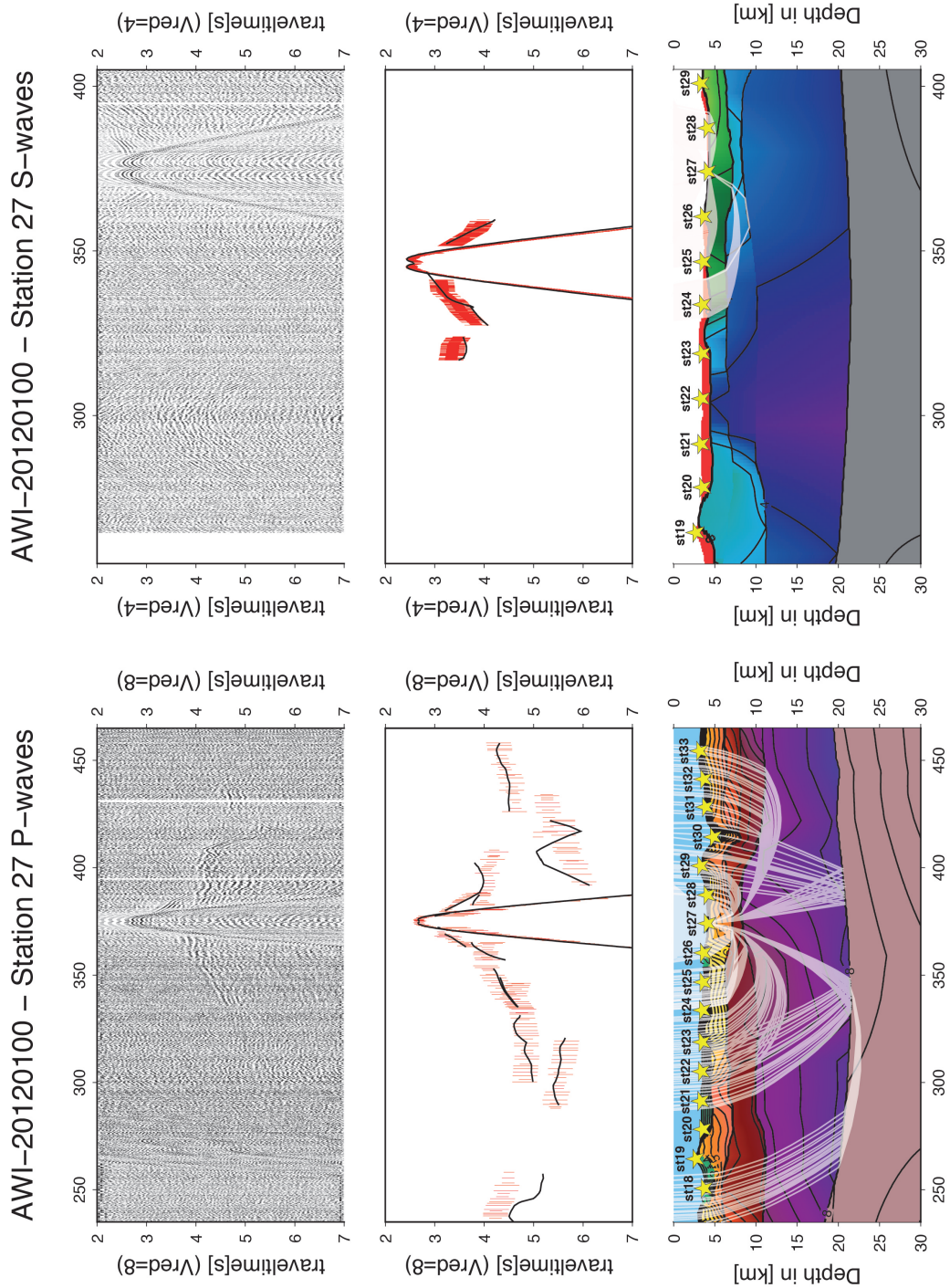


Figure A.25: P- and S-waves station 100st27 upper panel: seismogram, middle panel: picked and modeled arrival times, lower panel: resulting velocity model



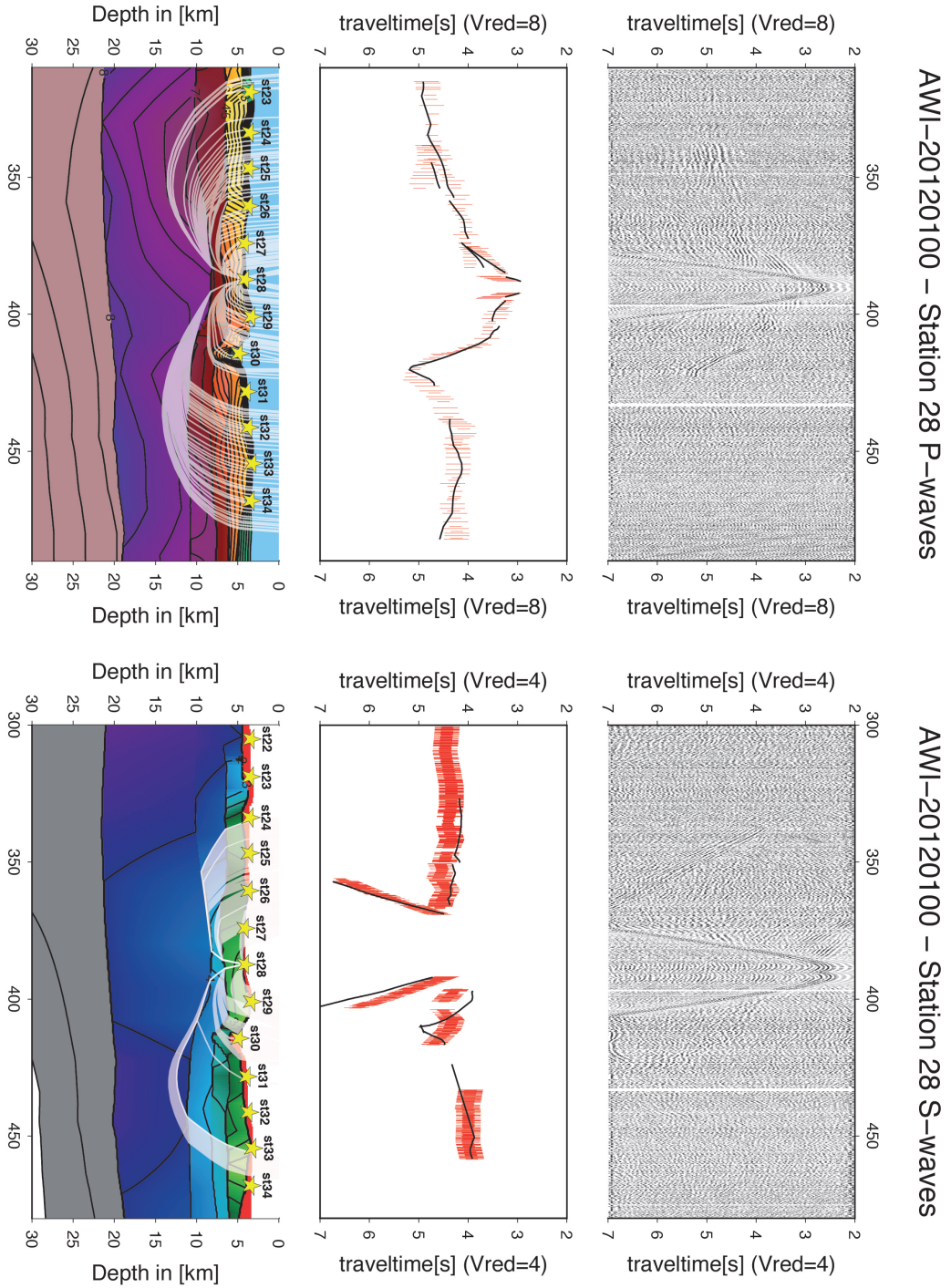


Figure A.26: P- and S-waves station 100st28 upper panel: seismogram, middle panel: picked and modeled arrival times, lower panel: resulting velocity model

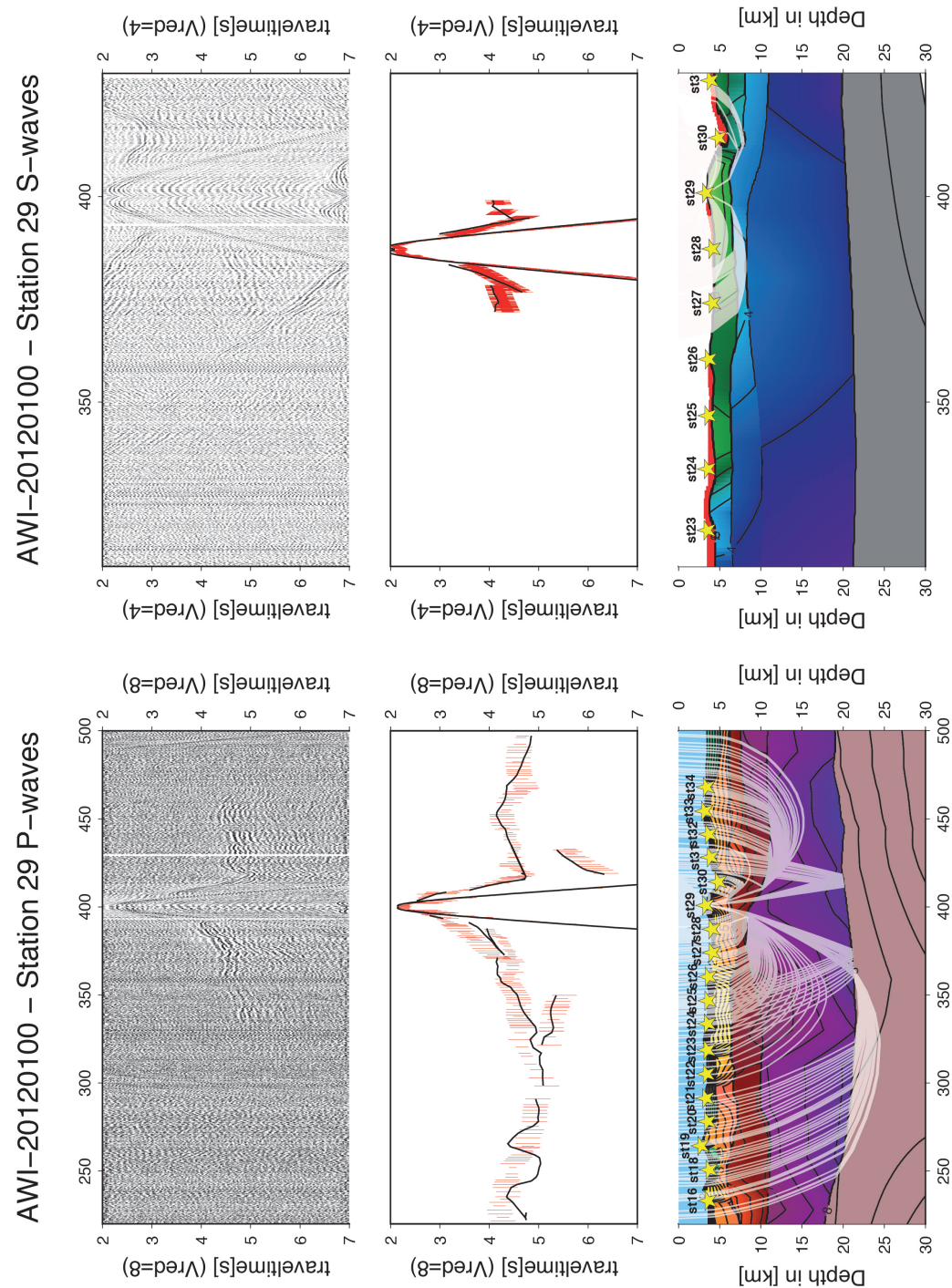
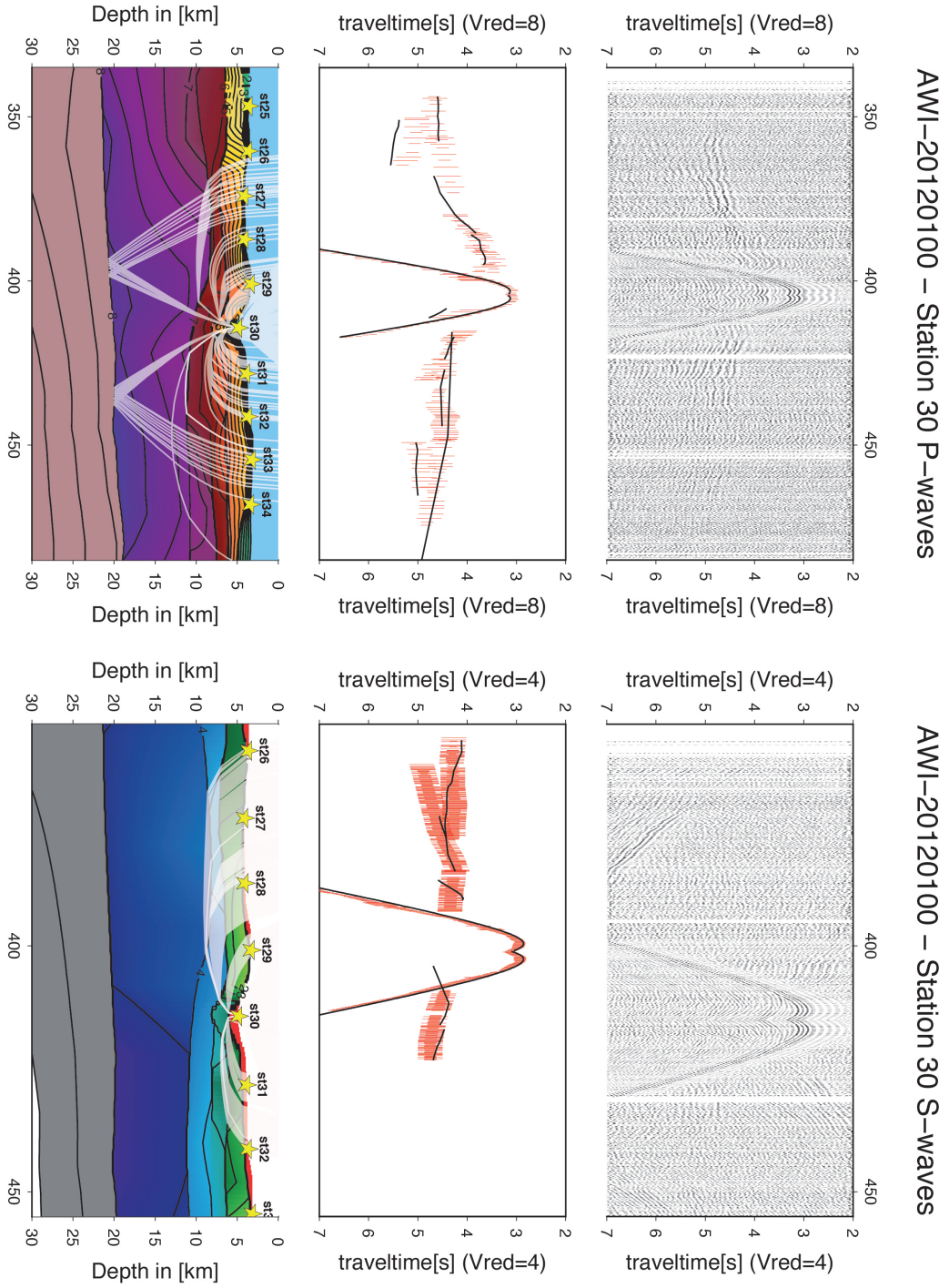


Figure A.27: P- and S-waves station 100st29 upper panel: seismogram, middle panel: picked and modeled arrival times, lower panel: resulting velocity model





**Figure A.28:** P- and S-waves station 100st30 upper panel: seismogram, middle panel: picked and modeled arrival times, lower panel: resulting velocity model

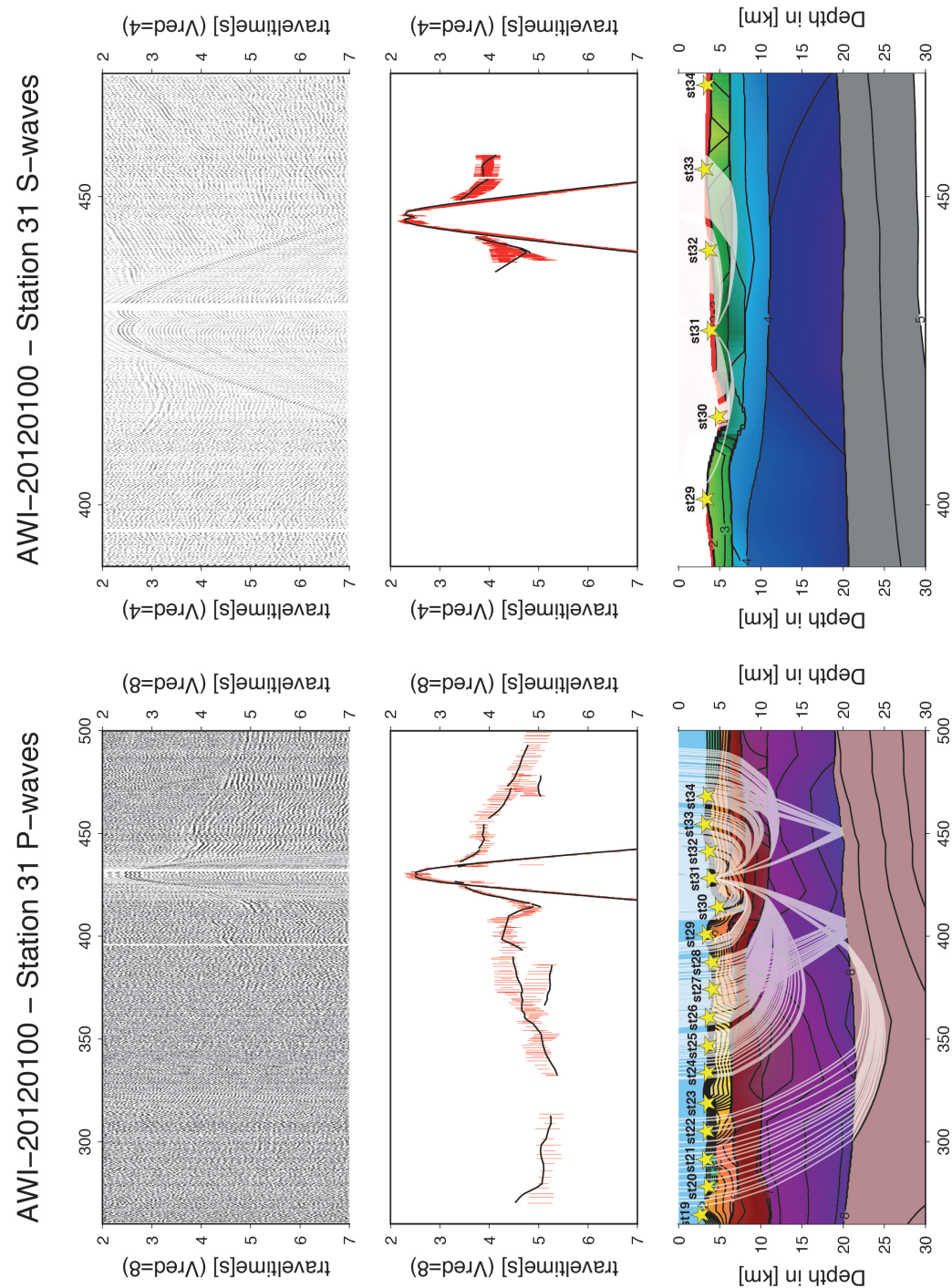
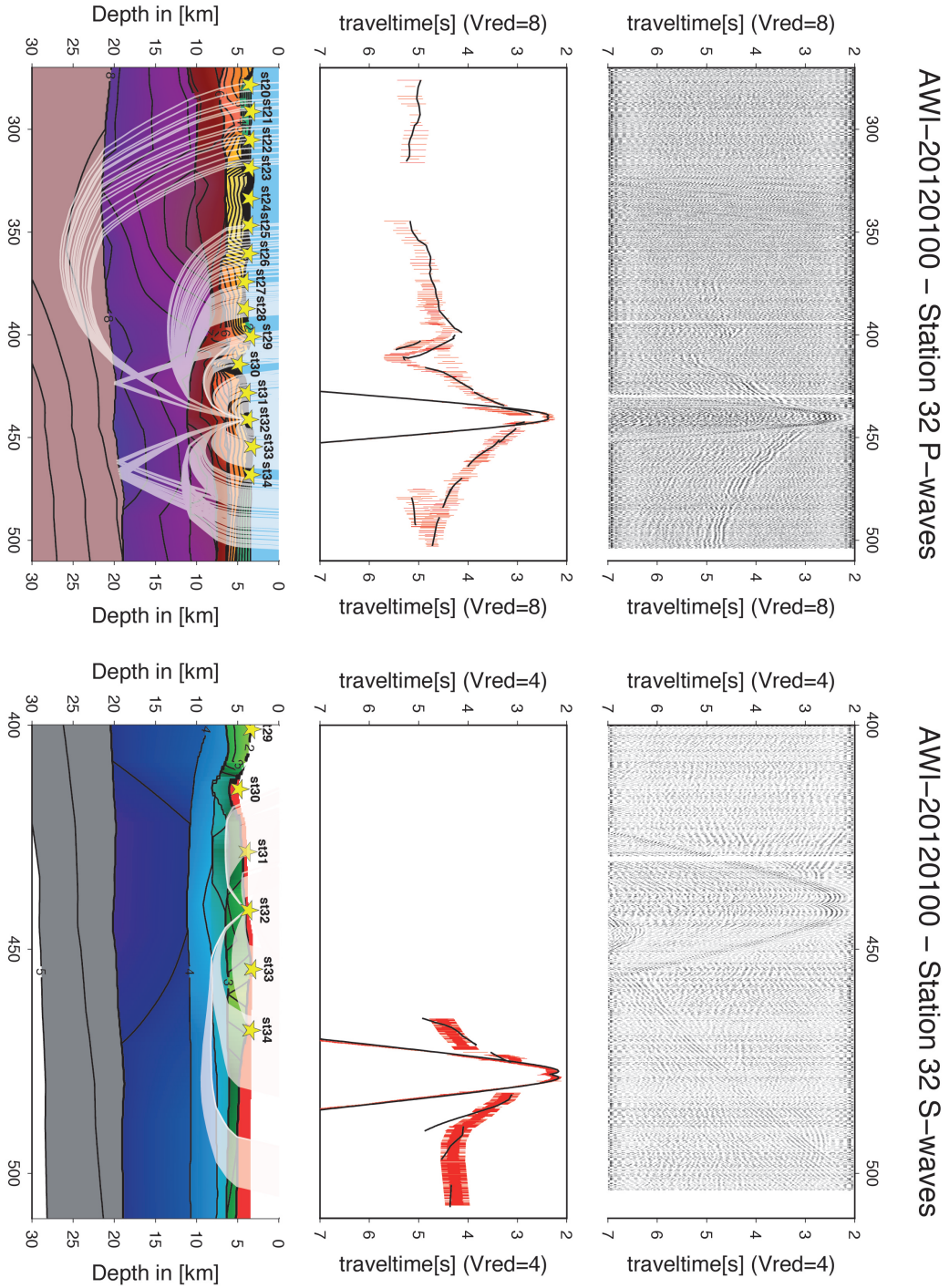


Figure A.29: P- and S-waves station 100st31 upper panel: seismogram, middle panel: picked and modeled arrival times, lower panel: resulting velocity model



**Figure A.30:** P- and S-waves station 100st32 upper panel: seismogram, middle panel: picked and modeled arrival times, lower panel: resulting velocity model



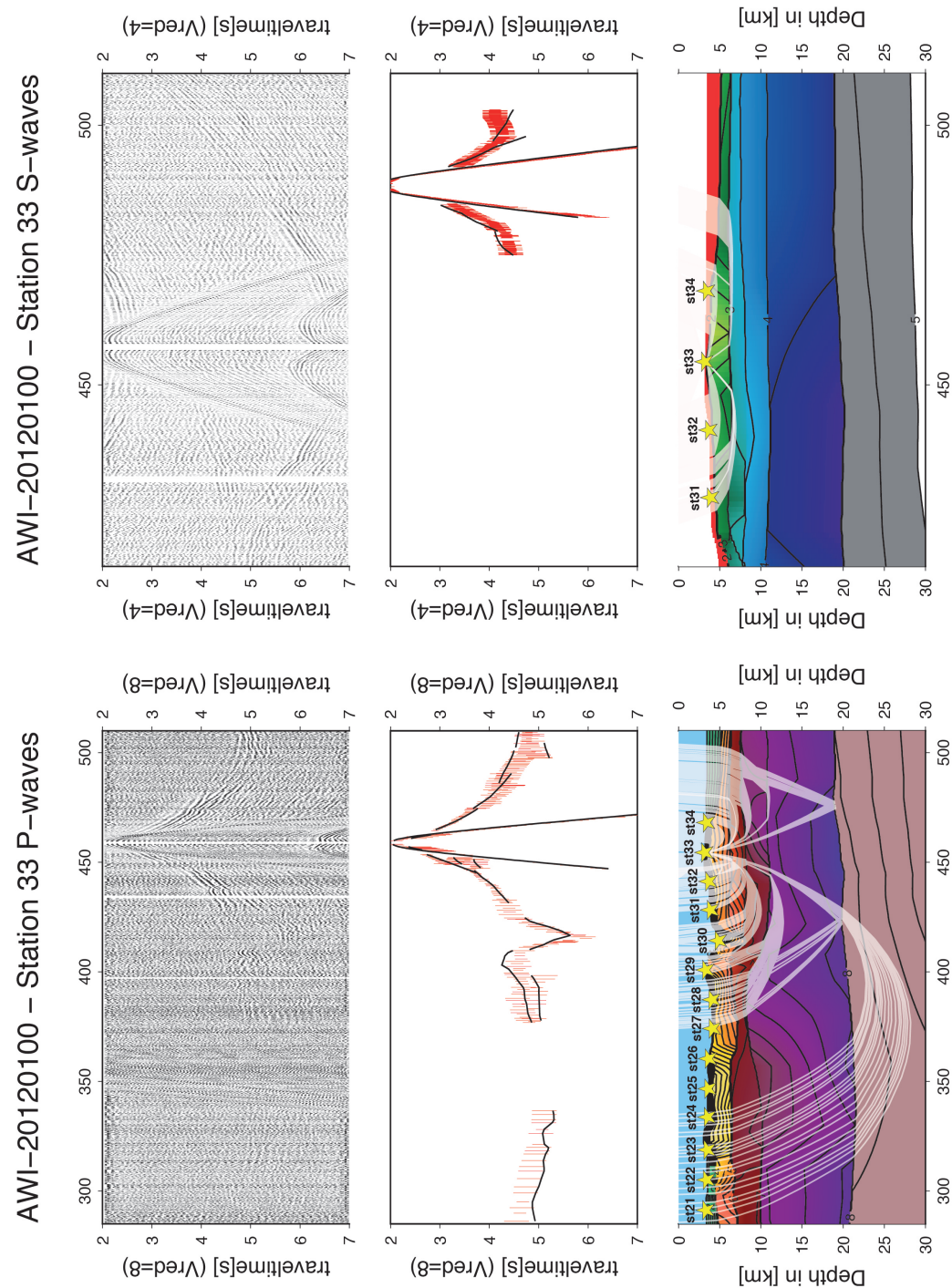
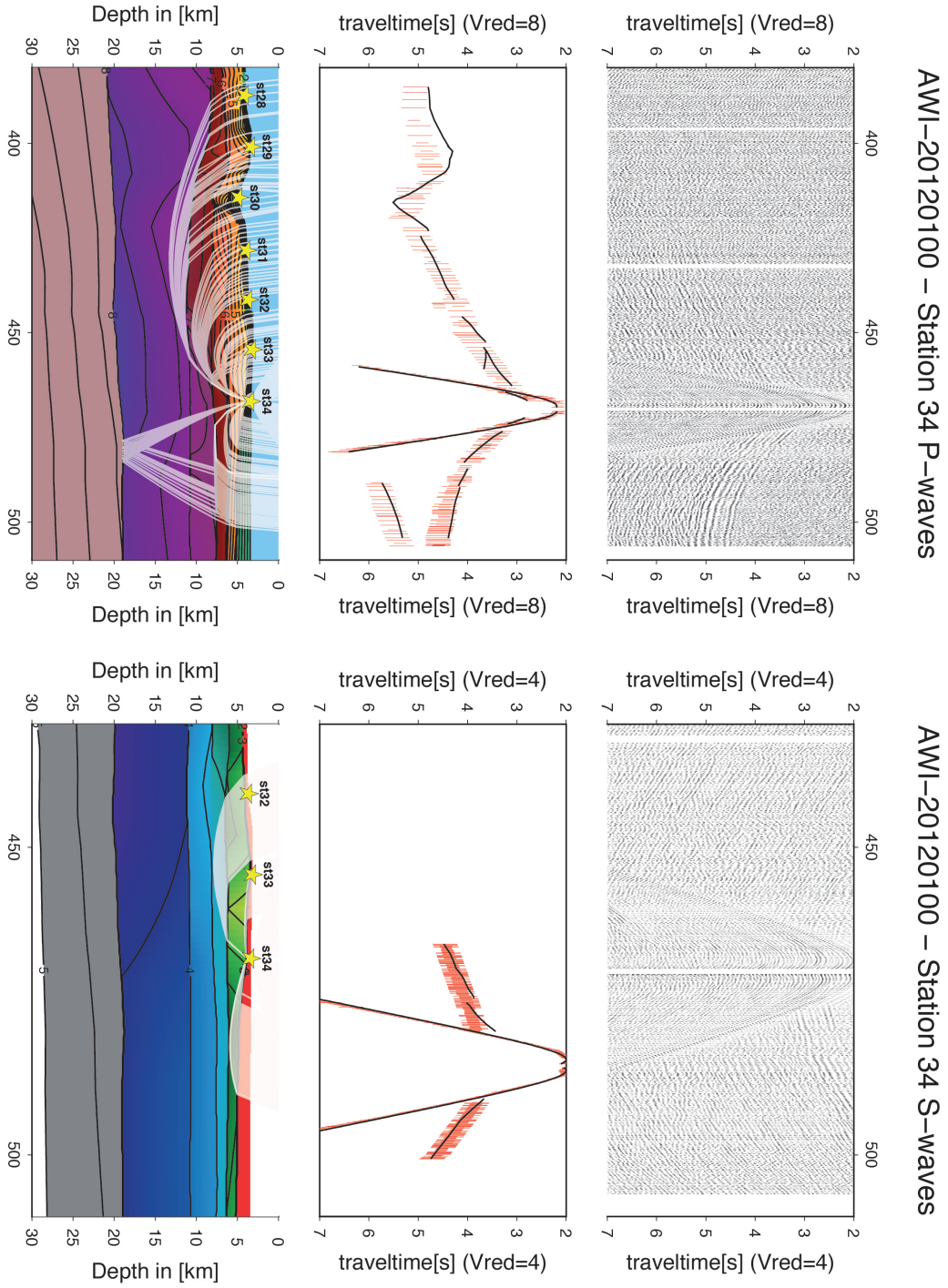
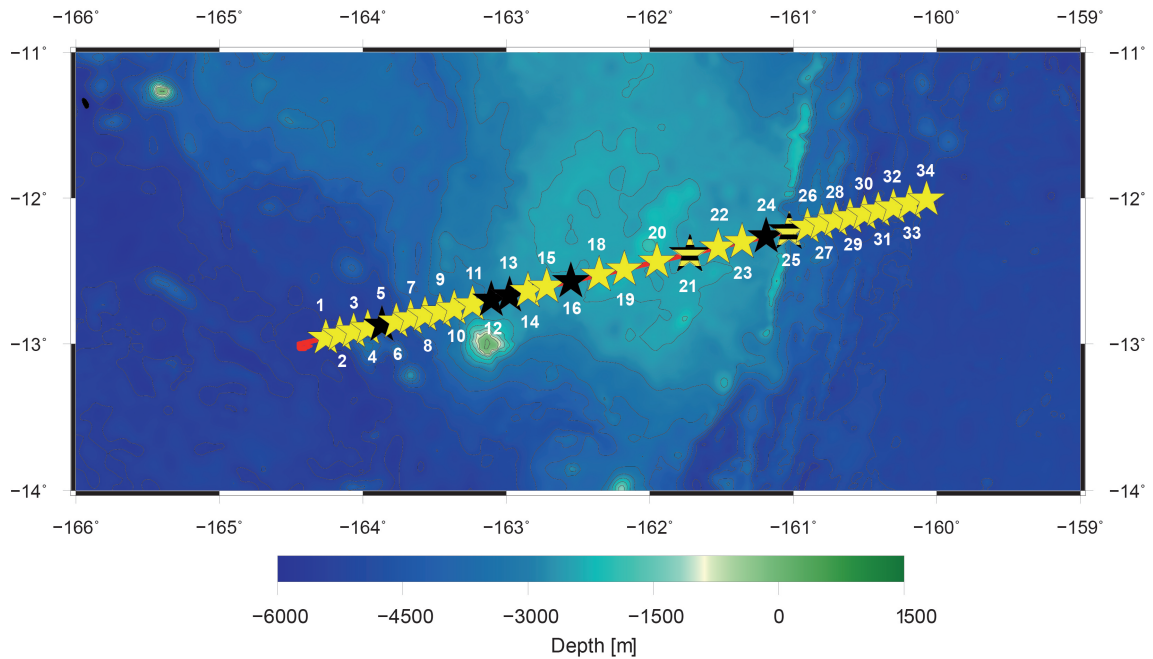


Figure A.31: P- and S-wave station 100st33 upper panel: seismogram, middle panel: picked and modeled arrival times, lower panel: resulting velocity model



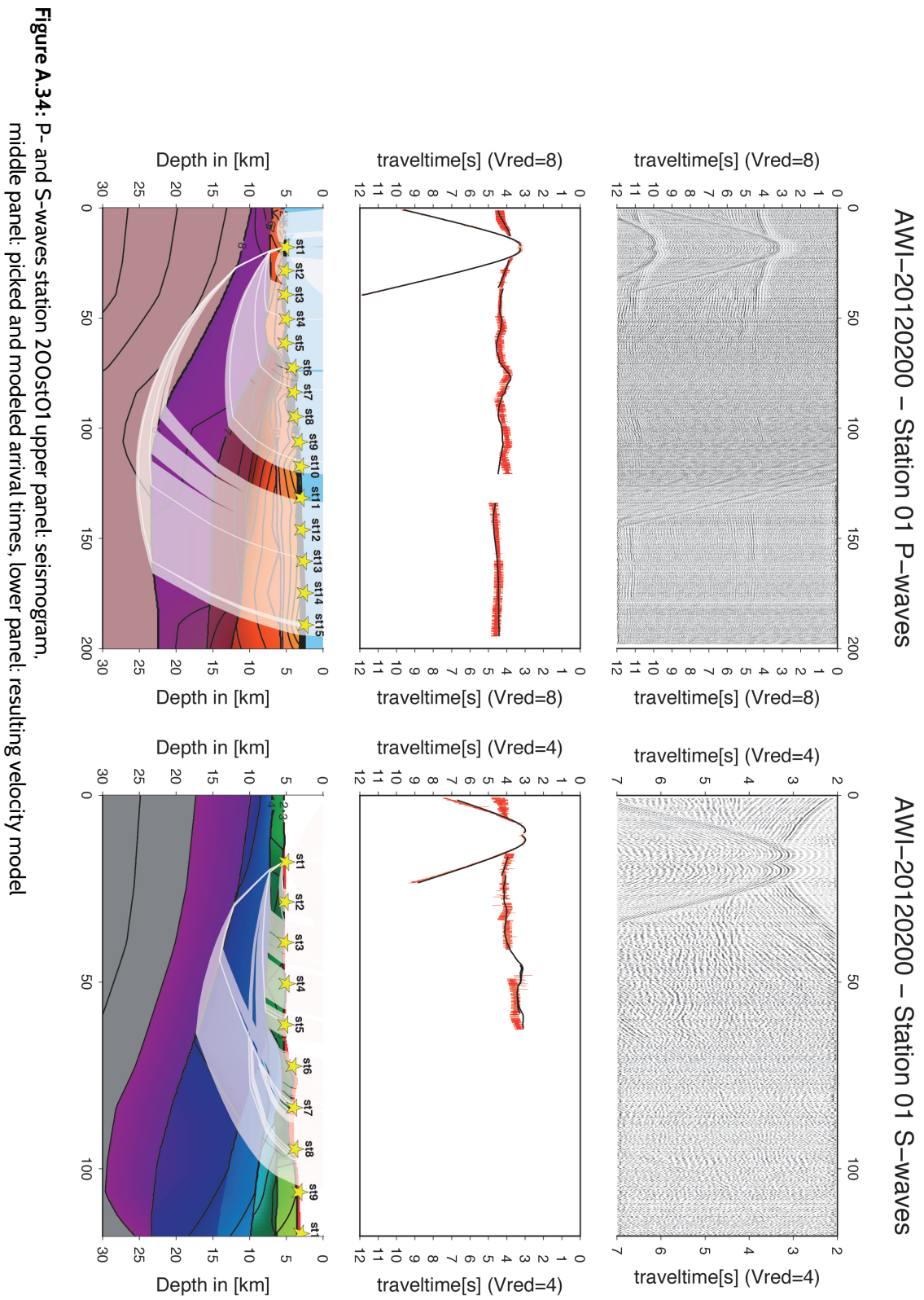
**Figure A.32:** P- and S-waves station 100st34 upper panel: seismogram, middle panel: picked and modeled arrival times, lower panel: resulting velocity model

#### A.4 OBS/OBH stations of AWI-20120200



**Figure A.33:** Bathymetric map of AWI-20120200 across the High Plateau of the Manihiki Plateau, yellow stars indicate stations, which provided P- and S-wave data, black stars indicate stations, which did not return any data, yellow and black striped stars indicate stations, which only returned usable P-wave data





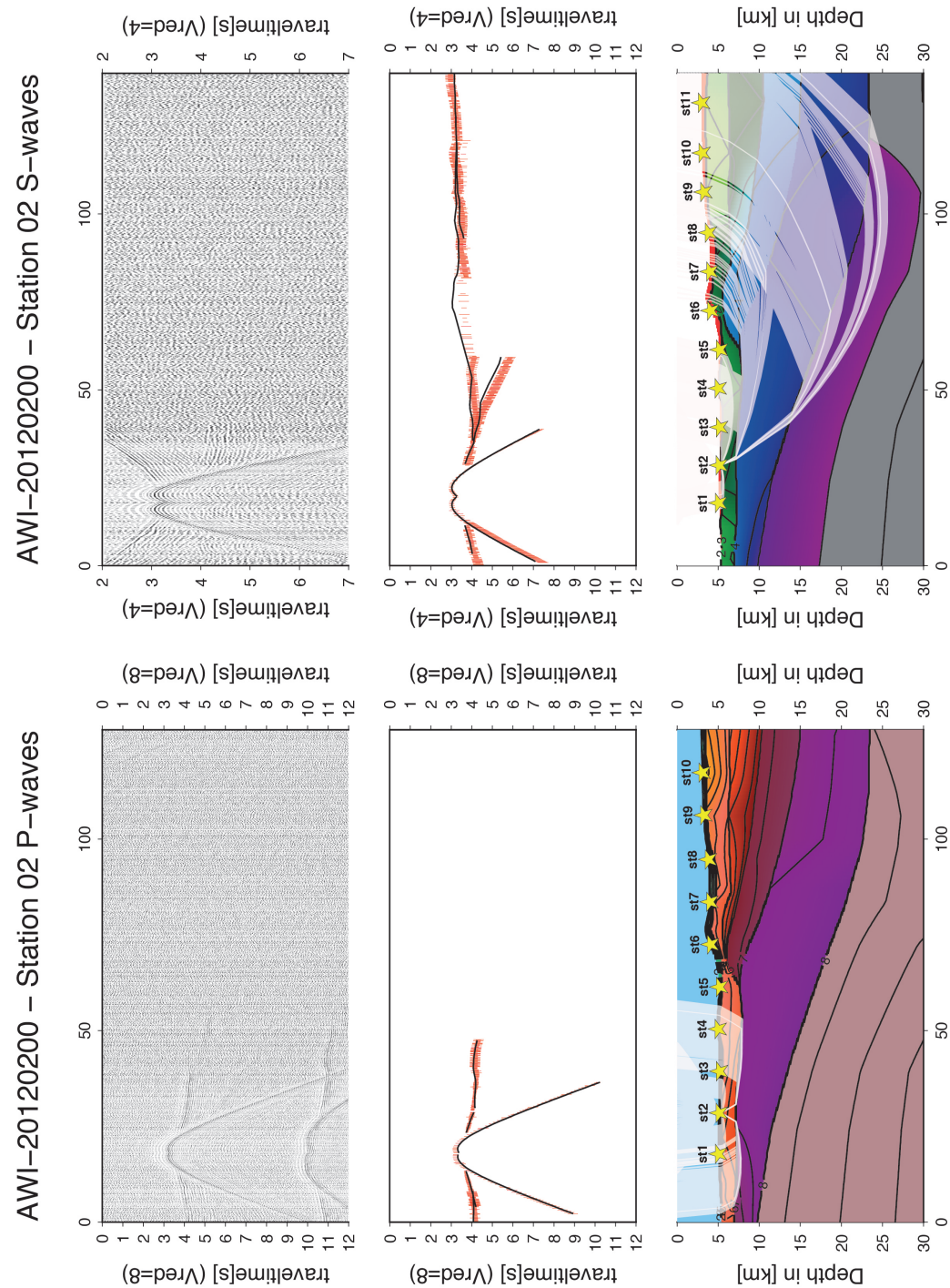


Figure A.35: P- and S-waves station 200st02 upper panel: seismogram, middle panel: picked and modeled arrival times, lower panel: resulting velocity model

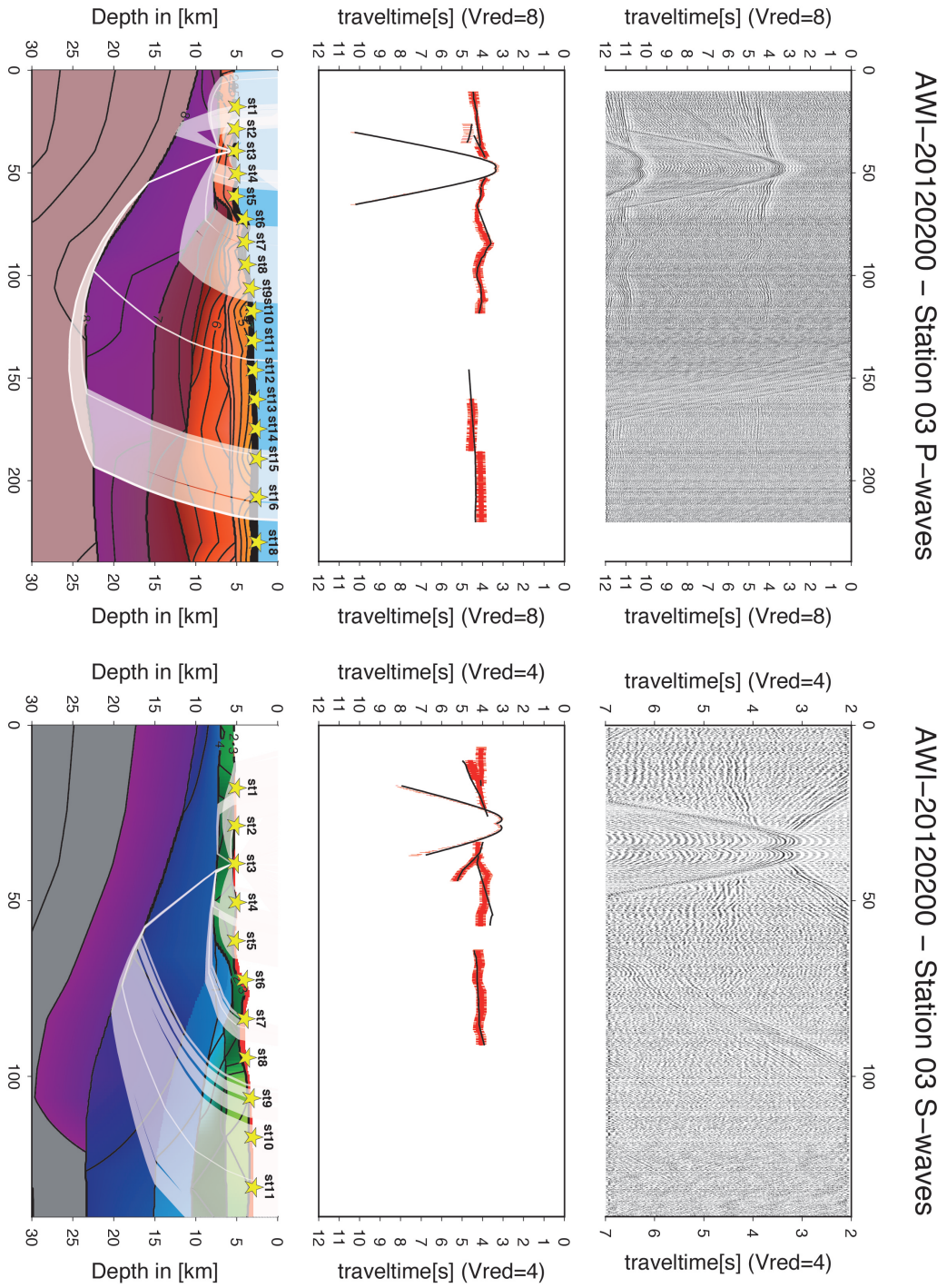


Figure A.36: P- and S-waves station 200st03 upper panel: seismogram, middle panel: picked and modeled arrival times, lower panel: resulting velocity model



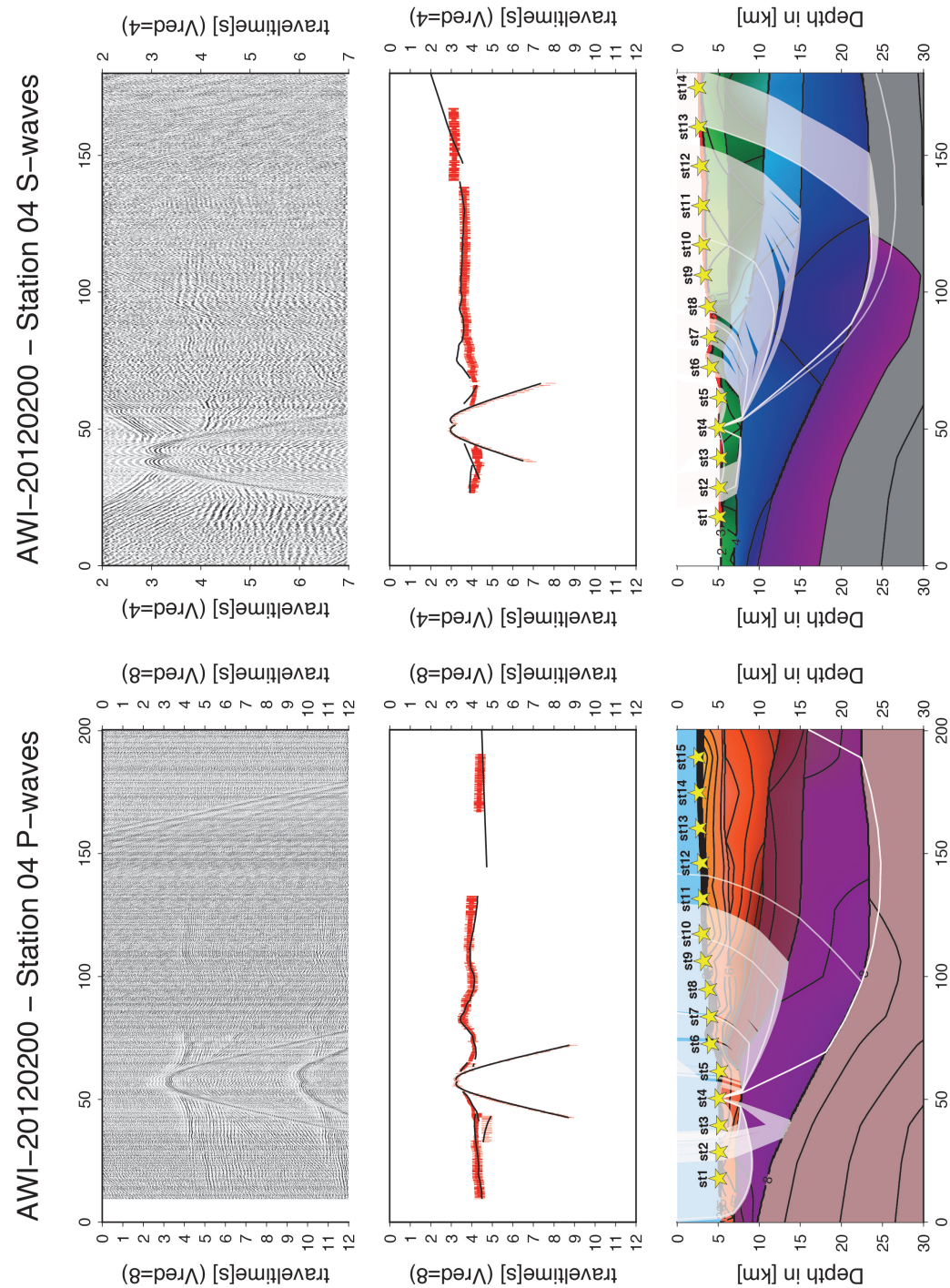
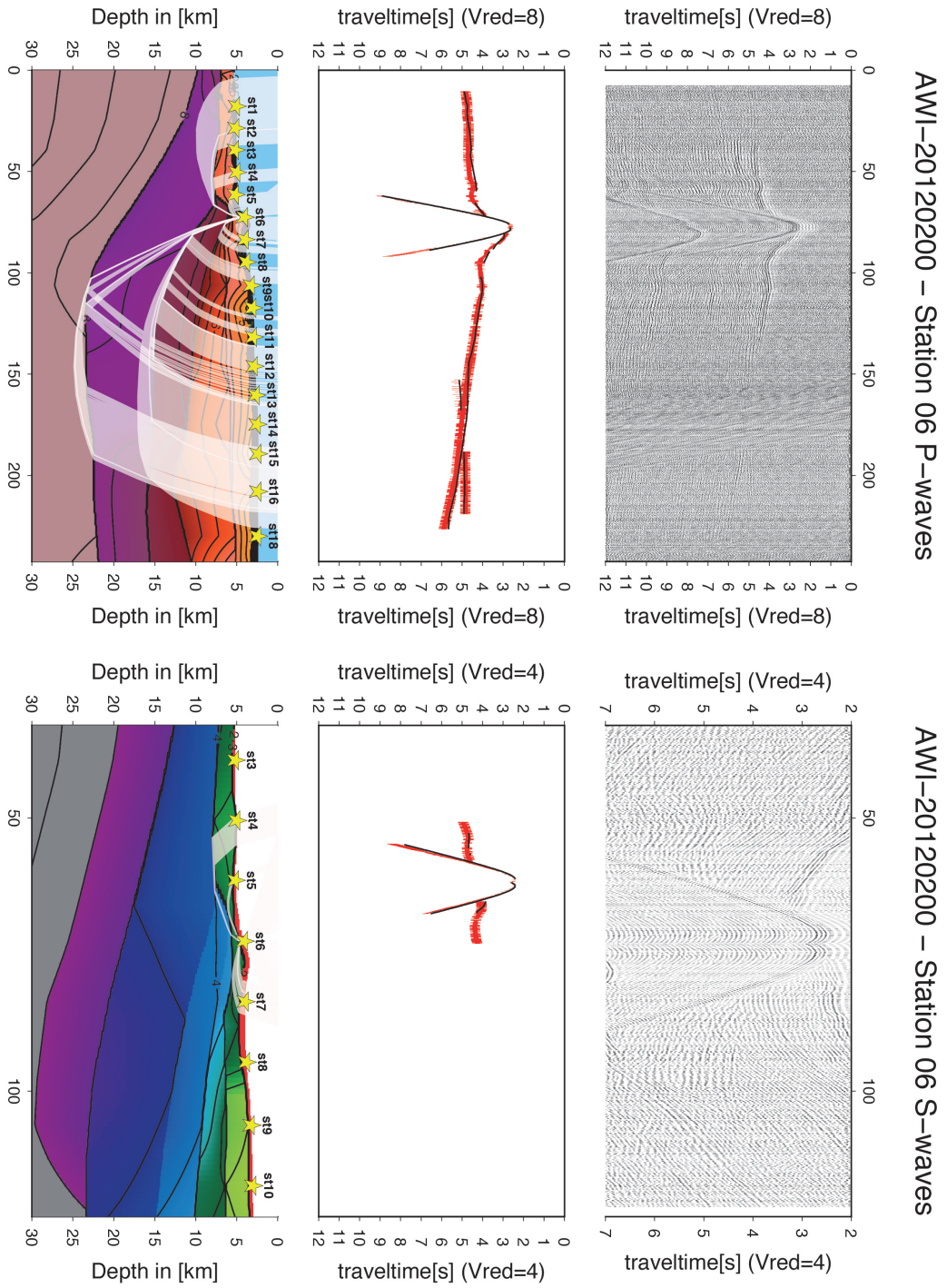


Figure A.37: P- and S-waves station 200st04 upper panel: seismogram, middle panel: picked and modeled arrival times, lower panel: resulting velocity model



**Figure A.38:** P- and S-waves station 200st06 upper panel: seismogram, middle panel: picked and modeled arrival times, lower panel: resulting velocity model

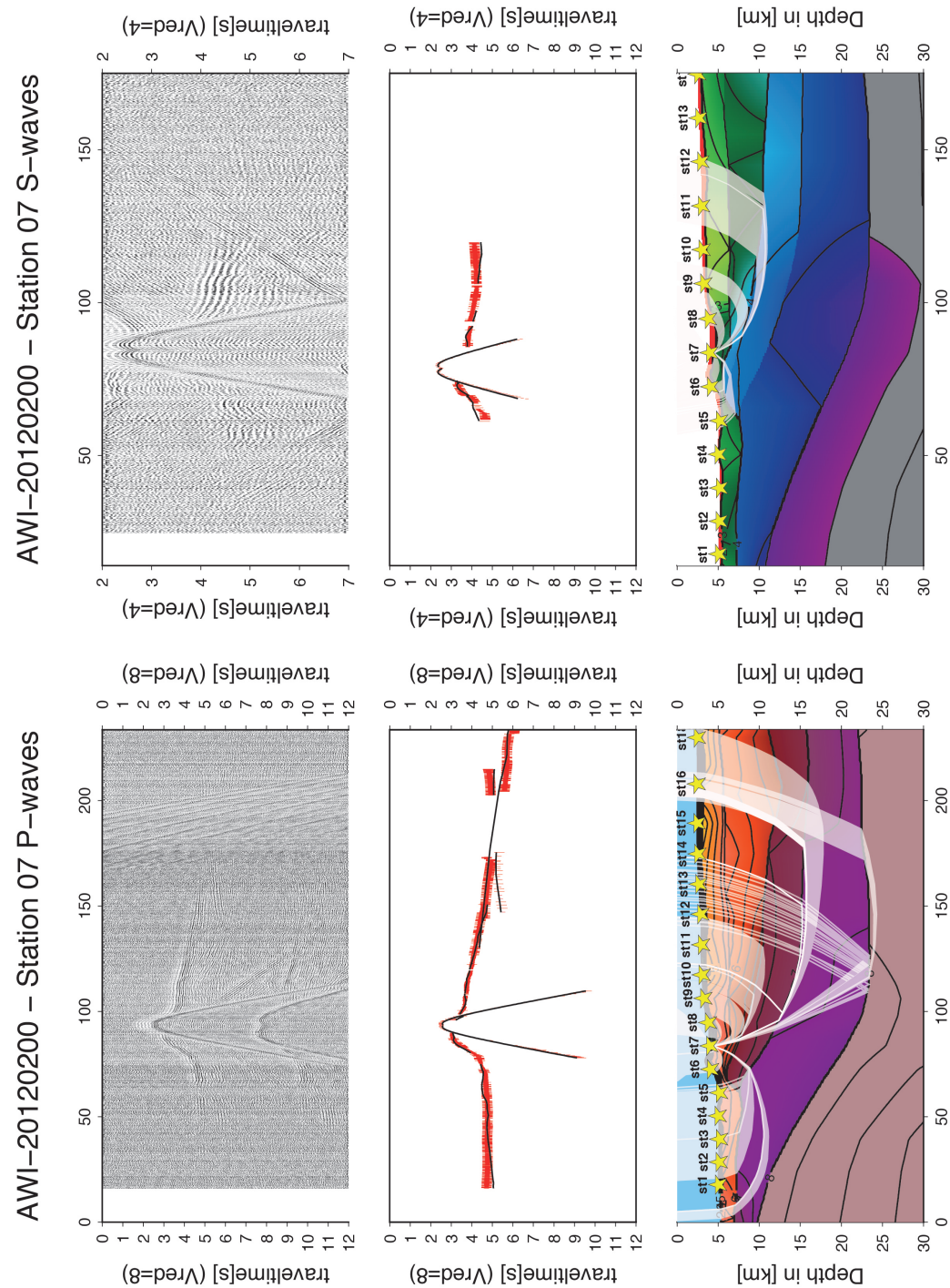


Figure A.39: P- and S-waves station 200st07 upper panel: seismogram, middle panel: picked and modeled arrival times, lower panel: resulting velocity model



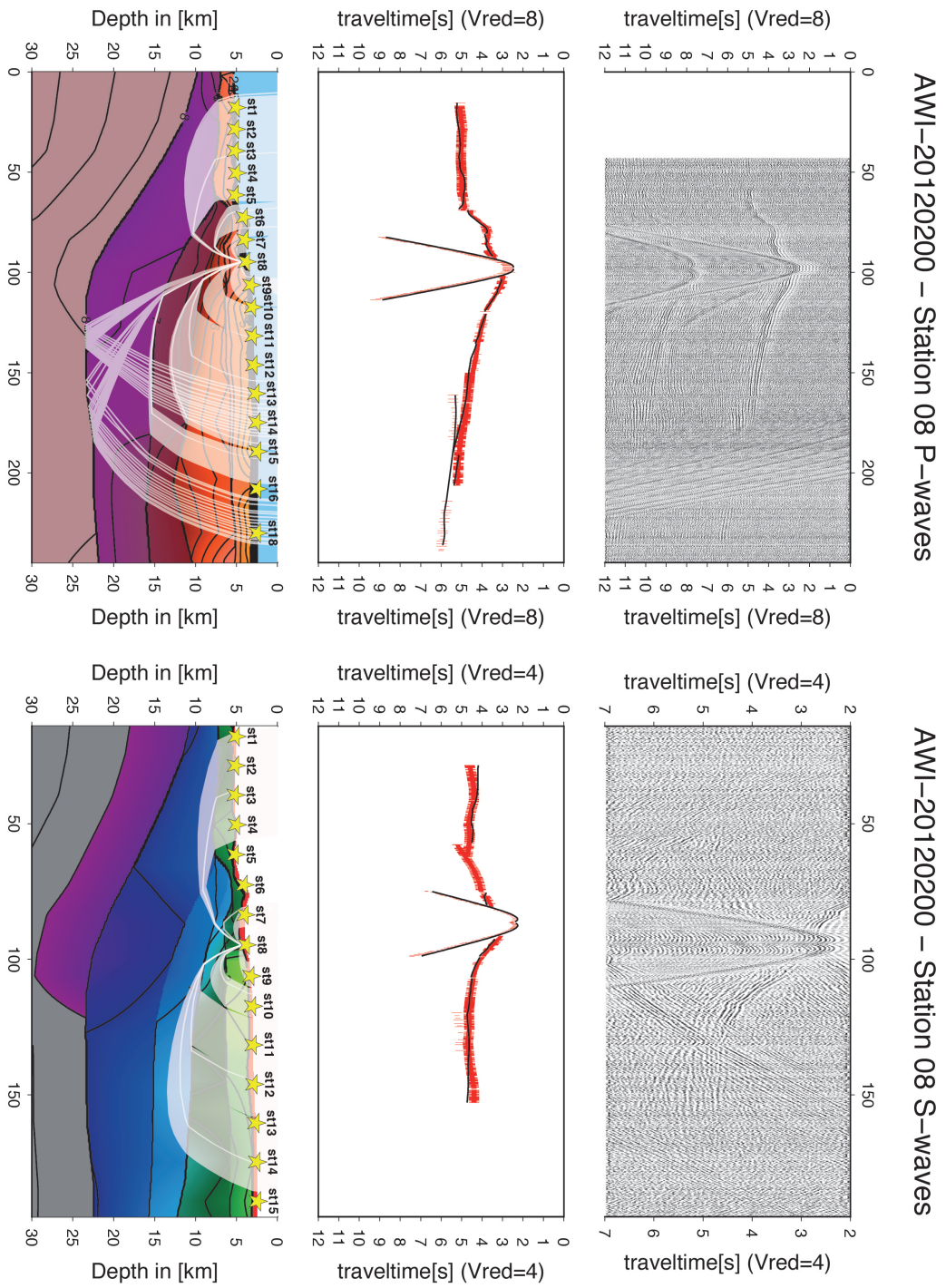
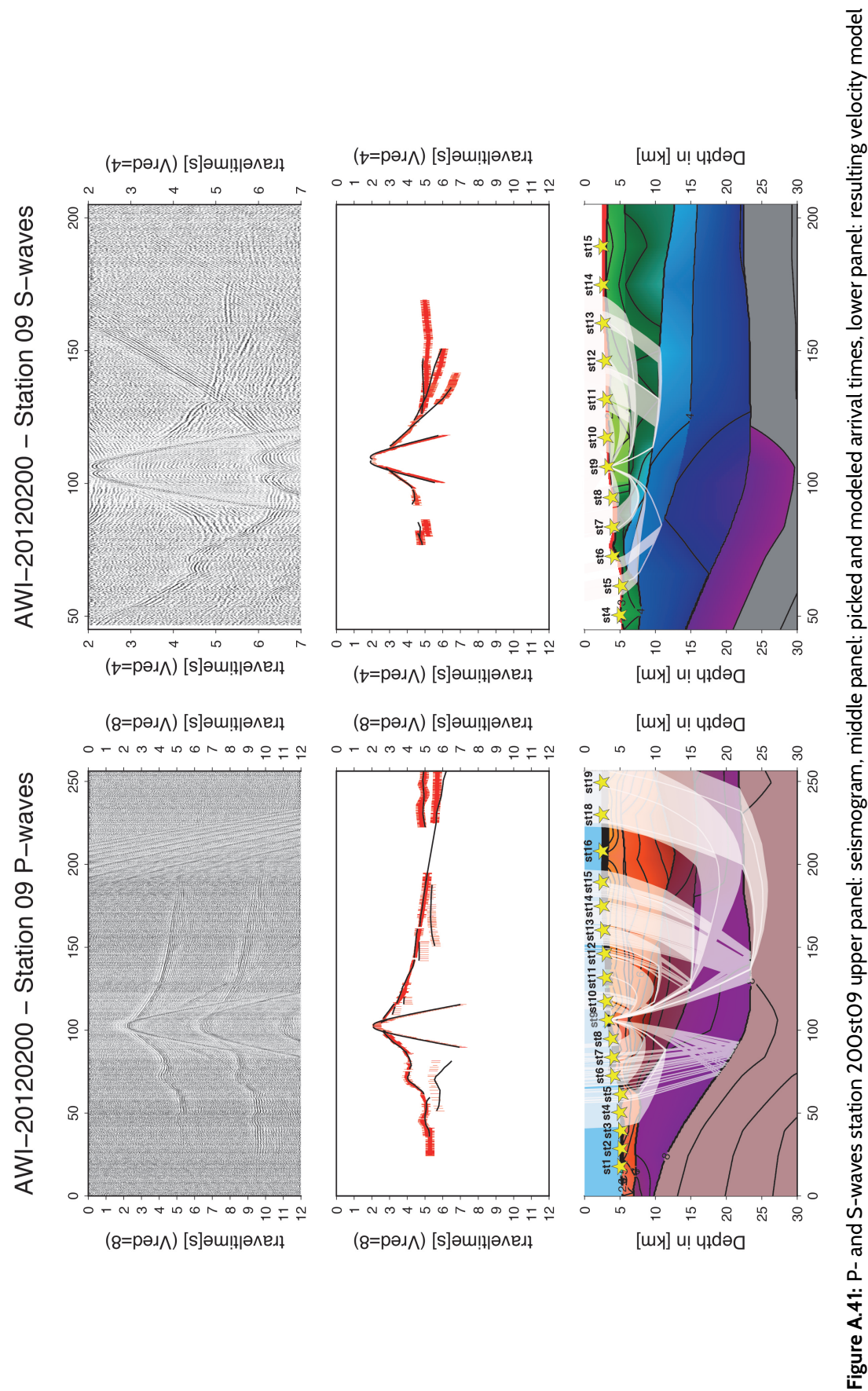
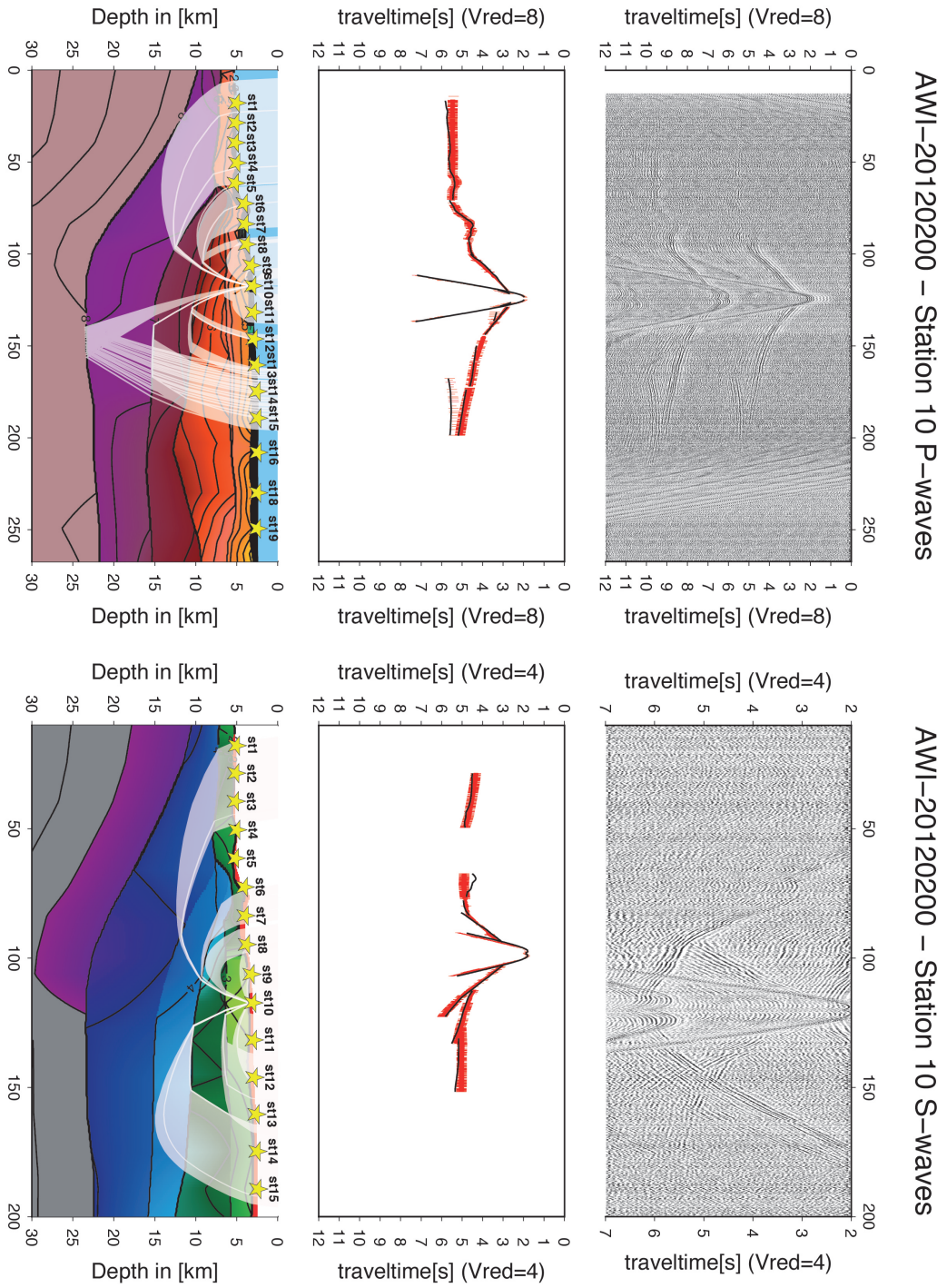


Figure A.40: P- and S-waves station 200st08 upper panel: seismogram, middle panel: picked and modeled arrival times, lower panel: resulting velocity model







**Figure A.42:** P- and S-waves station 200st10 upper panel: seismogram, middle panel: picked and modeled arrival times, lower panel: resulting velocity model

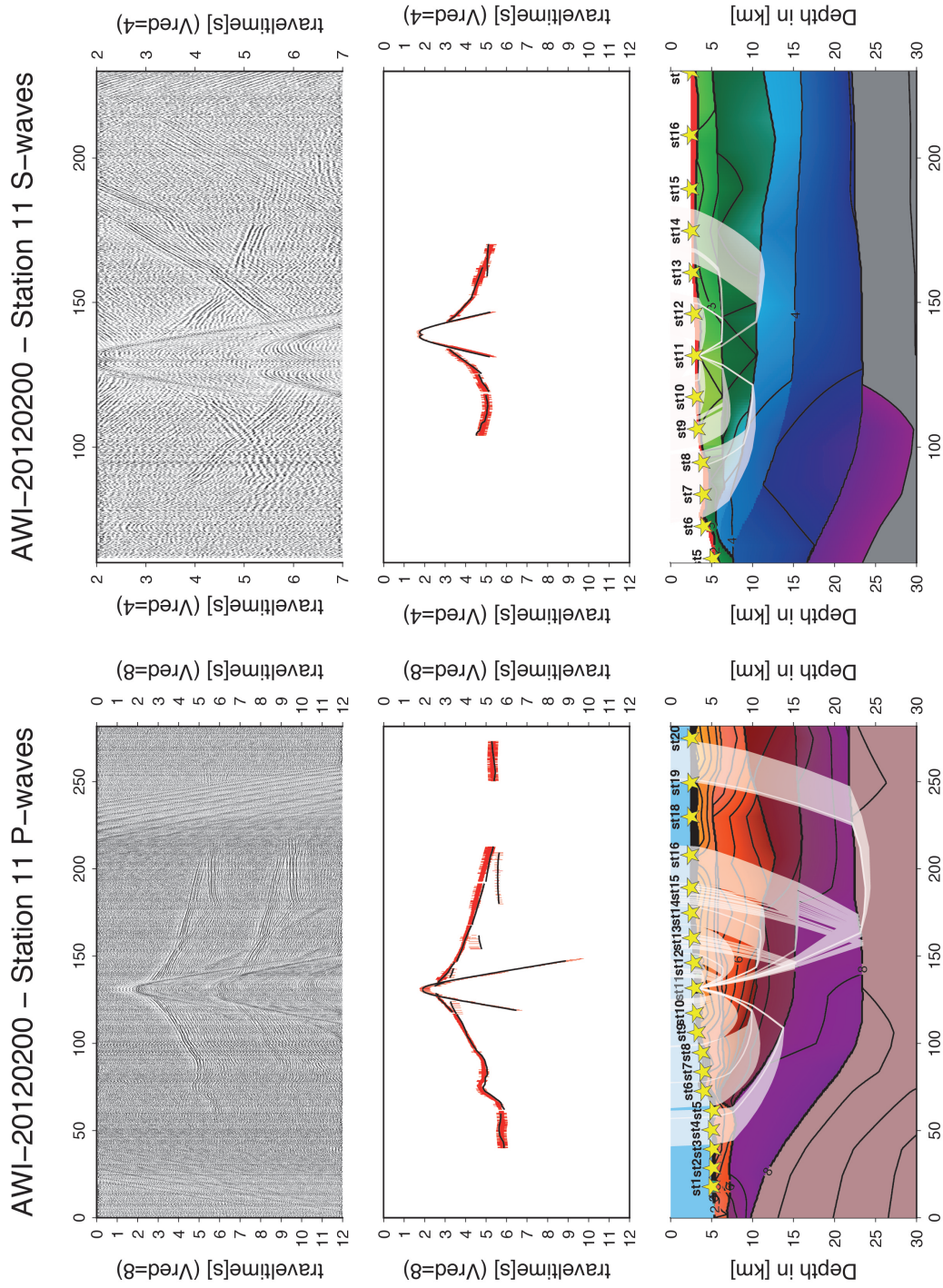


Figure A.43: P- and S-waves station 200st11 upper panel: seismogram, middle panel: picked and modeled arrival times, lower panel: resulting velocity model



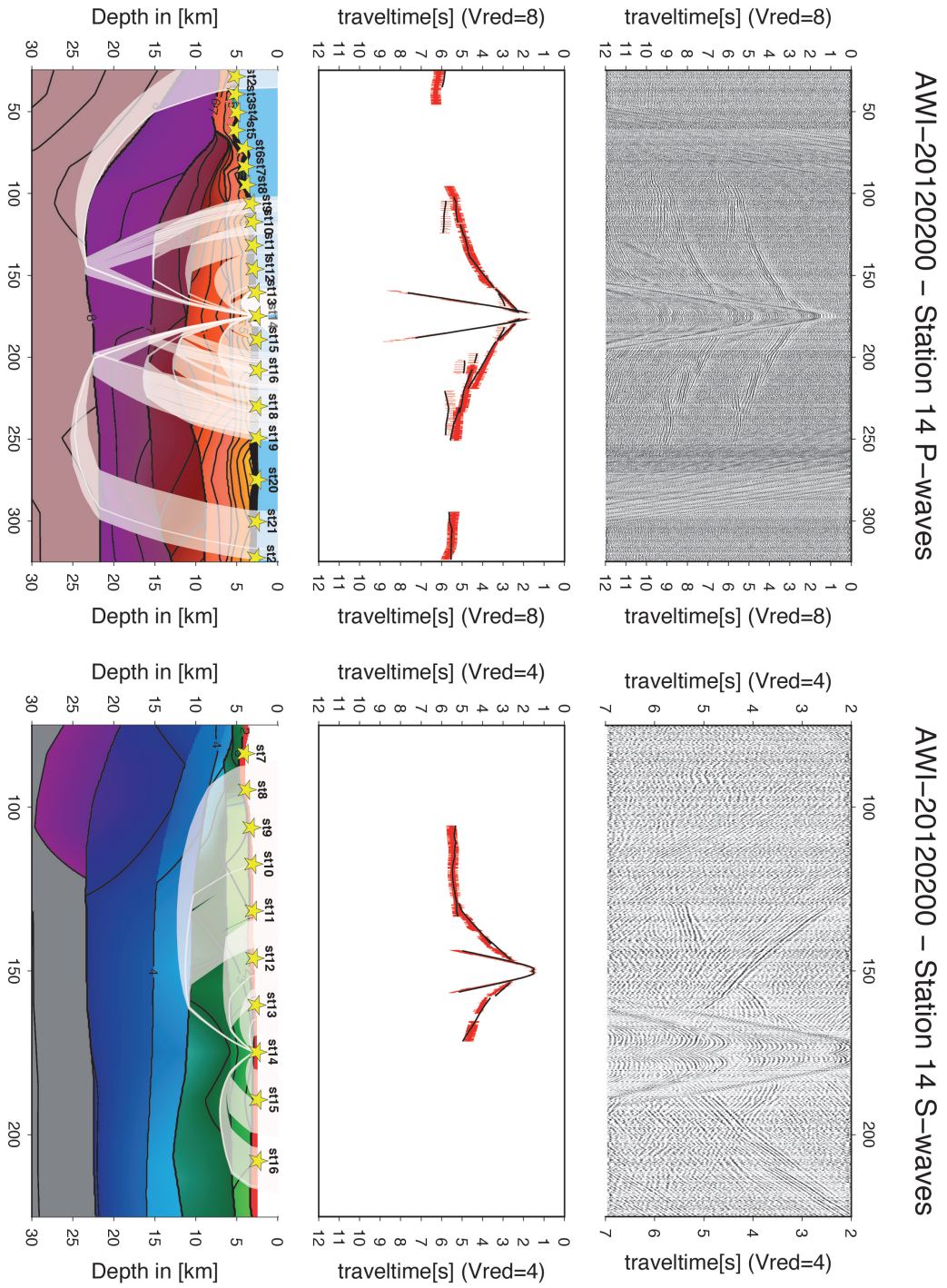


Figure A.44: P- and S-waves station 200st14 upper panel: seismogram, middle panel: picked and modeled arrival times, lower panel: resulting velocity model

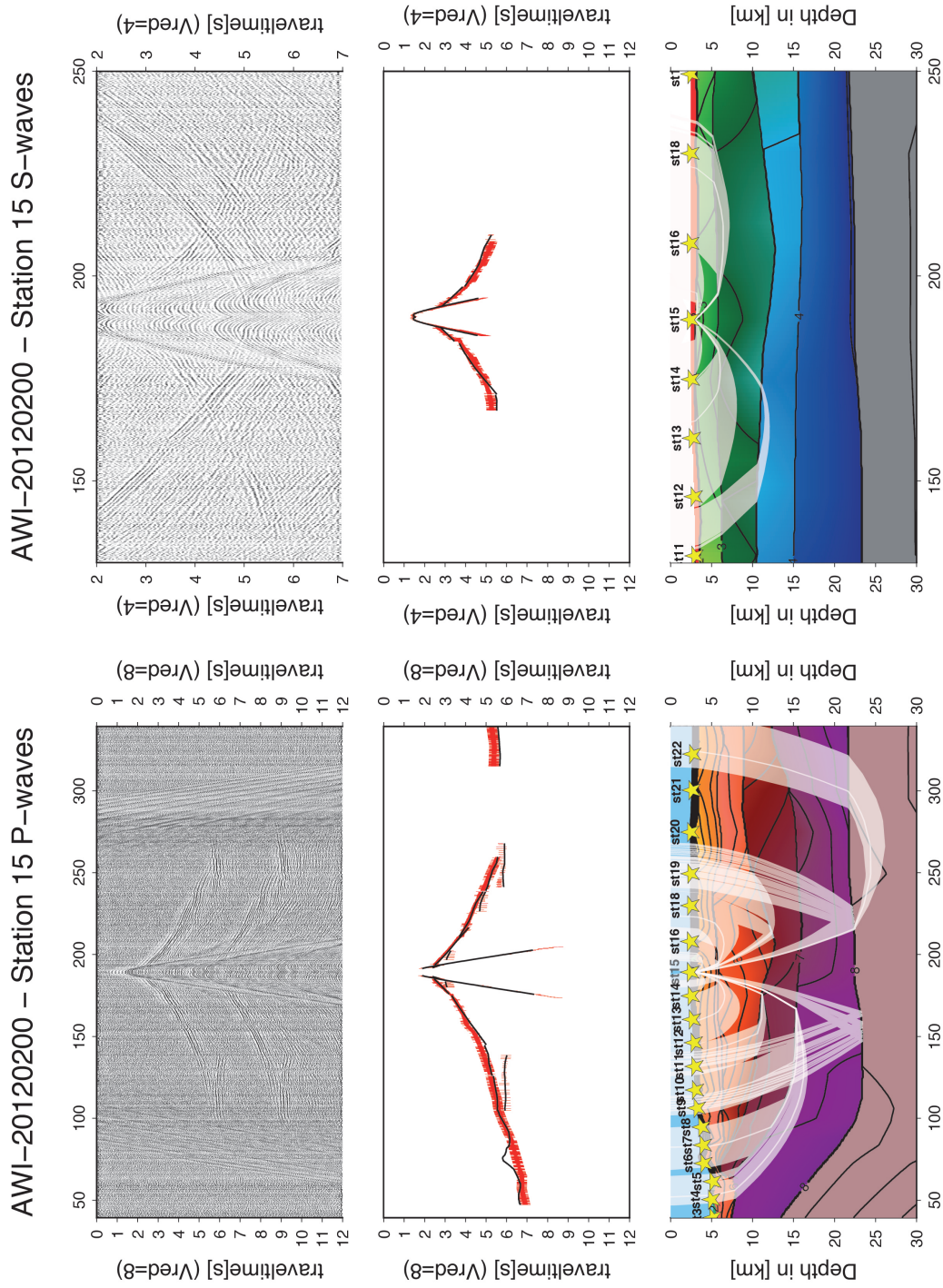
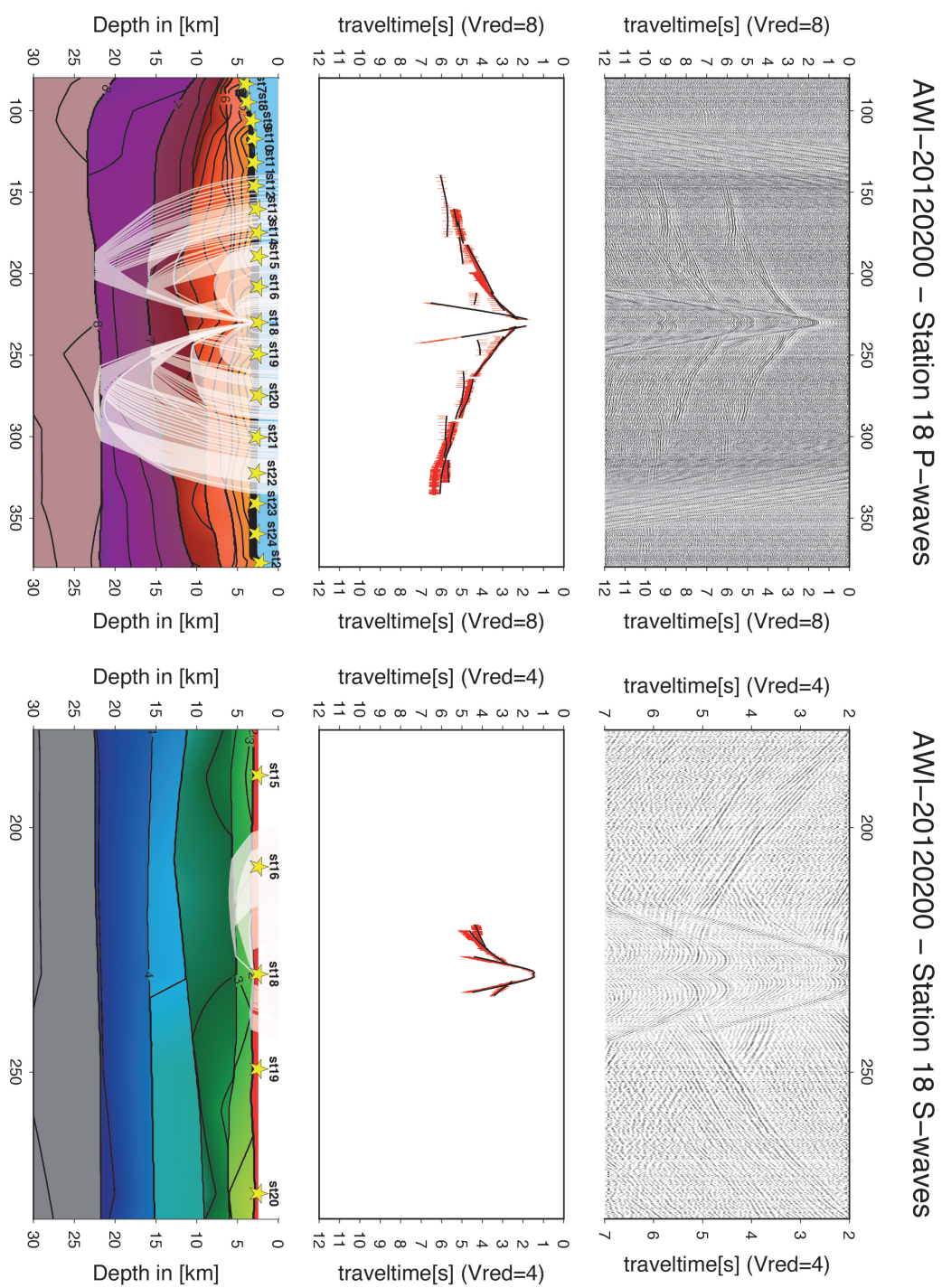


Figure A.45: P- and S-wave station 200st15 upper panel: seismogram, middle panel: picked and modeled arrival times, lower panel: resulting velocity model





**Figure A.46:** P- and S-waves station 20Ost8 upper panel: seismogram, middle panel: picked and modeled arrival times, lower panel: resulting velocity model

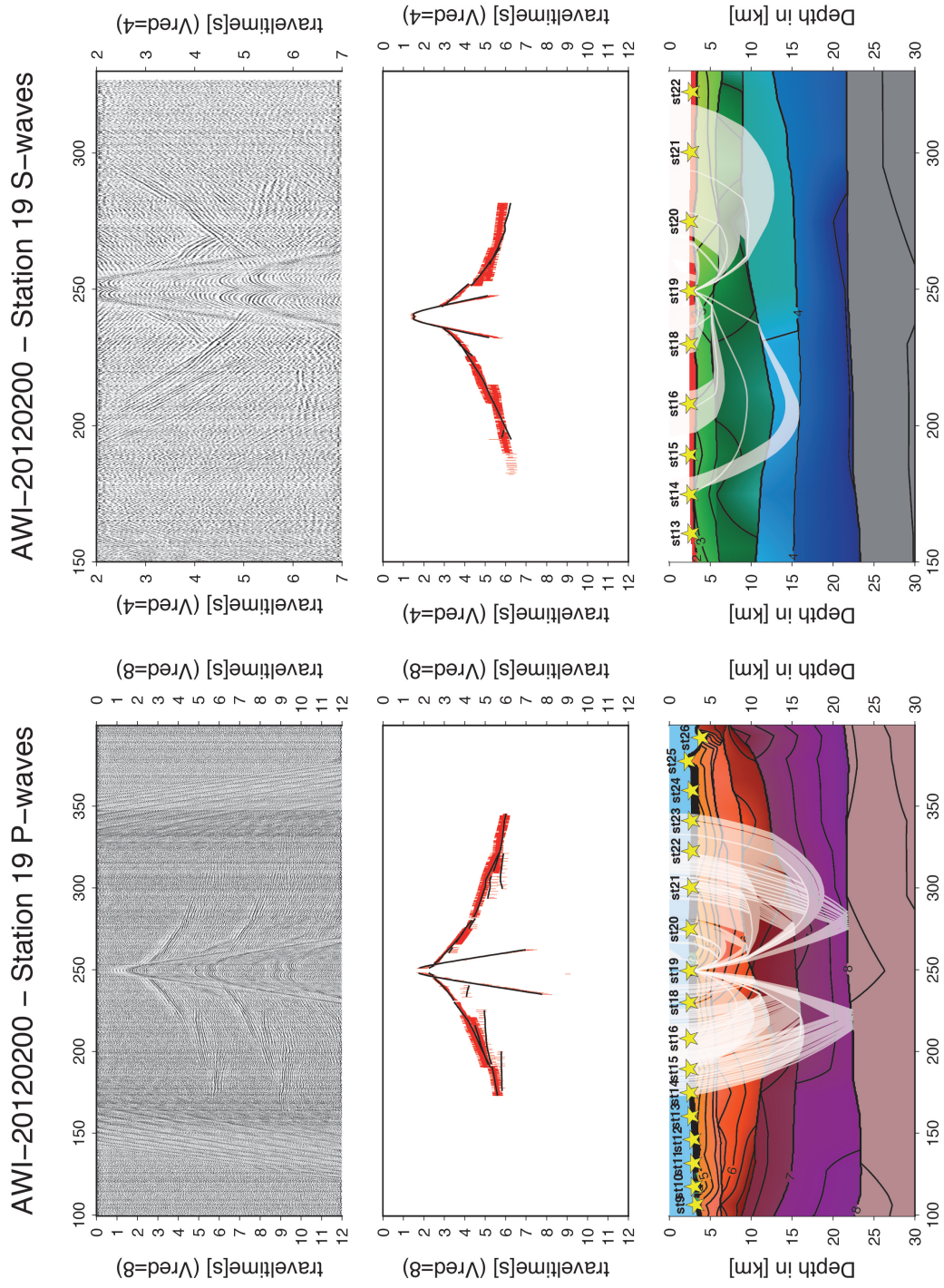
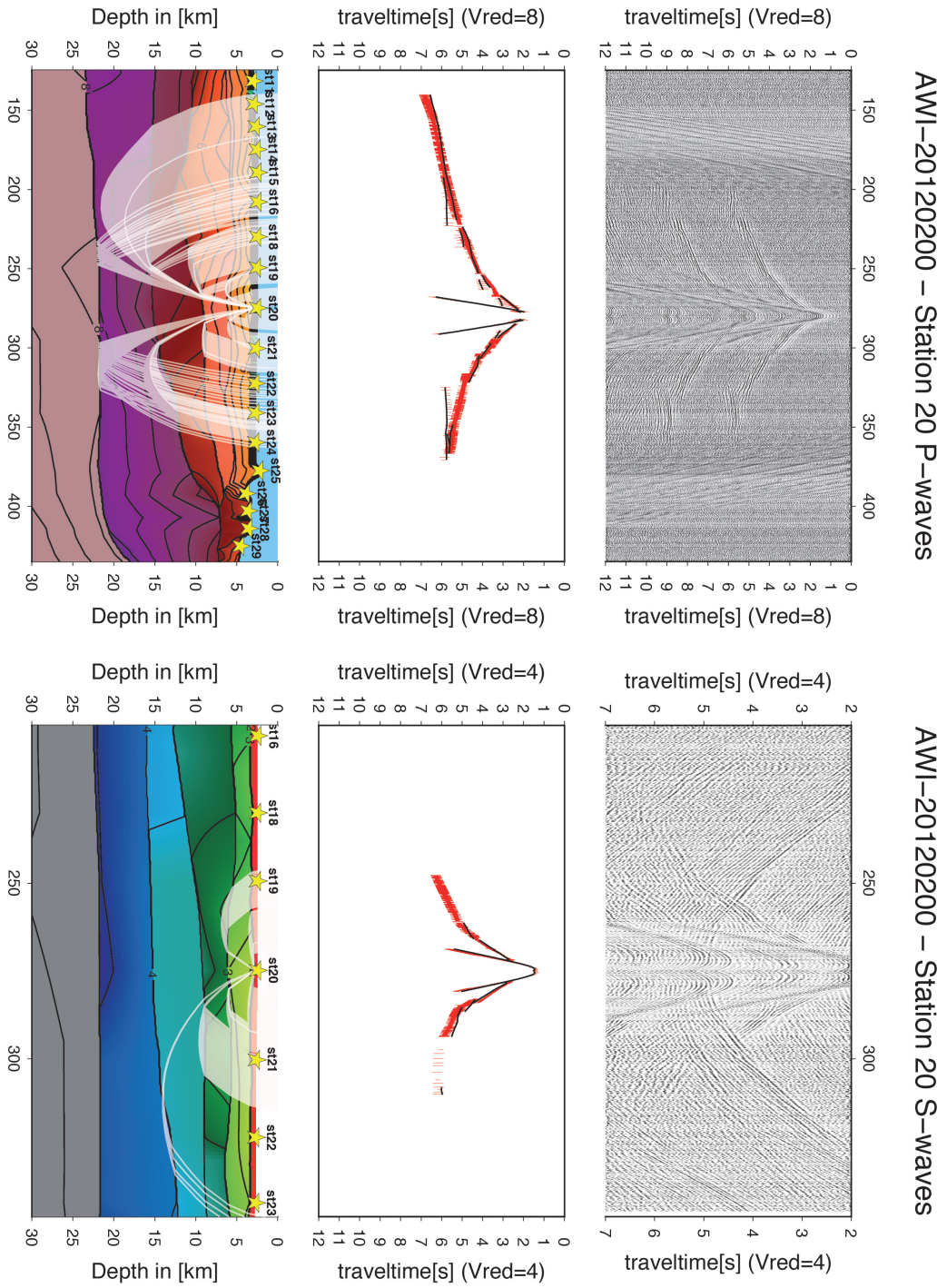


Figure A.47: P- and S-waves station 200st19 upper panel: seismogram, middle panel: picked and modeled arrival times, lower panel: resulting velocity model





**Figure A.48:** P- and S-waves station 200st20 upper panel: seismogram, middle panel: picked and modeled arrival times, lower panel: resulting velocity model

### AWI-20120200 – Station 21 P-waves

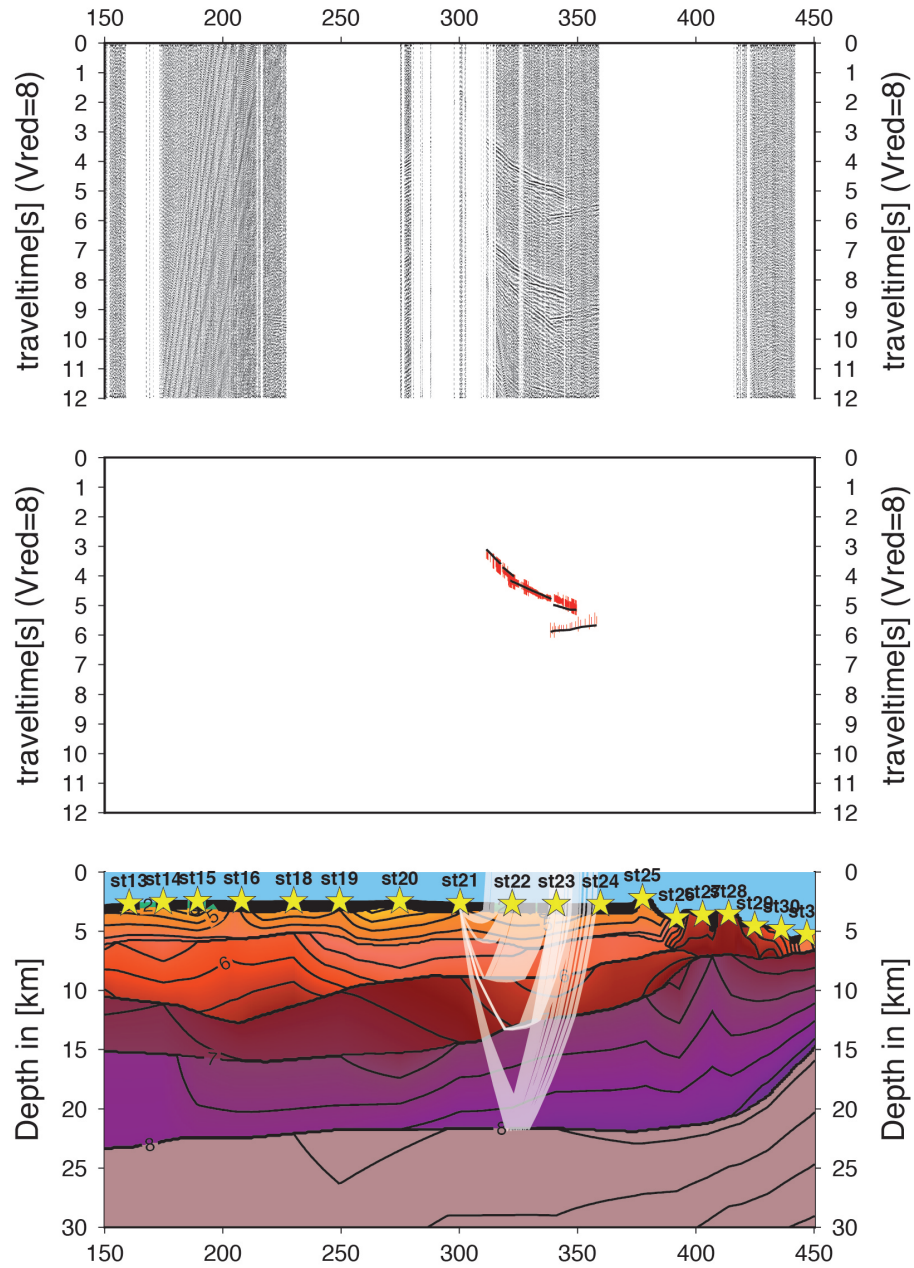


**Figure A.49:** P-waves station 200st21 upper panel: seismogram, middle panel: picked and modeled arrival times, lower panel: resulting velocity model

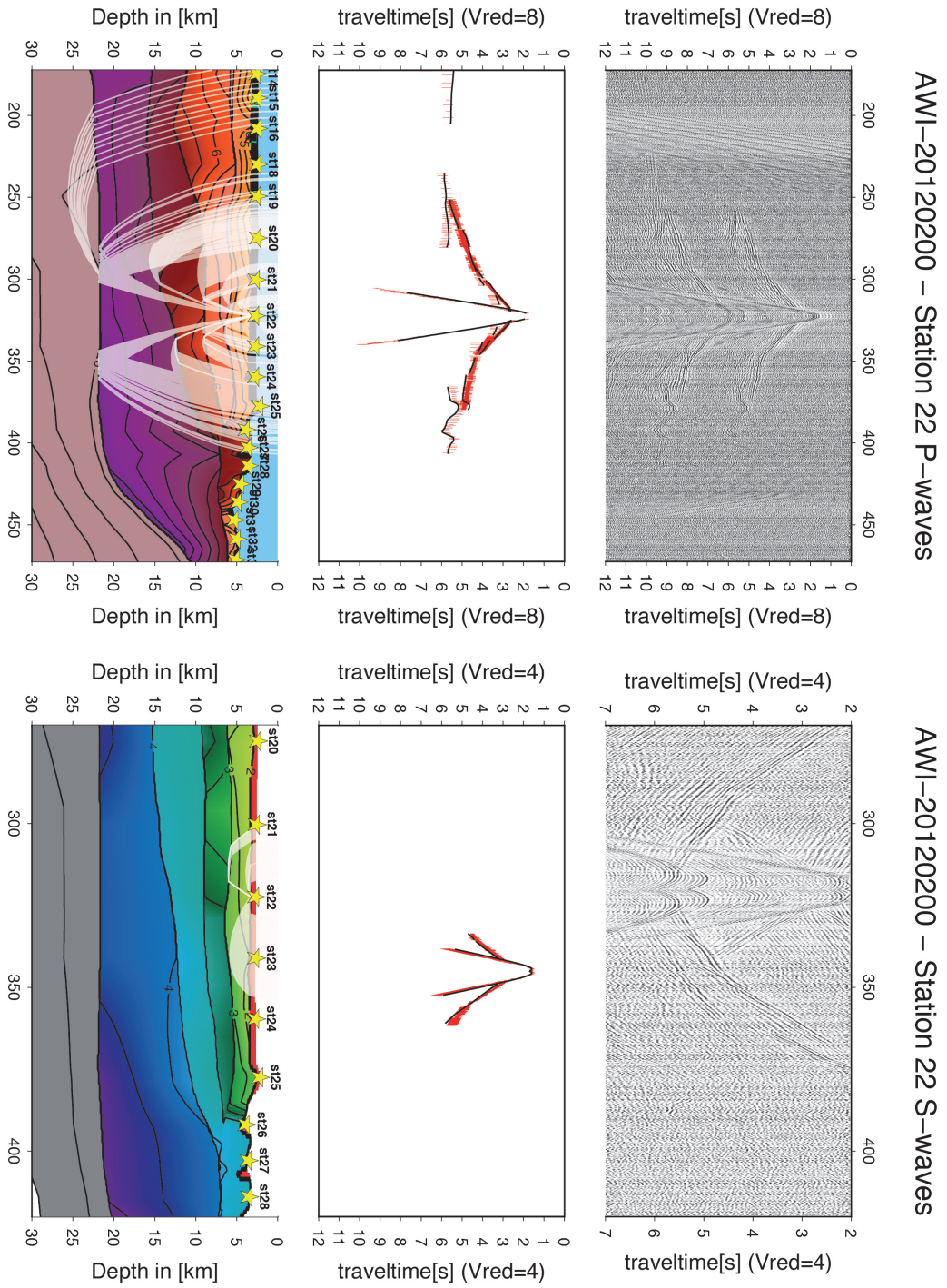


**Figure A.50:** P- and S-waves station 200st22 upper panel: seismogram, middle panel: picked and modeled arrival times, lower panel: resulting velocity model



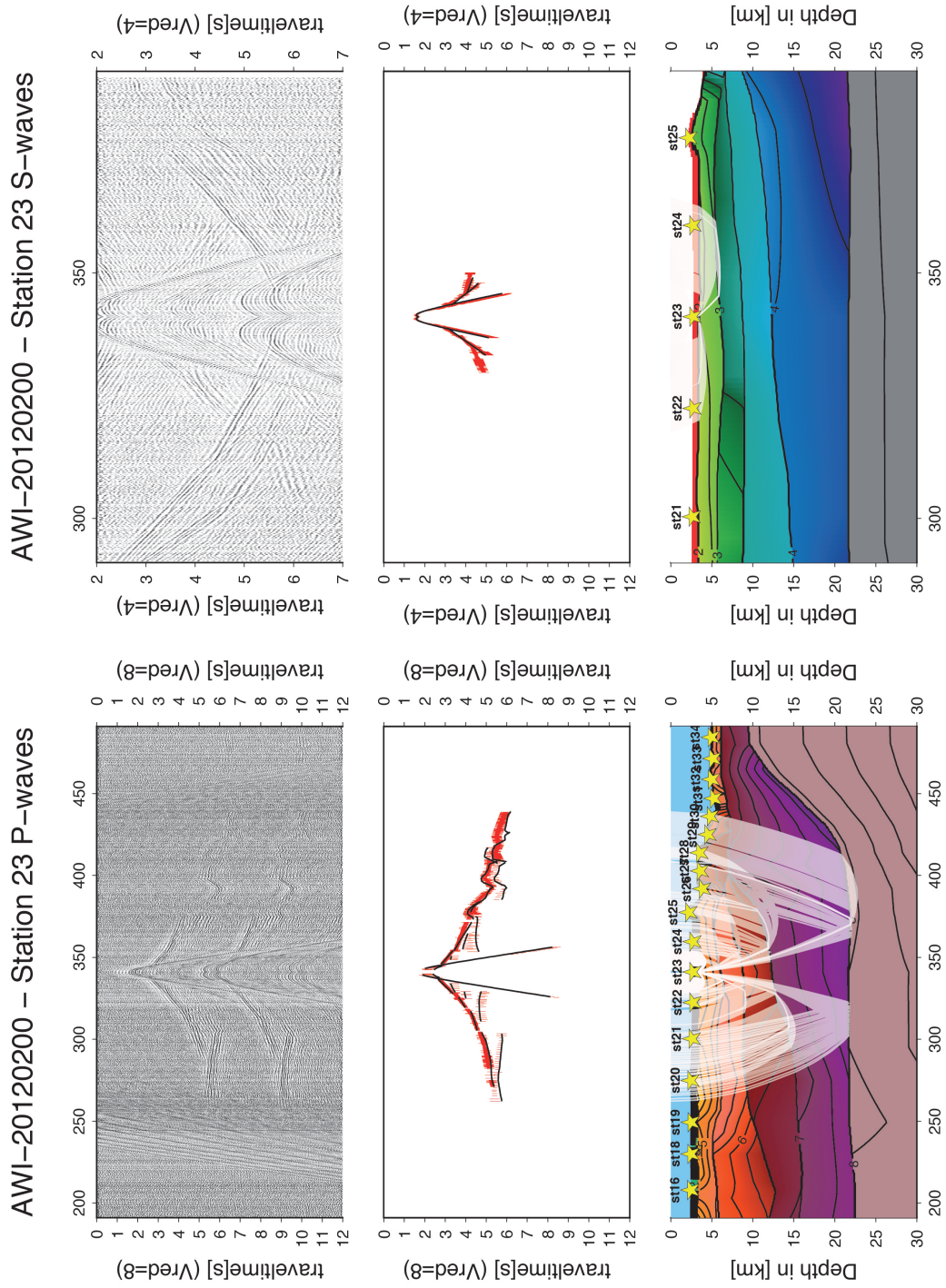


Figure A.51: P- and S-waves station 200st23 upper panel: seismogram, middle panel: picked and modeled arrival times, lower panel: resulting velocity model



## AWI-20120200 – Station 25 P-waves

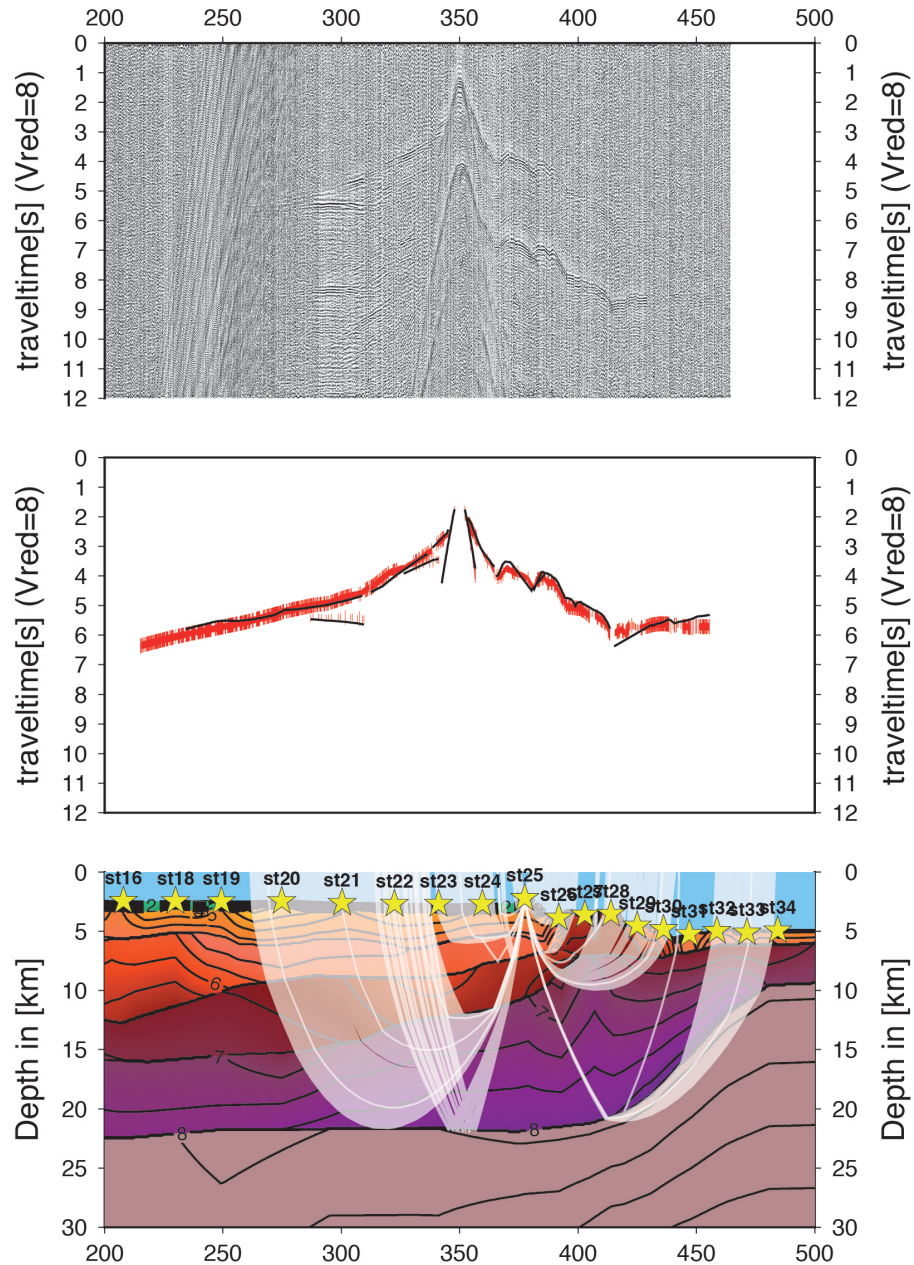


Figure A.52: P- waves station 200st25 upper panel: seismogram, middle panel: picked and modeled arrival times, lower panel: resulting velocity model

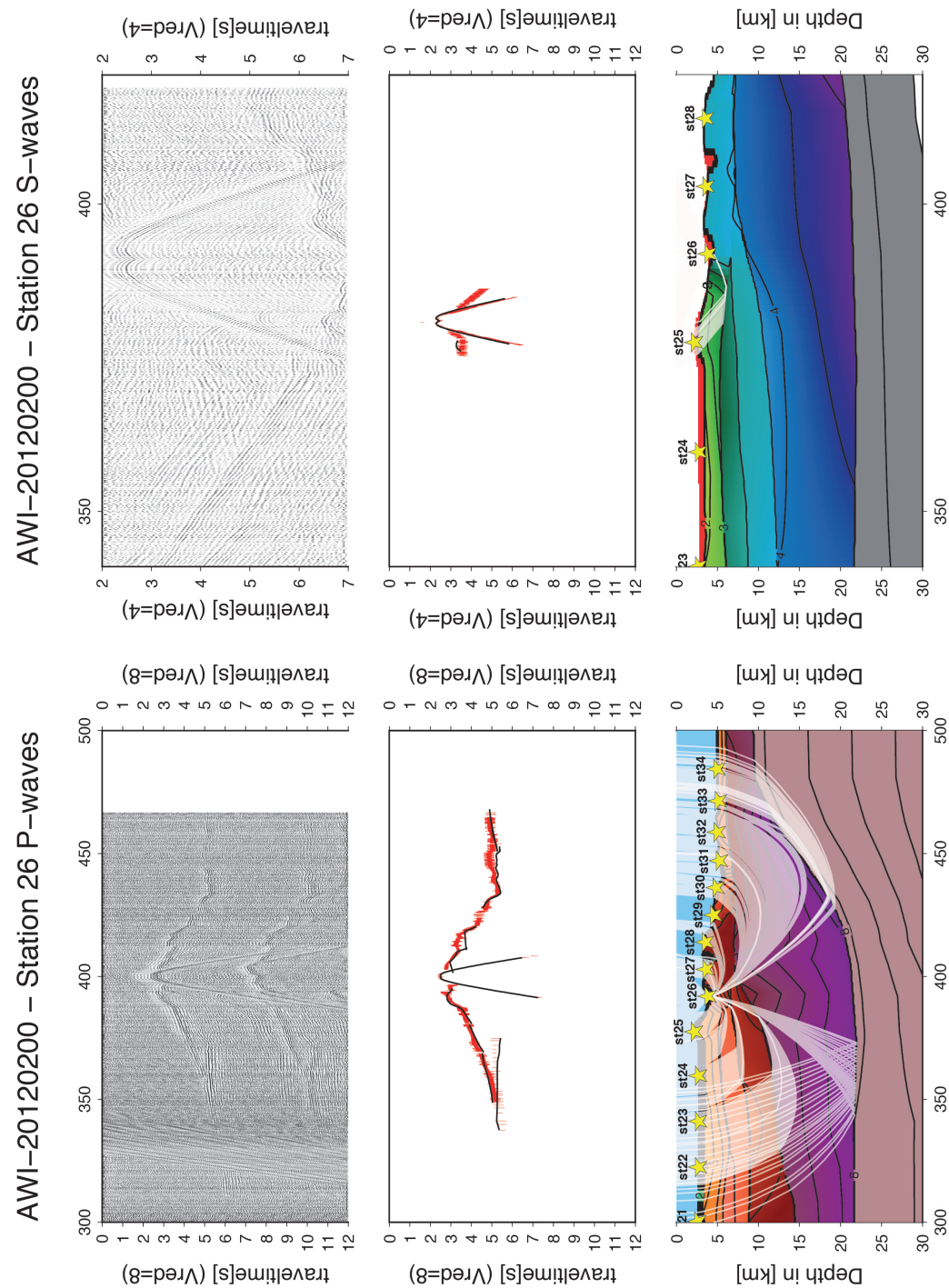


Figure A.53: P- and S-wave station 200st26 upper panel: seismogram, middle panel: picked and modeled arrival times, lower panel: resulting velocity model

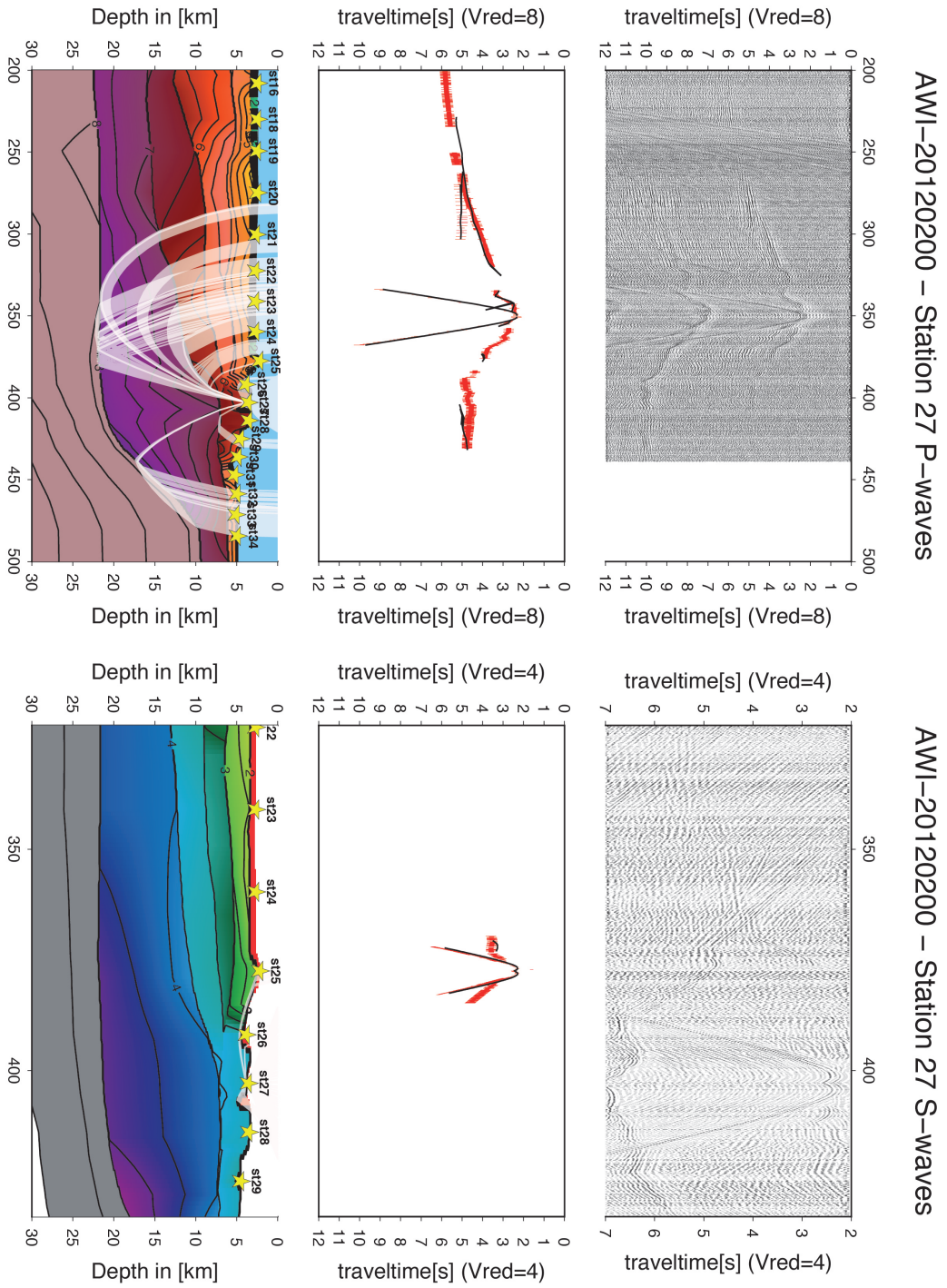


Figure A.54: P- and S-waves station 200st27 upper panel: seismogram, middle panel: picked and modeled arrival times, lower panel: resulting velocity model



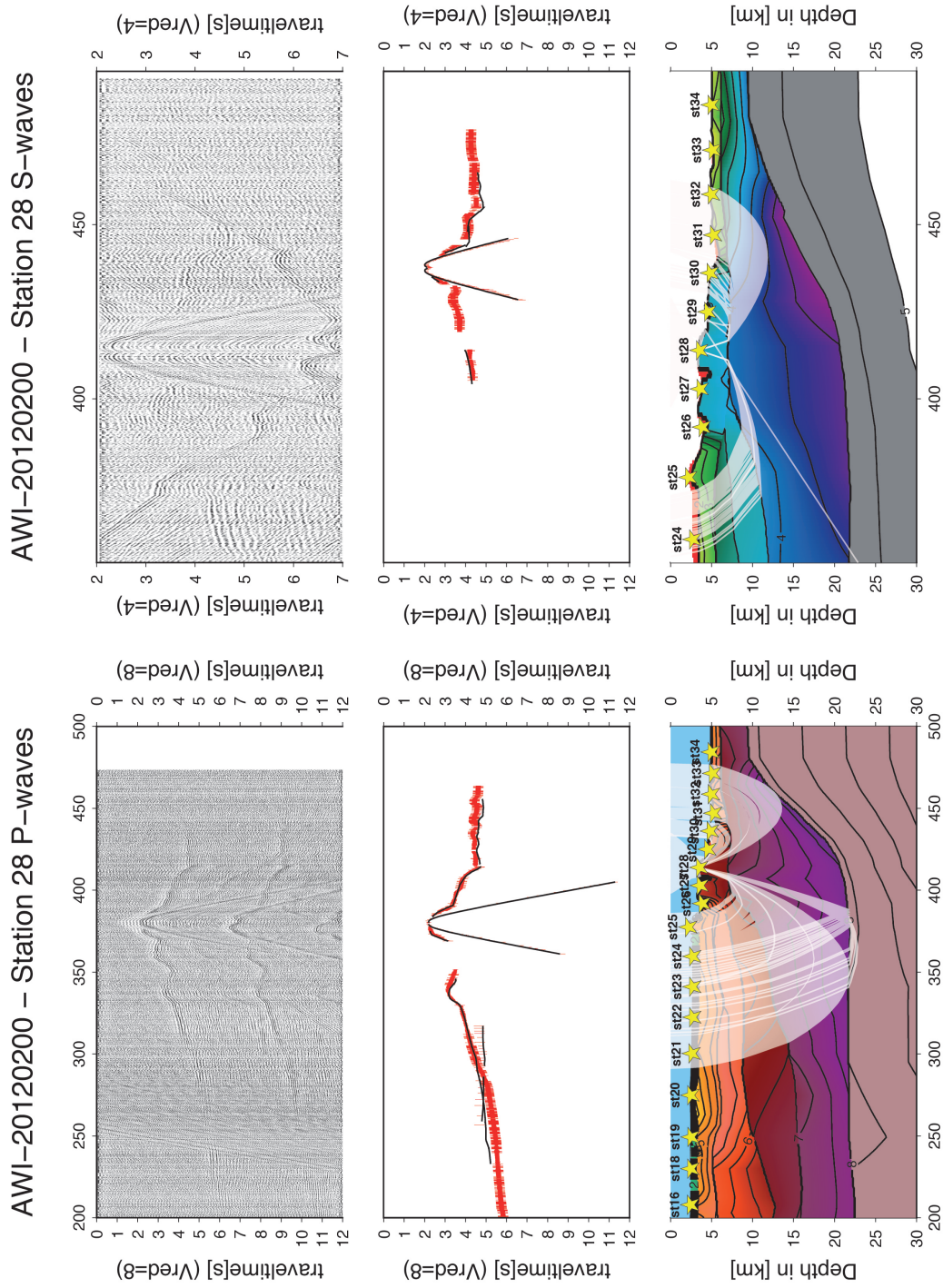


Figure A.55: P- and S-waves station 200st28 upper panel: seismogram, middle panel: picked and modeled arrival times, lower panel: resulting velocity model

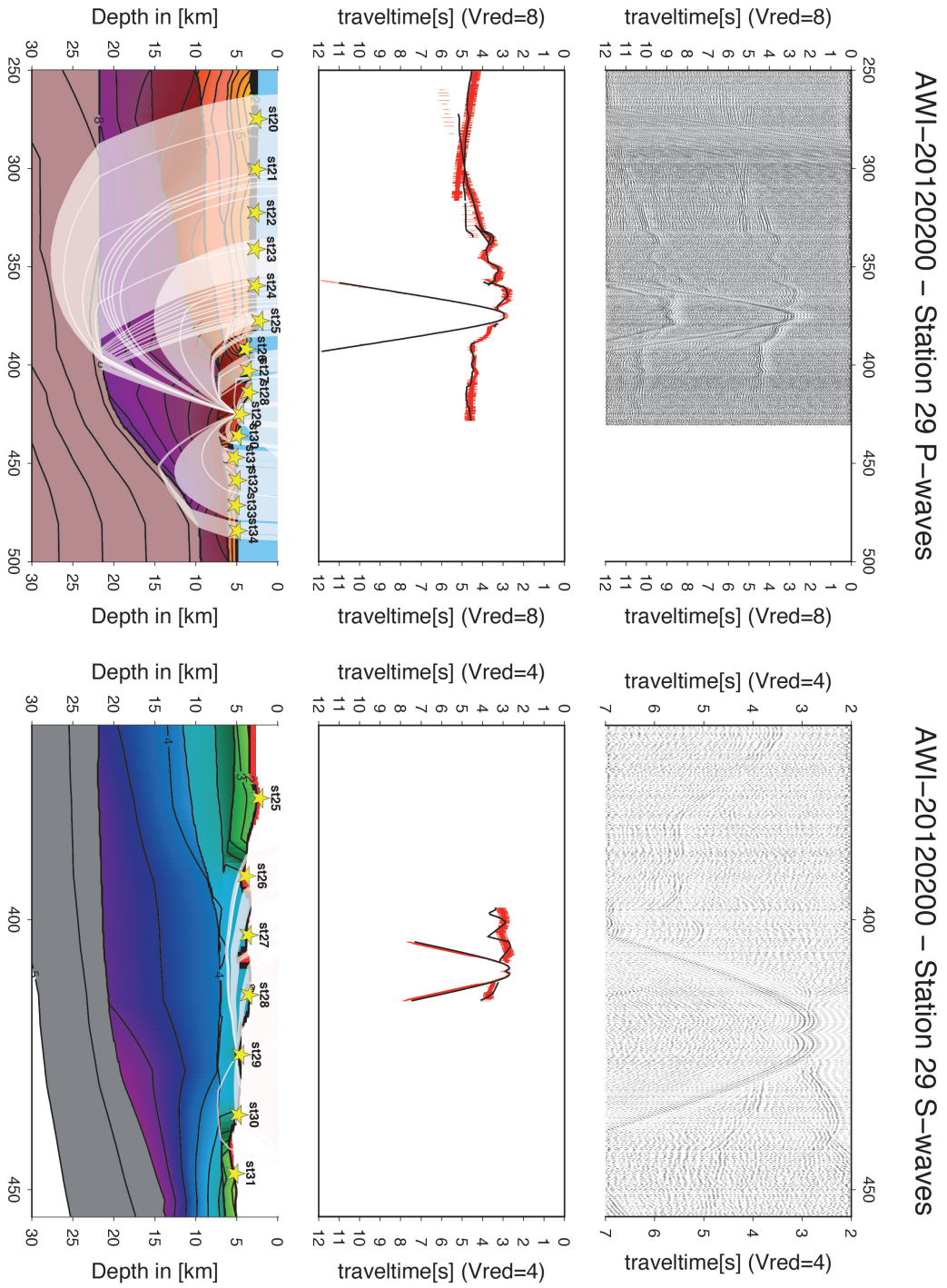


Figure A.56: P- and S-waves station 200st29 upper panel: seismogram, middle panel: picked and modeled arrival times, lower panel: resulting velocity model



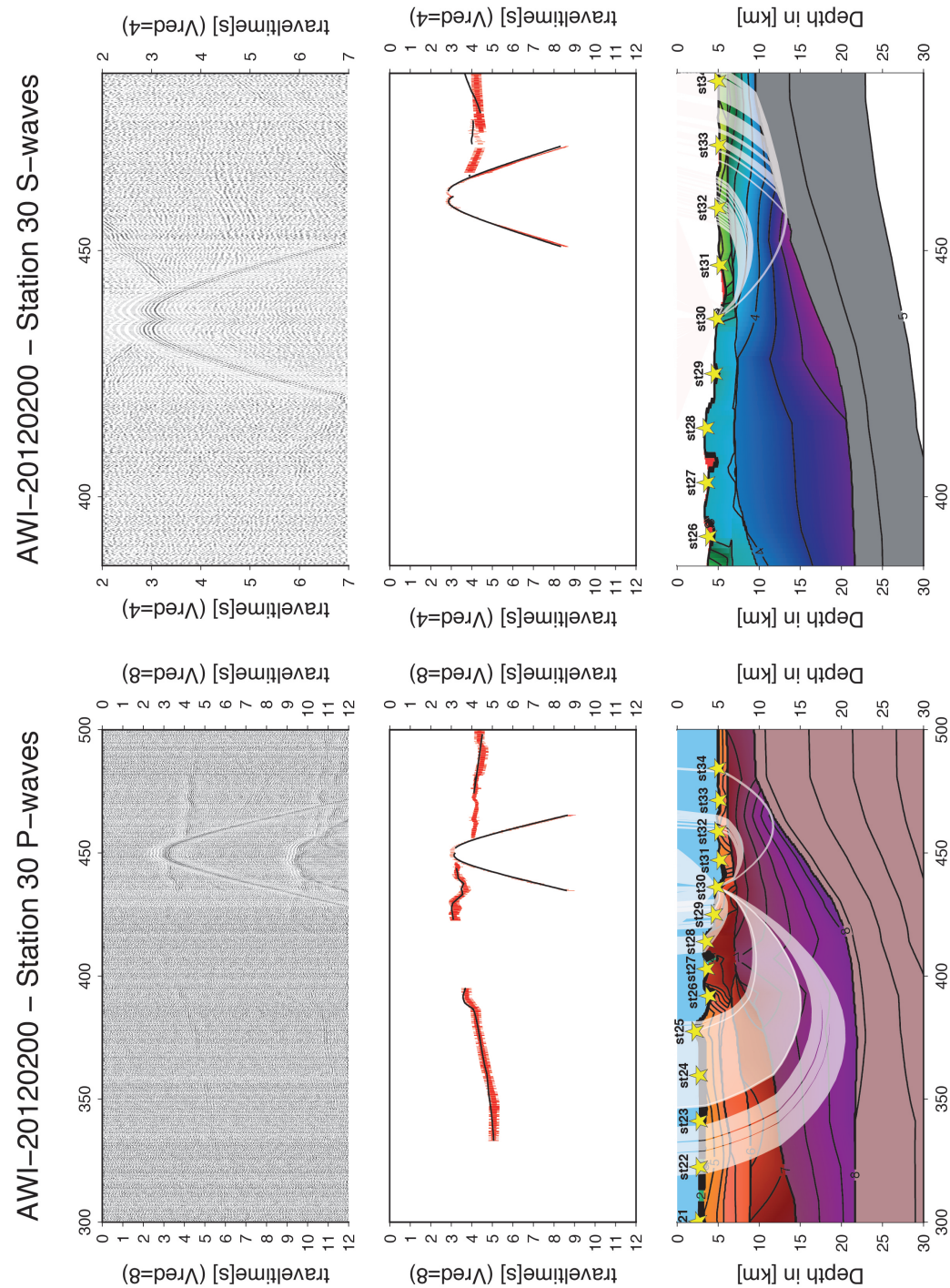
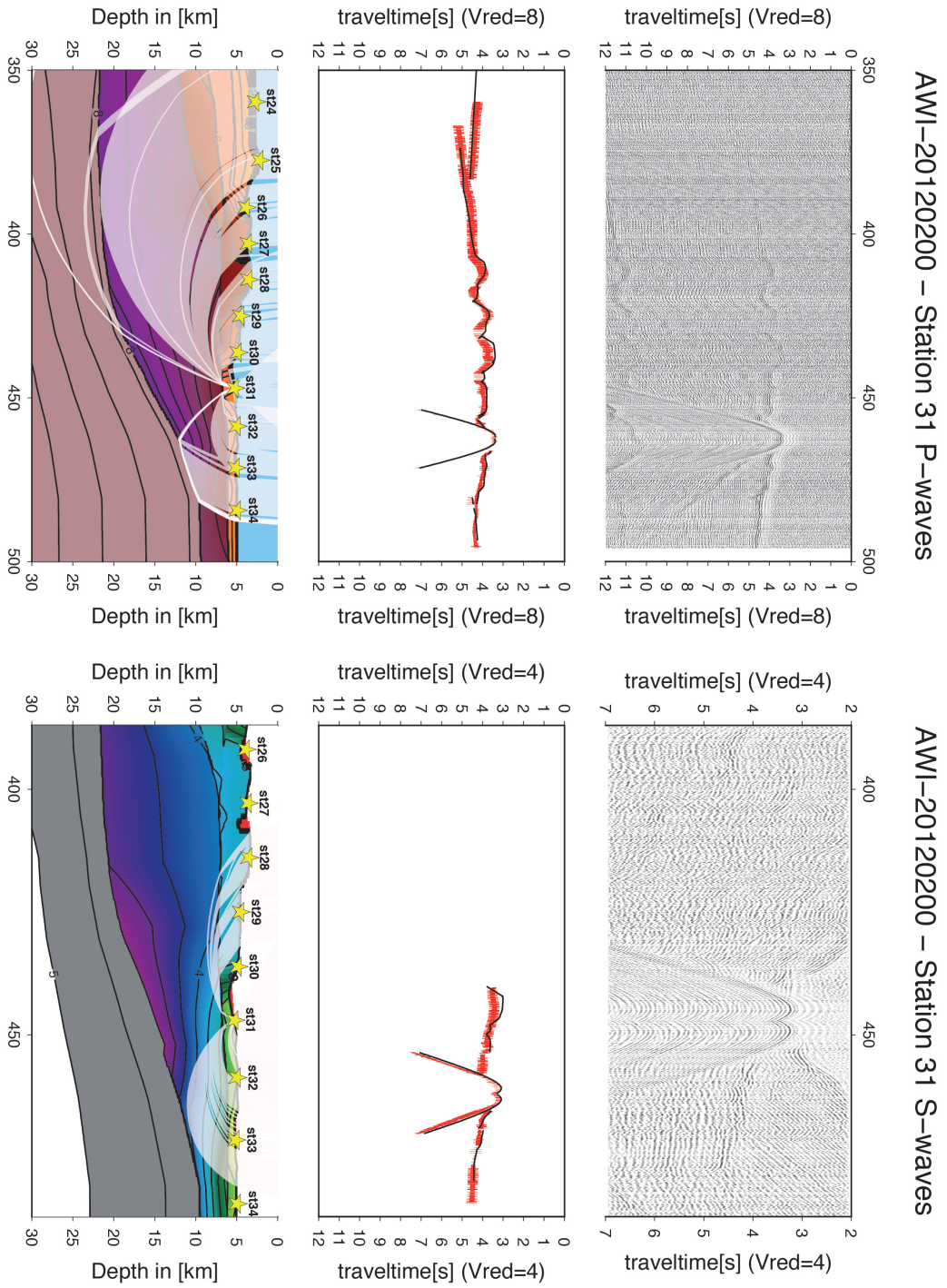


Figure A.57: P- and S-waves station 200st30 upper panel: seismogram, middle panel: picked and modeled arrival times, lower panel: resulting velocity model



**Figure A.58:** P- and S-waves station 200st31 upper panel: seismogram, middle panel: picked and modeled arrival times, lower panel: resulting velocity model

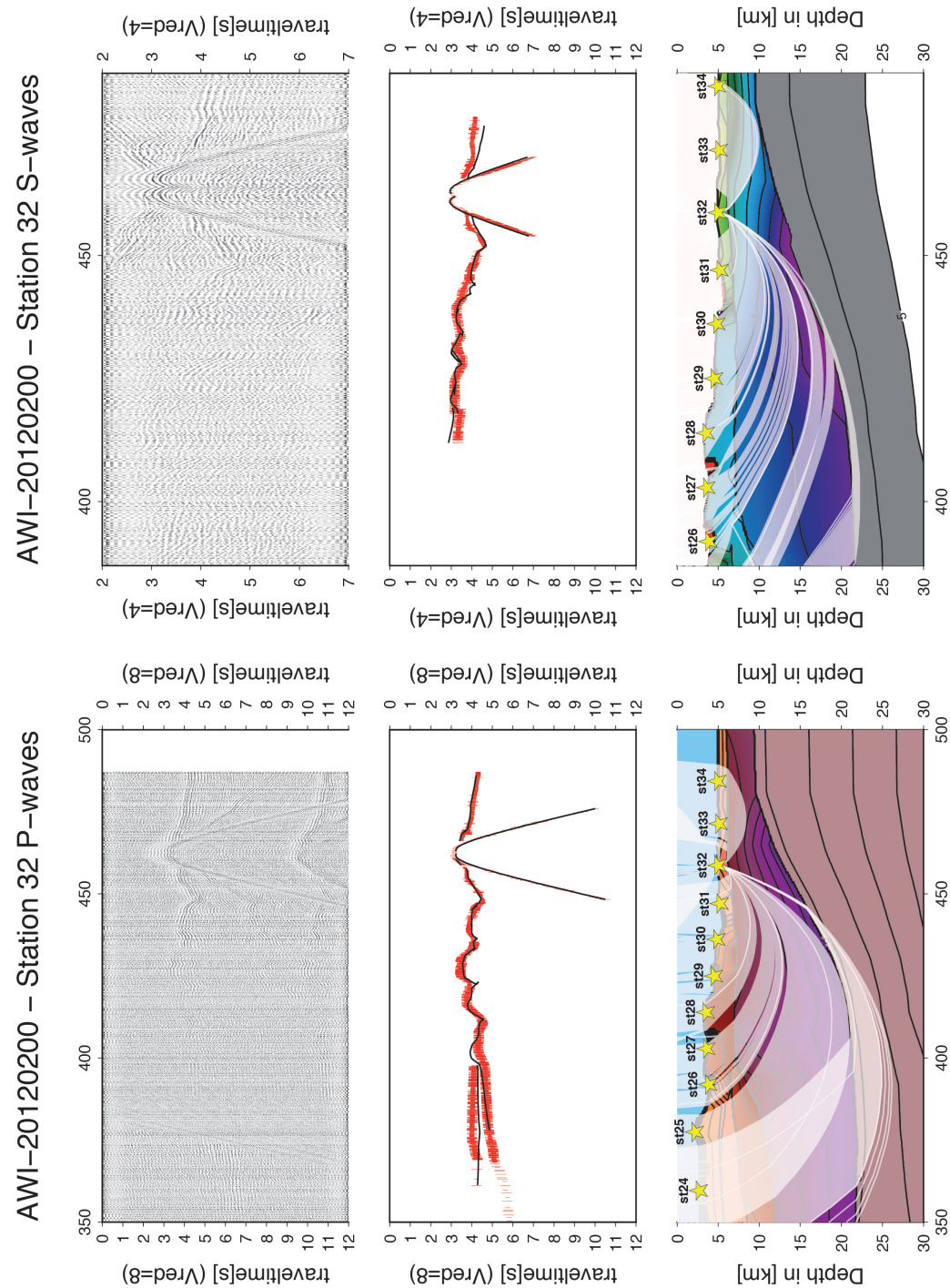


Figure A.59: P- and S-waves station 200st32 upper panel: seismogram, middle panel: picked and modeled arrival times, lower panel: resulting velocity model



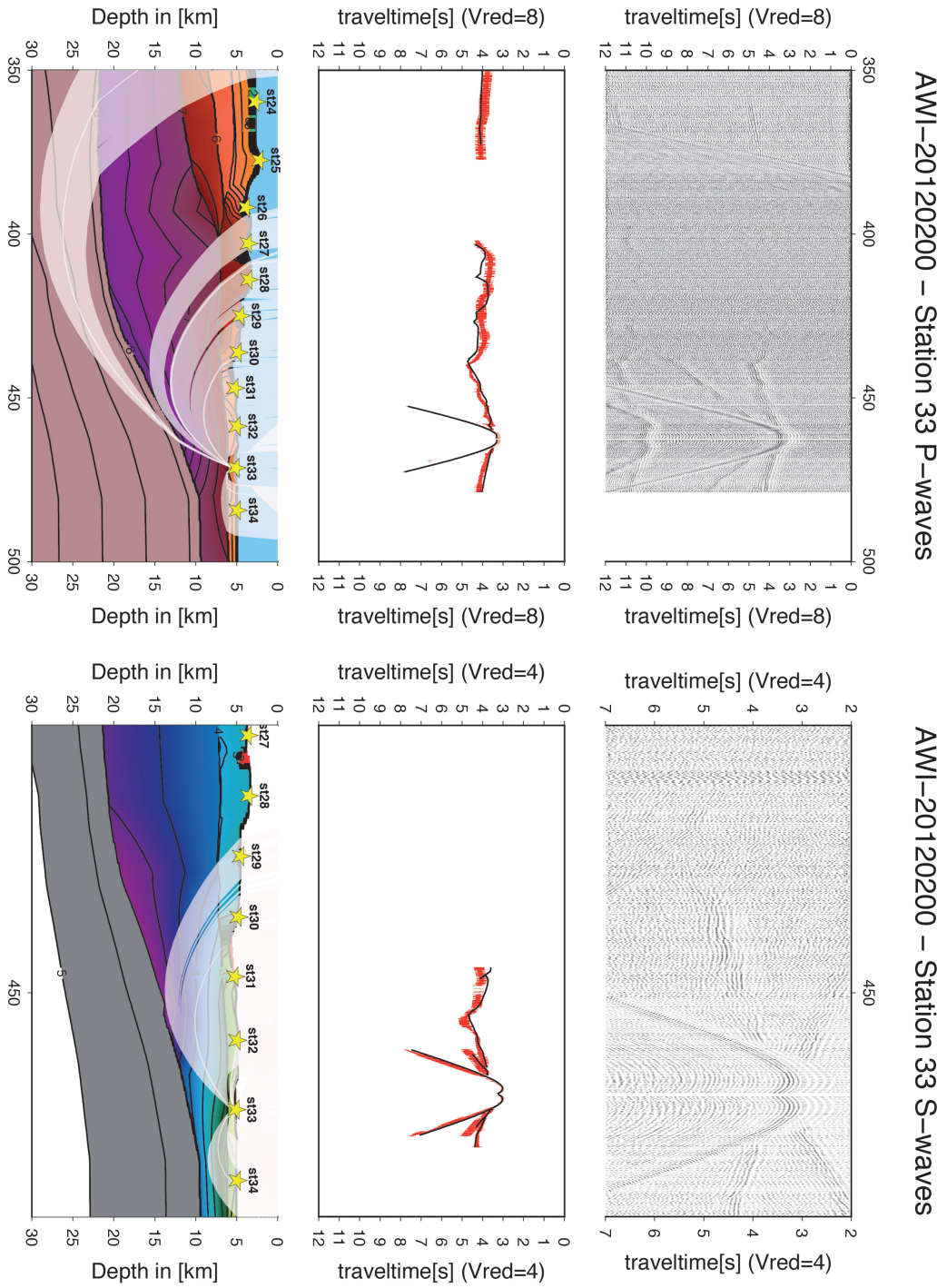


Figure A.60: P- and S-waves station 2000st33 upper panel: seismogram, middle panel: picked and modeled arrival times, lower panel: resulting velocity model

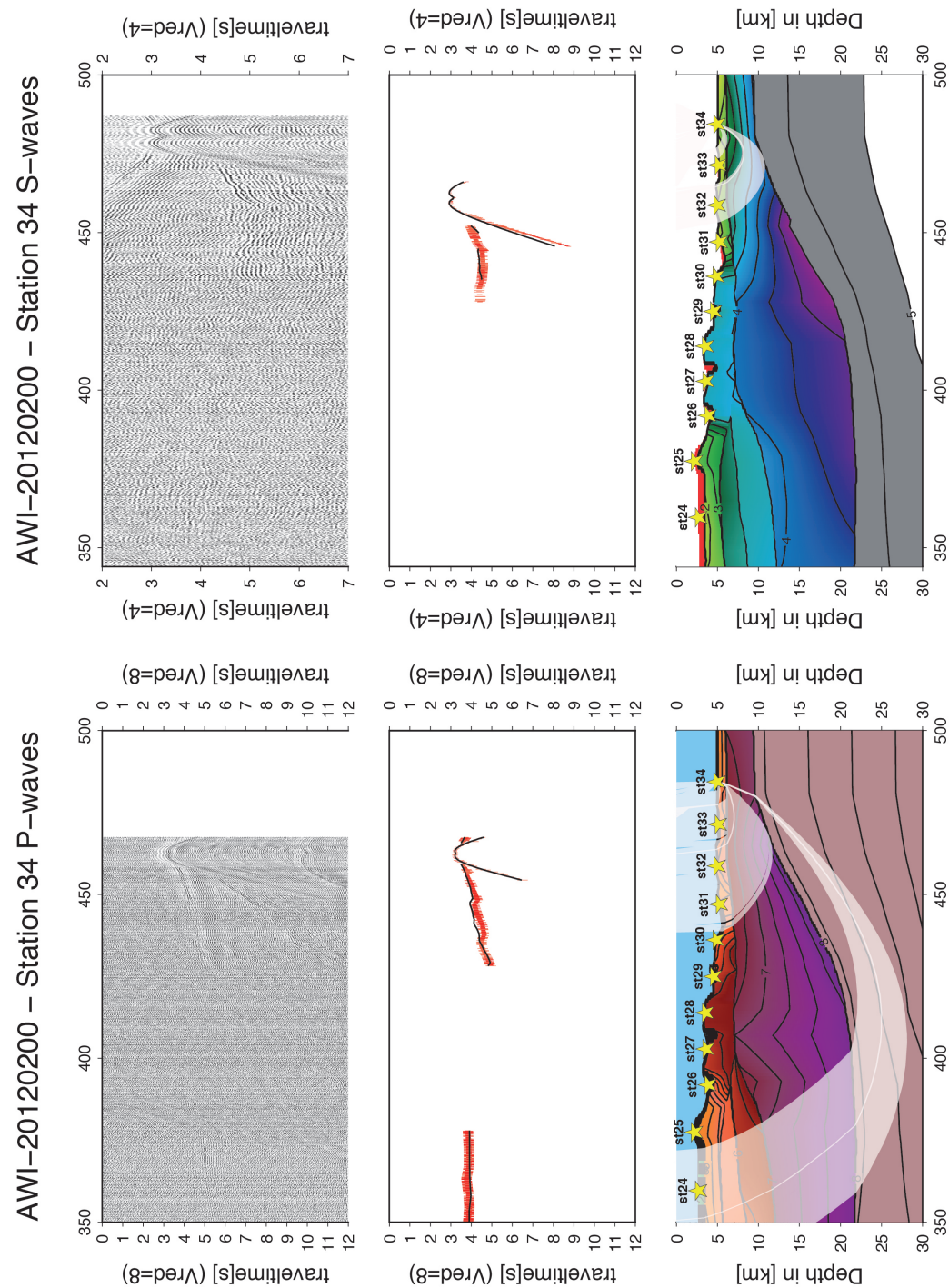
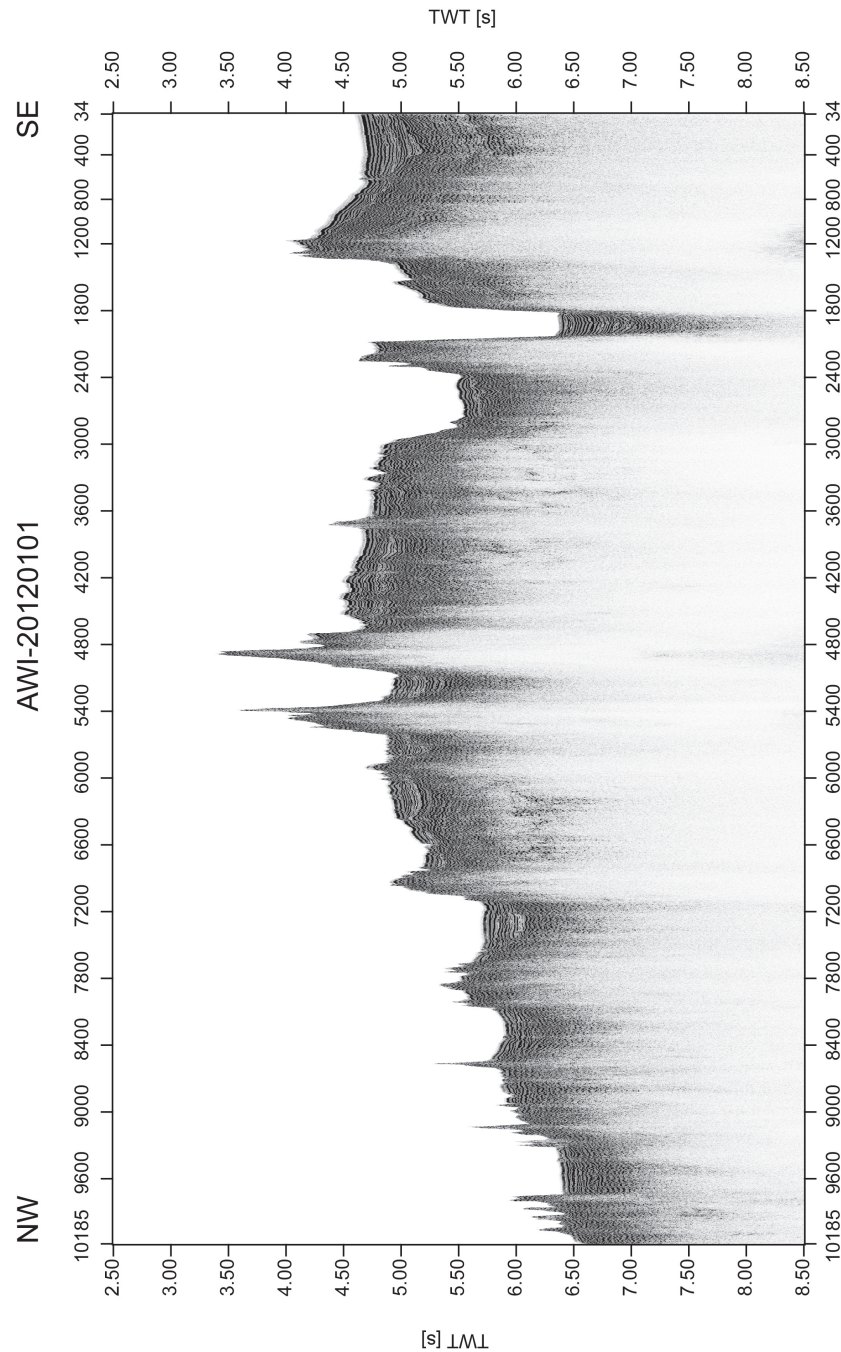


Figure A.61: P- and S-waves station 200st34 upper panel: seismogram, middle panel: picked and modeled arrival times, lower panel: resulting velocity model



## A.5 Reflection seismic data of So-224 along refraction seismic profile

### A.5.1 AWI-20120101



**Figure A.62:** Seismic reflection data profile AWI-20120101 corresponding to refraction seismic profile AWI-20120100; for more information on experimental set-up and processing refer to (Pietsch and Uenzelmann-Neben, 2015; Uenzelmann-Neben, 2012). This section has been processed by G. Uenzelmann-Neben.

## A.5.2 AWI-20120201

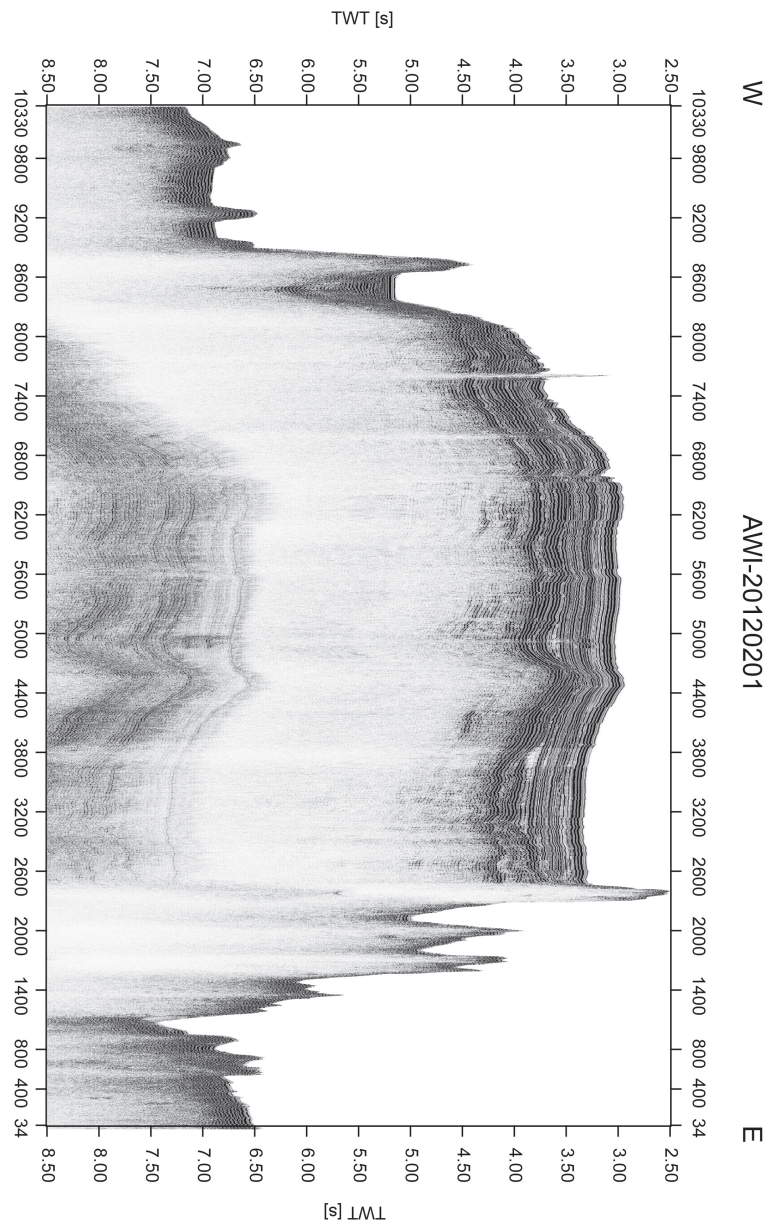


**Figure A.63:** Seismic reflection data profile AWI-20120201 corresponding to refraction seismic profile AWI-20120200; for more information on experimental set-up and processing refer to (Pietsch and Uenzelmann-Neben, 2015; Uenzelmann-Neben, 2012). This section has been processed by R. Pietsch.

## B Plate kinematic reconstruction with *GPlates*

### B.1 Plate IDs used in the plate tectonic reconstruction of the western Pacific

Plate ID	Plate	Plate ID	Plate
458	Proto East Pacific Rise	814	Bellingshausen Sea
474	spreading Chasca-Catequil	833	Lord Howe Rise
701	Africa	860	Challenger Plateau
790	FZ correction	901	Pacific
791	FZ correction	902	Farallon
792	FZ correction	908	Chasca Plate southern Farallon
793	FZ correction	879	Chatham Rise
794	FZ correction	919	Phoenix
795	FZ correction	926	Izanagi
796	FZ correction	963	High Plateau
801	Australia	964	Western Plateaus
802	Australia	965	Northern Plateau
803	Antarctic Peninsula	966	Robbie Ridge
804	Marie Byrd Land	967	Northeast Manihiki
806	North Island NZ	968	East Manihiki
807	South Island NZ	981	Ontong Java Plateau
808	Thurston Island	983	Hikurangi Plateau
813	Champell Plateau	984-987	Catequil Plate Phoenix Plate

**Table B.1:** Plate IDs of the western Pacific as used for chapter 6, the highlighted rows are additional Plate IDs to *Seton et al.* (2012)